Dinitrogen fixation in oxygen minimum zones

DISSERTATION
ZUR ERLANGUNG DES DOKTORGRADES
DER MATHEMATISCHEN-NATURWISSENSCHAFTLICHEN FAKULTÄT
DER CHRISTIAN-ALBRECHTS-UNIVERSITÄT ZU KIEL

vorgelegt von

Tobias Großkopf

Kiel, März 2012

Referent:	Prof. Dr. Julie LaRoche
Ko-Referent:	Prof. Dr. Ruth A. Schmitz
Tag der mündlichen Prüfung:	
Zum Druck genehmigt:	

Für meinen Vater

Summary

The fixation of dinitrogen (N_2) is the most important process of nitrogen (N) input to the oceans. Historically, this process has been primarily linked to surface waters where the limiting availability of N precludes further phytoplankton growth, thereby allowing the growth of N_2-fixers (diazotrophs) without competition. More recent findings suggest nutrient-rich but oxygen-depleted areas, termed oxygen minimum zones (OMZs), to be another important site for N_2 fixation. The aim of this thesis was to investigate the influence of oxygen on N_2 fixation and to assess the importance of diazotrophs in oxygen minimum zones.

In a first set of laboratory experiments, the unicellular diazotrophic cyanobacterium *Crocosphaera watsonii* WH8501 was used as a model organism to gain insight on the effect of oxygen on N_2 fixation (chapter 2.1). The removal of oxygen to protect the oxygen sensitive nitrogenase enzyme was responisble for over half of the cellular carbon storage drawdown during the dark phase (60%), at oxygen concentrations similar to those found in the surface oceans (20%). When the oxygen concentration was lowered to resemble values like found in the oxyclines of OMZs (5%), the cells performed N_2 fixation at slightly higher rates without any excess carbon consumption due to oxygen removal. *C. watsonii* showed no response to nitrate additions up to 800 µM. However, a comparison of the costs of N_2 reduction to ammonium relative to the costs of assimilatory nitrate reduction to ammonium revealed that these two processes are bioenergetically on a par at low oxygen concentrations, leading to the prediction that diazotrophy should not be limited to the oligotrophic (nutrient-poor) surface oceans, but would also be likely to occur inside OMZs, where nitrate concentrations can be high.

This prediction was tested in the Peruvian upwelling system, which is part of the largest OMZ of the world. The whole Peruvian shelf area (5°S - 15°S) is characterized by upwelling of cold, nutrient rich water leading to high primary productivity. High residual phosphate concentrations (high P*) due to N-loss processes in the area between Lima and Pisco (12°S - 14°S) lead to a N-limitation of phytoplankton and related overproduction of organic carbon relative to organic N, as observed in a nutrient addition experiment at 17.45°S 073°W (chapter 2.2).

The highest N_2 fixation rate during the cruise was measured in the area of highest P* values at 12.2°S 077°W with 840 µmol N m^{-2} d^{-1}, a value comparable to those measured in blooms of the diazotrophic cyanobacterium *Trichodesmium*. Several novel clusters of diazotrophs were detected in the Peruvian upwelling system by *nifH* cloning and quantified by cluster specific TaqMan qPCR. Each cluster showed a unique pattern of distribution and some had highest numbers within the OMZ at elevated nitrate concentrations. The incorporation of ^{15}N, added as $^{15}N_2$ gas to incubations, into biomass

confirmed the N_2 fixation activity within the OMZ. Glucose addition to bulk incubations of seawater always resulted in a stimulation of N_2 fixation, indicating a major importance of heterotrophic diazotrophs in the system. These results confirmed the assumption that diazotrophs can inhabit waters low in dissolved oxygen concentrations, where nitrate concentrations can be high (chapter 2.3).

Chapter 2.4 reports on a laboratory experiment on the equilibration time of a $^{15}N_2$ gas bubble with the N_2 gas in seawater, whose results have led to the conclusion that the most commonly applied method to measure N_2 fixation in the ocean, the $^{15}N_2$ tracer assay (Montoya *et al.* 1996), has lead to a signifficant and variable underestimation of N_2 fixation rates due to a slow equilibration between the $^{15}N_2$ tracer added as a gas bubble to incubations and the incubated seawater. The implications of this finding were tested on two cruises throughout the Atlantic Ocean, by parallel incubations of the $^{15}N_2$ tracer method and a revised protocol (chapter 2.5). The revised method yielded areal N_2 fixation rates on average 72% higher than the $^{15}N_2$ tracer method, leading to a revised estimate by direct measurements of global N_2 fixation of 180 Tg N yr^{-1}. Further, the magnitude of the difference between the methods was affected by the diazotrophic community composition. Areas dominated by *Trichodesmium* showed the least underestimation by the $^{15}N_2$ tracer method, while areas where the diazotrophic community was dominated by unicellular and heterocystous cyanobacteria and γ-proteobacteria suffered the largest underestimation. This effect most certainly has led to a biased view of the key organisms in marine N_2 fixation.

Zusammenfassung

Die biologische Fixierung von Distickstoff (N_2) ist der wichtigste Prozess des Stickstoffeintrags in die Ozeane. Dieser Prozess wurde vornehmlich mit Bereichen der Oberflächenozeane in Verbindung gebracht, in denen die Verfügbarkeit von Stickstoff (N) das weitere Wachstum von Phytoplankton limitiert und die daher ein konkurrenzloses Wachstum von Stickstofffixierern (Diazotrophen) erlauben. Neueren Ergebnissen zufolge sind auch Sauerstoffminimumzonen, Bereiche hohen Nährstoffgehaltes und verminderter Sauerstoffkonzentration ein wichtiger Ort der Stickstofffixierung. Ziel dieser Arbeit war es, den Einfluss von Sauerstoff auf die Stickstofffixierung und die Wichtigkeit von Diazotrophen in Sauerstoffminimumzonen zu untersuchen.

In einer ersten Serie von Laborversuchen wurde die einzellige stickstofffixierende Cyanobakterie *Crocosphaera watsonii* WH8501 als Modellorganismus verwendet, um zu verstehen, wie sich die Sauerstoffkonzentration auf den Energiehaushalt von Diazotrophen auswirkt (Kapitel 2.1). Unter normalen Sauerstoffkonzentrationen (20%), wie sie etwa im Oberflächenozean vorkommen, war über die Hälfte der nächtlichen Kohlenstoffabnahme (60%) in *C. watsonii* allein auf die Beseitigung des für die Nitrogenase schädlichen Sauerstoffs zurückzuführen. Wurde der Sauerstoffgehalt hingegen auf Konzentrationen gesenkt, wie sie etwa in Sauerstoffgradienten ober- und unterhalb von ausgeprägten Sauerstoffminimumzonen anzutreffen sind (5%), zeigten die Zellen eine leicht erhöhte Stickstofffixierungsrate bei gleichzeitigem Ausbleiben einer nächtlichen Kohlenstoffabnahme, die allein auf Sauerstoffbeseitigung zurückzuführen wäre. *C. watsonii* zeigte keienerlei Stimulanz durch die Zugabe von bis zu 800 µM Nitrat zum Nährmedium. Der Vergleich der bioenergetischen Kosten, die durch Stickstofffixierung oder durch Nitratassimilation entstehen, zeigte, dass bei niedriger Sauerstoffkonzentration, also ohne Kohlenstoffabnahme zur Sauerstoffbeseitigung, beide N-Aufnahmewege energetisch gleichgestellt sind und somit kein Nachteil von Diazotrophen gegenüber Nitratassimilierern zu erwarten wäre. Dieser Vergleich führte uns zu der Annahme, dass Diazotrophe neben den Oberflächenozeanen auch Sauerstoffminimumzonen besiedeln könnten, wo die Nitratkonzentrationen mitunter sehr hoch sind.

Diese Vorhersage konnte im Auftriebsgebiet von Peru untersucht werden, das zu der größten Sauerstoffminimumzone der Welt im tropischen und subtropischen Ostpazifik gehört. Der gesamte peruanische Kontinentalsockel (5°S - 15°S) ist von Auftriebsströmungen geprägt, die kaltes, nährstoffreiches Tiefenwasser an die Oberfläche befördern und zu vermehrter Primärproduktion führen. Durch Stickstoffverlustprozesse im Bereich zwischen Lima und Pisco (12°S - 14°S) kam es zu einer hohen Konzentration an Phosphat bei gleichzeitig sehr geringer Nitratkonzentration (hohe P* Konzentration) in der Wassersäule, was zu einer Stickstofflimitierung der Primärproduktion und einer Überpro-

duktion von Kohlenstoff im südlichen Auftriebsgebiet von Peru führte, wie es anhand eines Nährstoffzugabeexperiments bei 17.45°S 073°W zu beobachten war (Kapitel 2.2).

Die höchsten Stickstofffixierungsraten der gesamten Ausfahrt wurden in dem Bereich der höchsten P* Konzentrationen bei 12.2°S 077°W gemessen, mit 840 µmol N m^{-2} d^{-1}, einem Wert wie er etwa in größeren *Trichodesmium*-Blüten erreicht wird. Sieben neue Cluster im Stammbaum der Diazotorophen wurden mittels Klonierung des *nifH* Gens im Auftriebsgebiet von Peru entdeckt und konnten durch TaqMan qPCR quantifiziert werden. Dabei zeigte sich ein einzigartiges Verbreitungsmuster für jeden Cluster, wobei einige der Cluster ihr Häufigkeitsmaximum in der Sauerstoffminimumschicht bei hohen Nitratkonzentrationen zeigten. Die Aktivität der Diazotrophen vor Peru konnte über den Nachweis des Einbaus des schweren Stickstoffisotops $^{15}N_2$ in die Biomasse bestätigt werden. Dabei führte die Zugabe von Glukose immer zu einer Stimulation der Sickstoffixierungsraten, was auf eine Beteiligung von heterotrophen Stickstoffixierern in dem System hinweist. Diese Ergebnisse haben die Annahme bestätigt, das Stickstoffixierer Bereiche der Ozeane besiedeln können, in denen die Nitratkonzentration hoch, aber gleichzeitig der Sauerstoffgehalt gering ist (Kapitel 2.3).

Kapitel 2.4 zeigt Ergebnisse eines Experiments zum Gasgleichgewicht zwischen Gas und Wasserphase einer Inkubation mit $^{15}N_2$ aus denen resultierte, dass Messungen der Stickstofffixierung mit der weit verbreiteten $^{15}N_2$ Spurengasmethode (Montoya *et al.* 1996) zu einer signifikanten und variablen Unterschätzung der Stickstofffixierungsraten führen. Die Konsequenzen dieser Entdeckung wurde mittels zweier Ausfahrten im Atlantischen Ozean überpüft, bei denen Parallelmessungen mit der $^{15}N_2$ Spurengasmethode und einer überarbeiteten Methode durchgeführt wurden. Die überarbeitete Methode zeigte im Durchschnitt 72 % höhere flächenbezogene Stickstofffixierungsraten als die $^{15}N_2$ Spurengasmethode, was zu einer Korrektur der globalen Stickstoffixierungsrate durch direkte Messungen auf 180 Tg N a^{-1} führte. Dabei war der Unterschied der mit den beiden Methoden gemessenen Raten variabel, zeigte aber eine deutliche Tendenz zu höherer Unterschätzung von Stockstofffixierungsraten mit der $^{15}N_2$ Spurengasmethode in Bereichen, die von einzelligen und heterocystenbildenden diazotrophen Cyanobakterien und δ-Proteobakterien dominiert wurden. Raten, gemessen in Regionen in denen *Trichodesmium* vorherrschend war, wiesen hingegen geringere Unterschiede zwischen den Methoden auf. Ein solcher Effekt hat sicherlich zu einer verschobenen Wahrnehmung in Bezug auf die Schlüsselorganismen der Stickstoffixierung geführt.

Contents

Summary VII

Zusammenfassung IX

1 Introduction 3

1.1 Nitrogen fixation 3
1.2 The marine nitrogen cycle 10
1.3 Oxygen minimum zones 12
1.4 Aim of this thesis 14

2 Results 19

2.1 Bioenergetics of N_2 fixation 23
2.2 The Peruvian upwelling system 49
2.3 Heterotropphic N_2 fixation in the Peruvian OMZ 83
2.4 Underestimation of N_2 fixation 107
2.5 Closing the Gap 117

3 Discussion 163

References 169

Acknowledgements 181

Eidesstattliche Erklärung 183

1 Introduction

1 Introduction

Together with carbon (C), nitrogen (N) is the most important nutrient element for all living matter. The oceans hold a considerable amount of N in the form of reactive N (N_r, N that is available to biology, mainly nitrate, nitrite, ammonium and dissolved organic N (DIN)), yet a fraction of this N_r is continuously lost by processes occurring in oxygen minimum zones (OMZs) and suboxic sediments. The largest supply route of new N_r to the oceans is the microbial mediated fixation of gaseous dinitrogen (N_2). Only specialized groups of bacteria and archea, called diazotrophs, are capable of breaking the chemically highly stable triple bond in the N_2 molecule and reducing it to ammonium. These diazotrophs, although only responsible for about 1.6% of marine primary productivity, are therefore key organisms in controlling the marine carbon cycle and the sequestration of CO_2 from the atmosphere (Falkowski 1997). Should all diazotrophs cease to exist in one instance, the oceans would be completely sterile after 1000 -2000 years (ignoring terrestrial inputs and given the continuation of N-loss) (Duce *et al.* 2008). This thesis focuses on the fixation of N_2 in oxygen minimum zones. These large areas of low oxygen concentration are well known for their high activity of N-loss pathways, yet little is known about N-input by N_2 fixation.

1.1 Nitrogen fixation

The Haber-Bosch process

In 1909 the German chemist Fritz Haber discovered that hydrogen gas (H_2) would combine with the highly inert nitrogen gas (N_2) to form ammonia (NH_3) at a temperature of around 500° C, a pressure of 150 -200 atmospheres, and in presence of an iron catalyst. Carl Bosch upscaled the process to industrial levels and took the idea to the chemical company BASF, where the commercial production of ammonia started in 1913 (Smil 1999). Since then the Haber-Bosch process has supplied the exponentially growing human population with the ammonia needed as fertilizer for high efficiency agriculture. Today, about 130 Tg of ammonia are produced by the Haber-Bosch process each year (Galloway *et al.* 2004, Gruber & Galloway 2008). The energetic expense invested is immense: About 1% of the total human energy production is consumed by the Haber-Bosch process. The fixation reaction itself is an exothermic (energy yielding) process at room temperature (eq. 1).

$$0.5N_2 + 1.5H_2 \leftrightarrow NH_3 \qquad G'_0 = -45.7KJmol^{-1} \tag{1}$$

However, to break the triple bond in the N_2 molecule a high activation energy is required that is overcome by using high temperature and pressure, making the industrial process expensive energetically.

Nitrogenase

The process of biological fixation of N_2 arose a few billion years before its rediscovery by Haber and Bosch. The reaction is catalyzed by the nitrogenase enzyme complex, which has its evolutionary origin in a completely reduced atmosphere some 2 x 10^9 years ago (Cheng 2008, Boyd *et al.* 2011). The ancient form of nitrogenase contains molybdenum and iron, but alternative enzymes free of molybdenum exist, instead using a vanadium-iron (*vnfDK*) or iron only (*anfDK*) cofactor (Hales *et al.* 1986, Chisnell *et al.* 1988). The following description of nitrogenase will focus on the molybdenum containing nitrogenase, encoded by the *nif*-operon, which is the best studied of the nitrogenases. The core enzyme of nitrogenase is known as the MoFe protein. It is a heterotetramer, consisting of two alpha and two beta subunits, encoded by the *nifD* and *nifK* genes (Schindelin *et al.* 1997). The MoFe protein binds the N_2 substrate and reduces it to ammonium in a three step reaction, a fourth cycle reduces two protons to yield hydrogen gas (H_2) (Pickett 1996). The low potential electrons that are needed for the reduction of N_2 are provided by the nitrogenase reductase, a heterodimer protein with an iron cofactor bound between the subunits, encoded by the *nifH* gene (Brigle *et al.* 1985). Per electron transferred, the iron protein hydrolyzes two molecules of ATP to ADP (Hallenbeck 1983), which is required for lowering the midpoint potential of the iron protein as well as for the conformational change that allows the binding to the MoFe protein (Danyal *et al.* 2011). The overall reaction of the nitrogenase enzyme complex is summarized in equation 2 (Burgess & Lowe 1996).

$$N_2 + 8e^- + 8H^+ + 16ATP \leftrightarrow 2NH_3 + H_2 + 16ADP + 16Pi \tag{2}$$

Similar to the Haber-Bosch process, large amounts of energy are invested (in form of ATP), presumably to increase the kinetics of the reaction. The electrons that are delivered by the Fe protein to nitrogenase are very low potential electrons that stem from reduced ferredoxin or flavodoxin (Shah *et al.* 1983). Nitrogenase in vitro shows a midpoint potential of -473 mV. When the redox potential is set to more negative values, the ATP consumption of nitrogenase approaches two moles ATP per mol electrons transferred. At higher redox potentials (more oxidizing conditions), the ATP consumption per electron transferred increases rapidly (Hallenbeck 1983). Oxygen, if present, increases the redox potential and therefore the ATP requirement of nitrogenase. This finding already implies that the enzyme is sensitive to oxygen and needs to be kept in a completely reduced environment for most efficient operation. Although a respiratory chain proves very useful to supply the large amounts of ATP required by the reduction of N_2 to ammonium, both the MoFe and the Fe protein are rapidly destroyed on contact with oxygen, presumably by the action of peroxide or superoxide radicals (Fay 1992). Therefore, all diazotrophs show adaptations to protect their nitrogenase enzyme from oxygen, either by respiratory

removal of oxygen (Peschek *et al.* 1991), the exclusion of oxygen via diffusion barriers (Walsby 2007), the conformational protection of the enzyme (Fay 1992) or the complete inhibition of nitrogenase gene expression in the presence of oxygen (Schmitz *et al.* 2002).

Diazotrophs (N_2 fixers)

The occurrence of a *nif* operon is strictly limited to genomes within the bacteria and archaea. Nevertheless, many plants make use of the process of N_2 fixation to colonize areas low in fixed N compounds like nitrate (NO_3^-), nitrite (NO_2^-) or ammonium (NH_4^+) by offering space, protection and nutrients to certain prokaryotes, that in turn supply the plant with fixed nitrogen in form of ammonium. The best known of these symbiont interactions is represented by the legumes, one of the largest families within the plant kingdom. Several lineages therein show a symbiosis with diazotrophic (α- and β-) proteobacteria commonly known by the name rhizobia. When growing on soil devoid of fixed N, these plants attract rhizobia to live in globular structures generated along the roots of the plant. The plant then produces leghemoglobine, an oxygen binding protein that both keeps the oxygen pressure at low levels and at the same time guarantees a steady flow of oxygen to fuel rhizobial respiratory needs (Long 1989).

While rhizobia are the most important terrestrial diazotrophs, in the marine environment most of the biological N_2 fixation is performed by cyanobacteria, the only prokaryotes containing both chlorophyll a and b, besides other accessory pigments. Cyanobacteria are capable of oxygenic photosynthesis, since they possess two photosystems, photosystem I (PSI) and photosystem II (PSII), which allows them to reduce CO_2 to carbohydrates with electrons derived from water. An interesting exception to the rule is represented by a novel cyanobacterium UCYN-A, that lacks PSII (Zehr *et al.* 2008) and therefore does not evolve oxygen. Cyanobacteria populate the euphotic layer of the oceans, the top 200 meters, which are penetrated by sufficient amount of sunlight to permit photosynthesis (Ting et al. 2002). Within the cyanobacteria, several species are capable of N_2 fixation. Diazotrophic cyanobacteria are confronted with the problem of combining the oxygen evolving lifestyle of photoautotrophy with the anoxic process of N_2 fixation. They have evolved four different strategies to circumvent this problem, allowing the classification of diazotrophic cyanobacteria into four groups: Heterocystous, filamentous non-heterocystous and single cell cyanobacteria, with the UCYN-A as a special case.

Heterocystous cyanobacteria form linear or branched chains of cells called filaments. When growing in the absence of fixed N like nitrate or ammonium, some cells along a filament develop into heterocysts (Ramos & Guerrero 1983). These cells grow a thick glycolipid layer, that acts as a diffusion barrier for molecular oxygen (Paerl *et al.*. 1995). The heterocysts have no PSII and are highly enriched in PSI, which plays a role in generating ATP, together with the terminal oxidase of the respiratory chain (Milligan

et al. 2007, Valladares *et al.* 2007). The heterocysts are the only cells along the filaments with active nitrogenase enzymes. The ammonium produced in these cells is shared with neighboring cells in exchange for reduced carbon compounds (sugars). In the ocean the occurrence of free living heterocystous cyanobacteria is limited to brackish water systems, like the Baltic Sea, where they can form large and sometimes toxic surface blooms in the summer, after the nitrate has been consumed (Ohlendieck *et al.* 2000, Seppala *et al.* 2007). In the open ocean, heterocystous cyanobacteria of the genera *Richelia* and *Calothrix* occur in the form of symbionts of diatoms (Carpenter *et al.* 1999, Foster *et al.* 2007, Foster *et al.* 2009).

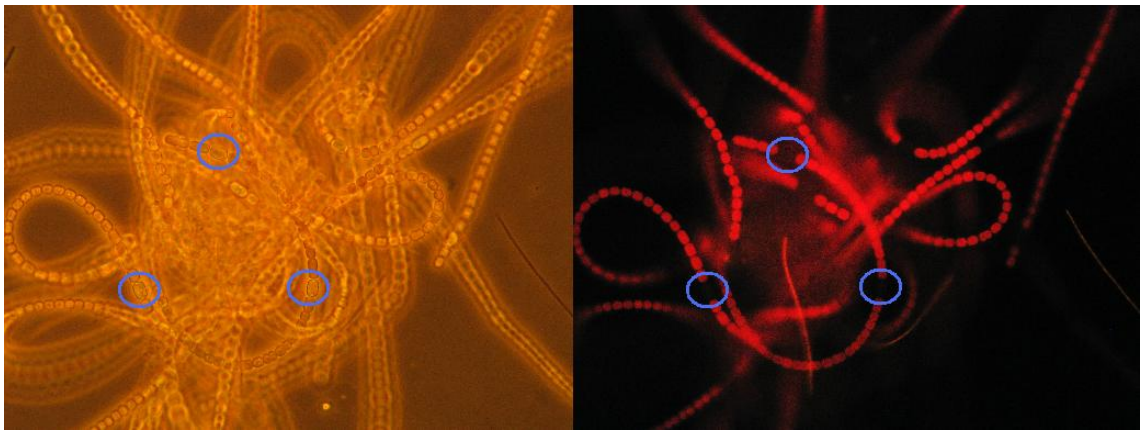

Figure 1: Picture of *Anabaena* collected in the Eckernförde bay (Baltic Sea) from the sailing boat *Pisco Sour* in 2009. Left panel shows a light microscope image of entangled filaments. Right panel shows the same view with a long pass filter and exited by blue light. Red fluorescence is emitted by chlorophyll from PS II. Circles show the position of heterocysts, specialized N_2-fixing cells which lack PSII and exhibit no fluorescence.

One of the most important diazotrophs in the ocean is the filamentous non-heterocystous cyanobacterium *Trichodesmium* (Capone *et al.* 1997). Although the single cells are about 8 -10 µm wide and 5 - 21 µm in diameter, these organisms form colonies of thousands of cells arranged in hundreds of filaments that are visible to the naked eye (LaRoche & Breitbarth 2005). *Trichodesmium* is able to fix N_2 above temperatures of 20°C, with maximum rates in the temperature range between 24° and 30°C (Breitbarth *et al.* 2007). This confines its distribution to the tropical and subtropical oceans, where it can grow to large numbers, forming patches of high biomass that are detectable from space (Subramaniam *et al.* 2002). Such blooms of *Trichodesmium* are associated with a shallow mixed layer and the input of iron to the surface ocean by aeolian dust deposition (Tyrrell *et al.* 2003). Colonies of *Trichodesmium* have an adaptive advantage over other diazotrophs in regions with high atmospheric dust input due to their ability of accessing particle-bound iron (Rubin *et al.* 2011). The ability to switch to alternative P sources like inorganic phosphate or phosphonates (Dyhrman & Haley 2006), the plasticity of the cellular C:P ratio that allows low cellular P quota (Fu *et al.* 2005) and the high iron requirements of *Trichodesmium*

(Tuit *et al.* 2004) suggest that the distribution of these organisms is controlled by the availability of iron in the environment rather than phosphate (Moutin *et al.* 2008). In contrast to the heterocystous cyanobacteria, *Trichodesmium* does not show specialized cells that exclusively perform N_2 fixation. In principle every cell is competent to produce nitrogenase, but since N_2 fixation and photosynthetic oxygen evolution are happening in parallel in the same filament, there is separation at the cellular level (Berman-Frank *et al.* 2001). Cells that are fixing N_2 exhibit increased PSI activity, light driven oxygen consumption via the Mehler reaction (Kupper *et al.* 2004, Milligan *et al.* 2007) and increased cytochrome c oxidase activity (Bergman *et al.* 1993). The consumption of oxygen during the N_2 fixation period likely exceeds the purely energetic demands, since N_2 fixation is negatively correlated with ambient oxygen concentration in these cyanobacteria (Staal *et al.* 2007). The dominance of *Trichodesmium* in the tropical oceans creates a paradox, since apparently the heterocystous cyanobacteria are better equipped to confront high oxygen concentrations, due to their diffusion barrier. It seems likely however, that at high temperatures such as those observed in the tropical oceans, respiratory protection, the removal of oxygen by PSI or terminal oxidases, presents a better strategy to remove oxygen than the development of heterocysts (Staal *et al.* 2003).

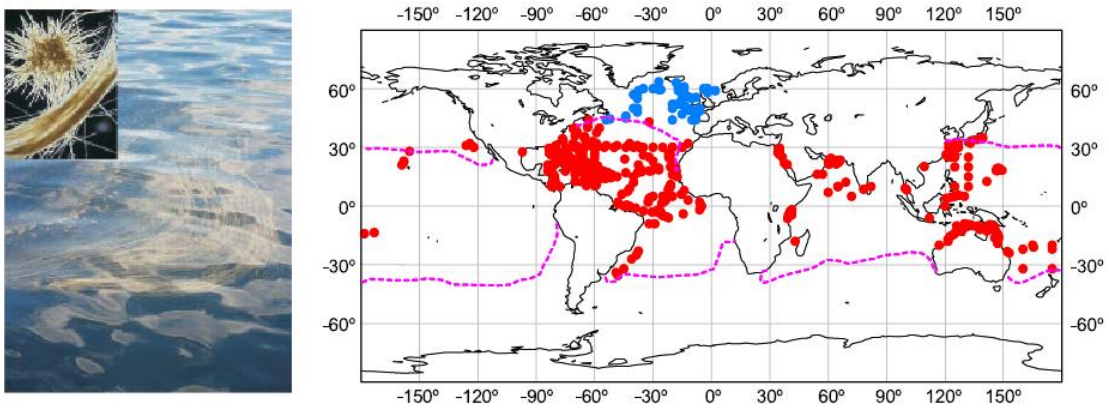

Figure 2: *Trichodesmium*, a key player in the marine N-cycle. Left panel shows surface bloom of *Trichodesmium* with inlay showing *Trichodesmium* colonies. Picture from: (Kasting & Siefert 2002). Right panel shows observations of *Trichodesmium* in waters warmer than (red dots) or cooler than 20° C (blue dots). Dashed line shows 20°C isotherm of annual mean SST. Source: (LaRoche & Breitbarth 2005).

In *Crocosphaera* and *Cyanothece*, two genera with important representatives in the marine habitat, the fixation of N_2 is restricted to the night period (ColonLopez *et al.* 1997, Mohr *et al.* 2010b). During the light period the cells exhibit a photoautotrophic lifestyle, fixing CO_2 and accumulating storage carbohydrates (Schneegurt *et al.* 1994). At the beginning of the dark period photosynthesis genes are down-regulated and the genes for respiration and N_2 fixation up-regulated (Colon-Lopez & Sherman 1998, Stoeckel *et al.*

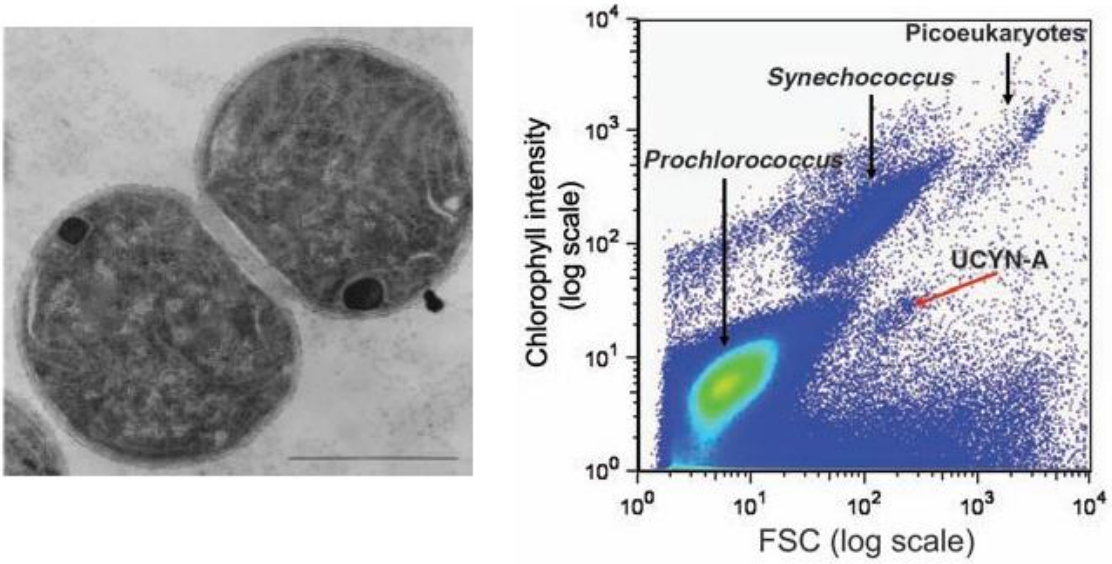

Figure 3: Unicellular diazotrophic cyanobacteria. Left panel: Electron micrograph of *Crocosphaera watsonii* WH 8501. Scale bar = 1 µm. Source: (Zehr *et al.* 2001). Right panel: first report on detection of Group A (UCYN-A) canobacteria in a flow cytometry sample. Source: (Zehr *et al.* 2008).

2008, Mohr *et al.* 2010b). The cells switch to a heterotrophic lifestyle, fueling the energetic demands of N_2 fixation by the oxidation of carbohydrates acquired during the light period (Sherman *et al.* 1998, Shi *et al.* 2010). Respiration not only provides energy for basal metabolism and N_2 fixation during the dark period, but probably also represents the mechanism by which these unicellular bacteria keep their cellular interior at low oxygen concentrations during the period of N_2 fixation, a mechanism termed respiratory protection (Peschek *et al.* 1991). Some unicellular cyanobacteria produce external polysaccharides that generate a mucus matrix around clusters of cells (Webb *et al.* 2009) that could additionally slow the diffusion of oxygen and assist during N_2 fixation. Unicellular cyanobacteria seem to be better competitors for iron than *Trichodesmium*, since the major iron requiring processes, N_2 fixation and photosynthesis, are separated in time (Tuit *et al.* 2004). In *Crocosphaera* a strategy coined hotbunking consist of the movement of iron atoms between the nitrogenase enzymes and the proteins involved in photosynthesis, thus allowing the cells to lower their iron requirements (Saito *et al.* 2011).

Being the only cyanobacteria that lack the oxygen evolving PS II, the recently discovered UCYN-A express their *nifH* gene during the day (Church *et al.* 2005, Zehr *et al.* 2008), a strategy that would enable them to make use of ATP generated by PSI activity in the light to fuel N_2 fixation. No cultured representative of the UCYN-A exists to date, which limits the information about their lifestyle and physiology. However, the information obtained by DNA-sequencing of flow cytometry sorted environmental samples suggests that UCYN-A exist in a symbiotic relationship, since their genome lacks

some essential biosynthesis pathways (Tripp *et al.* 2010). If this proves to be the case, the nitrogenase enzyme of UCYN-A could be protected from oxygen by respiratory activity or diffusion barrriers of the host cell. While *Trichodesmium* and *Crocosphaera* thrive mainly in water temperatures above 25°C, the UCYN-A show abundance maxima in waters between 19° and 24° C (Langlois *et al.* 2008, Moisander *et al.* 2010).

Recent culture independent methods suggest that non-cyanobacterial sequences are much more frequent in the oceanic community of diazotrophs than previously thought (Gaby & Buckley 2011). Proteobacterial sequences dominate within the non-cyanobacterial *nifH* sequences obtained from clone libraries (Farnelid *et al.* 2011) and certain proteobacteria are present at high abundances even in oligotrophic ocean areas (Langlois *et al.* 2008). Recently, non-cyanobacterial *nifH* sequences were recovered from the Northern and Southern Eastern Tropical Pacific oxygen minimum zones (Fernandez *et al.* 2011, Hamersley *et al.* 2011), indicating the importance of these organisms in low oxygen environments. Furthermore, the South Pacific gyre, one of the largest ecosystems in the world, seems to be dominated by heterotrophic diazotrophs (Halm *et al.* 2011). Despite accumulating reports about abundance and activity of non-cyanobacterial diazotrophs in the oceans, their contribution to global marine N_2 fixation and their role in the marine ecosystem is still an open issue (Riemann *et al.* 2010). Most of the diazotrophs are exclusively known by their *nifH* gene sequence and any conclusion about their physiology is speculative. Therefore the ways that non-cyanobacterial diazotrophs protect their nitrogenase from oxygen might be as diverse as their phylogeny suggests. Protective mechanisms in cultivated proteobacteria include respiratory protection (Bertsova *et al.* 2001), tolerance of the nitrogenase towards oxygen by oxygen reduction at the enzyme itself (Thorneley & Ashby 1989) and shut down of enzyme synthesis in contact with oxygen (Schmitz *et al.* 2002, Martinez-Argudo *et al.* 2004).

Measuring N_2 fixation

The dynamics of nutrient concentrations in the oceans have repeatedly been used to derive global N_2 fixation rates (Gruber & Sarmiento 1997, Deutsch *et al.* 2007). The P* parameter for example displays the excess or lack of inorganic phosphate (P) relative to nitrate in the water, given Redfield stochiometry (N:P = 16:1) (eq. 3). The assumptions needed in order to estimate N_2 fixation from P* are that non-diazotrophic phytoplankton growth and remineralisation of non-diazotrophic biomass will always remove and supply N and P from the environment in the relation 16:1 and that only N_2 fixation and N-loss processes can alter the concentration of N relative to 16 x P. Combining knowledge of P* and ocean circulation allows the calculation of changes in P* over time (given steady-state P* conditions in space), that must result either from N_2 fixation (P* decrease) or N-loss

(P* increase), given the above assumptions (Deutsch *et al.* 2007).

$$P^* = [PO_4^{3-}] - [NO_3^-]/16 \quad (3)$$

The strength of this approach is that it uses the concentrations of inorganic N and P, which are routinely measured on nearly every oceanographic cruise, therefore it relies on a huge dataset that facilitates global extrapolations of N_2 fixation. The weakness however, is that differences in nutrient stoichiometry result from the integration of several metabolic processes and do not necessarily reflect N-loss or N-input processes exclusively. Non-Redfield production, the growth of phytoplankton with a stoichiometry of PON:POP (particulate organic N: particulate organic P) other than 16:1, is one way of changing the nutrient N:P ratio without the alteration of the total fixed-N budget. Therefore such estimates of global N_2 fixation derived from the distribution and dynamics of geochemical parameters cannot replace direct measurements of N_2 fixation in the field. The two most applied methods to measure environmental N_2 fixation are the acetylene reduction assay (Capone 1993) and the $^{15}N_2$ tracer assay (Montoya *et al.* 1996). While the former uses the capability of nitrogenase to reduce the alternative substrate acetylene to ethylene, thereby monitoring its activity *in vivo*, the latter relies on the incorporation of the stable nitrogen isotope ^{15}N into diazotrophic biomass. The $^{15}N_2$ tracer technique is more frequently used for oligotrophic bulk water incubations, with incubations ideally lasting 24 hours to cover one full day and night period. The cyclic behavior of the N_2 fixation activity in many diazotrophs prohibits an exact determination of the daily N_2 fixation rate in incubations lasting less than a day, unless the diazotrophic species composition is entirely determined.

1.2 The marine nitrogen cycle

Only the top 200 meters of the ocean, the euphotic zone, receive enough sunlight for phytoplankton to grow. Life in the on average 3600 meters below is fueled by the flux of organic material from above. The biological processes that dominate in the deep ocean are respiration and degradation of organic material (or biomineralization), resulting in the depletion of oxygen and the buildup of dissolved inorganic carbon (DIC, C), N and P. It is therefore not surprising that the relative abundances of C, N and P in the deep ocean reflect the composition of average phytoplankton biomass (C:N:P = 106:16:1, the Redfield ratio) (Redfield 1958).

While C, Fe and P are supplied to the surface ocean mainly from abiotic sources, both the sources and the sinks of N in the ocean are controlled by marine microbes. Therefore the N-cycle is believed to ultimately limit marine primary productivity (Falkowski 1997). Nitrate is the most abundant form of N in the ocean. With a few exceptions phy-

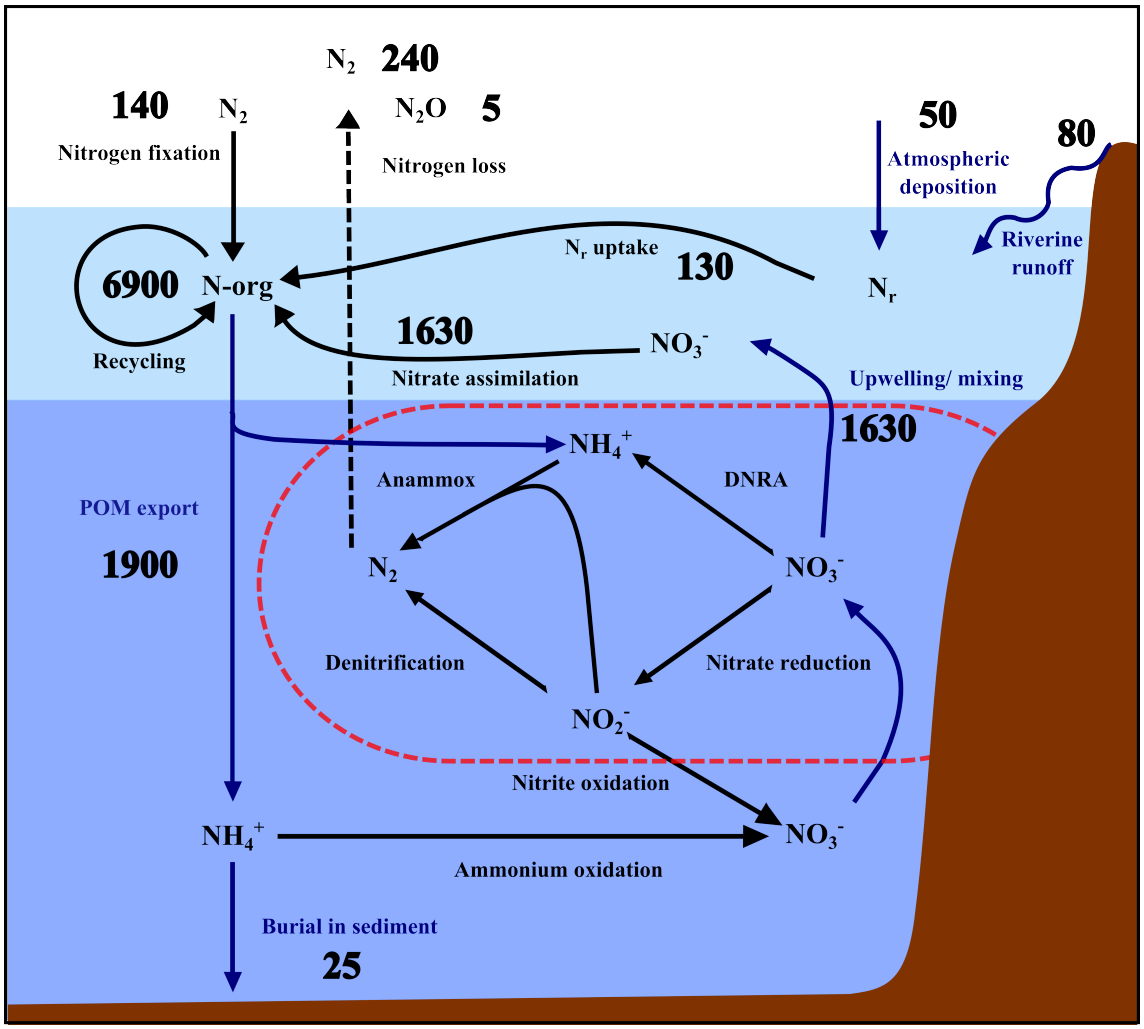

Figure 4: Schematic diagram of the marine N cycle. The energy consuming processes of N_2 fixation and nitrate assimilation dominate in the euphotic zone, while energy yielding N-conversions are dominant in the deep ocean. In areas of low oxygen concentration (red dashed line) the conversion of fixed N to N_2 gas is favored. Blue arrows are transport processes, black arrows are biological conversions. All numbers represent fluxes in Tg N yr^{-1}, adapted from (Duce *et al.* 2008) and (Gruber & Galloway 2008). The euphotic zone is indicated by light blue shading. DNRA, dissimilatory nitrate reduction to ammonium; anammox, anoxic ammonium oxidation, POM, particulate organic matter, N-org, organic nitrogen, N_r, reactive nitrogen (all non-gaseous N-compounds).

toplankton species are capable to assimilate nitrate by reducing it to ammonium which is further used to make amino acids. The phytoplankton biomass is either exported in form of particulate organic matter (POM) to the deep ocean, or it is degraded in the euphotic zone, whereby ammonium is liberated and fuels recycled production. After ammonium and nitrate, the most important N-source for phytoplankton is the fixation of N_2 (Karl *et al.* 2002). Since 80% of the earth's atmosphere is composed of N_2, the availability of N_2 gas should not be limiting. Rather the relatively high costs of N_2 fixation in the surface ocean restrict diazotrophs (N_2-fixers) mostly to areas where nitrate and ammonium concentrations are low. While nitrate and ammonium uptake and remineralization do not alter the total stock of N in the ocean, since one form of N is transformed into another, N_2 fixation presents a true input process of N to the oceans, besides riverine input, groundwater discharge or the deposition of N via rain or dust (Gruber & Galloway 2008). The ways that N can leave the ocean is by deposition into the sediments or by transformation of fixed N forms (nitrate, nitrite, and ammonium) into the gaseous N_2 form by denitrification and anammox (minor amounts are lost as N_2O and NO) (Kuypers *et al.* 2005, Duce *et al.* 2008, Ward *et al.* 2009). While denitrification, the reduction of nitrite to N_2 is (mostly) a heterotrophic process, the anammox reaction is performed by autotrophic anaerobic ammonium oxidizers with nitrite as oxidant (Lam & Kuypers 2011). Ammonium for the anammox reaction is supplied by remineralisation, dissimilatory nitrate reduction to ammonium (DNRA) and, possibly, via N_2 fixation, while nitrite is a product of heterotrophic nitrate reduction (Lam et al. 2009). Figure 4 displays the nitrogen cycle in the ocean with N-conversion flux estimates from the current literature. Most of these estimates have large error terms attached and while some authors produce a closed oceanic N-budget using an estimated N-loss of 245 Tg N yr^{-1} (Gruber & Sarmiento 1997, Gruber & Galloway 2008) others suggest a much higher N loss term of 450 Tg N yr^{-1}, therefore leaving a major gap on the N-input side (Galloway *et al.* 2004, Codispoti 2007). This gap, however, represents a gap in our knowledge about the N-cycle rather than a real gap between N-input and N-loss processes in the ocean, since such a difference in magnitudes of the two processes would lead to a net loss of fixed N from the ocean, which has not been observed in the recent history of the N-cycle as recorded in the sediments (Altabet 2007). On a local scale the two processes, N-loss and N-imput, can be out of balance, like e.g. in oxygen minimum zones, where the N-losses exceed the N-input processes and therefore the N:P ratio is lower than expected from Redfield stochiometry.

1.3 Oxygen minimum zones

The mixed layer of the ocean is almost always close to 100% oxygen saturation. The concentration of oxygen at equilibrium is a function of temperature and salinity and can

vary by about a factor of two in the surface ocean (Weiss 1970). Photosynthetic oxygen production and respiration can alter the concentration of oxygen in seawater, but as long as the water is in contact with the atmosphere, any deviation from the saturated state will be adjusted by air-sea gas exchange. Once the water sinks below the mixed layer and forms part of intermediate water masses or deep water, the oxygen concentration can only change through watermass mixing or biological activity (mainly respiration). Ventilation, the bulk transport of water masses, is the main route that brings new oxygen to the deep ocean. Areas with sluggish ventilation of deep water and increased respiration rates through remineralization of sinking organic material have lower concentrations of oxygen than the surrounding water masses and are called oxygen minimum zones (OMZ) (Wyrtki 1962). Such areas have developed at the eastern boundary of the Tropical Atlantic and Pacific Ocean basins, where the trade winds blow perpendicular to the coast and generate an offshore flow of surface water, which is replaced by cold subsurface water, a process called upwelling. The high primary productivity stimulated by the nutrient-rich deep water in turn results in increased export fluxes of organic material, which is remineralized in deeper waters, thereby lowering the concentration of dissolved oxygen there (Dugdale 1972). Therefore, the upwelling systems of the Peru-Humbold current in the South-Eastern and the California-current in the North-Eastern Pacific Ocean as well as the Canary-current in the North-Eastern and the Benguela-current in the South-Eastern Atlantic Ocean are areas of both very high productivity in surface and an oxygen minimum zone underneath (Carr & Kearns 2003). Additionally, the northern Indian Ocean is characterized by very low oxygen values in subsurface waters, due to low ventilation and monsoon driven upwelling (Morrison *et al.* 1999).

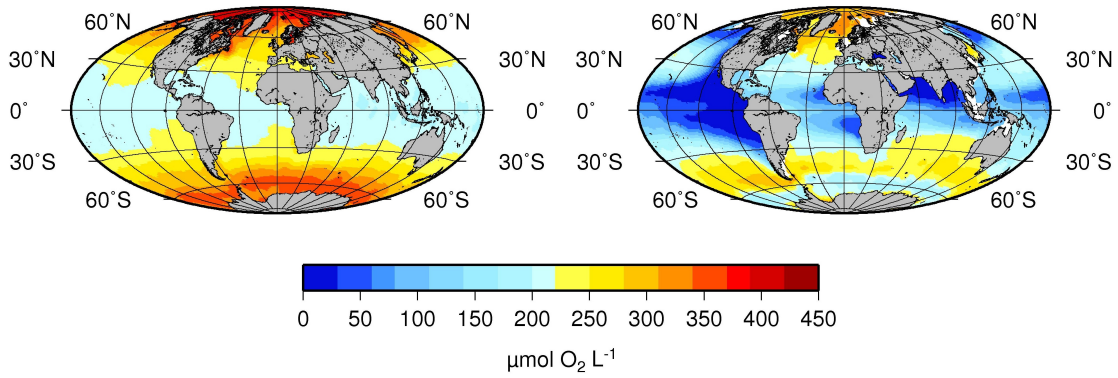

Figure 5: Oxygen concentration in the world's oceans at sea surface (left panel) and 400 m depth (right panel). Data from World Ocean Atlas 2009 (Garcia 2010).

About 7% of the total oceanic volume has an oxygen concentration of 20 µM or less, which is considered the OMZ core regions (Paulmier & Ruiz-Pino 2009). Over the last 50 years an ongoing deoxygenation and vertical growth of the main oxygen minimum zones in the Atlantic and Pacific Ocean has occurred (Stramma *et al.* 2008, Stramma *et al.*

2009). Anthropogenic climate change and increased usage of fertilizers and concomitant runoff of nutrients into the ocean has been shown to increase the number of coastal anoxic events as well as the volume of suboxic water in the tropical ocean (Diaz & Rosenberg 2008, Stramma *et al.* 2008). Although oxygen minimum zones only represent a minor fraction of the oceans water volume, they have the potential to impact global nutrient cycles far more than suggested by their extension, since unique biological and chemical reactions can happen under low oxgygen conditions. Many reactions in the N-cycle are sensitive to oxygen, like N_2 fixation or denitrification (Robson & Postgate 1980, Knowles 1982). Therefore oxygen minimum zones represent hotspot areas in the N-cycle, where the inventory of fixed N can be altered and the ratio of N:P may be significantly lower than the Redfield ratio (Zehr 2009). However, the N-loss within the core OMZ and the accumulation of phosphate in surface waters was hypothesized to stimulate N_2 fixation, which then would gradually resupply fixed N and remove the excess P (Deutsch *et al.* 2007).

1.4 Aim of this thesis

When I started my thesis in late 2008, little was known about the N_2 fixation in OMZs. The high productivity due to upwelling of nutrient rich waters, loaded with nitrate and sometimes nitrite and ammonium seemed an inappropriate habitat for organisms relying on the expensive acquisition of atmospheric N_2 as N source. However, a model study by Deutsch *et al.* from 2007 predicted that the bulk N_2 fixation in the ocean should happen in close proximity to the areas where N gets lost, hence the OMZs. At the same time the suggestion that the N-loss processes are of much greater magnitude than previously believed, the discovery of unicellular cyanobacteria with an important role in the marine N-cycle and the accumulation of literally thousands of different non-cyanobacterial *nifH* sequences from oceanic clone libraries led to the conclusion that the global magnitude of N_2 fixation is currently grossly underestimated. The aim at the beginning of my thesis was to evaluate if OMZs present a possible habitat for diazotrophs and if N_2 fixation is happening in or above OMZs. Further, it was a main interest to understand what kind of organisms inhabit this possible niche, how abundant they are and how they are distributed in the water column along gradients of biological, physical and chemical parameters. First, I derived a hypothesis from a laboratory experiment on the unicellar diazotrophic cyanobacterium *Crocosphaera watsonii*, predicting the occurrence of diazotrophs at low oxygen, even when nitrate concentrations are high (chapter 2.1). The second and third manuscripts of this thesis focus on the Peruvian upwelling system, which forms part of the largest OMZ in the world. The detection of high numbers of so far unknown heterotrophic diazotrophs and the fixation of high amounts of N_2 right in the OMZ core

area demonstrated that the theoretical foundations of my thesis were justified and lay the foundation for future in depth research on heterotrophic and other non-cyanobacterial diazotrophs in OMZs. The last chapter was nothing planned at the beginning of my thesis. It was a colleague, Wiebke Mohr, who came across a discrepancy between the N_2 fixation rates measured with the $^{15}N_2$-tracer assay in her *Crocosphaera watsonii* culture and the observed growth rates of the culture. I had previously detected that the acetylene reduction assay, a second method to measure N_2 fixation, potentially suffers from an incomplete equilibration between gas phase and liquid phase, when the ratio of gas to liquid phase is lower than 2:1 (vol:vol). We hypothesized that a similar effect could apply to the $^{15}N_2$-tracer method and explain the results on the *C. watsonii* culture experiment. In a first manuscript (chapter 2.4) we could show that the kinetic of equilibration between a $^{15}N_2$ gas bubble and the surrounding seawater was slower than the time of a typical incubation period of 24 hours, leading to a variable underestimation of measured N_2 fixation rates. In a second manuscript (chapter 2.5) we assessed the average magnitude of this effect on field samples from the Atlantic Ocean, which enabled us to extrapolate our findings over published values of N_2 fixation and to generate a revised global estimate of N_2 fixation, derived from direct measurements.

2 Results

2 Results

The following manuscripts form part of this thesis:

2.1 Bioenergetics of N_2 fixation

Großkopf, T., LaRoche, J. (2012) Direct and indirect costs of dinitrogen fixation in *Crocosphaera watsonii* WH8501 and possible implications for the nitrogen cycle Submitted to *Frontiers in Aquatic Microbiology*

Contribution: T.G. designed and performed the experiments, analyzed the data and wrote the manuscript. J.LR. helped with experimental design and analysis of the data and to improve the manuscript.

2.2 The Peruvian upwelling system

Großkopf, T., Löscher, C.R., Schunck, H., Lavik, G., Kuypers, M.M.M., Kolber, Z., Friedrich, G., Chavez, F., Schmitz, R.A., LaRoche, J. (2012) High coastal productivity drives Southern Peruvian upwelling system into N limitation. In preparation for submission.

Contribution: T.G., C.R.L., H.S. and J.LR. performed the experiments and collected the data. G.F. measured CO_2 concentrations and Fv/Fm values. T.G. measured the smamples, analyzed the data and wrote the manuscript. G.L., M.M.M.K., Z.K., G.F., F.C., R.A.S. and J.L.R. helped to analyze the data and to improve the manuscript.

2.3 Heterotropphic N_2 fixation in the Peruvian OMZ

Loescher, C.R., **Großkopf, T.**, Gill, D., Schunck, H., Pinnow, N., Desai, F., Lavik, G., Kuypers, M.M.M., LaRoche, J., Schmitz, R.A. (2012) Niche separation of novel groups of bacterial diazotrophs in the largest oxygen minimum zone of the world's ocean. In preparation for submission.

Contribution: C.R.L., T.G., H.S. and J.LR. collected the samples and performed the experiments. C.R.L. and D.G. did the extraction and qPCR of *nifH* DNA from transect stations. C.R.L., T.G.,N.P., F.D. and D.G. did cloning of *nifH* DNA and cDNA. T.G. and H.S. extracted DNA and RNA from experimental stations. T.G. and C.R.L. did qPCR with *nifH* DNA of experimental stations. T.G. performed flow cytometry measurements and analyzed the C and N fixation data. C.R.L wrote the manuscript with T.G., R.A.S. and J.LR.. M.M.M.K., G.L., R.A.S., J.LR., T.G. and C.R.L. designed the experiments and analyzed the data.

2.4 Underestimation of N_2 fixation

Mohr, W., **Grosskopf, T.**, Wallace, D. W. R. & LaRoche, J. Methodological Underestimation of Oceanic Nitrogen Fixation Rates. Plos One 5 (9), e12583. doi:10.1371/journal.pone. 0012583 (2010).

Contribution: W.M. designed the research, carried out the experiments and measurements, analyzed the data and wrote the manuscript. T.G., D.W.R.W. and J.L.R. assisted with the design and analysis of the data and commented on the prepared manuscript.

2.5 Closing the Gap

Großkopf, T., Mohr, W., Baustian, T., Schunck, H., Gill, D., Kuypers, M.M.M., Lavik, G., Schmitz, R.A., Wallace, D.W.R., LaRoche, J. (2012) Closing the gap - Doubling in global N_2 fixation rates by direct measurements. In review at *Nature*

Contribution: W.M. designed the dissolution method. T.G., T.B., H.S. and D.G. collected samples and performed nifH gene quantification, M.M.M.K. and G.L. did the measurements on the mass spectrometer. T.G. wrote the manuscript with W.M. and J.LR. M.M.M.K., G.L., R.A.S., D.W.R.W., J.L.R, W.M. and T.G. designed the experiments and analyzed the data.

Further contributions that do not form part of this thesis:

Schunck, H., Lavik, G., Desai, D.K., **Großkopf, T.**, Kalvelage, T., Löscher, C.R., Contreras, S., Paulmier, A., Mußman, M., Holtappels, M., Rosenstiel, P., Schillhabel, M., Graco, M., Siegel, H., Schmitz, R.A., Kuypers, M.M.M., LaRoche, J. (2012) Metatranscriptomic profiling of the (chemolithoautotrophic) microbial community active in sulfidic waters of the Peruvian oxygen minimum zone. In preparation for submission.

2.1 Bioenergetics of N_2 fixation

Direct and indirect costs of dinitrogen fixation in Crocosphaera watsonii WH8501 and possible implications for the nitrogen cycle

Tobias Großkopf and Julie LaRoche

Standard Text:	This Provisional PDF corresponds to the article as it appeared upon acceptance, after rigorous peer-review. Fully formatted PDF and full text (HTML) versions will be made available soon.
Journal Name:	Frontiers in Microbiology
ISSN:	1664-302X
Article type:	Original Research Article
Received on:	09 Mar 2012
Frontiers website link:	www.frontiersin.org

Direct and indirect costs of dinitrogen fixation in *Crocosphaera watsonii* WH8501 and possible implications for the nitrogen cycle

Running title: **OMZs present niches for diazotrophs**

Tobias Großkopf[*1] and Julie LaRoche[1]
[1] Helmholtz-Centre for Ocean Research Kiel (GEOMAR), Düsternbrooker Weg 20, 24105 Kiel, Germany

*Correspondence
Tobias Großkopf
Helmholtz-Centre for Ocean Research Kiel (GEOMAR)
Düsternbrooker Weg 20
24105 Kiel
Email: tgrosskopf@geomar.de

The recent detection of heterotrophic nitrogen (N_2) fixation in deep waters of the southern Californian and Peruvian OMZ questions our current understanding of marine N_2 fixation as a process confined to oligotrophic surface waters of the oceans. In experiments with *Crocosphaera watsonii* WH8501, a marine unicellular diazotrophic (N_2-fixing) cyanobacterium, we demonstrated that the presence of high nitrate concentrations (up to 800 µM) had no inhibitory effect on growth and N_2 fixation over a period of two weeks. In contrast, the environmental oxygen concentration significantly influenced rates of N_2 fixation and respiration, as well as carbon and nitrogen cellular content of *C. watsonii* over a 24 hour period. Cells grown under lowered oxygen atmosphere (5%) had a higher nitrogenase activity and respired less carbon during the dark cycle than under normal oxygen atmosphere (20%). Respiratory oxygen drawdown during the dark period could be fully explained (104%) by energetic needs due to basal metabolism and N_2 fixation at low oxygen, while at normal oxygen these two processes could only account for 40% of the measured respiration rate. Our results revealed that under normal oxygen concentration most of the energetic costs during N_2 fixation (~60%) are not derived from the process of N_2 fixation per se but rather from the indirect costs incurred for the removal of intracellular oxygen or by the reversal of oxidative damage (e.g. nitrogenase de novo synthesis). Theoretical calculations suggest a slight energetic advantage of N_2 fixation relative to assimilatory nitrate uptake for heterotrophic and phototrophic growth, when oxygen supply is in balance with the oxygen requirement for cellular respiration (i.e. energy generation for basal metabolism and N_2 fixation). Taken together our results imply the existence of a niche for diazotrophic organisms inside oxygen minimum zones, which are predicted to further expand in the future ocean.

Introduction

The classical view on marine N_2 fixation assumes that the preferred ecological niche of diazotrophs is largely limited to surface waters of oligotrophic areas, characteristically depleted of fixed N, saturated in dissolved oxygen and subjected to high light intensities (Howarth et al. 1988, Karl et al. 2002). However, recent surveys of the phylogenetic diversity and distributions of *nifH*, the functional gene marker for diazotrophy, demonstrated the presence of diazotrophs throughout all marine environments, ranging from deep-sea vents to highly productive shelf areas (Braun et al. 1999, Steppe & Paerl 2002, Mehta et al. 2003, Zehr et al. 2003, Church et al. 2005, Langlois et al. 2005, Farnelid et al. 2011, Fernandez et al. 2011, Hamersley et al. 2011). Furthermore, in the euphotic zone of the Atlantic and Pacific oceans N_2 fixation has been reported at high concentrations of ambient nitrate (Voss et al. 2004, Moisander et al. 2010, Sohm et al. 2011). Despite the broad diversity and distribution of diazotrophs, current research on oceanic N_2 fixation focuses mainly on a few groups of cyanobacteria inhabiting the mixed layer, mainly the upper 200 meters of the water column (Zehr et al. 2001, Voss et al. 2004, Staal et al. 2007a, Langlois et al. 2008, Zehr et al. 2008, Moisander et al. 2010, Monteiro et al. 2010).

The high energetic costs associated with the process of N_2 fixation has led to the general expectation that diazotrophs will be outcompeted by other microorganisms when nitrate is available. However, the costs of N_2 fixation have mainly three origins, which need to be treated separately in order to understand why diazotrophs are poor competitors in eutrophic surface ocean areas. There are the costs of daily synthesis and degradation of the nitogenase enzyme (Sherman et al. 1998, Taniuchi & Ohki 2007, Mohr et al. 2010), there are the direct costs, in form of ATP and low potential electrons, to fuel the actual N_2 fixation reaction (eq. 1) and there are the indirect costs due to the removal of oxygen from the cellular interior during the period of N_2 fixation.

Nitrogenase is highly sensitive to oxygen and is irreversibly inactivated on contact with molecular oxygen (Robson & Postgate 1980, Gallon & Hamadi 1984, Fay 1992, Karl et al. 2002). In well oxygenated waters, such as the euphotic zone of oligotrophic oceans, diazotrophs must overcome the problem of removing dissolved oxygen from the immediate surroundings of the nitrogenase enzyme, at least during the period of active N_2 fixation (Robson & Postgate 1980, Gallon & Hamadi 1984, Fay 1992). For diazotrophic cyanobacteria not only the oxygen in the surrounding water becomes a problem, but also the oxygen generated by photosynthesis, since so far all cyanobacteria, with the exception of UCYN-A carry out oxygen-evolving photosynthesis (Bergman et al. 1997, Berman-Frank et al. 2003, Zehr et al. 2008, Tripp et al. 2010). Several strategies are employed by cyanobacteria to avoid oxidative damage during N_2 fixation and all can be summarized as temporal or spatial separation of N_2 fixation and photosynthetic oxygen evolution (Berman-Frank et al. 2001, Berman-Frank et al. 2003). Heterocystous filamentous cyanobacteria have developed specialized cells, called heterocysts where N_2 fixation takes place. These cells lack oxygenic photosystem II and have a thick glycolipid layer that decreases diffusion of oxygen into the cell. They represent the classical example of spatial separation of N_2 fixation and photosynthesis in an aerobic environment. Heterocysts rely on reduced carbon compounds from neighboring cells as energy source and donate amino acids in exchange (Staal et al. 2003, Milligan et al. 2007). The costs for the removal of oxygen in heterocystous cyanobacteria are represented by the excess energy invested into producing a thick glycolipid

layer to envelop the heterocysts. The unicellular diazotrophic cyanobacteria, which carry out photosynthesis and N_2 fixation within the same cell, are at the other end of the spectrum. Most have developed a strategy of temporal separation, with oxygenic photosynthesis and carbon fixation during the light period and N_2 fixation during the dark period when no oxygen evolution takes place (Mitsui et al. 1986, Sherman et al. 1998, Stoeckel et al. 2008, Toepel et al. 2008, Mohr et al. 2010, Shi et al. 2010). There are two theories of how unicellular diazotrophs overcome damage by oxygen: A strategy termed 'respiratory protection', consisting of increased respiration rates during the dark period, insures the removal of residual intracellular oxygen, thereby providing an anoxic environment for the nitrogenase enzyme to function properly (Peschek et al. 1991, Bergman et al. 1993). In the diazotrophic proteobacterium *Azotobacter vinelandii* an uncoupled cytochrome *bd* oxidase, that lacks the proton pumping activity and hence does not participate in energy production is active at elevated oxygen pressures (Poole & Hill 1997). The alternative route for respiratory electrons towards a high affinity, low energy conserving oxidase acts like a relief valve during N_2 fixation at high oxygen concentrations (Robson & Postgate 1980). In cyanobacteria, genetic evidence points towards branched respiratory chains, with the possible involvement of uncoupled terminal oxidases like those in *Azotobacter*, but so far their activity has not been observed in vivo (Peschek et al. 1991, Peschek et al. 2004, Hart et al. 2005, Paumann et al. 2005). The second strategy, termed autoprotection, implies that oxygen is permitted to diffuse into the cell but is removed by reduction through the nitrogenase enzyme itself, therefore competing with respiration and N_2 fixation for electrons derived from storage carbohydrates (Oelze 2000).

Both the respiratory protection and autoprotection mechanisms use electrons to reduce oxygen, either at the cell membrane or by the enzyme itself. Regardless of which strategy may be used by unicellular diazotrophic cyanobacteria, they present good model organisms to monitor the costs of N_2 fixation, since the electrons used to reduce oxygen to water stem from reduced carbohydrates, buildup through photosynthesis during the daily light phase and thus can be monitored by the cellular carbon quota. We conducted laboratory experiments exposing cultures of *C. watsonii* WH8501, a unicellular diazotrophic cyanobacterium of approx. 2.5- 3 µm in diameter, to normal (20%) and low (5%) oxygen concentrations, measuring key physiological parameters over a 24 hour period to establish an energetic budget of N_2 fixing cells. Further, we calculated the direct costs of N_2 fixation and compared them with the costs of NO_3^- assimilation, the major competing nitrogen uptake process in the marine environment. We used the model organism *C. watsonii* to differentiate between the direct costs of N_2 fixation, arising from the enzymatic reaction and the indirect costs arising from the combined removal of oxygen from the cellular interior and the repair of the nitrogenase due to oxidative damage. We found that this differentiation of the costs associated with N_2 fixation is crucial when trying to understand how diazotrophs will compete along a vertical gradient in the ocean, when oxygen concentrations decrease but at the same time the availability of nitrate increases.

Material and methods

Culturing

All cultures of *Crocosphaera watsonii* WH8501 (Waterbury & Willey 1988) were grown in YBCII Medium (Chen et al. 1996) at 28°C and 150 µmol Photons x m^{-2} x s^{-1} white illumination on a 12/12 light/dark cycle. Cultures where maintained in exponential growth phase and adapted to experimental conditions eight days prior to the experiment. Subculturing

was done in the exponential growth phase and 1/10 of the stock was used as inoculum. Cultures were held in one liter Schott Duran glass bottles with magnetic stirrers at medium stirring speed to prevent sedimentation of cells during the experiment and bubbled with sterile filtered air (referred to as normal oxygen) or with a 94.962 % N_2, 5% oxygen and 0.038% CO_2 mixture (referred to as low oxygen) (BASI-GASE). Daily cell counts where performed in a counting chamber (Neubauer improved) under the microscope. For the experiments, triplicate cultures were incubated under one given experimental condition (low or normal oxygen) and all parameters were measured every three hours during a 24 hour day cycle (L1, L2, L3, L4 are 0, 3, 6, and 9 hours after the beginning of the light phase. L5/D1 is the beginning of the dark phase and D2, D3, D4 and D5 are 3, 6, 9 and 12 hours into the dark phase, respectively). Linear regression analysis for growth rates of the nitrate experiment was performed with the statistics package of SigmaPlot (SYSTAT SOFTWARE).

Oxygen measurements

Measurements of oxygen consumption and production where done in triplicates with an Oxytherm (Hansatech) Clark-type electrode unit with temperature stabilizer. Aliquots of 25 mL culture were centrifuged in a Beckman Avanti J-25 centrifuge at 4000 g for 6 minutes. The pellet was resuspended in 2.5 mL of fresh YBCII medium. Two mL of this concentrated culture were placed in the cuvette of the oxygen electrode and the oxygen level was set to the approximate incubation level by gently bubbling with N_2 gas or compressed air. After 10 minutes of initial dark adjustment the light was turned on three times at 150 $\mu mol\ Photons\ x\ m^{-2}\ x\ s^{-1}$ for five minutes with five minute dark intervals in between. Since the oxygen evolution and consumption rates showed an adaptive feature after switching the light that lasted for 1-2 minutes, rates for photosynthesis and respiration were calculated from the last three minutes of the light and dark phases respectively, using the Oxygraph software (Hansatech) and normalized to cell numbers.

Acetylene reduction measurements

Duplicate 2 ml culture aliquots were pipetted into 8.5 ml glass vials and sealed gas tight with a crimp cap containing a butyl rubber septum. Two vials containing sterile YBCII medium served as controls. The vials and medium were flushed with the appropriate gas mixture (5% or 20% Oxygen) for 60 seconds injected through a syringe needle. A second syringe needle served to release the pressure from the vial. Next, 650 µl acetylene were added to all vials with a gastight syringe (HAMILTON). Samples and controls were then incubated for two hours at the corresponding temperature and light regime on a shaker (Wt 17; BIOMETRA). After the incubation period 250 µl of headspace gas from each vial were injected into a gas chromatograph (SHIMADZU GC-14B) equipped with a flame ionization detector. The area of the ethylene peak was converted to ppm with a calibration curve obtained by injecting 250 µl of 1, 10, 100, and 1000 ppm pure ethylene standards (Capone 1993, Breitbarth et al. 2004).

Particulate Organic Carbon/ Particulate Organic Nitrogen (POC/PON)

Duplicates of 20 ml culture were filtered onto precombusted (12 hours, 450°C) GF/F filters (WHATMAN). Filters were frozen and stored at -20°C until measurement. Blank filters served as control. Before measuring the nitrogen and carbon content, filters were placed over fuming HCl for 8 hours and left to dry overnight at 60°C to remove remaining liquids and inorganic carbon. Filters were folded, rolled and packed tightly in a tin cup which was then combusted in a gas chromatograph (Elemental Analyzer, EUROVECTOR).

Results

Acetylene reduction, nitrogen fixation and growth

The exponential growth rates established by cell counts during the course of the experiment were 0.28 +/- 0.05 and 0.28 +/- 0.02 for the low and normal oxygen treatments respectively. Although no differences in growth rates were observed between the low and normal oxygen treatments, other biochemical pathways showed distinct activity patterns during the diel cycle as a function of oxygen concentration. In cultures grown under a 12/12 light/dark cycle, acetylene reduction (AR) activity in *C. watsonii* began in the early dark phase, peaked around the middle of the dark phase and returned below the detection limit in the early light phase. At normal oxygen levels, peak rates of AR were reached six hours after the beginning of the dark phase (D3) with 2.14 +/- 0.34 fmol C_2H_2 $cell^{-1}$ h^{-1}. Under low oxygen conditions, peak rates were slightly but not significantly higher (2.48 +/- 0.46 fmol C_2H_2 $cell^{-1}$ h^{-1}) but the AR activity started around three hours earlier (D2) (Fig. 1). When cells grown at low oxygen were exposed to normal oxygen concentrations at the middle of the night phase (D3) they showed decreased AR rates, while cells acclimated to normal oxygen but bubbled with low oxygen immediately prior to AR rate measurements showed no change in their AR rate (Fig.2). This indicates that the nitrogenase activity is not limited by oxygen availability down to at least 5% ambient oxygen concentration. On the other hand a short-term increase in oxygen above the acclimated level led to an inhibition of the nitrogenase activity, possibly via the competition for electrons with respiration or the direct damage and inactivation of the enzyme from the contact with oxygen.

Oxygen evolution and consumption

The rates of net oxygen evolution (light phase) and consumption (dark phase) were integrated over the corresponding 12h period and the results summarized in Table 1. Photosynthetic oxygen evolution peaked during the light phase and was higher in the normal oxygen compared to low oxygen treatment (13.1 +/- 2.3 fmol $cell^{-1}$ h^{-1} and 10.2 +/- 0.2 fmol $cell^{-1}$ h^{-1} for normal and low oxygen respectively), although the 12 hour integrated photosynthesis rate and total carbon buildup during the light phase showed no significant differences (Fig. 3, Table 1). The minimum in oxygen evolution was observed in both treatments in the middle of the dark phase (1.4 +/- 0.4 fmol $cell^{-1}$ h^{-1} and 1.3 +/- 1.6 fmol $cell^{-1}$ h^{-1} for normal and low oxygen respectively) (Fig. 3). The reduced capacity for oxygen evolution in the dark was paralleled by a decrease in Fv/Fm ratio that reached near zero values during the dark phase (data not shown). In contrast, the respiration rates peaked around six hours after beginning of the dark phase (D3) and thus mirrored the AR activity. Under normal oxygen concentrations, the respiration rate in the dark increased by over a factor of ten compared to background levels in the light phase (0.8 +/- 1.4 fmol $cell^{-1}$ h^{-1} at L3 and 11.3 +/- 0.8 fmol $cell^{-1}$ h^{-1} at D3 respectively). The respiration rates during the dark phase were significantly lower in the low oxygen growth conditions compared to the normal oxygen conditions and only reached peak values of 4.1 +/- 0.5 fmol $cell^{-1}$ h^{-1}, although the background respiration rates during the light phase were comparable to those of the normal oxygen grown cultures (1.3 +/- 0.4 fmol $cell^{-1}$ h^{-1} at L3) (Fig. 3).

Carbon and nitrogen content

The cellular carbon content increased during the light phase at comparable rates in both normal and low oxygen cultures. During the dark phase a significant decrease of cellular carbon content could only be measured in the culture grown under normal oxygen conditions,

where about 30% of the cellular carbon levels at the end of the light phase were consumed again during the dark phase (Fig. 4A). The cellular nitrogen content increased throughout the whole dark phase (D1-D5) in the low oxygen treatments, while at normal oxygen concentrations the cellular nitrogen content only increased between 3 to 9 hours after the beginning of the dark phase (Fig. 4B). At the end of the dark phase both treatments reached a cellular nitrogen level of around 150% of the level at the end of the light phase (L5/D1), thus fixing all nitrogen needed for a cell doubling in two consecutive nights. The molar C:N ratio in the low oxygen treatment decreased from the peak value of 9.7 +/- 0.7 at D1 to 6 +/- 0.6 at D5 over the course of the dark phase. In the normal oxygen treatment the decrease in the C:N ratio was more pronounced, due to the higher respiration and carbon drawdown rate. The value dropped from 10.5 +/- 0.8 at D1 to 5.1 +/- 0.1 at D5 (Fig. 4C). In both the low and the normal oxygen treatment, the buildup of carbon during the day matched quite closely with the photosynthetic oxygen evolution integrated over the light cycle. However, the observed drawdown of carbon from D1 to D5 did not match the respiration rate integrated over the dark period. The difference between carbon drawdown and respiratory oxygen consumption had the same magnitude in both treatments, although the oxygen consumption and the cellular carbon drawdown differed by a factor of 2.7 and 6.4 between the treatments, respectively (Table 1). If carbon fixation continued during the dark, this would have masked the drawdown of storage carbohydrates. One enzyme that performs carbon fixation without consuming electrons is for example the phosphoenolpyruvate carboxylase (EC 4.1.1.31, Gene bank accession: ZP_00517310) that produces oxaloacetic acid from phosphoenolpyruvate and CO_2 consuming ATP. Oxaloacetic acid is an important precursor of many amino acids, so the phosphoenolpyruvate carboxylase could be used to produce carbon skeletons for N_2 fixation in the dark. The electron imbalance could also arise from compounds in the cell other than carbon serving as electron donors or by a partial oxidation of carbon compounds without releasing them from the cell.

Energy utilization during N_2 fixation

The moles of oxygen (O_2) consumed per mol of nitrogen (N) fixed were 9.3:1 and 3.2:1 at normal and low oxygen respectively (Table 1). Using an ATP production of 4.28 mol ATP per mole of oxygen respired (Raven 2009), the observed oxygen drawdown during the dark phase can be converted to 40 and 14 mol ATP per mol of nitrogen (N) fixed at normal and low oxygen, respectively. Table 1 sums up the cellular budget of oxygen, nitrogen and carbon during the light and dark cycle for low and normal oxygen. According to eq. 1, 8 mol ATP are needed for the direct reduction of 0.5 mol N_2 to ammonium, so the nitrogenase enzyme reaction consumes 20% and 57% of the cellular energy produced in the dark at normal and low oxygen respectively. If a respiration rate of 1.5 fmol O_2 $cell^{-1}$ h^{-1} is assumed to meet the energetic demands of the basal metabolism (~ background respiration at L3), 17.6% and 47% of the oxygen consumption during the dark phase can be accounted for at normal and low oxygen, respectively. Therefore, at low oxygen conditions the observed oxygen drawdown matches the calculated expenses of the cell (104%), whereas about 60% of the observed oxygen consumption at normal oxygen conditions appears in excess of the combined needs for N_2 fixation and the basal metabolism. We assumed that the excess respiration represents the percentage of respiration invested into protection of the nitrogenase enzyme, either in the form of intracellular oxygen removal or energy necessary to repair the nitrogenase enzyme after oxidative damage.

Growth on nitrate

To test the growth rate of *Crocosphaera* in the presence of nitrate, we grew batch cultures in YBCII medium amended with 25, 50, 100, 500 and 800 µM nitrate and an unamended control. There was no effect of nitrate concentration detectable on the growth rate (linear regression analysis of growth rate versus nitrate concentration, slope not significantly different from 0, p = 0.6806). Cell numbers increased at the same rate over the course of 14 days in all five treatments and the control. Nitrogenase activity measured by acetylene reduction did not show a decrease under elevated levels of nitrate at day four after amendment with nitrate. Growth rates and acetylene reduction rates decrease with time (e.g. day 11 vs day 4), but trends were identical for all of the treatments (Fig. 5). Hence, it seems *Crocosphaera* behaves indifferently towards nitrate, and is neither inhibited nor stimulated by its presence in the culture media. Although nitrate was shown to inhibit the nitrogenase activity in the filamentous cyanobacteria *Anabaena* and *Trichodesmium* (Ramos & Guerrero 1983, Mulholland et al. 2001) our results are in agreement with recent experiments on the utilization of nitrate by *Crocosphaera*, that showed no reduction in the N_2 fixation activity after additions of up to 10 µM nitrate (Dekaezemacker & Bonnet 2011).

Costs of N_2 fixation compared to assimilatory nitrate reduction

The net reaction for N_2 fixation is

$$N_2 + 8H^+ + 8Fd_{red} + 16ATP = 2NH_3 + 16ADP + 16P_i + 8Fd_{ox} + H_2 \quad (1)$$

With Fd_{red} and Fd_{ox}, representing reduced and oxidized ferredoxin, respectively and P_i, inorganic phosphate. It has been shown that diazotrophic cyanobacteria can recycle the two electrons from hydrogen with high efficiency through an uptake hydrogenase that uses ferredoxin as an electron acceptor (Robson & Postgate 1980, Wilson et al. 2010), reducing eq. 1 to 3 mol electrons (from reduced ferredoxin) and 8 mol ATP needed to convert half a mol of N_2 into one mol of NH_3. Assimilatory NO_3^- reduction requires 8 mol electrons to reduce NO_3^- to NH_3 and one mol of ATP to get NO_3^- into the cell per mol NH_3 produced if an ATP-hydrolyzing NO_3^- transporter is used (Herrero et al. 2001). Taking carbohydrates (e.g. glucose) as a common currency for both electrons and ATP sources, we can calculate the electrons and ATP requirements of both N_2 fixation and assimilatory NO_3^- reduction in terms of carbohydrate units. Table 2 summarizes the costs to produce one mol of NH_3 using carbohydrate compounds as energy and electron donors. The calculations are made on the assumptions that one mole of glucose generates either 36 mol ATP via glycolysis and oxidative phosphorylation or 24 mol electrons. Some authors suggest a value of 30 mol ATP per mol glucose respired is reasonable (Raven 2009), others quote 36 mol for mitochondria and heterotrophic bacteria (Martin & Muller 1998). Figure 6 shows how the carbohydrate demand for N_2 fixation and assimilatory nitrate reduction behaves over a range of theoretical ATP per glucose production rates from 30 to 38 (mol mol^{-1}). Under the given conditions, the amount of energy generated by respiration is crucial in determining which N assimilation strategy is energetically more favorable, since it represents the converting agent of electrons into ATP. N_2 fixation consumes more ATP, assimilatory nitrate reduction more low potential electrons. The higher the ATP yield per electron, the more favorable will the conditions be towards N_2 fixation. The costs of N_2 fixation are on a par with NO_3^- assimilation at higher yields of ATP per mol glucose and could even be considered to show a slight advantage in terms of lower carbohydrate consumption per mol of NH_3 assimilated, depending on the ATP production per mol of glucose respired (the efficiency of the respiratory energy conversion) (Figure 6). In phototrophic organisms, the assimilatory reduction of nitrate is mediated by electrons coming directly from photosynthesis. These electrons on the other hand could be invested into carbon fixation, if not used for nitrate reduction. Therefore, in theory, it makes no difference, if the cell reduces CO_2 to sugar with light energy and later uses the reduced

carbon compounds to reduce nitrogen, or reduces nitrogen directly with light energy. In practice however, during every chemical conversion some of the energy is lost in form of heat. Therefore the indirect reduction of nitrogen via reduced carbohydrates should have a certain penalty attached. This specifically applies to unicellular phototrophic diazotrophs fixing N_2 during the dark period, like *C. watsonii*. Other cyanobacteria, like the UCYN-A, capable of fixing N_2 during the light period, could also directly use electrons from photosynthetic light reactions (Needoba et al. 2007, Tripp et al. 2010).

Discussion

The fact that diazotrophs need to protect the nitrogenase against high oxygen concentrations is well-known, consequently diazotrophs should thrive at low oxygen levels (Robson & Postgate 1980, Fay 1992, Staal et al. 2007b, Compaore & Stal 2010). However, deeper layers of the ocean often hold substantially higher nitrate concentrations, presenting an N source alternative to N_2 fixation. Although the direct energetic costs of N_2 reduction to ammonium via nitrogenase are explicit and remain constant regardless of the environmental conditions, the costs associated with oxygen removal in diazotrophic cyanobacteria will vary with the dissolved oxygen concentration present in their habitat. Our results indicate that oxygen removal must be by far the largest energy sink in the daily life of a unicellular cyanobacterial diazotroph inhabiting fully oxygenated surface waters. The electrons from reduced carbon compounds serve a double function: They are used to reduce N_2 to ammonium by the nitrogenase enzyme and they are channeled through the respiratory chain to generate energy in form of ATP. Thereby oxygen, the final electron acceptor in respiration, gets reduced to water. However, if the diffusion of oxygen into a *C. watsonii* cell is in excess of the respiratory demand, respiration has to increase along with the oxygen concentration of the environment to prevent oxidative damage of the nitrogenase enzymes thereby creating an extra sink for electrons from storage carbohydrates. This generates a futile cycle consisting of an excess synthesis of carbohydrates during the light period needed to provide the reducing potential during the dark period to remove oxygen and protect nitrogenase. Very low oxygen concentrations will inhibit N_2 fixation due to energy limitation (shortage of ATP production), while high oxygen concentrations necessitate an investment of extra energy into a protective mechanism. Between the two extremes is a narrow optimum, where oxygen is supplied at a concentration that meets, but does not exceed, the cellular energy demands thus circumventing the need to protect the nitrogenase against irreversible oxidative damage. This optimum will vary with the size and metabolic activity of the organism, with temperature, salinity and energy supply (i.e. light regime in the case of *C. watsonii*), since all these parameters determine either the diffusion of oxygen into the cell or the oxygen demand by cellular respiration. During our experiment, the oxygen concentration of 5% oxygen (~50 µmol L^{-1}) could be considered close to the optimum for *C.watsonii*, since 104% of the observed respiration could be accounted for by energetic needs of basal metabolism or N_2 fixation.

Our results obtained with *C. watsonii* suggest that for diazotrophs inhabiting the oxygenated surface waters of the ocean the removal of oxygen at night to a level suitable for N_2 fixation represents the largest expenditure in the energetic budget of the cells, exceeding the cost of the enzymatice reduction of N_2 to ammonium. This extra energy expenditure to generate intracellular anaerobiosis in an aerobic environment likely contributes to the confinement of diazotrophs mostly to areas where fixed N compounds are scarce. The niche of surface ocean diazotrophs is therefore characterized by oligotrophy, or more specifically N-limitation. In

these regions elevated costs associated with N-acquisition (N_2 fixation) are not a disadvantage, simply because there is no competing option available.

We propose here that a second niche possibly exists for unicellular diazotrophs, when N_2 fixation reaches its energetic optimum at low oxygen concentrations. When omitting the additional costs arising from oxygen removal to protect the oxygen-labile nitrogenase, assimilatory NO_3^- reduction and N_2 fixation come in very close proximity in terms of energetic investment. Although several assumptions are necessary to calculate the energetic requirements, our calculations suggest that N_2 fixation is as effective or slightly more effective then NO_3^- uptake from a purely bioenergetics point of view, thus making N_2 fixation a competitive lifestyle strategy even in the presence of high NO_3^- concentrations. Hence, environments with low dissolved oxygen concentrations where diazotrophs do not need to expand extra energy for the removal of excess oxygen can be considered optimal from the point of view of N_2 fixation. The oxycline of an OMZ represents a gradient, where oxygen concentrations in some case range from fully saturated to zero or close to zero oxygen values. Along such a gradient, for any given diazotroph, there will be an oxygen concentration where the diffusion of oxygen into the cell meets the energetic demand of the diazotroph without creating an additional energy sink. Similar situations can be observed for rhizobia in a nodule of their host plant, in which the diazotroph will be supplied with just the right amount of oxygen necessary to meet the energetic demands of the N_2 fixation reaction (Long 1989). Unlike the situation for rhizobia, where the energy needed to reduce the oxygen concentration is supplied by the host plant (i.e. by the synthesis of leghaemoglobins), an OMZ presents a situation where the oxygen concentration is reduced without any metabolic costs to the diazotroph or a possible symbiont. In the upper oxycline of the large OMZs, light availability can overlap with low oxygen and high nitrate concentrations (Figure 7), highlighting possible areas of where phototrophic diazotrophs could grow competitively. Although these areas that would favor photosynthetic diazotrophs are currently limited, predicted future shoaling and expanse of the OMZs (Stramma et al. 2009) may also lead to an increase in this additional niche for diazotrophs. In addition to the oxycline of OMZs, such environments could develop at the surface of particles and aggregates where high community respiration rates may prevail (Paerl et al. 1995).

Furthermore, heterotrophs, living on energy sources low in ammonium compared to carbon (organic material with high C:N ratio) need extra N-sources to meet their nitrogen demand. Such organisms could assimilate nitrate or, if the oxygen concentration is lowered to an optimum level, fix N_2 despite high nitrate concentrations. We would therefore expect heterotrophic diazotrophy in oxygen minimum zones to be mostly depend on the C:N ratio of the energy supply, rather than on the DIN:DIP (dissolved inorganic nitrogen, dissolved inorganic phosphorous) ratio, like the diazotrophy of the surface oceans (Deutsch et al. 2007). The C:N ratio of phytoplankton primary production has been shown to increase with increasing atmospheric CO_2 concentrations (Riebesell et al. 2007). Increased carbon export and decreased oxygen concentrations (Oschlies et al. 2008) could trigger an increase in heterotrophic N_2 fixation in the oxygen minimum zones of the future.

Acknowledgements

We would like to thank Diana Gill, Tania Klüver, Steffani Sudhaus, Harald Schunck and Sebastian Krossa for their help with the experimental work and Kerstin Nachtigall for measurements on the elemental analyzer. We would also like to thank Professor John Raven

and Dr. Wiebke Mohr for critically reading the manuscript. We would like to thank the Bundesministerium für Bildung und Forschung (BMBF) for financial support through the SOPRAN II (Surface Ocean Processes in the Anthropocene) project. This work is a contribution of the Sonderforschungsbereich 754 "Climate - Biogeochemistry Interactions in the Tropical Ocean" (www.sfb754.de) which is supported by the Deutsche Forschungsgemeinschaft.

References

Bergman B, Gallon JR, Rai AN, Stal LJ (1997). N-2 fixation by non-heterocystous cyanobacteria. *Fems Microbiology Reviews*, 19:139-185

Bergman B, Siddiqui PJA, Carpenter EJ, Peschek GA (1993). Cytochrome-Oxidase - Subcellular-Distribution and Relationship to Nitrogenase Expression in the Nonheterocystous Marine Cyanobacterium Trichodesmium-Thiebautii. *Applied and Environmental Microbiology*, 59:3239-3244

Berman-Frank I, Lundgren P, Chen YB, Kupper H, Kolber Z, Bergman B, Falkowski P (2001). Segregation of nitrogen fixation and oxygenic photosynthesis in the marine cyanobacterium Trichodesmium. *Science*, 294:1534-1537

Berman-Frank I, Lundgren P, Falkowski P (2003). Nitrogen fixation and photosynthetic oxygen evolution in cyanobacteria. *Research in Microbiology*, 154:157-164

Braun ST, Proctor LM, Zani S, Mellon MT, Zehr JP (1999). Molecular evidence for zooplankton-associated nitrogen-fixing anaerobes based on amplification of the nifH gene. *Fems Microbiology Ecology*, 28:273-279

Breitbarth E, Mills MM, Friedrichs G, LaRoche J (2004). The Bunsen gas solubility coefficient of ethylene as a function of temperature and salinity and its importance for nitrogen fixation assays. *Limnology and Oceanography-Methods*, 2:282-288

Capone DG (1993). Determination of nitrogenase activity in aquatic samples using the acetylene reduction procedure. *E.B. Sherr [ed.] Handbook of methods in aquatic microbial ecology, Lewis*:621-631

Chen YB, Zehr JP, Mellon M (1996). Growth and nitrogen fixation of the diazotrophic filamentous nonheterocystous cyanobacterium Trichodesmium sp IMS 101 in defined media: Evidence for a circadian rhythm. *Journal of Phycology*, 32:916-923

Church MJ, Short CM, Jenkins BD, Karl DM, Zehr JP (2005). Temporal patterns of nitrogenase gene (nifH) expression in the oligotrophic North Pacific Ocean. *Applied and Environmental Microbiology*, 71:5362-5370

Compaore J, Stal LJ (2010). Effect of Temperature on the Sensitivity of Nitrogenase to Oxygen in Two Heterocystous Cyanobacteria. *Journal of Phycology*, 46:1172-1179

Dekaezemacker J, Bonnet S (2011). Sensitivity of N(2) fixation to combined nitrogen forms (NO(3)(-) and NH(4)(+)) in two strains of the marine diazotroph Crocosphaera watsonii (Cyanobacteria). *Marine Ecology-Progress Series*, 438:33-46

Deutsch C, Sarmiento JL, Sigman DM, Gruber N, Dunne JP (2007). Spatial coupling of nitrogen inputs and losses in the ocean. *Nature*, 445:163-167

Farnelid H, Andersson AF, Bertilsson S, Abu Al-Soud W, Hansen LH, Sorensen S, Steward GF, Hagstrom A, Riemann L (2011). Nitrogenase Gene Amplicons from Global Marine Surface Waters Are Dominated by Genes of Non-Cyanobacteria. *Plos One*, 6

Fay P (1992). Oxygen Relations of Nitrogen-Fixation in Cyanobacteria. *Microbiological Reviews*, 56:340-373

Fernandez C, Farias L, Ulloa O (2011). Nitrogen Fixation in Denitrified Marine Waters. *Plos One*, 6(6): e20539

Gallon JR, Hamadi AF (1984). Studies on the Effects of Oxygen on Acetylene-Reduction (Nitrogen-Fixation) in Gloeothece Sp Atcc27152. *Journal of General Microbiology*, 130:495-503

Garcia HE, R. A. Locarnini, T. P. Boyer, J. I. Antonov, O. K. Baranova, M. M. Zweng, and D. R. Johnson (2010). World Ocean Atlas 2009, Volume 3: Dissolved Oxygen, Apparent Oxygen Utilization, and Oxygen Saturation. *S. Levitus, Ed. NOAA Atlas NESDIS 70, U.S. Government Printing Office, Washington, D.C., 344 pp.* ,

Hamersley MR, Turk KA, Leinweber A, Gruber N, Zehr JP, Gunderson T, Capone DG (2011). Nitrogen fixation within the water column associated with two hypoxic basins in the Southern California Bight. *Aquatic Microbial Ecology*, 63:193-+

Hart SE, Schlarb-Ridley BG, Bendall DS, Howe CJ (2005). Terminal oxidases of cyanobacteria. *Biochemical Society Transactions*, 33:832-835

Herrero A, Muro-Pastor AM, Flores E (2001). Nitrogen control in cyanobacteria. *Journal of Bacteriology*, 183:411-425

Howarth RW, Marino R, Cole JJ (1988). Nitrogen-Fixation in Fresh-Water, Estuarine, and Marine Ecosystems .2. Biogeochemical Controls. *Limnology and Oceanography*, 33:688-701

Karl D, Michaels A, Bergman B, Capone D, Carpenter E, Letelier R, Lipschultz F, Paerl H, Sigman D, Stal L (2002). Dinitrogen fixation in the world's oceans. *Biogeochemistry*, 57:47-+

Langlois RJ, Hummer D, LaRoche J (2008). Abundances and distributions of the dominant nifH phylotypes in the Northern Atlantic Ocean. *Applied and Environmental Microbiology*, 74:1922-1931

Langlois RJ, LaRoche J, Raab PA (2005). Diazotrophic diversity and distribution in the tropical and subtropical Atlantic ocean. *Applied and Environmental Microbiology*, 71:7910-7919

Long SR (1989). Rhizobium-Legume Nodulation - Life Together in the Underground. *Cell*, 56:203-214

Martin W, Muller M (1998). The hydrogen hypothesis for the first eukaryote. *Nature*, 392:37-41

Mehta MP, Butterfield DA, Baross JA (2003). Phylogenetic diversity of nitrogenase (nifH) genes in deep-sea and hydrothermal vent environments of the Juan de Fuca ridge. *Applied and Environmental Microbiology*, 69:960-970

Milligan AJ, Berman-Frank I, Gerchman Y, Dismukes GC, Falkowski PG (2007). Light-dependent oxygen consumption in nitrogen-fixing cyanobacteria plays a key role in nitrogenase protection. *Journal of Phycology*, 43:845-852

Mitsui A, Kumazawa S, Takahashi A, Ikemoto H, Cao S, Arai T (1986). Strategy by Which Nitrogen-Fixing Unicellular Cyanobacteria Grow Photoautotrophically. *Nature*, 323:720-722

Mohr W, Intermaggio MP, LaRoche J (2010). Diel rhythm of nitrogen and carbon metabolism in the unicellular, diazotrophic cyanobacterium Crocosphaera watsonii WH8501. *Environmental Microbiology*, 12:412-421

Moisander PH, Beinart RA, Hewson I, White AE, Johnson KS, Carlson CA, Montoya JP, Zehr JP (2010). Unicellular Cyanobacterial Distributions Broaden the Oceanic N-2 Fixation Domain. *Science*, 327:1512-1514

Monteiro FM, Follows MJ, Dutkiewicz S (2010). Distribution of diverse nitrogen fixers in the global ocean. *Global Biogeochemical Cycles*, 24

Morel A, Huot Y, Gentili B, Werdell PJ, Hooker SB, Franz BA (2007). Examining the consistency of products derived from various ocean color sensors in open ocean (Case 1) waters in the perspective of a multi-sensor approach. *Remote Sensing of Environment*, 111:69-88

Mulholland MR, Ohki K, Capone DG (2001). Nutrient controls on nitrogen uptake and metabolism by natural populations and cultures of Trichodesmium (Cyanobacteria). *Journal of Phycology*, 37:1001-1009

Needoba JA, Foster RA, Sakamoto C, Zehr JP, Johnson KS (2007). Nitrogen fixation by unicellular diazotrophic cyanobacteria in the temperate oligotrophic North Pacific Ocean. *Limnology and Oceanography*, 52:1317-1327

Oelze J (2000). Respiratory protection of nitrogenase in Azotobacter species: is a widely held hypothesis unequivocally supported by experimental evidence? *Fems Microbiology Reviews*, 24:321-333

Oschlies A, Schulz KG, Riebesell U, Schmittner A (2008). Simulated 21st century's increase in oceanic suboxia by CO2-enhanced biotic carbon export. *Global Biogeochemical Cycles*, 22

Paerl HW, Pinckney JL, Kucera SA (1995). Clarification of the Structural and Functional Roles of Heterocysts and Anoxic Microzones in the Control of Pelagic Nitrogen-Fixation. *Limnology and Oceanography*, 40:634-638

Paumann M, Regelsberger G, Obinger C, Peschek GA (2005). The bioenergetic role of dioxygen and the terminal oxidase(s) in cyanobacteria. *Biochimica Et Biophysica Acta-Bioenergetics*, 1707:231-253

Peschek GA, Obinger C, Paumann M (2004). The respiratory chain of blue-green algae (cyanobacteria). *Physiologia Plantarum*, 120:358-369

Peschek GA, Villgrater K, Wastyn M (1991). Respiratory Protection of the Nitrogenase in Dinitrogen-Fixing Cyanobacteria. *Plant and Soil*, 137:17-24

Poole RK, Hill S (1997). Respiratory protection of nitrogenase activity in Azotobacter vinelandii - Roles of the terminal oxidases. *Bioscience Reports*, 17:303-317

Ramos JL, Guerrero MG (1983). Involvement of Ammonium Metabolism in the Nitrate Inhibition of Nitrogen-Fixation in Anabaena Sp Strain Atcc-33047. *Archives of Microbiology*, 136:81-83

Raven JA (2009). Functional evolution of photochemical energy transformations in oxygen-producing organisms. *Functional Plant Biology*, 36:505-515

Riebesell U, Schulz KG, Bellerby RGJ, Botros M, Fritsche P, Meyerhofer M, Neill C, Nondal G, Oschlies A, Wohlers J, Zollner E (2007). Enhanced biological carbon consumption in a high CO2 ocean. *Nature*, 450:545-U510

Robson RL, Postgate JR (1980). Oxygen and Hydrogen in Biological Nitrogen-Fixation. *Annual Review of Microbiology*, 34:183-207

Sherman LA, Meunier P, Colon-Lopez MS (1998). Diurnal rhythms in metabolism: A day in the life of a unicellular, diazotrophic cyanobacterium. *Photosynthesis Research*, 58:25-42

Shi T, Ilikchyan I, Rabouille S, Zehr JP (2010). Genome-wide analysis of diel gene expression in the unicellular N(2)-fixing cyanobacterium Crocosphaera watsonii WH 8501. *Isme Journal*, 4:621-632

Sohm JA, Hilton JA, Noble AE, Zehr JP, Saito MA, Webb EA (2011). Nitrogen fixation in the South Atlantic Gyre and the Benguela Upwelling System. *Geophysical Research Letters*, 38

Staal M, Hekkert ST, Brummer GJ, Veldhuis M, Sikkens C, Persijn S, Stal LJ (2007a). Nitrogen fixation along a north-south transect in the eastern Atlantic Ocean. *Limnology and Oceanography*, 52:1305-1316

Staal M, Meysman FJR, Stal LJ (2003). Temperature excludes N-2-fixing heterocystous cyanobacteria in the tropical oceans. *Nature*, 425:504-507

Staal M, Rabouille S, Stal LJ (2007b). On the role of oxygen for nitrogen fixation in the marine cyanobacterium Trichodesmium sp. *Environmental Microbiology*, 9:727-736

Steppe TF, Paerl HW (2002). Potential N-2 fixation by sulfate-reducing bacteria in a marine intertidal microbial mat. *Aquatic Microbial Ecology*, 28:1-12

Stoeckel J, Welsh EA, Liberton M, Kunnvakkam R, Aurora R, Pakrasi HB (2008). Global transcriptomic analysis of Cyanothece 51142 reveals robust diurnal oscillation of central metabolic processes. *Proceedings of the National Academy of Sciences of the United States of America*, 105:6156-6161

Stramma L, Visbeck M, Brandt P, Tanhua T, Wallace D (2009). Deoxygenation in the oxygen minimum zone of the eastern tropical North Atlantic. *Geophysical Research Letters*, 36

Taniuchi Y, Ohki K (2007). Relation between nitrogenase synthesis and activity in a marine unicellular diazotrophic strain, Gloeothece sp 68DGA (Cyanophyte), grown under different light/dark regimens. *Phycological Research*, 55:249-256

Toepel J, Welsh E, Summerfield TC, Pakrasi HB, Sherman LA (2008). Differential transcriptional analysis of the cyanobacterium Cyanothece sp strain ATCC 51142 during light-dark and continuous-light growth. *Journal of Bacteriology*, 190:3904-3913

Tripp HJ, Bench SR, Turk KA, Foster RA, Desany BA, Niazi F, Affourtit JP, Zehr JP (2010). Metabolic streamlining in an open-ocean nitrogen-fixing cyanobacterium. *Nature*, 464:90-94

Voss M, Croot P, Lochte K, Mills M, Peeken I (2004). Patterns of nitrogen fixation along 10N in the tropical Atlantic. *Geophysical Research Letters*, 31

Waterbury JB, Willey JM (1988). Isolation and Growth of Marine Planktonic Cyanobacteria. *Methods in Enzymology*, 167:100-105

Wilson ST, Foster RA, Zehr JP, Karl DM (2010). Hydrogen production by Trichodesmium erythraeum Cyanothece sp and Crocosphaera watsonii. *Aquatic Microbial Ecology*, 59:197-206

Zehr JP, Bench SR, Carter BJ, Hewson I, Niazi F, Shi T, Tripp HJ, Affourtit JP (2008). Globally Distributed Uncultivated Oceanic N-2-Fixing Cyanobacteria Lack Oxygenic Photosystem II. *Science*, 322:1110-1112

Zehr JP, Jenkins BD, Short SM, Steward GF (2003). Nitrogenase gene diversity and microbial community structure: a cross-system comparison. *Environmental Microbiology*, 5:539-554

Zehr JP, Waterbury JB, Turner PJ, Montoya JP, Omoregie E, Steward GF, Hansen A, Karl DM (2001). Unicellular cyanobacteria fix N-2 in the subtropical North Pacific Ocean. *Nature*, 412:635-638

Table and Figure legends

	5% Oxygen		**20% Oxygen**	
	fmol x $12h^{-1}$ x $cell^{-1}$	Electron equivalents (fmol)	fmol x $12h^{-1}$ x $cell^{-1}$	Electron equivalents (fmol)
Nett photosynthesis (O_2 evolution)	98	392	102	408
Cellular carbon buildup (C)	96	-384	105	-420
Sum		8		-12
Respiration (O_2 drawdown)	-38	-152	-102	-408
Nitrogen fixation (N buildup)	12	-36	11	-33
Cellular carbon breakdown (C)	-12	48	-77	308
Sum		-140		-133

Table 1: Cellular budget of electron sources and sinks during the light (upper, white area) and the dark cycle (lower, gray area). Oxygen and carbon are converted into electrons 4:1, nitrogen is converted 3:1.

	$^1/_2$ N_2	NO_3^-
mol electrons	3	8
Converted to mol <CH_2O>	0.75	2.00
mol ATP	8	1
Converted to mol <CH_2O>	1.33	0.17
mol <CH_2O> per NH_4^+ produced	**2.08**	**2.17**

Table 2: Costs of electrons and ATP needed to produce one mol of NH_3 and the conversion into carbohydrate units. It is assumed that 4 mol electrons or 6 ATP can be generated out of one mol of carbohydrates (<CH_2O>, 1/6 mol of glucose).

Figure 1: Cellular acetylene reduction (AR) activity over a period of 24 hours with cell numbers as an inlay (y-axis: cells x mL^{-1}, x-axis: days). White squares and solid line, normal (20%) oxygen cultures. Black triangles and dashed line, low (5%) oxygen cultures. Error bars denote standard deviations of triplicate cultures. Cultures where diluted with fresh medium on day six and the day cycle measurements were performed on day eight.

Figure 2: Acetylene reduction by cultures of *Crocosphaera watsonii* grown under 5% oxygen (left) and 20% oxygen (right). Black bars represent acetylene reduction measurements made under 5% oxygen atmosphere, white bars represent measurements made under 20% oxygen atmosphere. Error bars denote standard deviation of triplicate cultures.

Figure 3: Photosynthesis and oxygen consumption. Squares: Normal (20%) oxygen culture. Triangles: Low (5%) oxygen culture. Filled symbols represent oxygen consumption in the dark, white symbols represent net oxygen evolution in the light (photosynthesis). L1-L5 light phase, D1-D5 dark phase. Error bars denote standard deviations of triplicate cultures.

Figure 4: Development of carbon (A), nitrogen (B) content in fmol per cell and the C:N ratio (C) over the course of a 24 hour cycle. White squares and solid line, normal oxygen treatment. Filled triangles and dashed line, low oxygen treatment. L1-L5 light phase, D1-D5 dark phase. Error bars denote standard deviations of triplicate cultures.

Figure 5 (A): Cell numbers (logarithmic scale) of *Crocosphaera watsonii* grown under different nitrate concentrations for two weeks. (B): Acetylene reduction assays were performed on day 4 (filled circles) and day 11 (open squares). Shown are duplicate measurements of acetylene reduction.

Figure 6: Theoretical costs of ammonia assimilation in carbohydrate units (<CH_2O>) (mol mol^{-1}) for different efficiencies of respiratory glucose oxidation. Solid line: N_2 fixation. Dashed line: Assimilatory nitrate uptake.

Figure 7: Average light intensity at the depth of 25% oxygen saturation in µmol photons m^{-2} s^{-1}. Note that 25% oxygen concentration correspond to water equilibrated to a 5% oxygen containing atmosphere. Euphotic zone depth was derived from aquaMODIS satellite data of 2009 (http://oceancolor.gsfc.nasa.gov/) using the algorithm by Morel (Morel et al. 2007). Oxygen concentrations were taken from the World Ocean Atlas 2009 (Garcia 2010).

Figure 1.TIF

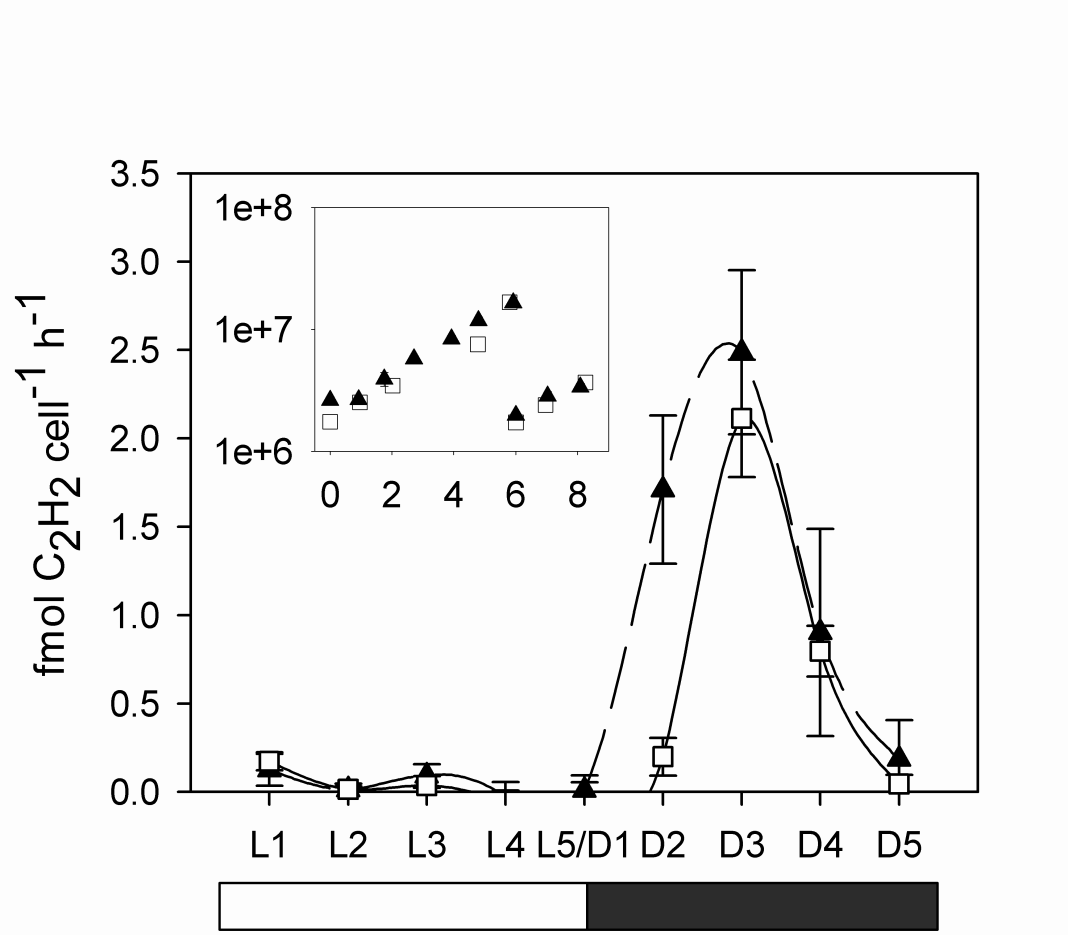
fmol C_2H_2 cell^{-1} h^{-1}
3.5
3.0
2.5
2.0
1.5
1.0
0.5
0.0
1e+8
1e+7
1e+6
0
2
4
6
8
L1
L2
L3
L4
L5/D1
D2
D3
D4
D5

Figure 2.TIF

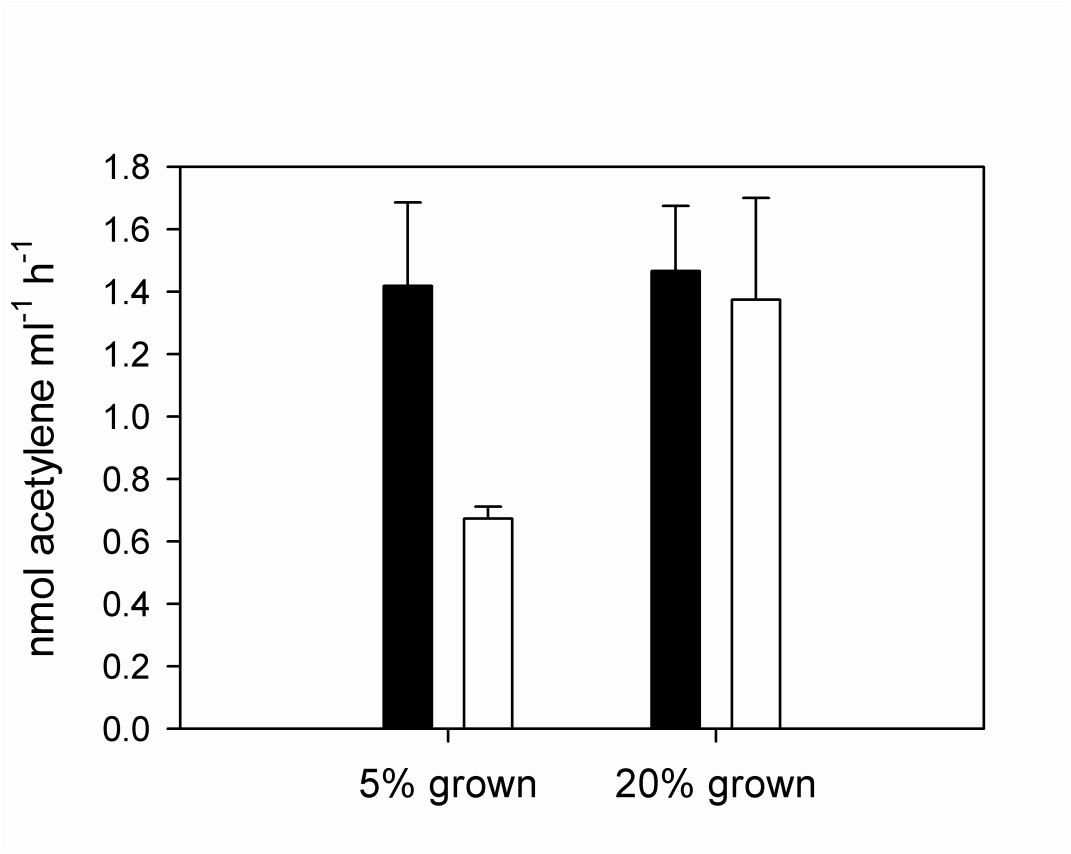
nmol acetylene ml-1 h-1
1.8
1.6
1.4
1.2
1.0
0.8
0.6
0.4
0.2
0.0
5% grown
20% grown

Figure 3.TIF

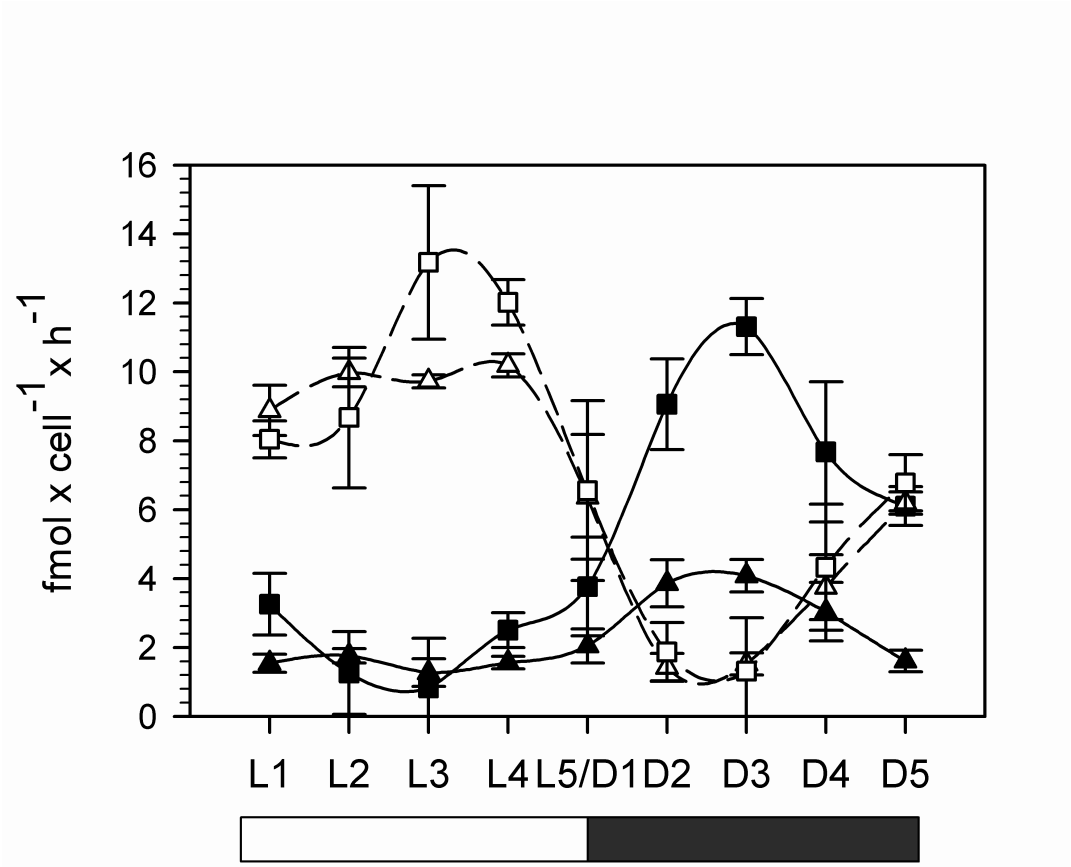

Figure 4.TIF

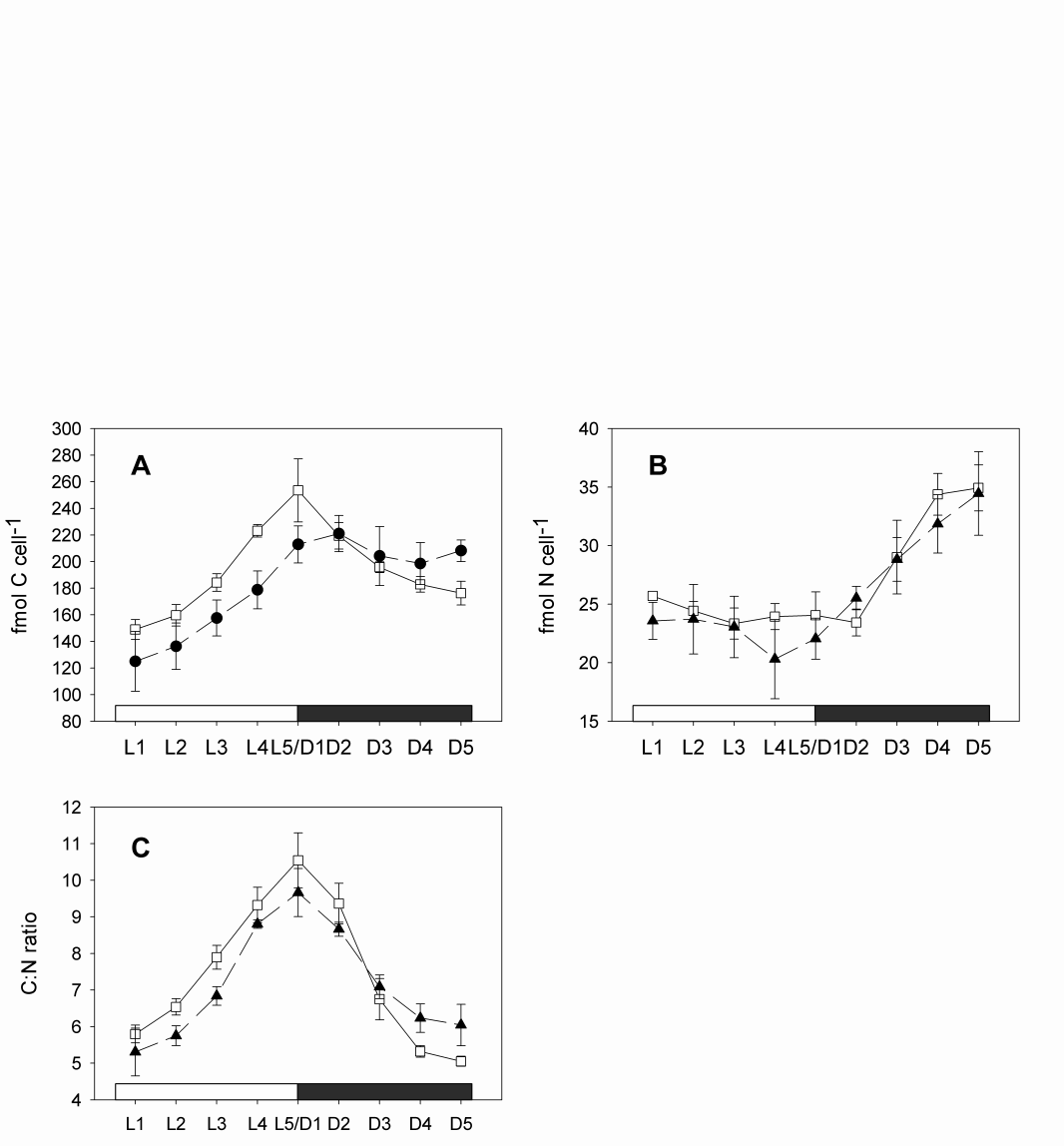
A
fmol C cell-1
300
280
260
240
220
200
180
160
140
120
100
80
L1 L2 L3 L4 L5/D1 D2 D3 D4 D5
B
fmol N cell-1
40
35
30
25
20
15
L1 L2 L3 L4 L5/D1 D2 D3 D4 D5
C
C:N ratio
12
11
10
9
8
7
6
5
4
L1 L2 L3 L4 L5/D1 D2 D3 D4 D5

Figure 5.TIF

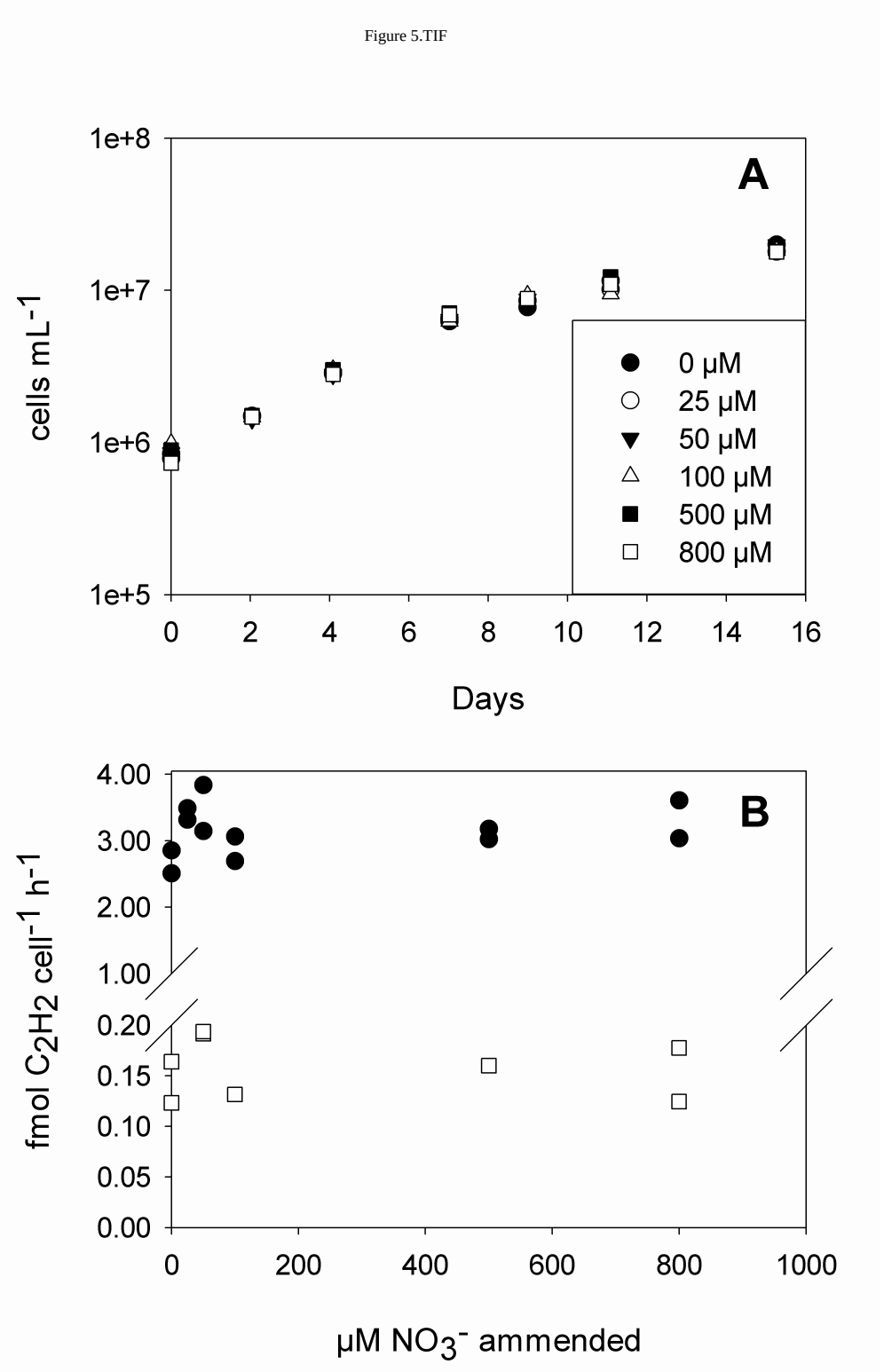
A
cells mL-1
1e+8
1e+7
1e+6
1e+5
0 µM
25 µM
50 µM
100 µM
500 µM
800 µM
0
2
4
6
8
10
12
14
16
Days
B
fmol C2H2 cell-1 h-1
4.00
3.00
2.00
1.00
0.20
0.15
0.10
0.05
0.00
0
200
400
600
800
1000
µM NO3- ammended

Figure 6.TIF

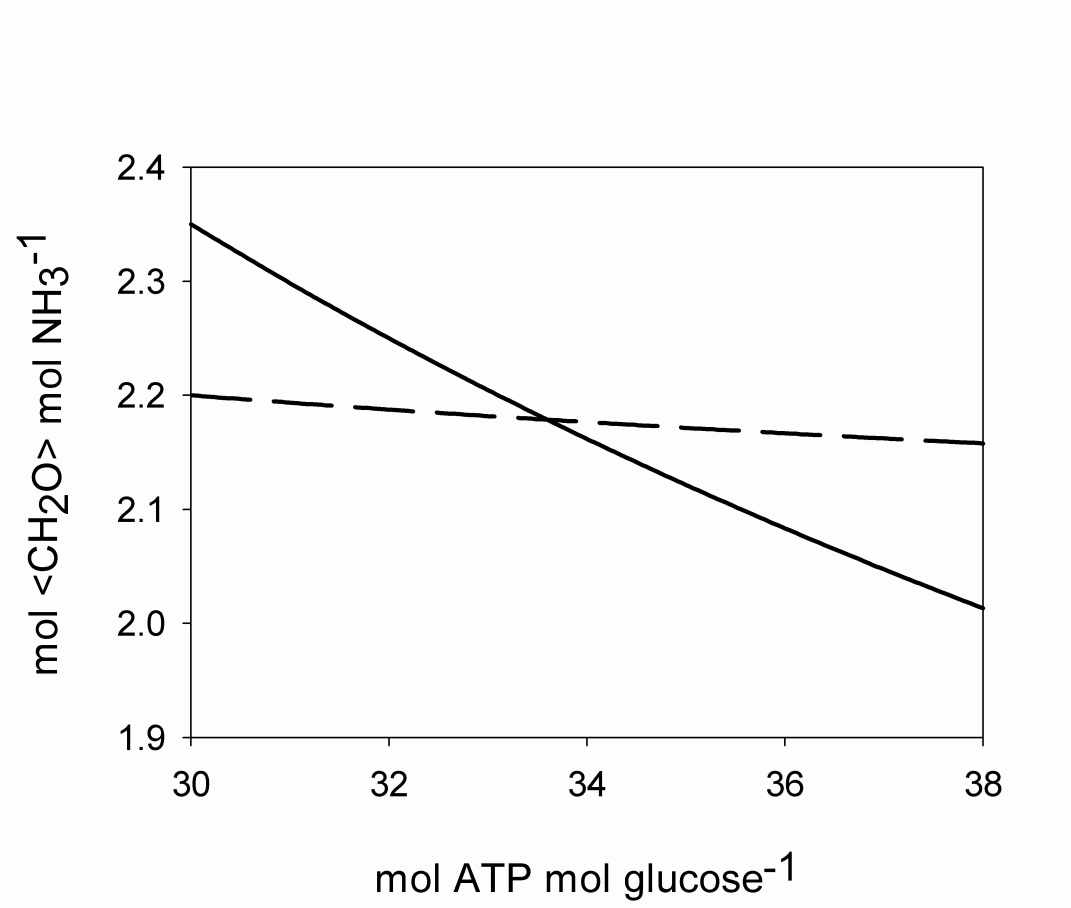
2.4
2.3
2.2
2.1
2.0
1.9
30
32
34
36
38
mol <CH2O> mol NH3-1
mol ATP mol glucose-1

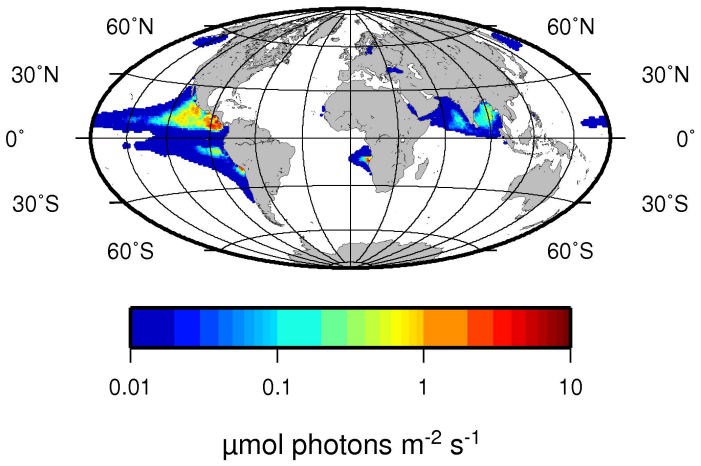
60˚N
60˚N
30˚N
30˚N
0˚
0˚
30˚S
30˚S
60˚S
60˚S
0.01
0.1
1
10
µmol photons m-2 s-1

2.2 The Peruvian upwelling system

High coastal productivity drives Southern Peruvian upwelling system into N limitation

T. Großkopf[1], C. Löscher[2], H. Schunck[1], G. Lavik[3], M.M.M. Kuypers[3], Z. Kolber[4], G. Friedrich[4], Francisco Chavez[4], Ruth A. Schmitz[2], J. LaRoche[1]

[1]Helmholtz-Centre for Ocean Research Kiel (GEOMAR), Düsternbrooker Weg 20, 24105 Kiel, Germany

[2]Institute for General Microbiology, Christian-Albrechts University Kiel, Am Botanischen Garten 1-9, 24118 Kiel, Germany

[3]Max-Planck-Institute for Marine Microbiology, Celsiusstraße 1, 28359 Bremen, Germany

[4]Monterey Bay Aquarium Research Institute (MBARI), 7700 Sandholdt Road Moss Landing, California 95039-9644

Summary

The continental shelf of Peru is one of the most productive ecosystems in the world. Wind driven upwelling supplies cold, nutrient rich water to the surface throughout the year, giving rise to high phytoplankton biomass. In contrast, the waters further offshore show HNLC (high nutrient low chlorophyll) characteristics, i.e. high concentration of nitrate and phosphate detectable in surface waters but low chlorophyll a concentrations. Here we present data on the distribution of picophytoplankton and bacterial cells collected during two research cruises from December 2008 to February 2009. In combination with FRR flurometry, nutrient addition experiments (bioassays) and CO_2 flux measurements we differentiate the Peruvian upwelling system into two biogeochemically distinct areas: The northern part of the system (0° - 12°S) showed incomplete N drawdown and a slight Si limitation of phytoplankton chlorophyll a in nutrient addition experiments. Iron and phosphate showed no response in chlorophyll a concentrations when added to incubations. High numbers of the picocyanobacteria *Synechococcus* and *Prochlorococcus* in surface waters and a cyclic pattern of the variable fluorescence of chlorophyll (Fv/Fm) over the day were observed by FRR flurometry, with dusk and dawn maxima and night time minima. In contrast, the southern part of the system (12°S -18°S) showed a complete drawdown of surface nitrate with still substantial phosphate concentrations (~ 0.5 µM). The Fv/Fm parameter was around 0.3 in offshore water, but did not show the pronounced cyclicity observed in the northern part of the system. In a nutrient addition experiment at 17.45° S, N amendment triggered a 4.7-fold increase in chlorophyll concentrations and a 3-fold increase in carbon fixation rates compared to non N-ammended tretaments. The Fv/Fm parameter recovered from 0.34 (s.d. = 0.04) in treatments without N-addition to 0.41 (s.d. = 0.03) in treatments with added N. Taken together, our data suggest that the strong upwelling in the area around Pisco (14° S) leads to a maximum in productivity, accompanied by elevated concentrations of P* in the underlying oxygen minimum zone, which drives the southern part of the system into N-limitation at the surface. In both the northern and southern region the respective growth limitations on phytoplankton prevent the complete uptake of CO_2 that has accumulated in the upwelling source water through hundreds of

years of remineralisation, thereby making the whole system a strong source of CO_2 to the atmosphere.

Introduction

The Pacific Ocean marks the end of the global conveyor belt, the ventilation route of deep water, therefore its deep water is enriched with N and P compared to the Atlantic Ocean from hundreds of years of accumulated remineralisation. Due to the mainly oxidative remineralization of organic matter and the lack of gas exchange with the atmosphere, the oxygen content of Pacific deep water is at any given point below the saturation concentration. The depletion of oxygen intensifies towards the east, where the productive upwelling regions of the Tropical and subtropical North and South Pacific generate extended oxygen minimum zones (OMZs) in the underlying water masses (Wyrtki 1962, Karstensen et al. 2008, Paulmier & Ruiz-Pino 2009). The Peruvian upwelling system is one of the most productive ecosystems in the world (Chavez & Messie 2009). The Peruvian coast alone supports a fishery of Anchovetta (Engraulis ringens) of up to 10^7 tons per year (0.01 pg yr^{-1}) (Montecino & Lange 2009). This incredible biomass of fish is sustained by a year round wind-driven upwelling that brings fresh, nutrient replete waters from the subsurface into the sunlit layers of the euphotic zone.

South-easterly Trade winds blowing parallel to the coast result in a westwards displacement of surface water, thereby creating a void that is filled with cold, nutrient rich subsurface water. Once the sun's energy penetrates the water, the combination of dissolved inorganic nitrogen (DIN (N), NO_3^-, NO_2^-, NH_4^+), dissolved inorganic phosphorus (DIP (P), mainly PO_4^{3-}), silicate (Si) and a handful of micronutrients such as iron (Fe) and molybdenum (Mo) create a fertile habitat for photosynthetic primary producers. Exponential growth of phytoplankton leads to depletion of surface nutrients, while grazing and viral lysis contribute to the continuous demise of the phytoplankton standing stock. Nutrients can get recycled by bacterial remineralisation of dissolved and particulate organic matter (DOM and POM, respectively) and re-enter the food chain at the phytoplankton level. However, a fraction of the nutrients ends up as export production, therefore, at some point in time the phytoplankton community will run out of an essential nutrient and primary production is haltered, if no additional supply of

nutrients is given.

In the Peruvian upwelling system, the phytoplankton standing stock is highest at the coast between 5°S and 15°S (Carr & Kearns 2003). Further offshore from the up to 150 km wide Peruvian shelf, chlorophyll concentration drops rapidly, while the macronutrients N and P are still available in surface waters. This situation is termed HNLC (high nutrients low chlorophyll) and has attracted researchers to investigate the factor that limits phytoplankton productivity in such regions. For the Peruvian upwelling system there have been reports about iron limitation (Hutchins et al. 2002), silicate limitation (Dugdale et al. 1995) and top down control of phytoplankton by grazing pressure matching the exponential growth rate of phytoplankton (Walsh 1976) leading to HNLC conditions.

Material and methods

From December 2008 to February 2009 two cruises, M77 leg 3 and 4, of the RV METEOR were conducted to the Peruvian upwelling system. In addition to routine CTD stations along the cruise transect, two transects along 10°S and 16°S were sampled at high resolution. Three nutrient addition experiments (bioassays) were performed at 10° S (082°W), 12°S (082°W) and 17.75° S (073°W) (Fig. 1).

Nutrients, oxygen

Nutrient samples for nitrate, nitrite, silicate and phosphate were taken from a CTD-rosette and frozen at -20°C for later analysis in the lab. Nutrient concentrations were measured according to (Grasshof et al. 1999). Oxygen was continuously measured with an oxygen electrode on the CTD rosette and calibrated with Winkler titrations from niskin bottles across all depths at several stations.

Fast repetition rate flurometry

Unfiltered seawater from the ships underway system was pumped with a constant flow rate through the flow through cuvette of a fast repetition rate flurometer (FRRf). Once every minute the instrument recorded a measurement to determine the dark adapted (F0) and maximum fluorescence (Fm) of photosystem II (PSII) after saturation with a series of sub microsecond excitation flashlets as described in Kolber et al. (Kolber et al. 1998). The difference in maximum and dark adapted fluorescence is called variable

fluorescence (Fm - F0 = Fv) and if normalized to Fm gives the maximal photochemical efficiency of PSII.

Flow cytometry

Samples for flow cytometry were taken from niskin bottles from surface to 400 m depth or from incubation bottles at the end of an experiment. At each depth 1.9 mL seawater were filled in a cryotube and 0.1 mL 20% glutaraldehyde were added, to give a final concentration of 1% glutaraldehyde (vol/vol). After mixing, samples were left for 8 -12 hours at 4°C for fixation and were frozen at -80°C until measurement. A FACS calibur flow cytometer with 488 nm blue laser excitation light and detectors for forward scatter, side scatter, 530 nm (green) fluorescence, 570 nm (orange) fluorescence and 670 nm (red) fluorescence was used to quantify bacteria and picophytoplankton. The flow rate was calibrated by using TZrucount calibration beads (BD Biosciences) and cell counts were calculated per milliliter according to the measured volume. After thawing, unstained samples were filtered through a 50 µm syringe filter and measured at low flow speed (~11 µL min^{-1}) for 10 minutes or until 50000 events were recorded. *Prochlorococcus* and *Synechococcus* were differentiated from picoeukaryotes due to their lower forward scatter and red fluorescence signal (Marie et al. 1997, Cavender-Bares et al. 2001). We did not make the subdivision into a nano- and ultraphytoplankton cluster, as described elsewhere, since these two clusters were often overlapping and hence did not allow a clear separation. Our picoeukaryote cluster is the sum of these two clusters (Cavender-Bares et al. 2001). The orange fluorescence only observed for phycoerythrin-containing cyanobacteria such as *Synechococcus* was used to differenciate the picocyanobacteria into *Prochlorococcus* and *Synechococcus*. Next, the remaining sample was stained with sybrgreen, a stain for nucleic acids. After 20 minutes staining at 4°C samples were measured for 3 minutes at low speed or until 50000 events were recorded. The staining protocol allowed the quantification of high nucleic acid (HNA) and low nucleic acid (LNA) containing bacteria (Marie et al. 1997, Cavender-Bares et al. 2001, Mary et al. 2006). Chlorophyll containing bacteria were electronically substracted (gated). The total number of non-green bacteria is HNA+LNA.

Chlorophyll

For chlorophyll a determination, 250 mL seawater were filtered on a GF/F filter with a vacuum of less than -200 mbar. The filters were placed in plastic tubes with 1 mL pure acetone and frozen at -20°C over 24 hours. Next, 9 mL $H2O_{deion}$ was added to the samples and mixed. For another three days, samples were stored at -20°C until the fluorescence of 5mL of the extract were measured in a Turner AU-10 flurometer . A spinach extracted chlorophyll solution (Sigma-Aldrich) was used as standard.

POC, PON and Carbon fixation

For carbon fixation measurements, 4.5 L of surface water were incubated in polycarbonate bottles in on-deck incubators, cooled with surface water flow through and shaded by one layer of blue lagoon light foil. Bottles were amended with 2 mL sodium ^{13}C-bicarbonate solution (0.24 M) at the beginning of the experiment. After 24 hours 1-3 L of water were filtered onto precombusted GF/F filters. Filters were oven dried at 50°C for 24 hours and stored in a desiccator until measurement. Samples for natural abundance of ^{13}C in particulate organic carbon (POC) were taken and used as blank for the enrichment of ^{13}C due to label uptake. For analysis, filters were fumed overnight with 37% HCl and dried for 2 hours at 60°C. Next, samples were analyzed for particulate organic carbon (POC) and nitrogen (PON) and isotopic composition using a CHN analyzer coupled to an isotope ratio monitoring mass spectrometer. Rates of primary production were calculated according to the relative enrichment of the ^{13}C isotope in biomass, like described elsewhere (Fernandez et al. 2009).

Nutrient addition experiments (Bioassays)

Trace-metal clean techniques were used throughout the whole bioassay experiments. Seawater for the experiments was collected by towing a trace metal clean seawater sampler at cruising speed at approximately 2 meters water depth. The seawater was directly channeled into the trace metal free laboratory, where a 200 L acid cleaned polycarbonate container was filled to about 60L before the onset of sampling, to guarantee sufficient homogeneity between the samples. From the container, 4.5 L of seawater were filled into polycarbonate bottles. The nutrients N (1 µM NH_4NO_3), P (0.2 µM NaH_2PO_4), Fe (2 nM $FeCl_3$) or Si (2 µM Na_2SiO_3) were added as simple additions or in combinations, to triplicate bottles. In total nine control bottles were filled without

added nutrients, three of which were filtered right away for POC/PON and chlorophyll concentration, three others after 24 hours and the remaining three at the end of the experiment after 48 hours. All bottles were filled with seawater to the top and capped bubble free. Next, bottles were placed in on deck incubators covered with one layer of blue lagoon light foil, simulating a 15 m water column. The temperature in the incubators was kept stable by flushing the incubators with surface seawater. After 24 hours 1 mL of ^{13}C labeled bicarbonate solution (1g $NaH^{13}CO_3$ 50 mL^{-1} H_2O_{deion}, Sigma-Aldrich) was added to each bottle in the clean lab. Bottles were incubated for another 24 hour period until filtration for POC/PON and chlorophyll measurements.

CO_2 fluxes

Measurements of pCO_2 were performed like described in (Friederich et al. 2008). Sea to air fluxes for CO_2 were calculated using salinity, temperature and wind strength data from the ships logging system according to the equations of Wanninkhof (Wanninkhof 1992).

Results

Temperature and Nutrients

The measured sea surface temperature (SST) during our cruise from December 2008 to February 2009 ranged from 14.2° C in the core of the upwelling at 13.5°S to 26.9° C at around 5°S, 85°W, 400 km offshore . Not surprisingly N, P and Si show a negative correlation with SST, due to the uptake of these nutrient elements by phytoplankton and the subsequent export out of the euphotic zone. The best fit was achieved for P, since the supply of P to surface waters is directly linked to upwelling strength. N on the other hand is lost in the core of the upwelling, at around 12-15°S. This is reflected in the growing P* values (P*= $[PO_4^{3-}]$ -$[NO_3^-]$/16) (Deutsch et al. 2007) towards the south in the neutral density layer y^n = 26.3 kg m^{-3} , which represents the lower end of the upper oxycline (Fig.2). Accordingly, the N/P value in the surface drops from ~12 in the north towards very low values in the south of the study region due to complete N depletion with still elevated P concentrations (~0.5 µM) due to upwelling of water with high P*.

Flow cytometry

The upwelling area showed a marked gradient in phytoplankton composition from west to east. The warmer offshore water was dominated by *Prochlorococcus* in surface, while *Synechococcus* was situated between the coastal, diatom dominated high productivity area (Franz e. al, submitted) and the HNLC type offshore waters (Fig.3). In the water column *Synechococcus* and picoeukaryotes inhabited the surface water down to 50 meters. Picoeukaryotes were mainly found on the shelf, except for in the middle of the 10° S transect, were up to 10^5 cells mL^{-1} were detected in the surface (Fig. 3). The highest abundance of both *Synechococcus* and picoeukaryotes was detected at 6° S on the shelf, with 1.57 x 10^5 picoeukaryote cells mL^{-1} and 4.4 x 10^5 *Synechococcus* cells mL^{-1} (Fig 3). *Synechococcus* was the only phytoplankter present in each surface sample measured with flow cytometry and the most abundant one in the top 10 meters, with average cell numbers of 1.45 x 10^5 cells mL^{-1} (range: 2 x 10^4 - 4.4 x 10^5 cells mL^{-1}). Extrapolated over an area of 1.75 x 10^6 km² (070°- 086° W, 0° - 18° S) there were 2.5 x 10^{24} *Synechococcus* cells in the top 10 meters of the Peruvian upwelling system present at the time of the survey. *Prochlorococcus* showed highest abundance in the warm surface waters to the northwest, peaking with 1.34 x 10^5 cells mL^{-1} at 084° W at the

west end of the 10°S transect. On the shelf *Prochlorococcus* cell numbers were very low and often undetectable in surface waters. A deep population of *Prochlorococcus* cells was found on the offshore end of the 10°S transect, with maximum numbers of 1.36 x 10^5 cells mL^{-1} at 80 meters depth at 10°S, 082°30' W (Fig. 4). This peak in deep *Prochlorococcus* coincided with an unexpected shoaling of the pycnocline, apparently not connected to the coastal upwelling (Fig.2). Closer towards the shelf the cell densities were lower and the subsurface peak of *Prochlorococcus* situated at shallower depths, roughly following the upper oxycline of the OMZ (Fig.4). This deep chlorophyll peak could be observed at the ends of the 10°S and 12°S transect via CTD fluorescence measurements (data not shown) and was situated right above the secondary nitrite peak within the OMZ (Fig.5). Throughout the 16°S transect a deep population of *Prochlorococcus* was present, but at much lower numbers than in the 10°S transect. In the middle of the southern transect, high *Prochlorococcus* numbers at around 20 - 40 meters depth extended from 075-077° W (Fig.6).

The number of non-green bacterial cells as established by flow cytometry was high throughout the whole surface (Fig.3). A general trend in bacterial numbers was high at the coast and decreasing towards the open ocean, but the variance was much lower than for other phytoplankton groups or environmental variables like carbon fixation. The range was below one order of magnitude, from 6.5 x 10^5 cells mL^{-1} at the south west end of the survey to 4.7 x 10^6 cells mL^{-1} in the coastal upwelling area at 10°S. The mean number of bacteria in surface was 1.98 x 10^6 cells mL^{-1} (st.dev. = 10^6 cells mL^{-1}). Along 10° S and 16° S the bacterial abundance was measured over a depth range from surface to 400 m and 200 m, respectively. The 10°S transect showed high numbers of bacteria in surface. Low nucleic acid containing (LNA) and high nucleic acid containing bacteria (HNA) equally contributed to the surface population. A minimum in bacterial abundance was observed at around 100 meters depth, while a secondary bacterial maximum with peak numbers around 10^6 cells mL was observed in the oxygen minimum zone at 300 meters depth. This deep peak had similar abundance of LNA and HNA bacteria, while a subsurface maximum on the shelf at 100 -150 meters depth was mainly composed by HNA bacteria (Fig.7). The peak on the shelf coincided with an accumulation of nitrite and a decrease in nitrate concentrations (data not shown). At 16°S the numbers of HNA and LNA bacteria were again equal in the top 50 meters. Two peaks of bacteria dominated by HNA bacteria were observed at 100 -

200 meters depth, one on the shelf slope at 74.2 °W, the other one at 76.3° W in the middle of the transect (Fig.8). Both peaks showed elevated nitrite concentrations and it seems likely that the Peru-Chile or Poleward undercurrent (PCU) that flows from north to south along the shelf around 100-300 meters depth (Penven et al. 2005, Czeschel et al. 2011) carries this signal of HNA bacteria out into the middle of the 16°S transect, while the peak of high nitrite and HNA bacteria at the coast is produced by high productivity on the shelf.

FRR flurometry, primary productivity and Bioassays

The variable fluorescence emitted by chlorophyll a compared to the maximum fluorescence (Fv/Fm) is often used as a fitness parameter to infer the nutrient status of the phytoplankton community (Kolber et al. 1998). Nutrient replete phytoplankton cultures show a maximum Fv/Fm value of ~0.65 (Kolber et al. 1994), however there is considerable difference between phytoplankton groups that originates from their unique physiology (Suggett et al. 2009). Cyanobacteria for example show fluorescence of their phycobilisomes that contributes to the dark adapted fluorescence (F0) but is not affected by the redox state of PSII and hence the Fv/Fm parameter of cyanobacteria in culture is generally lower than that of other phytoplankton (Schreiber et al. 1995, Campbell et al. 1998, Suggett et al. 2009). In an environmental or mixed culture setting the Fv/Fm value therefore holds integrated information about the species composition and the individual species "fitness" of a given watermass (Suggett et al. 2009). High Fv/Fm values up to 0.57 were measured all along the coast, indicating a fast growing, nutrient replete phytoplankton community. Further offshore the values decreased with increasing temperature (Fig.9). Between 10°S and 12°S (80° W -84°W) the Fv/Fm parameter showed the lowest values observed (~0.15) during our cruise and a strong daily signal with peaks at sunrise and sunset, a low plateau during daytime and lowest values during the night (Fig.9). The appearance of low overall Fv/Fm values, together with nighttime depression and peaking values at sunrise and sunset has previously been characterized as flurometric fingerprint of the iron limited HNLC Equatorial Pacific upwelling (Behrenfeld & Kolber 1999, Behrenfeld et al. 2006). However two nutrient addition experiments at 082°W on the 10°S and 12°S transect showed no increase in chlorophyll a or carbon fixation rates in response to the addition of 2 nM iron over a period of 48 hours. Only the addition of Si resulted in an increase in carbon fixation and

total chl a values at the 12° S assay. Both at 10°S and 12°S the combined addition of N, P, Fe and Si showed a significant increase in chlorophyll a and carbon fixation compared to the unammended control over a period of 48 hours. However, the effect was only small and phytoplankton biomass was increasing in all bottles over time. A clear N limitation was observed in the third nutrient addition experiment at 17.8° S 73°W (Fig.10). Here, all bottles without added N showed high C/N values (mean = 8.3 mol mol^{-1}, s.d = 0.5), low carbon specific growth rates (mean = 0.1 mol mol^{-1} d^{-1}, s.d. = 0.02) and low chlorophyll a values (mean = 0.3 µg L^{-1}, s.d.= 0.1). When N was added to the bottles, the C/N values were closer to the redfield value of 6.7 (mean = 6.4 mol mol^{-1}, s.d. = 0.4) and carbon specific growth rates and chlorophyll a values increased by a factor of 3 and 4.7 compared to non N added treatments, respectively (C specific growth rate = 0.29 mol mol^{-1} d^{-1}, s.d. = 0.02, chla = 1.4 µg L^{-1}, s.d. = 0.2) (Fig.11). The decrease in growth rates and increase in C:N ratios in the treatments without N added indicate carbon overproduction by N limited phytoplankton.

The net primary production was very high on the shelf, especially in the area around pisco, where the highest carbon fixation rate of 413 mg C d^{-1} m^{-3} at 13.5° S 076.75° W was measured. Two stations nearby were showing second and third highest carbon fixation rates measured during the cruise (274 mg C d^{-1} m^{-3} at 12.35° S and 224 mg C d^{-1} m^{-3} at 13.75° S, respectively). The stations on the shelf at 6°S, 10°S and 17°S showed higher carbon fixation rates than offshore stations, but considerably lower rates than the shelf between Lima and Pisco (177 mg C d^{-1} m^{-3}, 172 mg C d^{-1} m^{-3} and 108 mg C d^{-1} m^{-3}, respectively). All seven stations within the upwelling area (water below 21°C) had a mean carbon fixation rate of 176 mg C d^{-1} m^{-3} (std. dev. = 143 mg C d^{-1} m^{-3}). The remaining stations can be considered offshore stations with a mean in carbon fixation of 46 mg C d^{-1} m^{-3} (std. dev. 48 mg C d^{-1} m^{-3}) (Table 1). The lowest value in carbon fixation was measured at the southernmost station (17.83° S 073° W) with 12 mg C d^{-1} m^{-3} (Fig.12).

CO_2

The mean CO_2 value measured three meters below the surface during the METEOR 77 cruise leg 3 was 497 µatm, the minimum 253 µatm and the maximum 1419 µatm (n = 33276). Only 9% of the measurements fell below the atmospheric value (384 µatm). The CO_2 concentration in surface water showed a cubic fit with SST (equation 1, r =

0.805, n = 33276) (Fig.13).

$$CO_2 = 18328.5 – 2274.1 \times SST + 95.9 \times SST^2 - 1.342 \times SST^3 \quad (1)$$

Surface water with a temperature below 21°C showed clear signatures of upwelled water. The CO_2 values were highest right in the cold, upwelled water, decreasing with warming and increasing residence time of the watermass at the surface. Water with temperatures above 22°C showed a signature that resembled water of oceanic origin or from the equatorial upwelling. This is apparent both in the species composition of phytoplankton as detected with flow cytometry and the flurometric (FRRf) signal. The warmer, offshore water shows higher abundance in LNA than HNA bacteria and higher *Prochlorococcus* cell numbers, while the upwelling water colder than 21°C has higher total bacterial cell numbers and the community is dominated by HNA bacteria (Table 1). The CO_2 content of water above 21°C was on average 444 µatm (std. dev. = 37 µatm, n = 17246). A further increase of surface temperature in these waters lead to a slight increase in CO_2, rather than a decrease, although CO_2 in the water was still above atmospheric concentrations, hence still outgassing to the atmosphere. An equilibration of ocean and atmosphere was not observed during our cruise, despite some local patches that showed extreme CO_2 drawdown below atmospheric values, due to high biological activity. The wind speed measured by an onboard anemometer was used to calculate the flux of CO_2 from sea to atmosphere (Wanninkhof 1992). The calculated flux of CO_2 ranged from -8.4 mol C m^{-2} yr^{-1} to 119 mol C m^{-2} yr^{-1}, with an average of 4.3 mol C m^{-2} yr^{-1} (std. dev. = 7.5 mol C m^{-2} yr^{-1}). The highest variability of the CO_2 flux was observed in the area of strongest upwelling around Pisco, where highest fluxes from ocean to atmosphere and from atmosphere to ocean were observed in close proximity (Fig. 13).

Discussion

The Peruvian upwelling system is a highly dynamic system that is mainly characterized by coastal upwelling and the subsequent heating of the water with associated decrease in nutrient and CO_2 concentrations. The surface water temperature shows an increasing trend with the time since its first contact with the atmosphere. Friedrich et al. measured

a SST warming of 0.11° C per day with a drifter released in the core of the Peruvian upwelling (Friederich et al. 2008). Unequal upwelling strength along the coast and eddy formations that can export coastal waters at different speeds towards the open ocean creates patchiness in the system. A good example is the occurrence of high numbers of picoeukaryotes in the middle of the 10°S transect (Figs. 3, 4), that were associated with a cold water tongue that extended from around 6- 8°S southwestwards and can be seen on satellite images of SST and chlorophyll. Nevertheless, two coarse environmental zones could be distinguished according to the limitation of phytoplankton growth: The northern Peruvian upwelling, with HNLC characteristics and the southern Peruvian upwelling, with a clear N limitation in surface waters.

In the northern part of the Peruvian upwelling (0°-12°S) the surface water had lower primary productivity rates on the shelf compared to the southern part. Further offshore low chlorophyll a and Fv/Fm values and high concentrations of N and P were observed, while primary productivity was low. The water that gets upwelled at the coast is already low in Si compared to N and the coastal diatom blooms efficiently export the remaining Si to the sediments. The phytoplankton community was dominated by the picocyanobacteria *Prochlorococcus* and *Synechococcus*. High total bacterial numbers throughout the whole area suggest that most of the primary production was recycled via the microbial loop. The northern Peru upwelling system was previously found to be iron limited (Hutchins et al. 2002, Bruland et al. 2005, DiTullio et al. 2005). The Fv/Fm values along the 10°S and 12°S transect showed a cyclic behavior that would also suggest iron limitation. Nevertheless, the addition of iron had no effect on the phytoplankton community in experiments performed over 48 hours. Rather, the two bioassays at 10° and 12°S showed a slight N and Si limitation, respectively. However, the increase in chlorophyll and primary productivity that was observed was much less pronounced than at the southernmost bioassay. The most likely scenario for the northern Peruvian upwelling system is the following: The combinations of Si limitation with high bacterial abundance and a phytoplankton community dominated by picocyanobacteria leads to a low export of organic matter and a nearly complete recycling of nutrients in the surface. The high CO_2 concentration that the water carries as a signature of its recent upwelling is not exported to deeper waters. High bacterial abundance throughout the mixed layer further increases the CO_2 concentration. The result is a constant flux of CO_2 from sea to air at moderate rates.

On the shelf, between 12° and 14°S the highest productivity was observed. This region around Pisco represents a transition zone between the northern part of the Peruvian upwelling and the southern, N limited one. The increased wind curl stress in this area creates Ekman pumping that is responsible for a shoaling of the thermocline (Albert et al. 2010). The upper edge of the oxygen minimum zone is elevated towards shallower depth and the coastal upwelling is fueled by water that is higher enriched with nutrients compared to the more northerly parts. This in term leads to an even further increase in productivity, high export fluxes and increased consumption of oxygen in the subsurface water. After the complete consumption of oxygen, N loss processes dominate, observable in an increase in P* (which in part can also arise from P leaching from the sediments). The increased N loss leads to a considerably lower N:P ratio and once the water gets upwelled and the nutrients available for phytoplankton, the primary productivity gets limited by the cession of N before all other nutrients. The southern part of the Peruvian upwelling is hence N limited and is characterized by high POC:PON ratios and Fv/Fm values around 0.3, that do not show the pronounced cyclicity like observed at 10°S. Like in the northern part, the net flux of CO_2 is from sea to air, since there is not enough N left in the surface water for phytoplankton to take up all the respiratory CO_2.

Acknowledgements

We thank the authorities of Peru for permission to conduct research in the Peruvian territorial waters. Further we would like to thank captain and crew of FS METEOR as well as chief scientists Martin Frank and Lothar Stramma. We thank K. Stange, F. Malien, V. Leon and P. Fritsche for oxygen and nutrient measurements. We thank G. Klockgether for assisting with mass spectrometry measurements. This work is a contribution of the Sonderforschungsbereich 754 "Climate - Biogeochemistry Interactions in the Tropical Ocean" (www.sfb754.de) which is supported by the Deutsche Forschungsgemeinschaft. We thank the Max Planck Gesellschaft for financial support. We thank the Bundesministerium für Bildung und Forschung (BMBF) for financial support through the SOPRAN II (Surface Ocean Processes in the Anthropocene) project.

References

Albert A, Echevin V, Levy M, Aumont O (2010) Impact of nearshore wind stress curl on coastal circulation and primary productivity in the Peru upwelling system. Journal of Geophysical Research-Oceans 115

Behrenfeld MJ, Kolber ZS (1999) Widespread iron limitation of phytoplankton in the South Pacific Ocean. Science 283:840-843

Behrenfeld MJ, Worthington K, Sherrell RM, Chavez FP, Strutton P, McPhaden M, Shea DM (2006) Controls on tropical Pacific Ocean productivity revealed through nutrient stress diagnostics. Nature 442:1025-1028

Bruland KW, Rue EL, Smith GJ, DiTullio GR (2005) Iron, macronutrients and diatom blooms in the Peru upwelling regime: brown and blue waters of Peru. Marine Chemistry 93:81-103

Campbell D, Hurry V, Clarke AK, Gustafsson P, Oquist G (1998) Chlorophyll fluorescence analysis of cyanobacterial photosynthesis and acclimation. Microbiology and Molecular Biology Reviews 62:667-+

Carr ME, Kearns EJ (2003) Production regimes in four Eastern Boundary Current systems. Deep-Sea Research Part Ii-Topical Studies in Oceanography 50:3199-3221

Cavender-Bares KK, Karl DM, Chisholm SW (2001) Nutrient gradients in the western North Atlantic Ocean: Relationship to microbial community structure and comparison to patterns in the Pacific Ocean. Deep-Sea Research Part I-Oceanographic Research Papers 48:2373-2395

Chavez FP, Messie M (2009) A comparison of Eastern Boundary Upwelling Ecosystems. Progress in Oceanography 83:80-96

Czeschel R, Stramma L, Schwarzkopf FU, Giese BS, Funk A, Karstensen J (2011) Middepth circulation of the eastern tropical South Pacific and its link to the oxygen minimum zone. Journal of Geophysical Research-Oceans 116

Deutsch C, Sarmiento JL, Sigman DM, Gruber N, Dunne JP (2007) Spatial coupling of nitrogen inputs and losses in the ocean. Nature 445:163-167

DiTullio GR, Geesey ME, Maucher JM, Alm MB, Riseman SF, Bruland KW (2005) Influence of iron on algal community composition and physiological status in the Peru upwelling system. Limnology and Oceanography 50:1887-1907

Dugdale RC, Wilkerson FP, Minas HJ (1995) The Role of a Silicate Pump in Driving New Production. Deep-Sea Research Part I-Oceanographic Research Papers 42:697-719

Fernandez C, Farias L, Alcaman ME (2009) Primary production and nitrogen regeneration processes in surface waters of the Peruvian upwelling system. Progress in Oceanography 83:159-168

Friederich GE, Ledesma J, Ulloa O, Chavez FP (2008) Air-sea carbon dioxide fluxes in the coastal southeastern tropical Pacific. Progress in Oceanography 79:156-166

Grasshof G, Kremling K, Erhardt M (1999) Methods of seawater analysis, Vol. Wiley VCH, Weinheim

Hutchins DA, Hare CE, Weaver RS, Zhang Y, Firme GF, DiTullio GR, Alm MB, Riseman SF, Maucher JM, Geesey ME, Trick CG, Smith GJ, Rue EL, Conn J, Bruland KW (2002) Phytoplankton iron limitation in the Humboldt Current and Peru Upwelling. Limnology and Oceanography 47:997-1011

Karstensen J, Stramma L, Visbeck M (2008) Oxygen minimum zones in the eastern tropical Atlantic and Pacific oceans. Progress in Oceanography 77:331-350

Kolber ZS, Barber RT, Coale KH, Fitzwater SE, Greene RM, Johnson KS, Lindley S, Falkowski PG (1994) Iron Limitation of Phytoplankton Photosynthesis in the Equatorial Pacific-Ocean. Nature 371:145-149

Kolber ZS, Prasil O, Falkowski PG (1998) Measurements of variable chlorophyll fluorescence using fast repetition rate techniques: defining methodology and experimental protocols. Biochimica Et Biophysica Acta-Bioenergetics 1367:88-106

Marie D, Partensky F, Jacquet S, Vaulot D (1997) Enumeration and cell cycle analysis of natural populations of marine picoplankton by flow cytometry using the nucleic acid stain SYBR Green I. Applied and Environmental Microbiology 63:186-193

Mary I, Heywood JL, Fuchs BM, Amann R, Tarran GA, Burkill PH, Zubkov MV (2006) SAR11 dominance among metabolically active low nucleic acid bacterioplankton in surface waters along an Atlantic meridional transect. Aquatic Microbial Ecology 45:107-113

Montecino V, Lange CB (2009) The Humboldt Current System: Ecosystem components and processes, fisheries, and sediment studies. Progress in Oceanography 83:65-79

Paulmier A, Ruiz-Pino D (2009) Oxygen minimum zones (OMZs) in the modern ocean. Progress in Oceanography 80:113-128

Penven P, Echevin V, Pasapera J, Colas F, Tam J (2005) Average circulation, seasonal cycle, and mesoscale dynamics of the Peru Current System: A modeling approach. Journal of Geophysical Research-Oceans 110

Schreiber U, Endo T, Mi HL, Asada K (1995) Quenching Analysis of Chlorophyll Fluorescence by the Saturation Pulse Method - Particular Aspects Relating to the Study of Eukaryotic Algae and Cyanobacteria. Plant and Cell Physiology 36:873-882

Suggett DJ, Moore CM, Hickman AE, Geider RJ (2009) Interpretation of fast repetition rate (FRR) fluorescence: signatures of phytoplankton community structure versus physiological state. Marine Ecology-Progress Series 376:1-19

Walsh JJ (1976) Herbivory as a factor in patterns of nutrient utilization in the sea. Limnology and Oceanography 21:1-13

Wanninkhof R (1992) Relationship between Wind-Speed and Gas-Exchange over the Ocean. Journal of Geophysical Research-Oceans 97:7373-7382

Wyrtki K (1962) The Oxygen Minima in Relation to Ocean Circulation. Deep-Sea Research 9:11-23

Tables and Figures

	Water with T < 21°C						Water with T ≥ 21°C					
Parameter	No. samples	**Mean**	Median	Min.	Max.	Std. dev.	No. samples	**Mean**	Median	Min.	Max.	Std. dev.
F_0	14013	**572.67**	446.70	3.76	3625.16	510.87	19629.00	**195.36**	111.51	2.01	2751.58	220.14
F_m	14013	**994.98**	757.58	4.57	4256.63	845.89	19629.00	**299.47**	160.93	2.32	3265.82	368.21
F_v	14013	**422.31**	305.23	0.75	1699.22	361.42	19629.00	**104.11**	49.52	0.15	1363.84	156.51
F_v/F_m	14013	**0.43**	0.43	0.03	0.57	0.06	19629.00	**0.31**	0.30	0.05	0.50	0.08
Sigma (A^2)	14013	**757.47**	744.47	58.70	1485.93	137.15	19629.00	**772.67**	766.53	39.82	1493.90	132.68
p	14013	**0.42**	0.44	0.00	0.70	0.11	19629.00	**0.22**	0.23	0.00	0.70	0.19
CO_2 (µatm)	12457	**594.52**	540.30	255.80	1419.30	192.92	20819.00	**439.26**	446.70	252.90	639.80	41.21
Wind speed ($m s^{-1}$)	14009	**5.72**	5.50	0.10	14.20	2.36	19351.00	**6.18**	6.10	0.90	11.70	1.80
CO_2 flux (mol m^{-2} yr^{-1})	12457	**7.40**	4.35	-5.55	118.90	11.25	20815.00	**2.47**	2.48	-8.43	13.35	2.48
NO_3 (µM)	23	**8**	8	0	21	4.9	17	**3**	2	0	11	3.9
NO_2 (µM)	23	**1**	1	0	7	1.6	17	**0**	0	0	1	0.3
NH_4 (µM)	23	**2**	2	1	3	0.7	17	**1**	1	0.4	2	0.3
PO_4 (µM)	23	**1**	1	0	3	0.6	17	**1**	1	0	2	0.6
Si (µM)	7	**7**	6	0	18	5.5	12	**1**	1	0	5	1.2
Prochlorococcus (cells mL^{-1})	11	**14606**	9838	0	63420	17971.3	10	**31754**	10334	0	134000	43389

Synechococcus (cells mL^{-1})	11	**207528**	172000	38100	439000	140444.9	10	**93413**	39466	23300	393000	115397.4
Picoeukaryotes (cells mL^{-1})	11	**52826**	45991	5860	157000	42041.2	10	**20628**	8037	0	102784	31959.4
Total non-green bacteria (cells mL^{-1})	11	**2906808**	2600000	1570000	4723339	916691.5	10	**1232752**	1037237	830000	2720000	565687.5
HNA bacteria (cells mL^{-1})	11	**1655725**	1490000	568000	3013562	729961	10	**484429**	450759	325000	912000	170963.4
LNA bacteria (cells mL^{-1})	11	**1250537**	1227513	796000	1930159	332360.1	10	**748823**	593193	476000	1810000	411124.8
POC ($g\ m^{-3}$)	7	**0.562**	0.638	0.072	1.181	0.377	11	**0.153**	0.100	0.070	0.607	0.153
PON ($g\ m^{-3}$)	7	**0.077**	0.089	0.010	0.131	0.045	11	**0.026**	0.018	0.013	0.100	0.025
POC/PON ratio	7	**8.4**	7.8	6.6	13.0	2.1	11	**6.8**	6.8	5.5	7.8	0.6
Carbon fixation ($g\ m^{-3}\ d^{-1}$)	7	**0.176**	0.172	0.016	0.413	0.143	11	**0.046**	0.026	0.012	0.177	0.048

Table 1: Various parameters of the Peruvian upwelling system, grouped into water with temperature above 21° C (oceanic) and water below 21°C (upwelling).

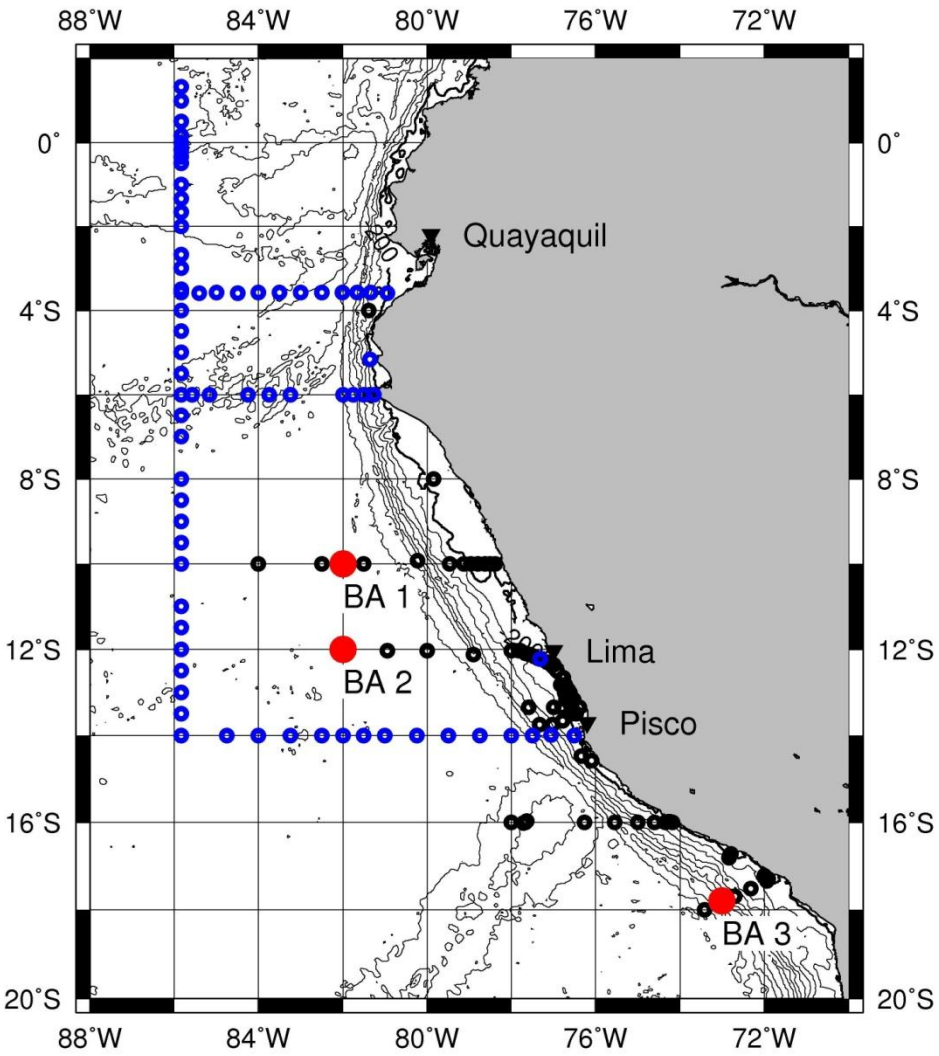

Figure 1: Overview of the Peruvian upwelling system. Sampled CTD stations during the Meteor cruises M77/3 (black circles) and M77/4 (blue circles) as well as the three bioassays conducted at 10°S (BA1), 12°S (BA2) and 17.8° S (BA3) are shown.

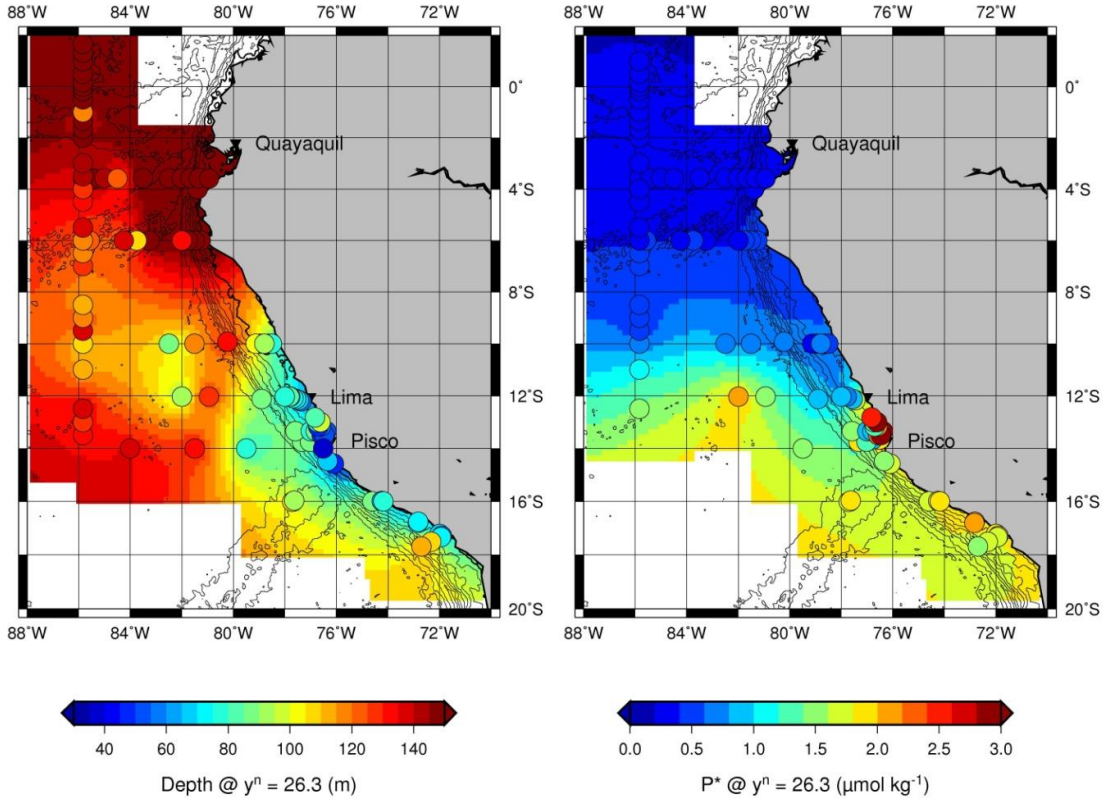

Figure 2: Depth of the neutral density layer y^n = 26.3 kg m^{-3} (left panel) and distribution of P* along that density layer (right panel). Observe the pronounced shoaling of the density layer off Pisco, with highest P* values associated.

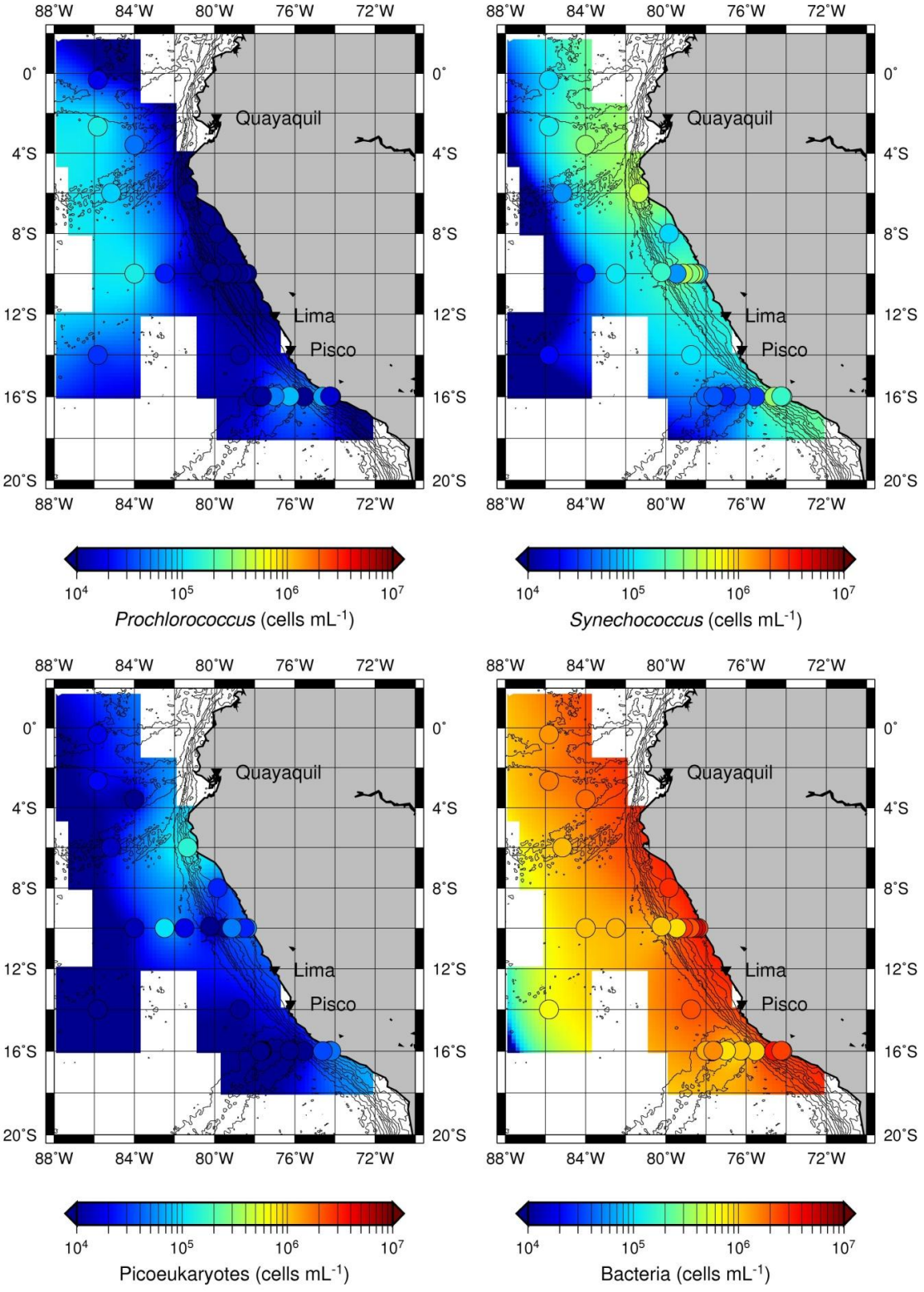

Figure 3: Distribution of *Prochlorococcus* (upper left), *Synechococcus* (upper right), picoeukaryotes (lower left) and total non-green bacteria (lower right) in the surface as counted in the flow cytometer. Note the logarithmic color scale is the same for all four groups.

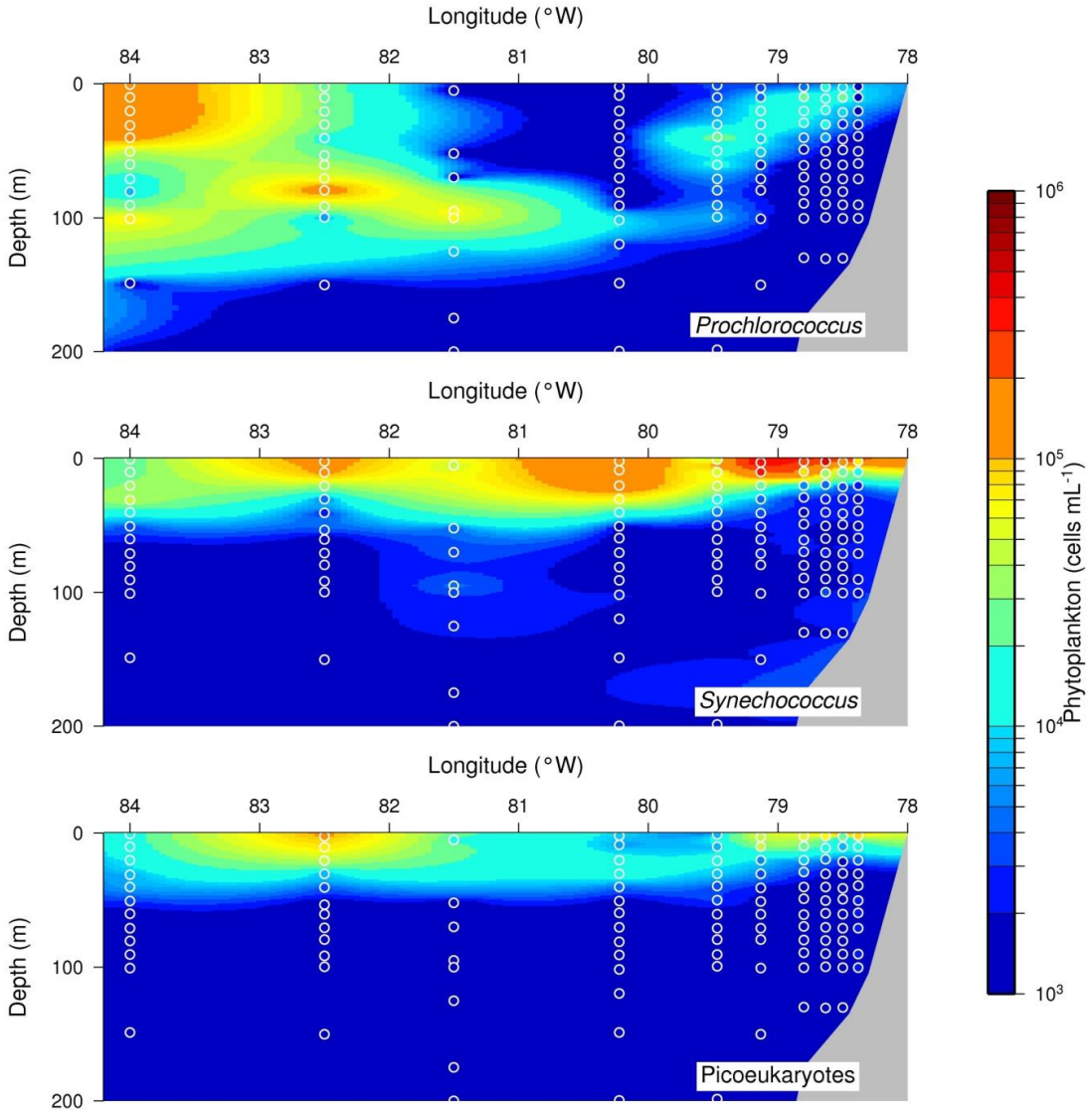

Figure 4: Distribution of the picocyanobacteria *Prochlorococcus* (upper panel) and *Synechococcus* (middle panel) and picoeukaryotes (lower panel) along the 10°S transect from surface to 200 meters. Note the logarithmic scale, which is the same for all groups.

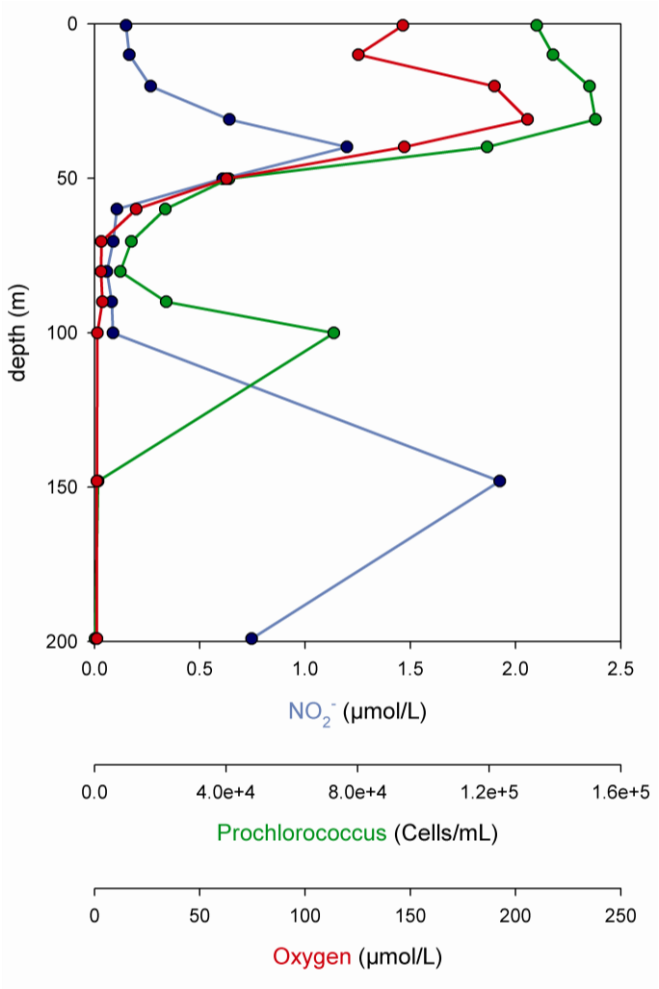

Figure 5: Vertical profile of station 5-1 (10° S 084° W). *Prochlorococcus* (green), oxygen (red) and nitrite (blue).

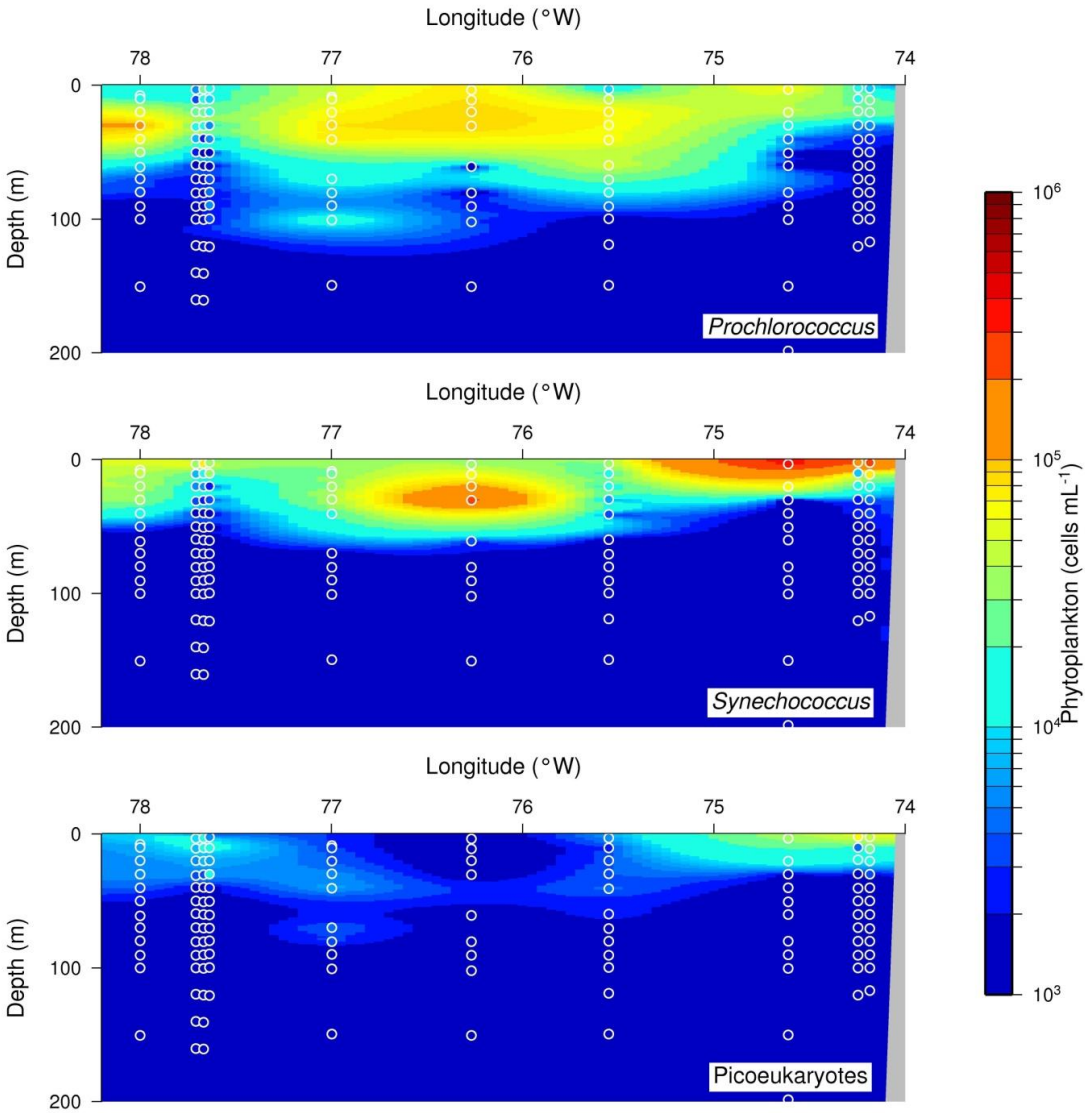

Figure 6: Distribution of the picocyanobacteria *Prochlorococcus* (upper panel) and *Synechococcus* (middle panel) and picoeukaryotes (lower panel) along the 16°S transect from surface to 200 meters. Note the logarithmic scale, which is the same for all groups.

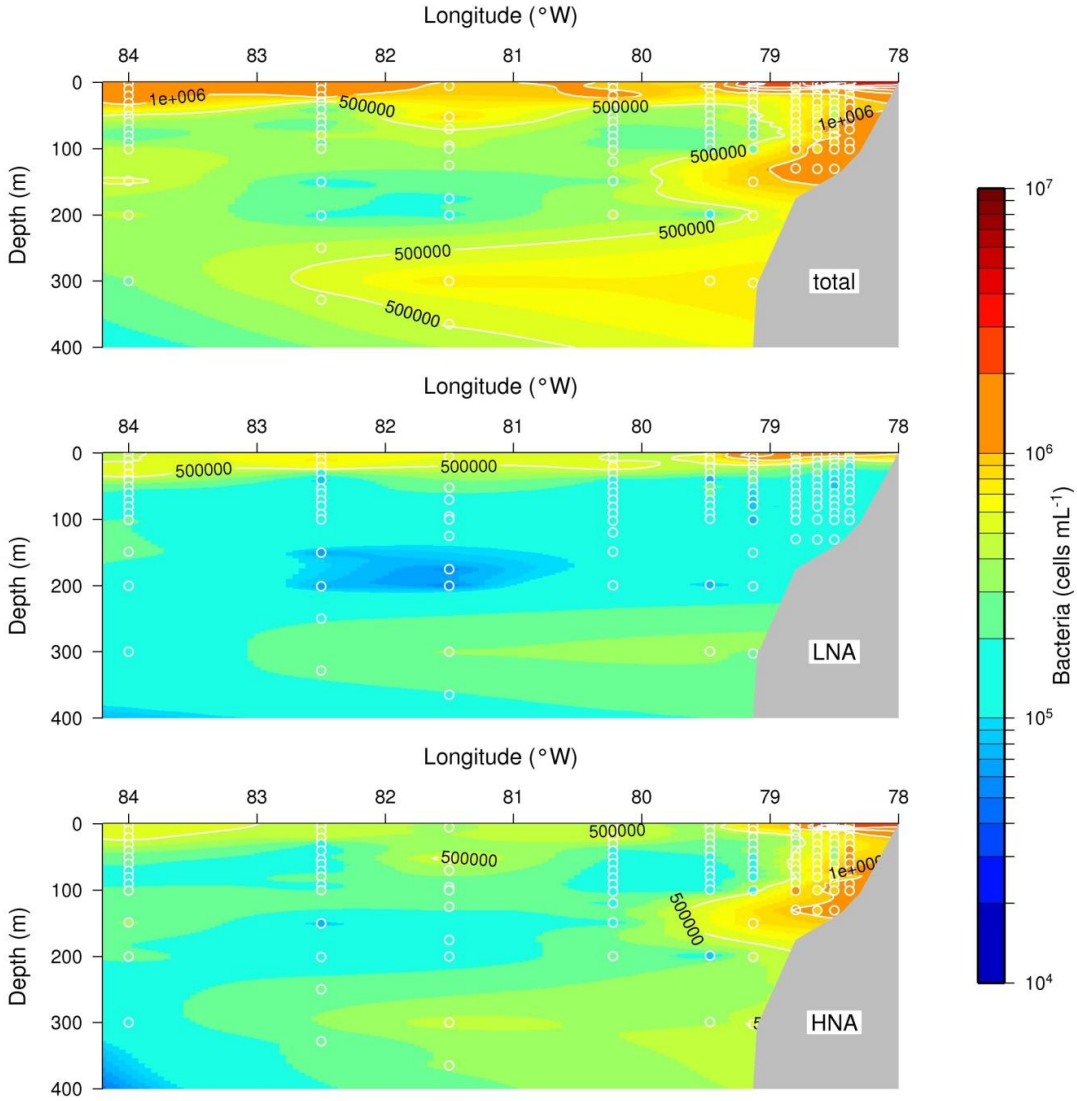

Figure 7: Cell numbers of total non-green (upper panel), low nucleic acid containing (LNA, middle panel) and high nucleic acid containing (HNA, lower panel) bacteria along the 10°S transect from surface to 400 meters.

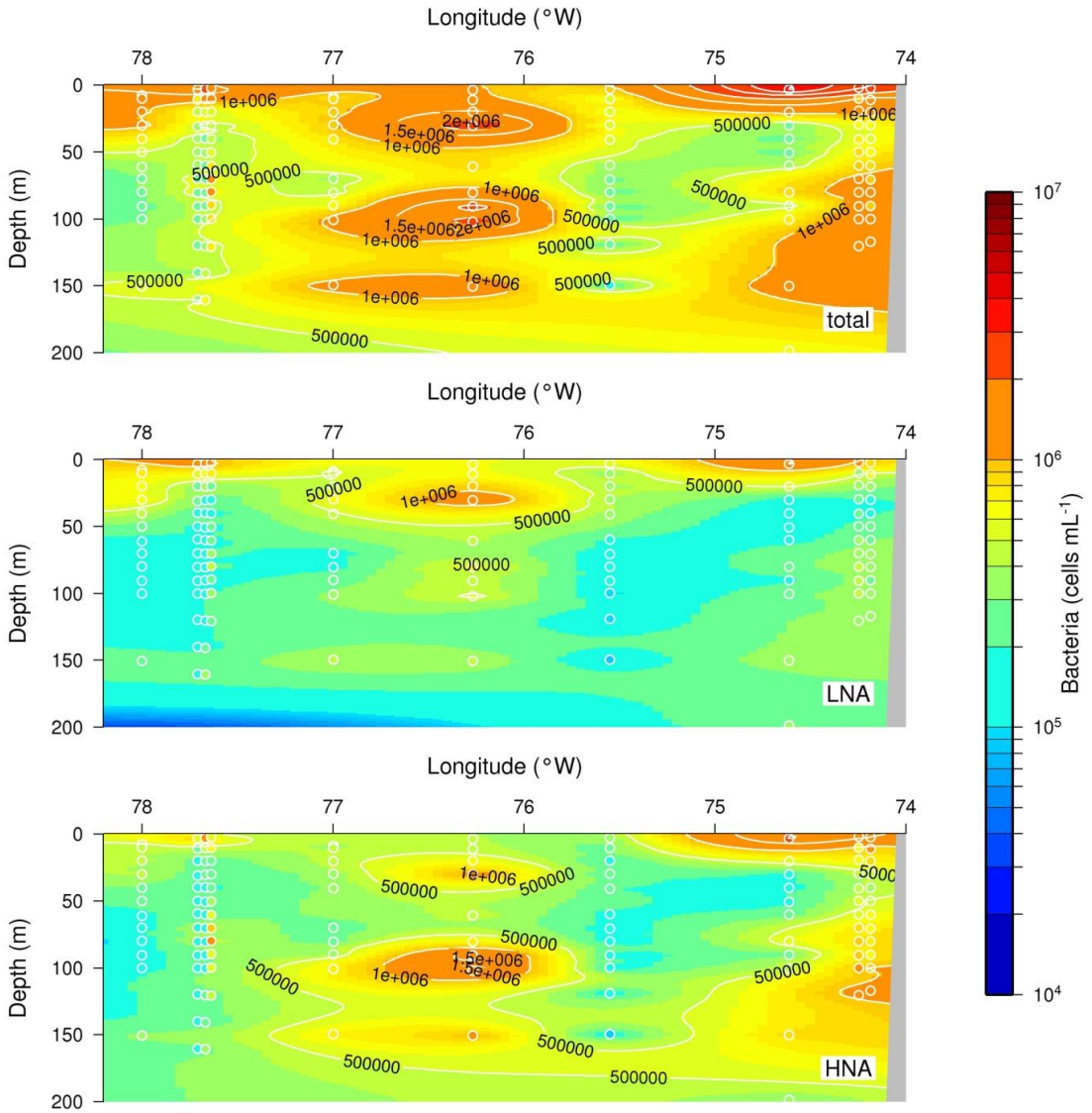

Figure 8: Cell numbers of total non-green (upper panel), low nucleic acid containing (LNA, middle panel) and high nucleic acid containing (HNA, lower panel) bacteria along the 16°S transect from surface to 200 meters.

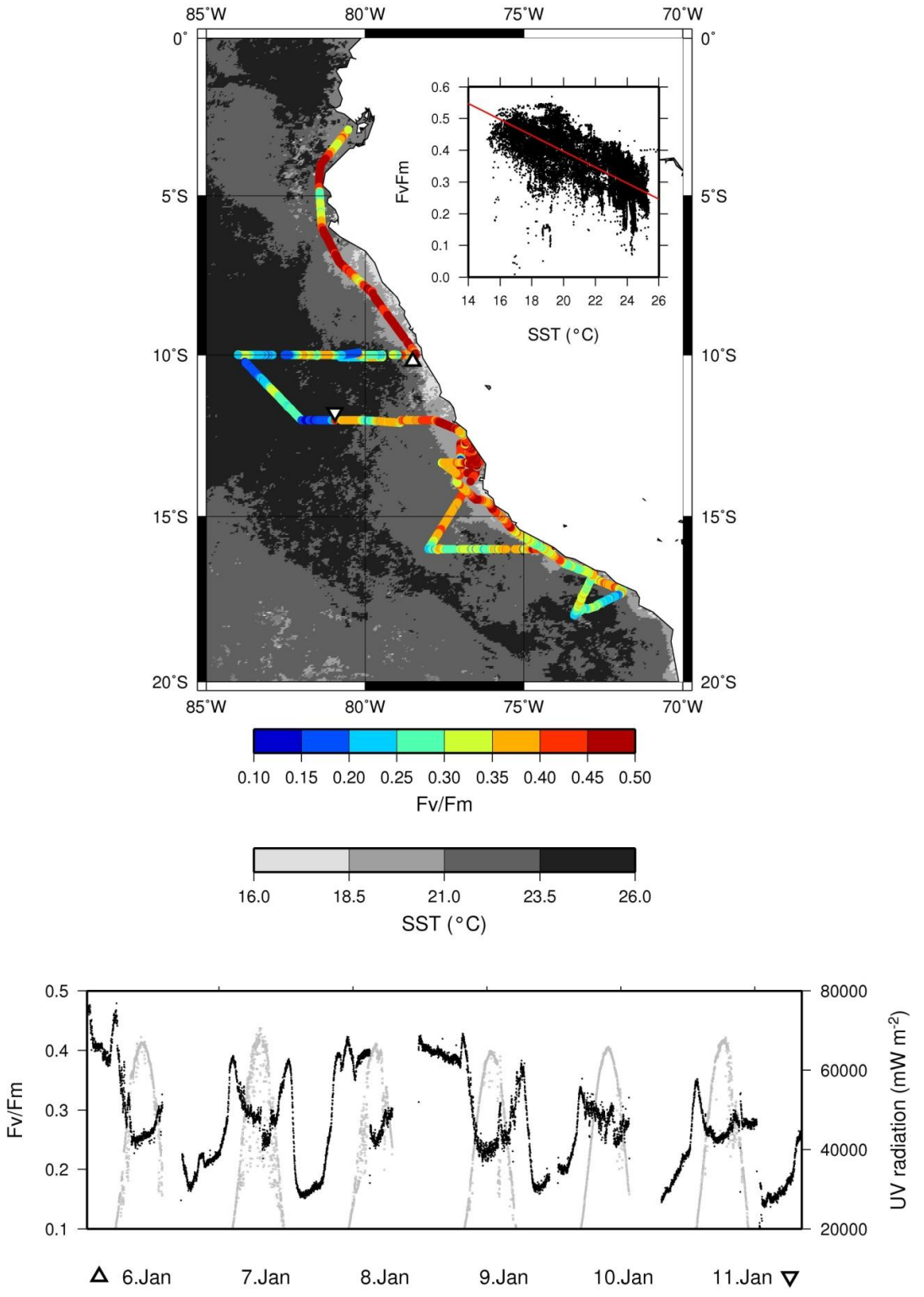

Figure 9: Plot of Satellite sea surface temperature (SST) used to show the distinction between the water below 21°C, that was classified as recently upwelled water and the water with temperatures higher than 21°C. Overlaid are the Fv/Fm values measured continuously by fast repetition rate flurometry in the water surface during the M77/3

cruise. The inlay in the upper right corner shows the correlation between Fv/Fm and the surface water temperature ($r^2 = 0.46$). The triangles on the map mark the start (triangle up) and the end (tiangle down) of the strong cyclic pattern observed in the Fv/Fm parameter(black dots), displayed in the lower panel along with UV irradiance (grey dots), with days (2009) on the x-axis.

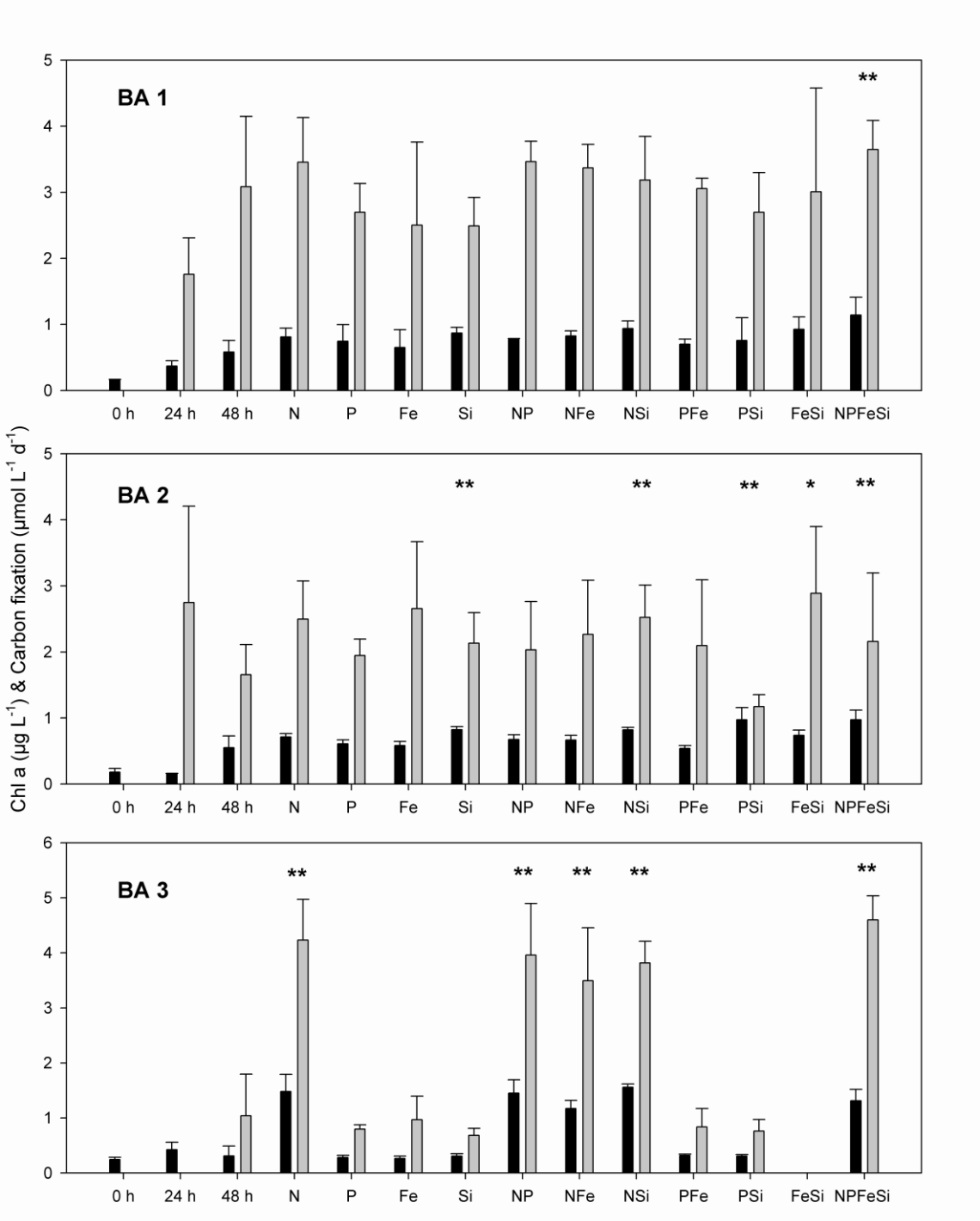

Figure 10: Response of the chlorophyll a concentration (black bars) and carbon fixation (grey bars) to nutrient amendments of 0.2 µM phosphate (P), 1 µM ammoniumnitrate (N), 1 µM silicate (Si), 2 nM iron (Fe) and combined treatments. Highlighted chlorophyll concentrations are significantly different from the 48 h treatment at the $p < 0.05$ (*) and $p < 0.001$ (**) level. Upper panel, bioassay 1 (BA 1, 10°S 082°W), middle panel, bioassay 2 (BA 2, 12°S 082°W), lower panel, bioassay 3 (BA 3, 17.45°S 073°W).

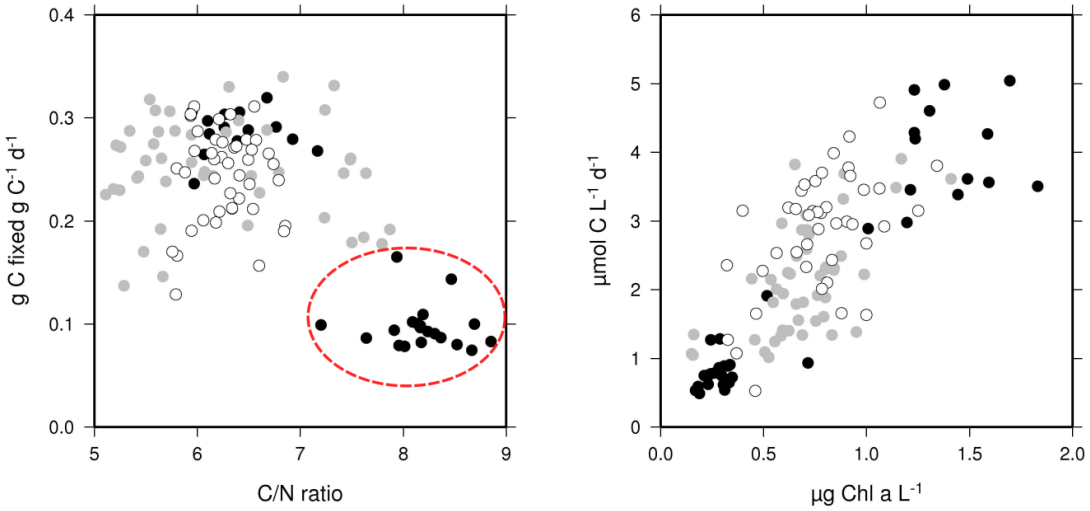

Figure 11: Left panel: An increase in C:N ratio was observed with decreasing carbon specific carbon fixation. The effect was especially pronounced in all treatments of bioassay 3 without added N (indicated by red dashed circle). Right panel: Carbon fixation versus chlorophyll content. Note the good linear correlation between the two parameters, despite different nutrient amendments. Bioassay 1, white circles, bioassay 2, grey circles, bioassay 3, black circles.

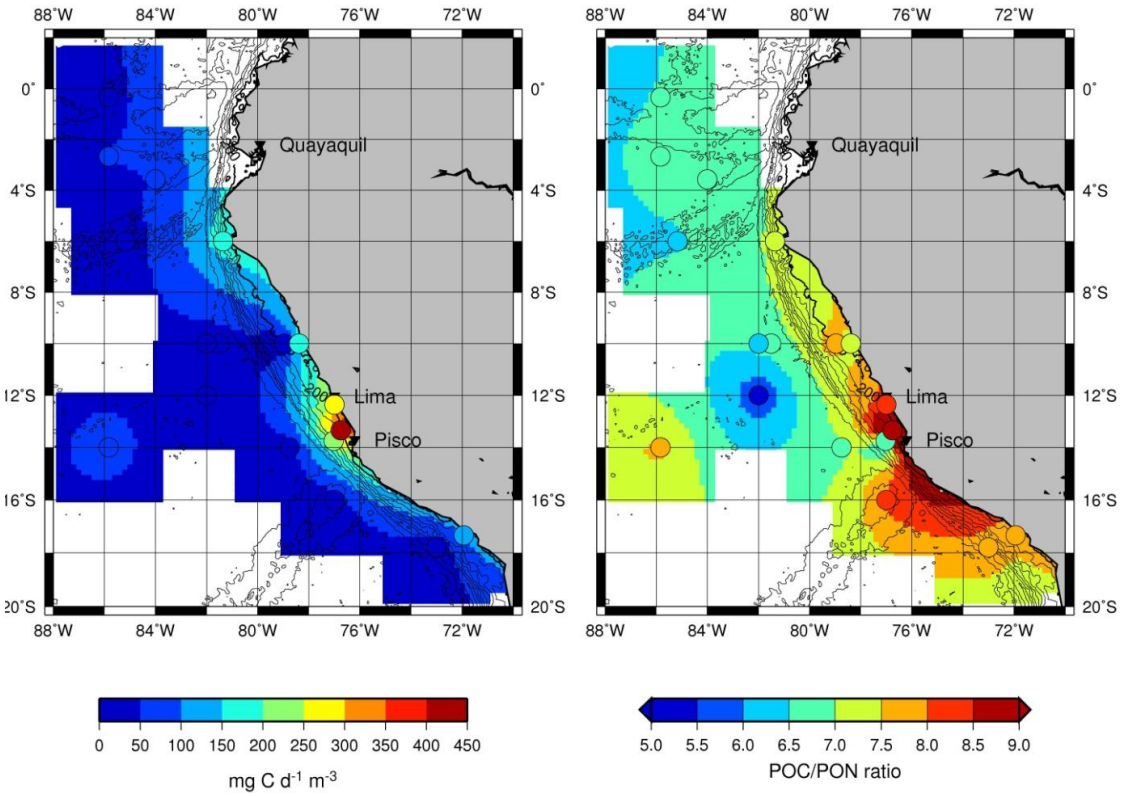

Figure 12: Carbon fixation (left) and POC:PON ration (right) in the surface of the Peruvian upwelling.

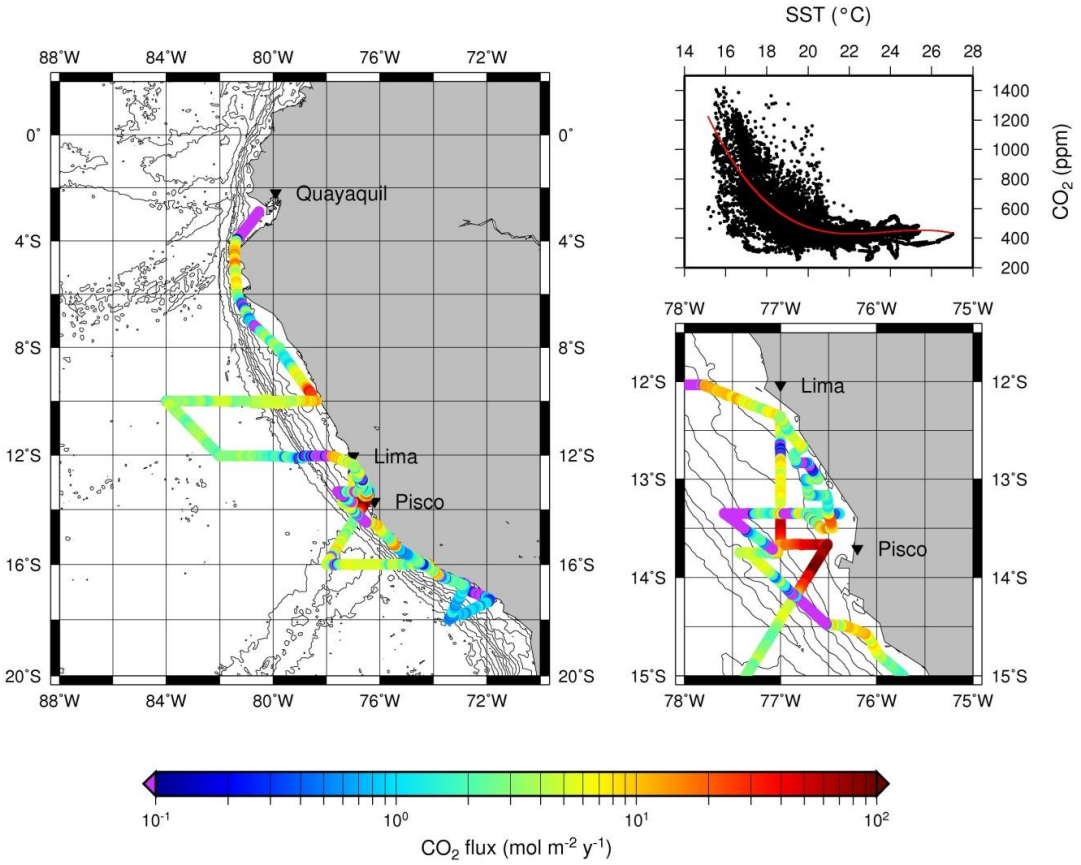

Figure 13: Left panel: Flux of CO_2 as measured on the M77/3 cruise. Purple color indicates CO_2 flux from atmosphere to ocean. The area around Pisco with highest overall fluxes of CO_2 from seawater to atmosphere and from atmosphere to seawater is shown on the bottom right. Upper right: Scatterplot of CO_2 concentration versus surface temperature. The red line represents the cubic fit function (equation 1).

2.3 Heterotropphic N_2 fixation in the Peruvian OMZ

Niche separation of novel groups of bacterial diazotrophs in the largest oxygen minimum zone of the world's ocean

Carolin R. Loescher[1*], Tobias Großkopf[2*], Diana Gill[2], Harald Schunck[2], Nicole Pinnow[1], Falguni Desai[2], Gaute Lavik[3], Marcel M.M. Kuypers[3], Julie LaRoche[2], Ruth A. Schmitz[1]

[1] Institut für Allgemeine Mikrobiologie, Christian-Albrechts-Universität Kiel, Am Botanischen Garten 1-9, 24118 Kiel, Germany

[2] RD2: Marine Biogeochemistry, Helmholtz-Centre for Ocean Research Kiel (GEOMAR), Düsternbrooker Weg 20, 24105 Kiel, Germany

[3] Max-Planck-Institut für marine Mikrobiologie, Celsiusstraße 1, 28359 Bremen, Germany

* Authors contributed equally to this work

Summary

Diazotrophy, the biological reduction of dinitrogen gas (N_2) to bioavailable ammonium (NH_4^+), is the largest source of fixed N compounds (nitrate, nitrite, ammonium) to the oceans. The classical view of the ecological niche for oceanic N_2-fixers (diazotrophs) is tropical oligotrophic surface waters, often completely depleted in fixed N, with microorganisms belonging to the cyanobacterial lineage as the main perpetrator of N_2 fixation. While this may be the case for large areas of the ocean, increasing reports of global diazotroph diversity [1, 2], and modelling studies of the oceanic N cycle [3] suggest that the oceanic diazotrophic niche may be much broader than previously thought. Here, we report on the distribution and relative abundance of novel clades of diazotrophs in the Eastern Tropical South Pacific and the Peru upwelling. The wide distribution of the novel clades throughout the water column extends the habitat of marine diazotrophs to low oxygen/ high nitrate areas. Nitrogen fixation was detected within OMZ waters and was stimulated by the addition of organic carbon sources. Moreover, the co-occurrence of the functional marker gene for N_2-fixation, *nifH*, and active N_2-fixation with key functional genes of nitrification, anammox and denitrification suggests that a close spatial coupling of N-input and N-loss processes exists in the OMZ off Peru. In view of the predicted increase in ocean deoxygenation as a result of global warming [4], our results indicate that the importance of OMZs as hotspots of N_2-fixation may increase in the future.

Introduction

The atmospheric pool of dinitrogen (N_2) is made available to life in the ocean by biological N_2-fixation, a process exclusively performed by diazotrophs, a special group of prokaryotes [5, 6]. Global estimates of N_2- fixation in surface waters (~150 Tg N y^{-1}) [7] cannot balance the nitrogen (N) loss (~ 400 Tg N y^{-1}) [8, 9] resulting from microbial processes such as anammox (the anaerobic oxidation of ammonium with nitrite to N_2 [10, 11]) and denitrification (the 4-step reduction of nitrate (NO_3^-) to N_2 [8, 12]). Both, N-loss processes and N_2-fixation, are strongly sensitive to dissolved oxygen (O_2) concentrations, yet oxygen minimum zones (OMZs) such as those found in the Arabian Sea and the Pacific Ocean [13], are only known for their importance as N-loss regions [5, 14]. It has been recently suggested that the excess phosphorus (P) [15], resulting from enhanced N-loss and from the release of reactive phosphate into the water column from the sediment [16], together with the availability of dissolved iron in OMZs provide environmental conditions favourable for N_2-fixation. Recent reports on the *nifH* gene diversity have suggested that the diazotrophic communities detected in OMZ waters differ

strongly from the classical cyanobacterial-dominated diazotrophic communities found in oligotrophic oceanic waters[17, 18 19-22]. Instead, DNA-based studies off the Californian coast and the Peru upwelling have reported a suite of broadly diverse nitrogenase (*nifH*) gene sequences related to heterotrophic bacteria and dominated by proteobacterial sequences [17, 18]. The role and importance of heterotrophic diazotrophs in the ocean is currently unclear and reports of contaminating *nifH* sequences from various sources call for a careful assessment of the *nifH* diversity based solely on a phylogenetic approach. Confirmation of their importance in OMZ waters requires information on the spatial distribution and relative abundance of diazotrophs present in OMZs.

Here, we present novel data from two cruises to the Eastern Tropical South Pacific (ETSP) off Peru (M77/3 and M77/4 on the German research vessel *Meteor*, Dec. 2008- Feb. 2009). By combining molecular tools with *in situ* rate measurements using $^{15}N_2$- incubations, seven novel *nifH* clusters have been identified with several of the clusters only distinctly related to previously described marine diazotrophs, some of them potentially heterotrophic as suggested by glucose addition experiments. The cluster-specific *nifH* abundance and expression were measured, together with N_2-fixation rate measurements throughout the water column. Further, the observed co-occurrence of genes involved in N_2-fixation and N-loss processes suggest a tight coupling between these opposing processes directly within the OMZs as well as in the overlaying waters.

Results

Diversity of novel *nifH* clusters in the OMZ off Peru

Unexpected high diazotrophic diversity in *nifH* sequences was detected in the OMZ off Peru. A total of 600 DNA and cDNA *nifH* sequences were obtained from clone libraries taken from various stations and depths during two cruises (M77/3, M77/4, 2008/2009) to the OMZ off Peru (Fig. 1, map). The bulk fraction of the *nifH* sequences grouped into seven clusters (further referred to as P1- P7). Those clusters were in large parts amplified from OMZ waters below the euphotic zone, pointing towards a non-phototrophic metabolism in those organisms. The P1 cluster was amplified throughout the water column of the OMZ off Peru, thus dominating large parts of the system. The clusters P1 and P2, whose closest relatives are found within the spirochaeta and archaea, respectively, represented the *nifH* sequences most distantly related to the other clades detected during our study. In addition to those deep branching clusters, the clusters P3-P7 were phylogenetically most closely related to various clades of the proteobacteria, with some similarity to *nifH* genes amplified from hypoxic

basins in the Californian Bight and the OMZs off Peru and Chile [17, 18] (Fig. 1). Sequences of the P8 cluster, have been previously detected in the Tropical South Pacific Ocean [17, 23], and were mainly present in clone libraries from M77/4 along the North-South transect at 85.83°W down to more than 4000m.

nifH sequences belonging to the filamentous non-heterocystous cyanobacterium *Trichodesmium sp.*, to the diatom endosymbiont *Richelia sp.* or to UCYN-A, all of which are considered key diazotrophs in the oligotrophic surface waters of the ocean [24-26] were conspicuously absent from our study area. Sequences of group B most closely related to *Crocosphaera* [27] were the only cyanobacterial sequences recovered to a small extent from some of our clone libraries (1 of ~300 sequences).

Distribution and relative abundance of novel clusters

We designed cluster-specific qPCR primers and TaqMan probes to assess the spatial distribution and relative abundance of the *nifH* gene of the novel diazotrophic clusters throughout the water column of the OMZ off Peru, from surface waters down to 300 m,. Clusters P1 and P4 were present in abundances up to 10^5 *nifH* copies L^{-1}, thus dominating the diazotrophic community from the shelf to about 83°W at 10°S and to 77°W at 16°S (Fig. 2). The P1 cluster was associated with deeper waters (100- 300 m) and thus lower O_2 concentrations, while other clusters (P2, P3, P4, Fig. 2 and Fig. S1) were present in surface to sub-surface waters. Contrary to the general belief that diazotrophs thrive mainly in N-depleted waters, clusters P1, P4 and P8 were present at nitrate (NO_3^-) concentrations up to ~40 μM (Fig. 2). The clusters P1 and P4 showed the highest abundances in coastal stations, while cluster P8 was present throughout the Peruvian OMZ (Fig. 2, 3) and was the dominant diazotroph in the nutrient- depleted open ocean region along the north-south offshore transect (transect C, Fig. 1,3), with abundances reaching up to 10^6 copies L^{-1}. Thus, the abundances of P1 and P8 were inversely correlated with highest abundances on the shelf and off shore, respectively (Fig. S2). *Crocosphaera (CR)*, the only detected diazotroph that belonged to the cyanobacteria, was mainly present in low abundances offshore in waters with high NO_3^- concentrations. However, at 16°S, *nifH* genes affiliated to CR were detected on the shelf as well (Fig. 2). The distribution of CR suggests that parameters other than NO_3^- influence their presence or absence; however, abundances of CR were generally low compared to other diazotrophs and it is unclear if CR played an active role in fixing N_2 in the OMZ off Peru during our study.

***In situ* N_2-fixation**

The activity of the diazotrophic community was monitored by following the incorporation of $^{15}N_2$, added in trace amounts during a 24 hour incubation of water samples. A broad peak of N_2-fixation extending into the OMZ (beginning at ~ 40 m) could be observed offshore from 79.134°W to 81.361°W with up to 0.4 nmol N L^{-1} d^{-1} at 200 meters depth (Fig. 4, Fig. S3). Analysis of endpoints of $^{15}N_2$- incubation experiments (Fig. 4) demonstrated the exclusive presence of P1, P4 and P7 *nifH* genes in the different treatments at station #3 (10°S 81.3°W) (Fig. 4, Fig. S4 shows a similar experiment at a more coastal station). While the addition of glucose (2 µM) stimulated the growth of clusters P1, P4 and P7, the combined addition of glucose and oxygen (10 µM) promoted exclusively the growth of P7. Clusters P1 and P4 were negatively affected by the addition of oxygen, even in the presence of glucose. This suggests a potential switch to a dominance of members from the P7 cluster when O_2 is transported (e.g. by O_2 intrusions or lateral mixing) into the OMZ, thus demonstrating the capability of the diazotrophic community to react to rapidly changing O_2 conditions. Highest N_2-fixation rates in this experiment were measured along with an increase of *nifH* copy numbers of a combination of P1, P4 and P7 when glucose but no O_2 was added (in situ concentrations ~ 1.85 µM), thus pointing towards an heterotrophic mode of diazotrophy that might be limited by the availability of reduced carbon compounds.

Further south, N_2-fixation rates increased showing higher activity in surface waters than at depth, consistent with low N: P ratios (resulting in high P*), there. Highest N_2-fixation rates of 24.8 ± 8.4 nmol N d^{-1} L^{-1} were measured on the Peruvian shelf between Lima and Pisco (12.37°S/ 77°W) in surface waters, where *nifH* cDNA of CR, P1 and P5 were expressed (samples specifically collected for mRNA purification, Fig. 5). At this station, large parts of the water column were fully anoxic (Fig. 5), and hydrogen sulfide (H_2S) was present. Below 30 m depth, the water was depleted in NO_3^- and NO_2^-, the key substrates for anammox and denitrification, thus N-loss processes were likely limited by substrate availability. However, ammonia was present in concentrations of 2-4 µM below the oxycline. Integrated water column N_2-fixation exceeded 800 µmol N d^{-1} m^{-2}, a rate comparable to those reported from major *Trichodesmium* blooms [28]. The peak in P1 *nifH* expression present at 80 m along with a maximum in N_2-fixation, here, indicates an active involvement of this cluster in N_2-fixation at depth (Fig. 5).

Co-occurrence of N_2-fixation and N-loss processes

High *nifH* gene abundances of cluster P1, coincident with maxima in abundance of key genes of archaeal ammonia- oxidizers (archaeal *amoA*, coding for the ammonia monooxygenase), denitrifiers (*nirS*, coding for the cd1-containing nitrite reductase) and anammox bacteria (*hzo*, coding for the hydrazine oxidoreductase) suggests a close spatial coupling between N_2-fixation and N-loss (Fig. 3) as previously proposed by the model prediction of Deutsch *et al.* 2007 [15]. A close correlation of P1 and NO_2^- was detected, which is most pronounced along 10°S (Fig. S5). This finding is in line with the significant correlation of P1 and *hzo* ($n = 113$, $r = 0.591$) and P1 and archaeal *amoA* ($n = 237$, $r = 0.56$), at 10°S.

Of all key genes involved in N-cycling, archaeal ammonia oxidizer associated *amoA* sequences were the most frequently detected, sometimes accounting for up to 80% of total microbial cells assuming one *amoA* gene copy per cell (Fig. S6).

Conclusions

We detected seven novel clusters of diazoptrophs within the Peruvian upwelling system and its associated OMZ. Together with the cyanobacterium *Crocosphaera* and a cluster previously detected in the Tropical Pacific Ocean (P8), these novel clusters were widely distributed over the Peruvian upwelling system. The observed patterns of distribution suggest preferences and specialization of each cluster towards different environmental conditions. A major contribution of heterotrophic diazotrophs to N_2-fixation among the novel clusters was demonstrated in fertilization experiments with glucose. Further, the co-occurrence of cluster P1 with key functional genes for nitrification and anammox suggests a close spatial coupling of N-input and N-loss processes in the OMZ off Peru, with the potential to redress to some extent the N- deficit generated on the shelf area as the water flows towards the open ocean. Moreover, the measured high N_2-fixation rate detected at a sulphidic shelf station indicates that such transient events, which have previously been reported to occur in intense OMZs [29], might sporadically trigger significant N_2-fixation in N-depleted sulfidic waters.

The abundance of *nifH* throughout the water column down to 1000 m and the detection of active N_2 fixation inside the OMZ point towards a significant contribution of mesopelagic N_2-fixation in OMZ waters, suggesting significant N-input in the OMZ in addition to surface N_2-fixation. The activity of diazotrophs below the euphotic zone is currently not considered in estimate of global N_2 fixation rates either from biogeochemical models, or derived from geochemical tracers or by direct measurements. Therefore the extension of the diazotrophic

niche into the mesopelagic realm has far reaching consequences for budgeting of the marine nitrogen cycle.

Taken together our findings imply a major paradigm shifts in understanding oceanic N_2-fixation, by extending the niches of diazotrophs towards high nitrogen and low oxygen environments, demonstrating the co-occurrence of N_2-fixation and N-loss and indicating a major dependency of diazotrophic clusters on O_2 and reduced carbon compounds, rather than on the surface fixed N concentration.

Methods summary

Hydrographic parameters and nutrients

Samples for salinity, O_2 concentrations and nutrients were taken from a 24-Niskin- bottle rossette equipped with a CTD sensor or a pump-CTD. Oxygen concentrations were determined according to the Winkler method, salinity and nutrient concentrations were determined as decribed [30].

Molecular genetic methods

Samples for the extraction of DNA/ RNA were taken by filtering a volume of about 2 L (exact volumes were determined and recorded continuously) of seawater through 0.2 µm polyethersulfon membrane filters (Millipore, Billerica, MA, USA). The filters were immediately frozen and stored at -80°C. Specific RNA samples were taken by filtering recorded volumes of seawater for a time intervall not exceeding 20 min.

DNA and RNA was extracted using the Qiagen DNA/RNA All prep Kit (Qiagen, Hilden, Germany) according to the manufacturers protocol. Nucleic acid concentrations were determined using PicoGreen and RiboGreen (Invitrogen, Carlsbad, CA) measurements.

Residual DNA was removed from the purified RNA by a Dnase I treatment (Invitrogen, Carlsbad, CA). Purity of RNA was checked by 16S rDNA PCR amplification prior to reverse transcription. The extracted RNA was gene specifically reverse transcribed to cDNA using the Superscript III First Strand synthesis Kit (Invitrogen, Carlbad) following the manufacturers' protocol.

NifH was amplified by PCR with primers and probes according to [22, 31]. For the novel *nifH* clusters qPCR primers and probes were designed with the Primer Express software package, oligonucleotide sequences and qPCR conditions are given in Tab.1. *AmoA* PCRs and quantitative PCRs were performed as described in Loescher (submitted 2011); *nirS* and *hzo* were amplified according to Lam (2007) and Schmid (2010).

Cloning of PCR amplicons was performed using the Topo TA Cloning®Kit (Invitrogen, Carlsbad, CA) according to the manufacturers' instructions. Sanger sequencing was carried out by the Institute of Clinical Molecular Biology, Kiel. Sequences were analyzed using the ClustalW multiple alignment tool on a 321 bp fragment for *nifH*, sequence differences were set on a minimum of 5%, phylogenetic trees were made using distance-based neighbour-joining analysis.

$^{15}N_2$ seawater incubations

Seawater incubations were performed in triplicates at 6 stations in the OMZ off Peru (M77/3) as previously described [32, 33]. The method used might however lead to an underestimation of the true N_2 fixation rates, as suggested recently[34, 35]. P* was calculated according to Deutsch *et al.* 2007 [15].

References

1. Farnelid, H. et al. Nitrogenase Gene Amplicons from Global Marine Surface Waters Are Dominated by Genes of Non-Cyanobacteria. Plos One 6 (2011).
2. Gaby, J. C. & Buckley, D. H. A global census of nitrogenase diversity. Environmental Microbiology 13, 1790-1799 (2011).
3. Codispoti, L. A. An oceanic fixed nitrogen sink exceeding 400 Tg Na-1 vs the concept of homeostasis in the fixed-nitrogen inventory. Biogeosciences 4, 233-253 (2007).
4. Matear, R. J. & Hirst, A. C. Long-term changes in dissolved oxygen concentrations in the ocean caused by protracted global warming. Global Biogeochemical Cycles 17 (2003).
5. Capone, D. The marine nitrogen cycle. Microbe 3 (2008).
6. Moisander, P. H. et al. Unicellular Cyanobacterial Distributions Broaden the Oceanic N-2 Fixation Domain. Science 327, 1512-1514 (2010).
7. Gruber, N. & Galloway, J. N. An Earth-system perspective of the global nitrogen cycle. Nature 451, 293-296 (2008).
8. Codispoti, L. A. An oceanic fixed nitrogen sink exceeding 400 Tg Na(-1) vs the concept of homeostasis in the fixed-nitrogen inventory. Biogeosciences 4, 233-253 (2007).
9. Karl, D. et al. Dinitrogen fixation in the world's oceans. Biogeochemistry 57, 47-+ (2002).
10. Dalsgaard, T., Canfield, D. E., Petersen, J., Thamdrup, B. & Acuna-Gonzalez, J. N-2 production by the anammox reaction in the anoxic water column of Golfo Dulce, Costa Rica. Nature 422, 606-608 (2003).
11. Kuypers, M. M. M. et al. Anaerobic ammonium oxidation by anammox bacteria in the Black Sea. Nature 422, 608-611 (2003).
12. Falkowski, P. G. Evolution of the nitrogen cycle and its influence on the biological sequestration of CO2 in the ocean. Nature 387, 272-275 (1997).
13. Stramma, L., Johnson, G. C., Sprintall, J. & Mohrholz, V. Expanding oxygen-minimum zones in the tropical oceans. Science 320, 655-658 (2008).
14. Codispoti, L. A. Interesting Times for Marine N_2O. Science 327, 1339-1340 (2010).
15. Deutsch, C., Sarmiento, J. L., Sigman, D. M., Gruber, N. & Dunne, J. P. Spatial coupling of nitrogen inputs and losses in the ocean. Nature 445, 163-167 (2007).

16. Ingall, E. & Jahnke, R. Evidence for enhanced phosphorus regeneration from marine sediments overlain by oxygen depleted waters. Geochimica et Cosmochimica Acta 58, 2571-2575 (1994).
17. Fernandez, C., Farias, L. & Ulloa, O. Nitrogen Fixation in Denitrified Marine Waters. Plos One 6(6): e20539 (2011).
18. Hamersley, M. R. et al. Nitrogen fixation within the water column associated with two hypoxic basins in the Southern California Bight. Aquatic Microbial Ecology 63, 193-+ (2011).
19. Falcon, L. I., Cipriano, F., Chistoserdov, A. Y. & Carpenter, E. J. Diversity of diazotrophic unicellular cyanobacteria in the tropical North Atlantic Ocean. Applied and Environmental Microbiology 68, 5760-5764 (2002).
20. Zehr, J. P., Carpenter, E. J. & Villareal, T. A. New perspectives on nitrogen-fixing microorganisms in tropical and subtropical oceans. Trends in Microbiology 8, 68-73 (2000).
21. Zehr, J. P. & Turner, P. J. in Methods in Microbiology, Vol 30 271-286 (Academic Press Inc, San Diego, 2001).
22. Langlois, R. J., LaRoche, J. & Raab, P. A. Diazotrophic diversity and distribution in the tropical and subtropical Atlantic ocean. Applied and Environmental Microbiology 71, 7910-7919 (2005).
23. Halm, H. et al. Heterotrophic organisms dominate nitrogen fixation in the South Pacific Gyre. ISME J (2011).
24. Church, M. J., Jenkins, B. D., Karl, D. M. & Zehr, J. P. Vertical distributions of nitrogen-fixing phylotypes at Stn ALOHA in the oligotrophic North Pacific Ocean. Aquatic Microbial Ecology 38, 3-14 (2005).
25. Montoya, J. P. et al. High rates of N-2 fixation by unicellular diazotrophs in the oligotrophic Pacific Ocean. Nature 430, 1027-1031 (2004).
26. Zehr, J. P. & Ward, B. B. Nitrogen cycling in the ocean: New perspectives on processes and paradigms. Applied and Environmental Microbiology 68, 1015-1024 (2002).
27. Zehr, J. P., Mellon, M. T. & Zani, S. New nitrogen-fixing microorganisms detected in oligotrophic oceans by amplification of nitrogenase (nifH) genes (vol 64, pg 3444, 1998). Applied and Environmental Microbiology 64, 5067-5067 (1998).

28. Capone, D. G. et al. Nitrogen fixation by Trichodesmium spp.: An important source of new nitrogen to the tropical and subtropical North Atlantic Ocean. Global Biogeochemical Cycles 19, 17 (2005).
29. Naqvi, S. W. A. et al. Increased marine production of N_2O due to intensifying anoxia on the Indian continental shelf. Nature 408, 346-349 (2000).
30. Grasshoff, G., Kremling, K., Erhardt, M. . Methods of seawater analysis (Wiley VCH, Weinheim, 1999).
31. Zani, S., Mellon, M. T., Collier, J. L. & Zehr, J. P. Expression of nifH genes in natural microbial assemblages in Lake George, New York, detected by reverse transcriptase PCR. Applied and Environmental Microbiology 66, 3119-3124 (2000).
32. Capone, D. G. Marine nitrogen fixation: what's the fuss? Current Opinion in Microbiology 4, 341-348 (2001).
33. Montoya, J. P., Voss, M., Kahler, P. & Capone, D. G. A simple, high-precision, high-sensitivity tracer assay for N-2 fixation. Applied and Environmental Microbiology 62, 986-993 (1996).
34. Grosskopf, T. submitted.
35. Mohr, W., Grosskopf, T., Wallace, D. W. R. & LaRoche, J. Methodological underestimation of oceanic nitrogen fixation rates. PLoS One 5, e12583 (2010).
36. Turk, K. A. et al. Nitrogen fixation and nitrogenase (nifH) expression in tropical waters of the eastern North Atlantic. Isme Journal 5, 1201-1212 (2011).

Supplementary Information is linked to the online version of the paper at www.nature.com/nature

Acknowledgments

We thank the authorities Peru for the permission to work in their territorial waters. We acknowledge the support of the captain and crew R/V Meteor as well as the chief scientists Martin Frank and Lothar Stramma. Moreover, we thank I. Grefe for sampling during M77/4; we further thank K. Stange, F. Malien, V. Leon and P. Fritsche for oxygen and nutrient measurements. We thank G. Klockgether for assisting with the mass spectrometry. Financial support for this study was provided by the DFG Sonderforschungsbereich 754 (www.sfb754.de). G.L. was funded by the MPI Bremen.

Author contributions C.R.L., T.G., H.S. and J.LR. collected the samples and performed the experiments. C.R.L. and D.G. did the extraction and qPCR of *nifH* DNA from transect stations. C.R.L., T.G.,N.P., F.D. and D.G. did cloning of *nifH* DNA and cDNA. T.G. and H.S. extracted DNA and RNA from experimental stations. T.G. and C.R.L. did qPCR with *nifH* DNA of experimental stations. T.G. performed flow cytometry measurements and analyzed the C and N fixation data. C.R.L wrote the manuscript with T.G., R.A.S. and J.LR.. M.M.M.K., G.L., R.A.S., J.LR., T.G. and C.R.L. designed the experiments and analyzed the data.

Author information Reprints and permissions information is available at www.nature.com/reprints. The authors declare no competing financial interests. Correspondence and requests for materials should be addressed to cloescher@ifam.uni-kiel.de

Tab 1: Primers and PCR conditions. For real-time qPCR the initial denaturing step was 10 min at 95°C, annealing temperatures were the same as in the end point PCRs, no final extension step took place, 40 cycles were performed followed by melting curve analysis.

Cluster	reference sequence (GenBank accesion no.)	Forward primer 5'- 3'	Reverse primer 5'- 3'	Probe	annealing temperature [°C]
P1	M773_3_70_4	GGACTACATTCGGACTAG	GTCGTAACCACGATCTAG	TCTTCAAAATCCCGCGTCCCG (antisense)	60
P2	M773_3_150_7	GGTGTTCTATGTGTTGAA	GTAGGAGTTACGAATTGG	TCGCCTAGCACATCATAGATCAC (antisense)	50
P3	M773_56_100_1	CACAGTTAGAGAGGTAGG	CAAGGTCGTCAGTAAAAG	AGCTCGACAAGGTAATGTTCACA (sense)	
P4	M773_22_30_1	CTCGCACAGAAATCAGTG	GCATGTTAATGGAAGTGATG	ACGTCGAACTCGAAGACATCCG (sense)	60
	M773_56_85_3	GCTCAATCTACAATTATGC	GCTGTAATAACTCCTCTAC	ACCACCTGACTCAGTACAATTAATGT	50
P7	M773_28_115_1	GGTTCTGTTGAAGACATC	CGAAGTCTAAGTCTTCTTC	ATCGCTGTGATTACACCACGAC (antisense)	52
P8 (Halm, submitted)	M774_800m_11B14a	ACTCGTCTGACTTCAC	TTAATACATCGTTCCA	AAAGCACAGAATCATG	52

Figure legends

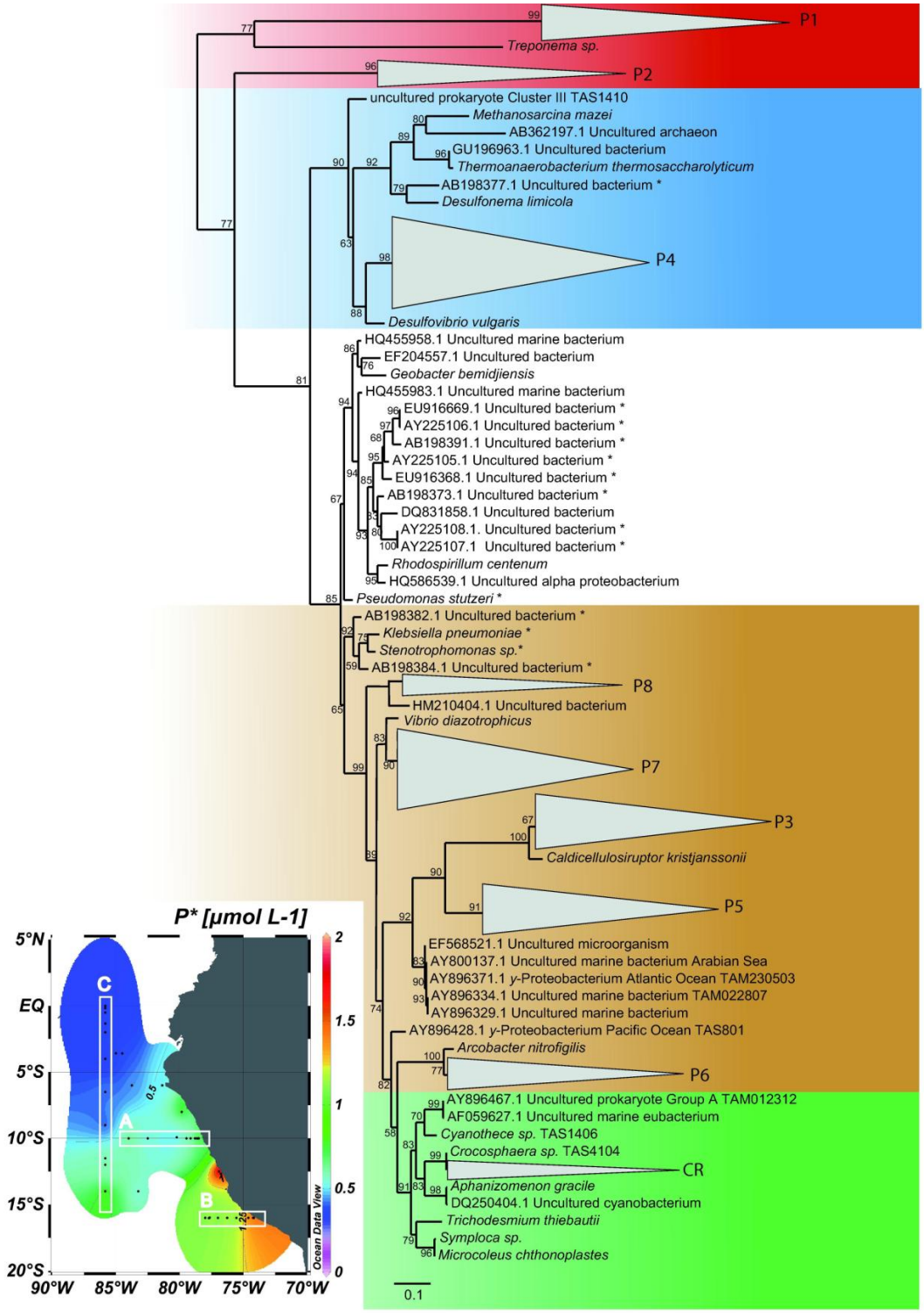

Fig. 1: Phylogenetic tree based on the analysis of ~600 nifH gene and transcript sequences retrieved in this study. The newly identified clusters are indicated by grey

triangles. Cyanobacterial sequences are highlighted in green, proteobacterial sequences are highlighted in brown, Cluster III sequences as defined by Zehr et al. (2000) [20] are shown in blue, and two novel deep branching clusters are highlighted red. Bootstrapped values (%) above 50, out of 100 are shown on branches. The scale bar represents 10% estimated sequence divergence. Sequences marked with an asterisk indicate likely contaminated PCR products previously reported by Turk et al. 2011[36], the novel clusters are mostly distant from those sequences.

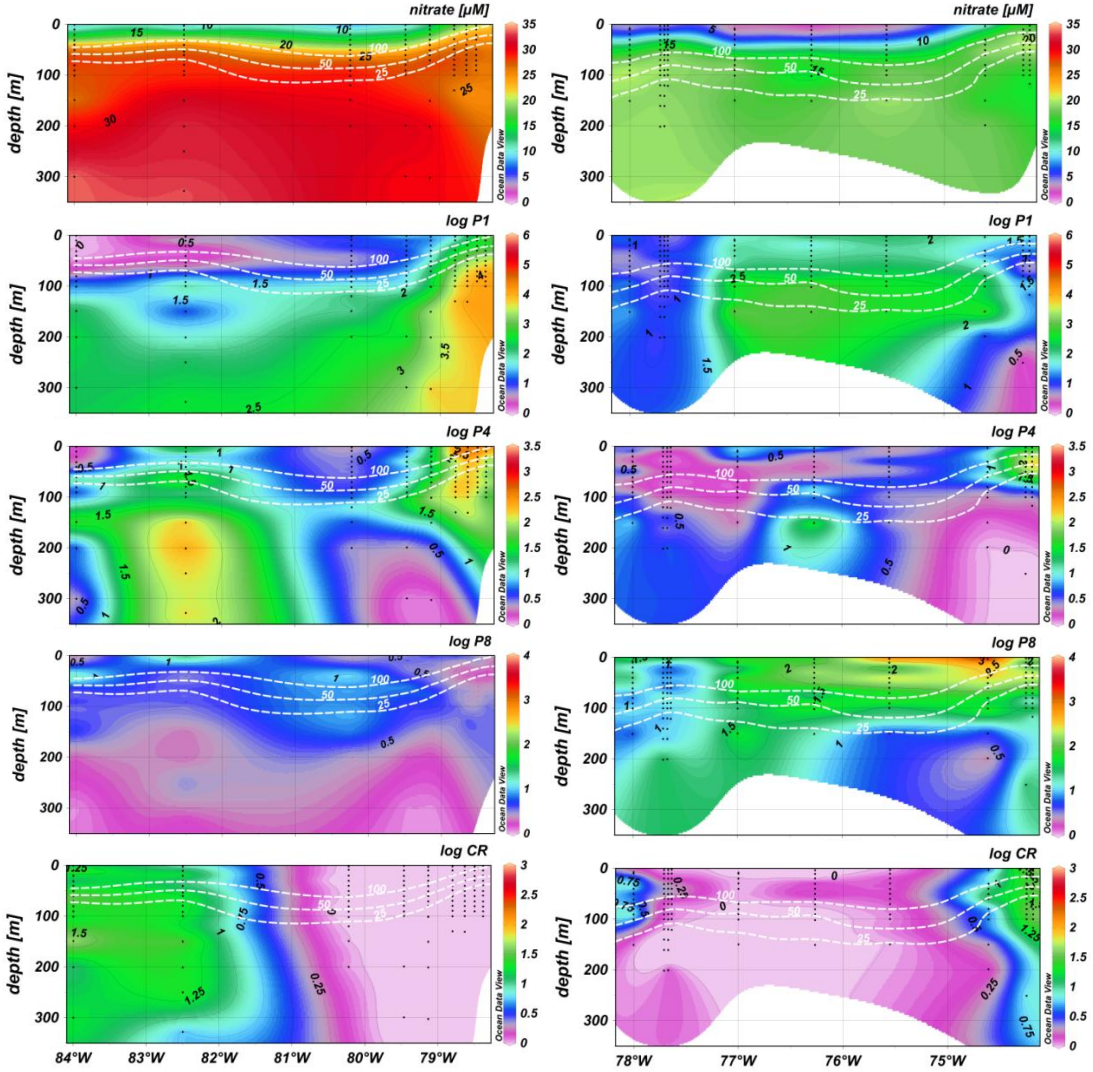

Fig. 2: Distribution of NO_3^-, O_2 and the newly identified *nifH* clusters: NO_3^- (µM), *nifH* clusters P1, P4, P8 and *Crocosphaera* (log_{10} copies L^{-1}) along (A) 10°S and (B) 16°S. The depth of 25, 50 and 100 µM oxygen concentration are indicated with white contour lines.

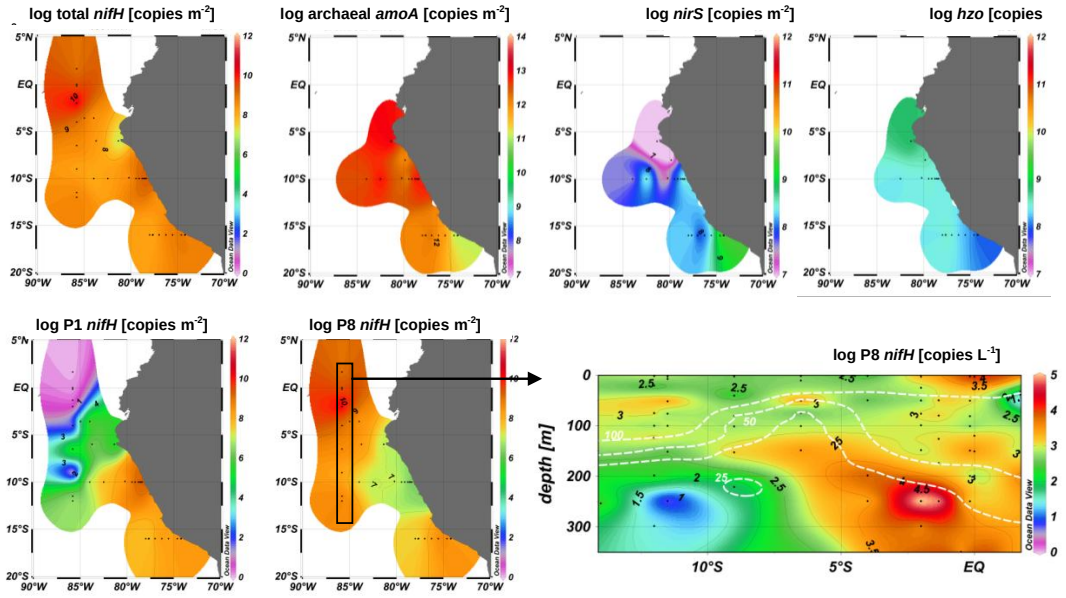

Fig. 3: Depth integrated horizontal distribution of functional key genes of N-loss processes and N_2-fixation in the upper 350 m in the Peruvian OMZ: archaeal *amoA* (functional marker for archaeal ammonia oxidation), *nirS* (functional marker for denitrification), *hzo* (functional marker for anammox), *nifH* for diazotrophs clusters P1, P8 and total *nifH* (log_{10} copies L^{-1}). The section shows the vertical distribution of the dominant *nifH* cluster P8 (log_{10} copies L^{-1}, measured by qPCR) along a North-South transect at 85.83°W as indicated by the black box on the map, the depth of 25, 50 and 100 µM oxygen concentration are indicated with white contour lines.

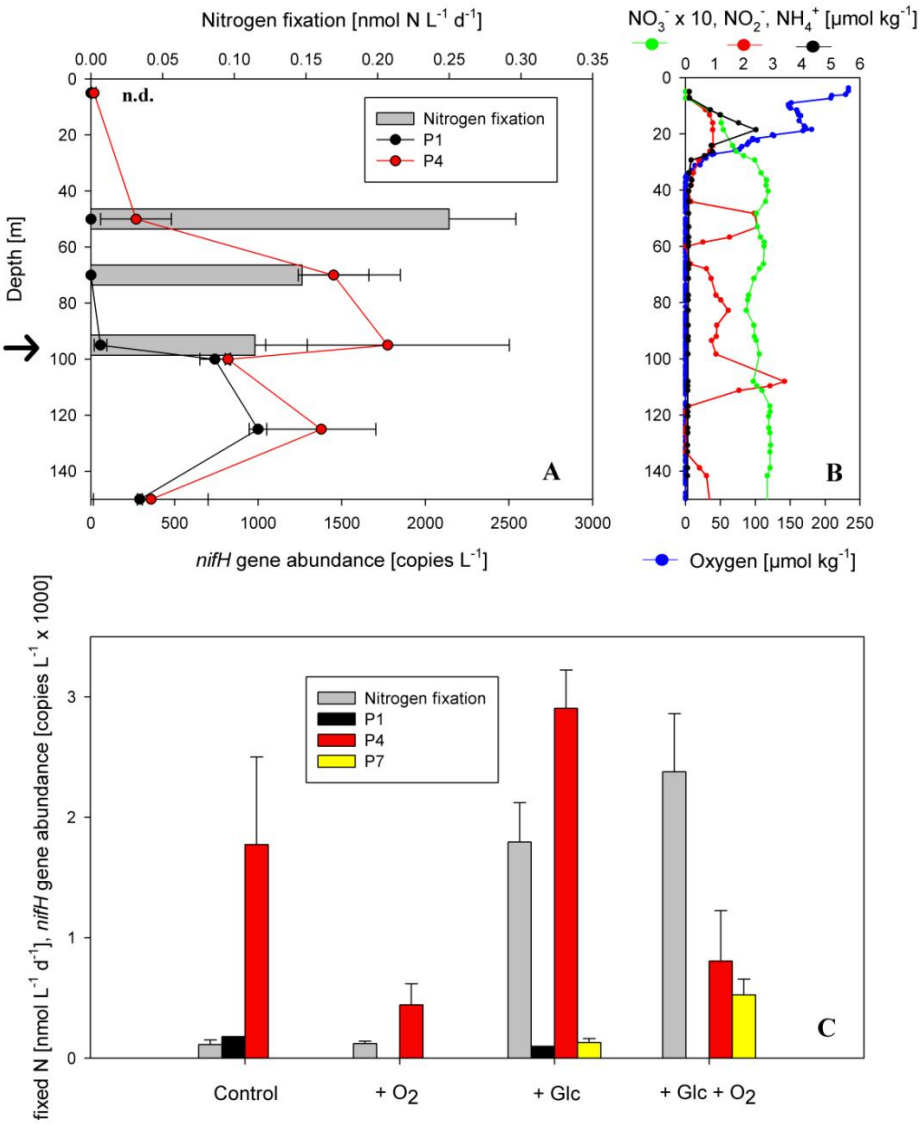

Fig. 4: **Vertical profiles of N_2- fixation**: (A) Water column N_2- fixation determined by 24h $^{15}N_2$- incubation experiments along with the initial vertical distribution of *nifH* clusters P1 and P4 at station #3 (Fig.1, map, 10°S/ 81.3°W). (B) O_2 and nutrient concentrations at the same station. (C) The effect to the addition of glucose (2µM) and oxygen (10 µM) on N_2-fixation as well as on the *nifH* gene abundances of the detectable clusters P1, P4 and P7 (both as end-point measurements in 24 h incubations, samples from 95m depth indicated by an arrow in panel A)) were determined.

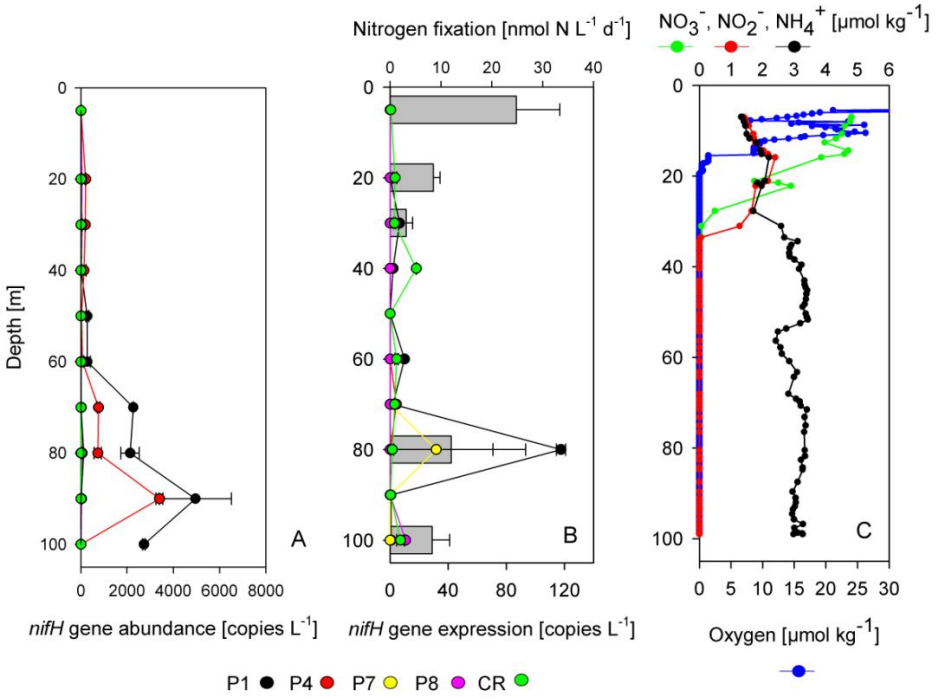

Fig. 5: Vertical distribution of (A) the *nifH* gene abundance, (B) the measured N_2-fixation and *nifH* gene expression (dashed line, second x- scale, samples have specifically collected for RNA extraction), and (C) chemical parameters (O_2, NO_3^-, NO_2^-, NH_4^+) at a coastal sulphidic station (M77/3, #19, 12.37°S/ 77°W)

Supplementary information

Distribution of additional novel *nifH* clusters

Although clusters P2, P3, P6 and P7 showed lower *nifH* abundance than the previously discussed clusters, they show a specific distribution along vertical and horizontal gradients. Generally, those clusters appear in higher abundance at 16°S, where N/P ratios were close to zero in surface and the OMZ had high P* values reaching 2 µM.

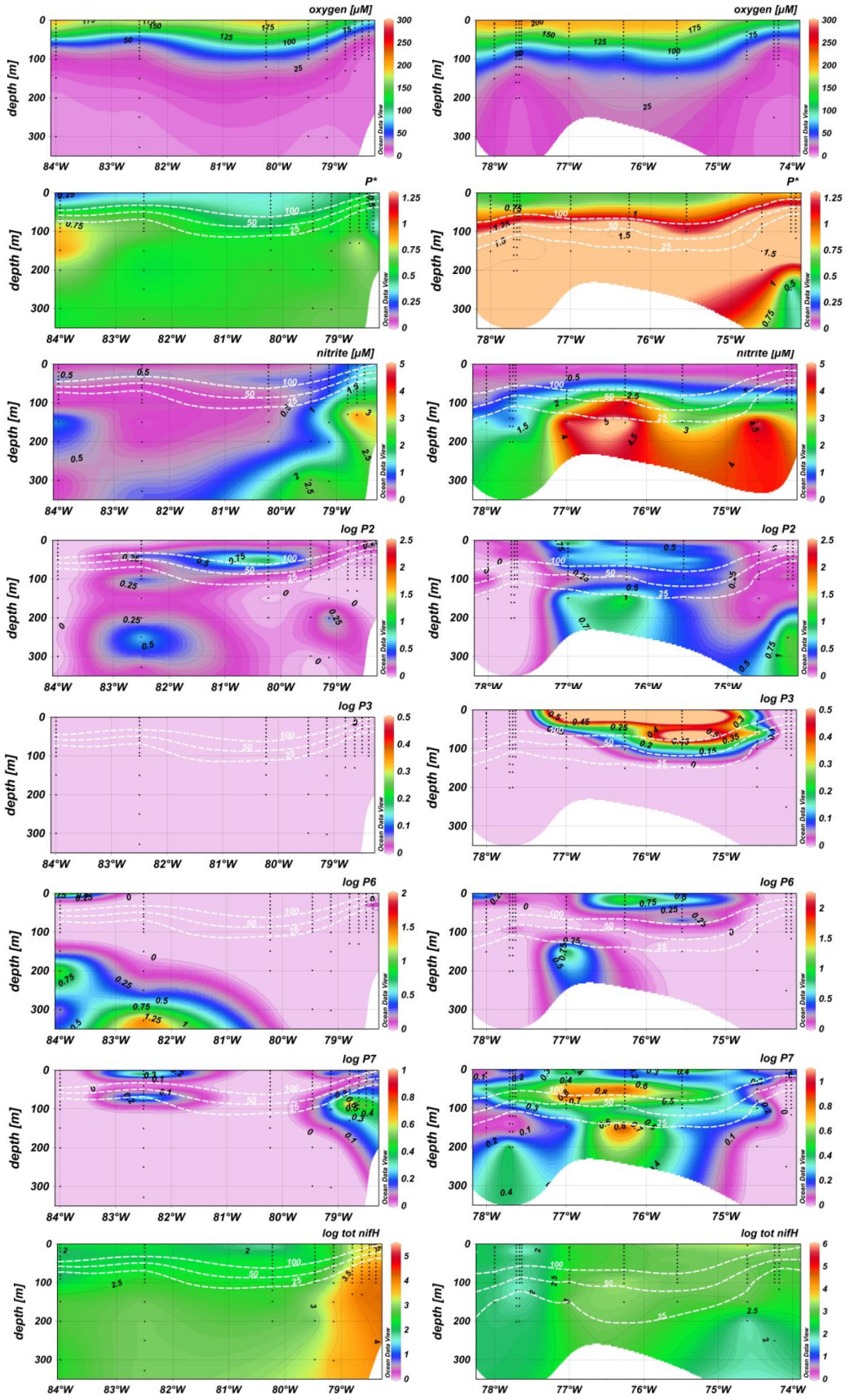
oxygen [µM]
P*
nitrite [µM]
log P2
log P3
log P6
log P7
log tot nifH
depth [m]
Ocean Data View
84°W 83°W 82°W 81°W 80°W 79°W
78°W 77°W 76°W 75°W 74°W

Fig. S1: Distribution of P*, NO_2^- and novel *nifH* clusters: Oxygen, P*, NO_2^- (µM), *nifH* clusters P2, P3, P6 and P7 and total nifH (log_{10} copies L^{-1}) along (A) 10°S and (B) 16°S. The 25, 50 and 100 µM oxygen concentrations are indicated with white contour lines.

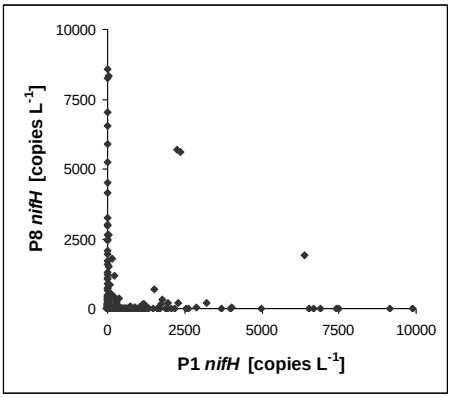

Fig. S2: P1 *nifH* gene abundance versus P8 *nifH* gene abundance, showing the mutual exclusion of the two clusters.

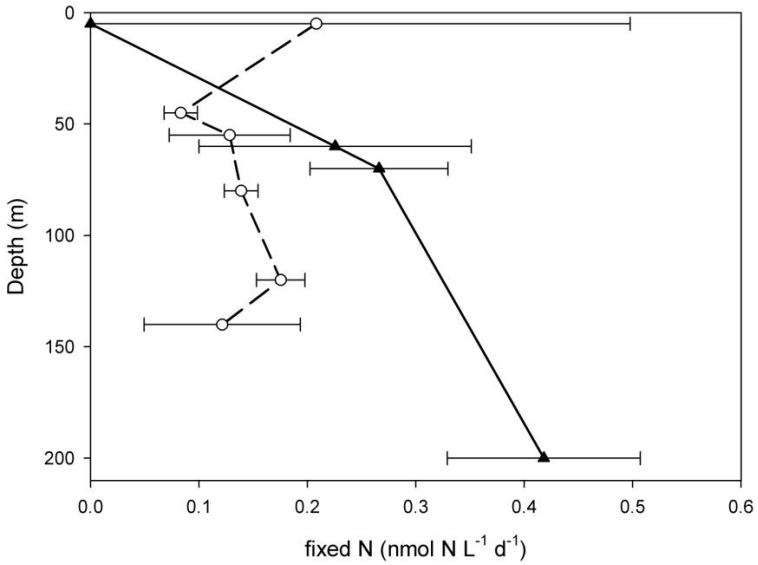

Fig. S3: **Vertical profiles of N_2- fixation**: 24h $^{15}N_2$- incubation experiments at two stations at 10°S (# 805 at 79.134°W and # 811 at 81.361°W, left panel).

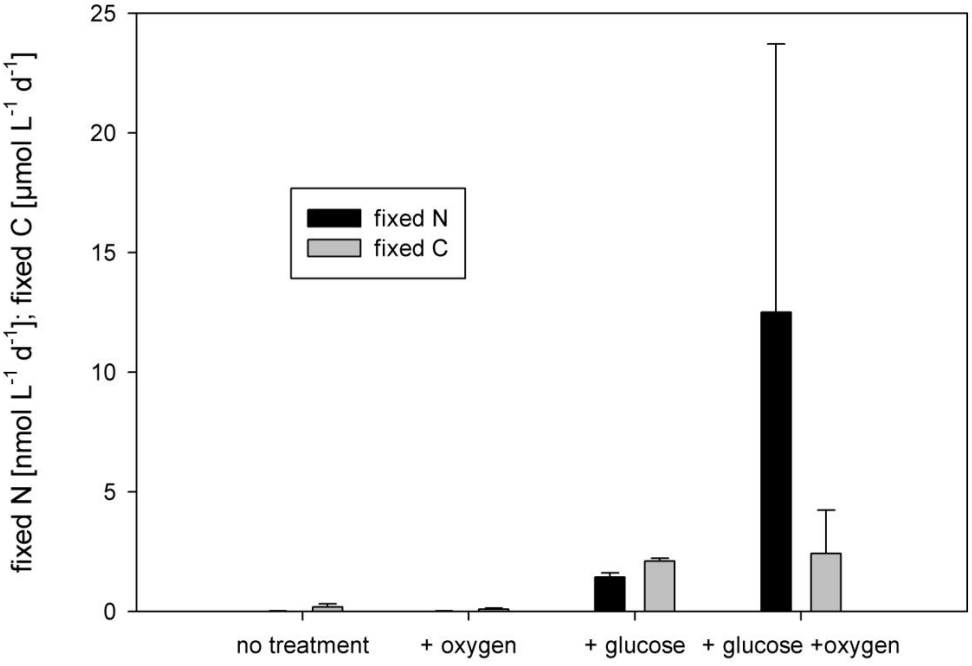

Fig. S4: N_2- fixation was triggered in incubation experiments (#807, 20 m depth) by glucose and glucose/ oxygen addition

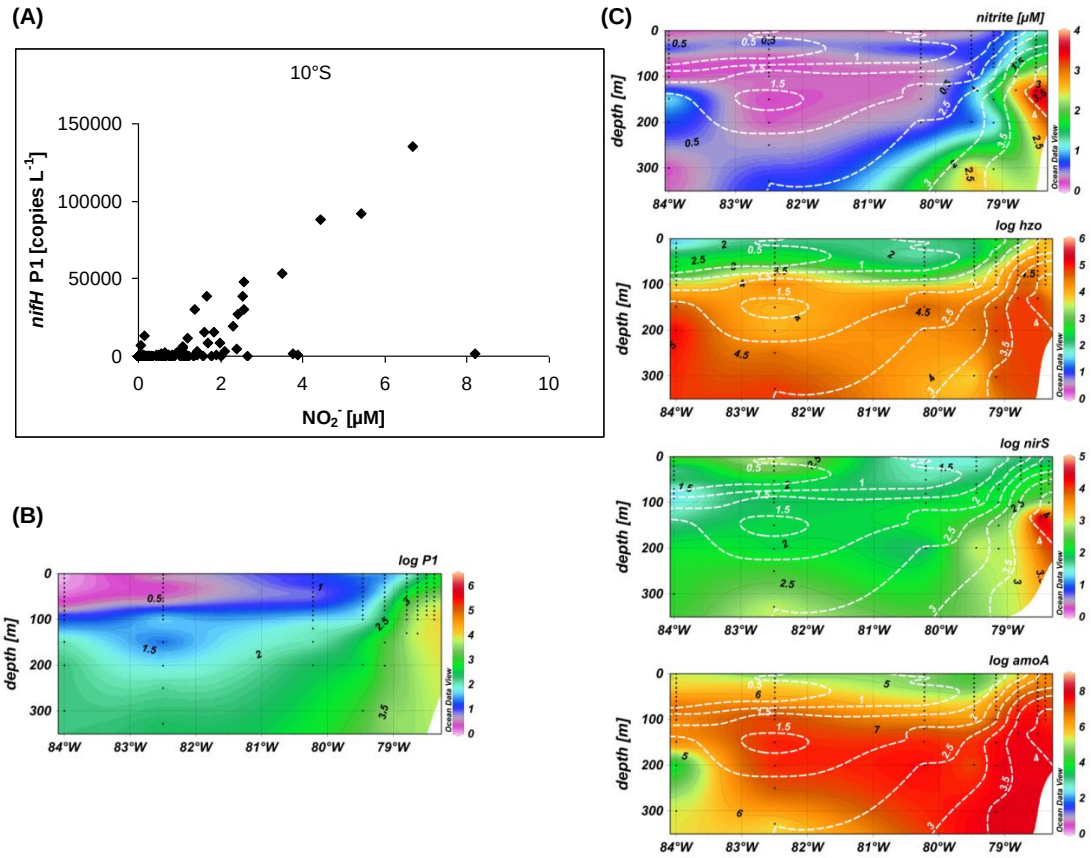

Fig. S5: Correlation of *nifH* P1 and NO_2^- : (A) A significant correlation of P1 and NO_2^- was detected along 10°S (n = 112, r = 0.799). This finding is in line with the significant correlation of P1 and *hzo* (n = 113, r = 0.591) and P1 and archaeal *amoA* (n = 237, r = 0.56), at 10°S. (B) Distribution of P1 nifH [$\log_{10}$ copies L^{-1}] along 10°S, (C) NO_2^- [µM], *nirS*, *hzo* and *amoA* sections section overlaid by P1 [$\log_{10}$ copies L^{-1}] indicated by dashed white contour lines.

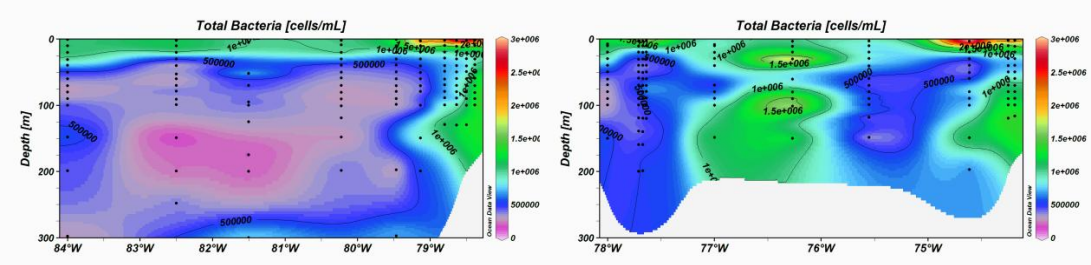

Fig. S6: Distribution of total non-green bacteria as detected in the flow cytometer along 10°S (left panel) and 16°S (right panel).

2.4 Underestimation of N_2 fixation

OPEN ACCESS Freely available online

PLoS one

Methodological Underestimation of Oceanic Nitrogen Fixation Rates

Wiebke Mohr*, Tobias Großkopf, Douglas W. R. Wallace, Julie LaRoche

Marine Biogeochemie, Leibniz-Institut für Meereswissenschaften (IFM-GEOMAR), Kiel, Germany

Abstract

The two commonly applied methods to assess dinitrogen (N_2) fixation rates are the $^{15}N_2$-tracer addition and the acetylene reduction assay (ARA). Discrepancies between the two methods as well as inconsistencies between N_2 fixation rates and biomass/growth rates in culture experiments have been attributed to variable excretion of recently fixed N_2. Here we demonstrate that the $^{15}N_2$-tracer addition method underestimates N_2 fixation rates significantly when the $^{15}N_2$ tracer is introduced as a gas bubble. The injected $^{15}N_2$ gas bubble does not attain equilibrium with the surrounding water leading to a $^{15}N_2$ concentration lower than assumed by the method used to calculate $^{15}N_2$-fixation rates. The resulting magnitude of underestimation varies with the incubation time, to a lesser extent on the amount of injected gas and is sensitive to the timing of the bubble injection relative to diel N_2 fixation patterns. Here, we propose and test a modified $^{15}N_2$ tracer method based on the addition of $^{15}N_2$-enriched seawater that provides an instantaneous, constant enrichment and allows more accurate calculation of N_2 fixation rates for both field and laboratory studies. We hypothesise that application of N_2 fixation measurements using this modified method will significantly reduce the apparent imbalances in the oceanic fixed-nitrogen budget.

Citation: Mohr W, Großkopf T, Wallace DWR, LaRoche J (2010) Methodological Underestimation of Oceanic Nitrogen Fixation Rates. PLoS ONE 5(9): e12583. doi:10.1371/journal.pone.0012583

Editor: Zoe Finkel, Mt. Alison University, Canada

Received July 2, 2010; **Accepted** August 11, 2010; **Published** September 3, 2010

Funding: This work is a contribution of the Collaborative Research Centre 754 "Climate - Biogeochemistry Interactions in the Tropical Ocean" (www.sfb754.de), which is supported by the German Research Association. The funders had no role in study design, data collection and analysis, decision to publish, or preparation of the manuscript.

Competing Interests: The authors have declared that no competing interests exist.

* E-mail: wmohr@ifm-geomar.de

Introduction

Biological dinitrogen (N_2) fixation is the major source of fixed nitrogen (N) in the oceanic N budget [1]. Current estimates of global oceanic N_2 fixation are ~100–200 Tg N a^{-1} [2]. N_2 fixation rates can be assessed through geochemical estimates, modelling of diazotroph abundances and growth rates [3] and direct measurements of N_2 fixation. Geochemical estimates rely on the measurement of, *e.g.*, nutrient stoichiometry and estimates or models of ocean circulation [4,5] or the distribution of stable isotope abundances (*e.g.*, [6]). Direct measurements of N_2 fixation are obtained either using the $^{15}N_2$-tracer addition method [7,8] or the acetylene reduction assay (ARA) [8,9]. However, direct measurements of N_2 fixation rates account for ≤50% of the geochemically-derived estimates [10]. Furthermore, the sink terms in the oceanic fixed N budget significantly exceed the current estimates of N_2 fixation and other source terms for fixed N [11,12]. This gap between sources and sinks of fixed N implies an oceanic nitrogen imbalance, which may reflect a non-steady-state of the oceanic fixed-N inventory, or result from over-estimation of loss processes and/or under-estimation of fixed nitrogen inputs [10,13]. However, isotopic signatures in sediments suggest that the fixed N budget is in a steady-state [14].

The comparison of N_2 fixation rates measured simultaneously using the $^{15}N_2$-tracer addition and the ARA shows that the $^{15}N_2$-tracer addition generally yields lower rates (for a summary see [15]). In addition, mass balance analyses of $^{15}N_2$-based N_2 fixation rates measured in experiments with cultured diazotrophs, indicate that the $^{15}N_2$-tracer addition method yields rates that are too low for sustaining the observed growth rates and biomass [16,17]. The discrepancies between the two methods and the lack of mass balance in culture experiments have often been attributed to the excretion of recently fixed nitrogen as ammonium (NH_4^+) or dissolved organic nitrogen (DON). The discrepancies have led to the operational definition of gross and net N_2 fixation [16,18] as measured by the ARA and the $^{15}N_2$-tracer addition approaches, respectively. However, the measured release of NH_4^+ or DON is rarely sufficient to balance the observed growth in culture, and even invoking recycling of the dissolved fixed N rarely accounts for the observed discrepancies between N_2 fixation rate and growth rate/biomass [16].

The apparent oceanic N imbalance, differences between geochemical estimates and measured rates of N_2 fixation, and the difficulties in reconciling discrepancies between ARA and $^{15}N_2$-based estimates of N_2 fixation in the field and in culture experiments, led us to re-assess the $^{15}N_2$-tracer addition method. This method is based on the direct injection of a $^{15}N_2$ gas bubble into a seawater sample [7] sufficient to yield a final enrichment of 2–5 atom percent (atom%) and incubation for 2–36 hours [19]. N_2 fixation rates are then retrieved from the incorporation of $^{15}N_2$ into the particulate organic nitrogen (PON). The method assumes implicitly that the injected gas fully and rapidly equilibrates with the surrounding water, and this assumption is the basis for calculation of the initial ^{15}N enrichment of the dissolved N_2 pool. Knowledge of this enrichment is pivotal to the calculation of N_2 fixation rates with this method as seen in equation 1 (equations

combined from [8]):

$$N_2\ fixation\ rate = \frac{\left(A_{PN}^{final} - A_{PN}^{t=0}\right)}{\left(A_{N_2} - A_{PN}^{t=0}\right)} \times \frac{[PN]}{\Delta t}$$

where A = atom% ^{15}N in the particulate organic nitrogen (*PN*) at the end (*final*) or beginning ($t = 0$) of the incubation or in the dissolved N_2 pool (N_2).

In applications of the method, all parameters of the equation are measured except for the atom% ^{15}N in the dissolved N_2 pool (A_{N2}). Equation 1 shows that calculation of N_2 fixation rates depends strongly on this value which is calculated from the predicted equilibrium dissolved N_2 concentration [20,21], its natural ^{15}N abundance, and the amount of $^{15}N_2$ tracer added with the bubble. The calculation assumes that there is complete isotopic equilibration between the injected bubble of $^{15}N_2$ and the surrounding water at the start of the incubation.

Here we report results of experiments that were designed to assess the rate of equilibration of an introduced $^{15}N_2$ gas bubble with the surrounding water. Based on results of these experiments, we developed a modified approach involving addition of $^{15}N_2$-enriched seawater which assured a well-defined and constant ^{15}N enrichment of the dissolved N_2 gas at the beginning of the incubations. We propose the application of the modified approach for future assessments of N_2 fixation rates in natural microbial communities and in laboratory cultures.

Results

Time-resolved equilibration of a bubble of $^{15}N_2$ in seawater

A first set of experiments (isotopic equilibration experiments) was carried out to assess the time required to attain isotopic equilibrium in the dissolved pool of N_2 gas after injection of a known amount of $^{15}N_2$ gas as a bubble into sterile filtered seawater. A gas bubble of pure $^{15}N_2$ was injected directly into incubation bottles which were manually inverted fifty-times (~3 min agitation) and left standing for up to 24 h. Concentration of dissolved $^{15}N_2$ was followed over the 24 h period to assess the degree of equilibration of the $^{15}N_2$ gas bubble with the surrounding water as a function of time. Dissolved $^{15}N_2$ concentrations in the seawater increased steadily with the incubation time (Fig. 1A). After eight hours, dissolved $^{15}N_2$ concentrations reached about 50% of the concentration calculated assuming complete isotopic equilibration of the injected bubble with the ambient dissolved N_2 gas in the seawater sample. At the end of the 24 h incubation, the dissolved $^{15}N_2$ concentration had increased to about 75% of the calculated concentration.

N_2 fixation rate underestimation due to incomplete $^{15}N_2$ gas bubble equilibration

Similar results were obtained in the incubation experiments with pure culture of *Crocosphaera watsonii* (culture experiments), which confirmed the incomplete and time-dependent equilibration of the injected bubble of $^{15}N_2$ gas with the surrounding water (Fig. 1B). These experiments also demonstrated the associated underestimation of N_2 fixation rates. Culture experiments were conducted after $^{15}N_2$ addition as a gas bubble and also after $^{15}N_2$ addition in the form of $^{15}N_2$-enriched seawater (our modified method, see Methods section). The incubation of *C. watsonii* after injection of a bubble of $^{15}N_2$ gas and without prior incubation of this bubble in algal-free media, gave a N_2 fixation rate which was

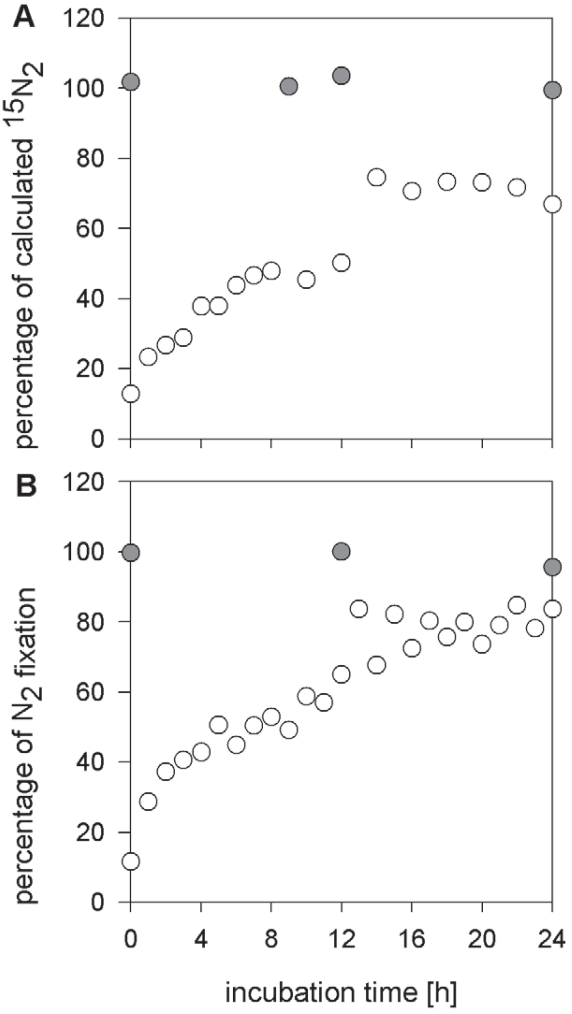

Figure 1. Time-dependence of the equilibration of a $^{15}N_2$ gas bubble with seawater. Results are presented as a function of the time after bubble injection (white symbols). (A) Measured dissolved $^{15}N_2$ concentrations as percentage of calculated concentration assuming rapid and complete isotopic equilibrium. (B) N_2 fixation rates by *C. watsonii* as percentage of the maximum rate measured during the experiments. For comparison, the addition of $^{15}N_2$-enriched water to samples yielded a constant $^{15}N_2$ enrichment over 24 h (A, grey symbols) or constant N_2 fixation rates (B, grey symbols).
doi:10.1371/journal.pone.0012583.g001

only 40% of the maximum rate measured in the incubations to which $^{15}N_2$-enriched seawater had been added. In other words, for the 12-h incubation period under the described experimental conditions, the N_2 fixation rate was underestimated by 60% when the $^{15}N_2$ was introduced as a gas bubble. In contrast, in both the isotopic equilibration and the culture experiments, the concentration of dissolved $^{15}N_2$ remained stable at the predicted value throughout the 24 h in incubations to which $^{15}N_2$-enriched water was added.

Factors influencing $^{15}N_2$ gas dissolution in N_2-saturated seawater

Continuous, vigorous shaking (50 rpm) greatly increased the concentration of $^{15}N_2$ in the media (Fig. 2) reaching ~67% of the calculated concentration after 30 minutes whereas the initial, manual agitation, *i.e.* inverting bottles 50 times (~3 min), resulted

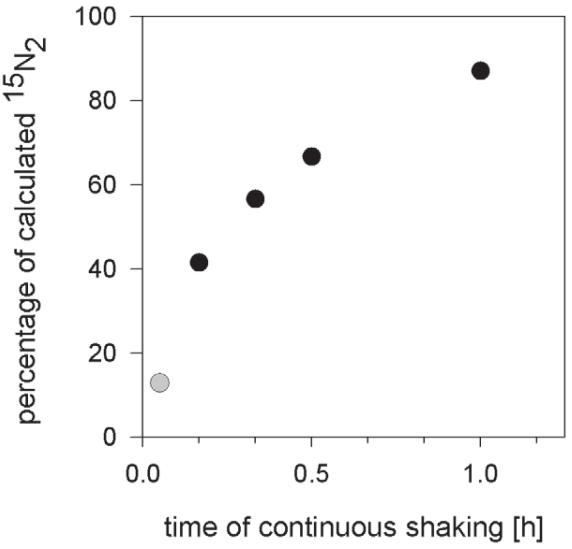

Figure 2. Agitation-dependent increase in dissolved $^{15}N_2$ using bubble incubations. Values are presented as a percentage of the calculated concentration. The manually-shaken (3 min) sample was added to the plot for comparison (grey symbol).
doi:10.1371/journal.pone.0012583.g002

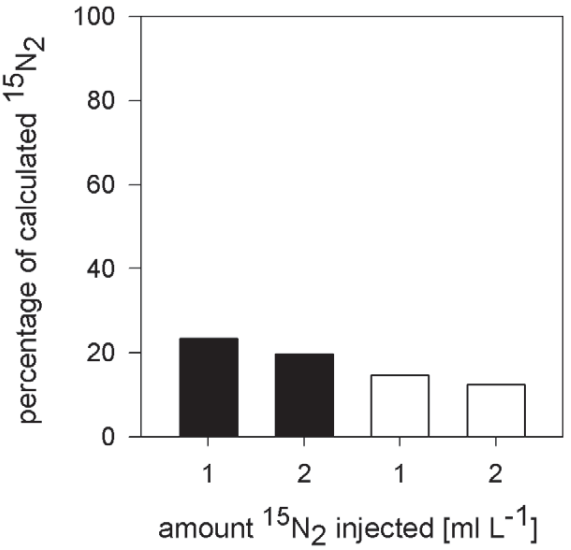

Figure 3. Dissolved $^{15}N_2$ concentration as a function of bottle size and amount of injected $^{15}N_2$ gas. Values are presented as a percentage of the calculated concentration. Bottles were incubated for 1 hour. Black bars, 0.13 L bottle and white bars, 1.15 L bottle.
doi:10.1371/journal.pone.0012583.g003

in only ~13% of the calculated concentration. Information on agitation is generally not provided in the published literature, but this is clearly a variable factor in incubations, especially if performed at sea. Continuous, vigorous shaking, as tested here (50 rpm; Fig. 2), is difficult to achieve in field experiments and may, in addition, be detrimental to some diazotrophs (*e.g.* *Trichodesmium* colonies).

Increasing the size of the incubation bottles, increasing the amount of gas injected per liter of seawater and the addition of dissolved organic matter (DOM) led in all cases except one to slower equilibration of the $^{15}N_2$ gas bubble with the surrounding water (Fig. 3 and 4A), even when bottles were shaken continuously for one hour (Fig. 4B). Only with the injection of 8 ml of $^{15}N_2$ gas per liter of water and one hour of continuous, vigorous shaking, was near-complete equilibration achieved (97% of calculated concentration).

Discussion

Both the isotopic equilibration and the culture experiments demonstrated clearly that the equilibration of $^{15}N_2$ gas injected as a bubble into N_2-saturated seawater is time-dependent and incomplete, even after 24 hours. The lack of complete equilibration causes the resulting calculated N_2 fixation rates to be variably and significantly underestimated (see Equation 1). The equilibration, *i.e.* the isotopic exchange between the $^{15}N_2$ gas in the bubble and the surrounding water is controlled primarily by diffusive processes. The major variables that influence the rate of isotopic exchange include the surface area to volume ratio of the bubble, the characteristics of the organic coating on the bubble surface [22], temperature and the rate of renewal of the water-bubble interface [23]. The renewal of the water-bubble interface appears to have the greatest effect on the isotopic exchange, as continuous vigorous shaking of the incubation bottles generated the highest enrichment of $^{15}N_2$ in the water phase. However, the calculated (equilibrium) enrichment in $^{15}N_2$ was not attained fully even after one-hour of continuous shaking at 50 rpm on a rotary shaker. Incubations carried out on board a research vessel will provide some agitation of the bubble but this will not approach the high and constant agitation tested in our experiments. The implication is that variable sea-state conditions encountered during sea-going incubations, and the details of individual experiments, will lead to variable $^{15}N_2$ enrichments and hence variable underestimation of N_2 fixation rates. Further, N_2 fixation studies in the oligotrophic regions of the ocean usually require the use of large incubation volumes (*e.g.*, 2–4 L), so that continuous shaking for one hour or more is not practical, and in addition would likely be detrimental to the natural microbial communities.

The experiments with variable bottle sizes and DOM additions (Fig. 3 and 4) demonstrated that there are factors in addition to the bubble incubation time that affect the equilibration. On the other hand, the addition of $^{15}N_2$-enriched seawater to the incubations led to a stable enrichment over the 24 h incubation time which was instantaneous and independent of the agitation of the bottles.

This study was motivated partly by the mismatches between the ARA and $^{15}N_2$-based measurements of N_2 fixation as well as imbalances between $^{15}N_2$-fixation rates and biomass-specific rates (~growth rate) or C:N fixation ratios (Table 1). Such mismatches have been observed in environmental studies and in culture studies, mainly with *Trichodesmium*. Although it has been shown that *Trichodesmium* can excrete recently fixed N_2 as NH_4^+ or DON [16,24], the excretion of $^{15}NH_4^+$ or DO^{15}N rarely accounts for the observed discrepancies [16,17]. The operational definition of gross and net N_2 fixation as obtained through ARA and $^{15}N_2$ incubations, respectively, has been mainly based on the mismatch between the rates measured by the two methods. Our results demonstrate that N_2 fixation rates, as measured with the $^{15}N_2$ method [7] are underestimated. Therefore, the magnitude of the exudation of recently fixed nitrogen and the conditions promoting this process should be re-evaluated, taking into account the results presented here.

We reviewed published studies that have used the direct injection of a $^{15}N_2$ gas bubble to assess N_2 fixation rates in order to

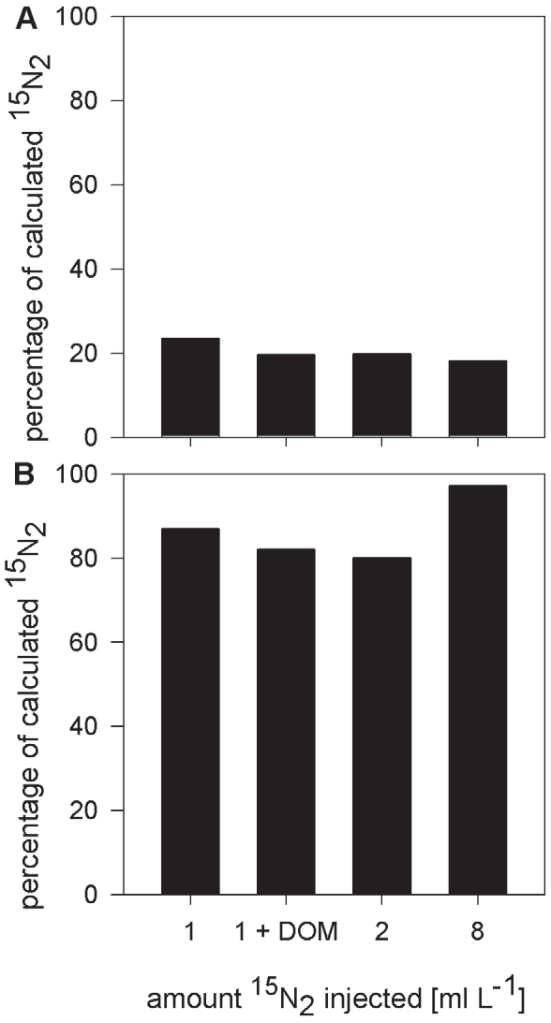

Figure 4. Dissolved $^{15}N_2$ concentration as a function of the amount of injected gas and agitation. Values are presented as a percentage of the calculated concentration (A) after 1 hour incubation in manually (3 min shaking and 1 h subsequent incubation), and (B) in continuously (1 h) shaken samples.
doi:10.1371/journal.pone.0012583.g004

evaluate the magnitude of under-estimation. However, first attempts to assess the degree of underestimation of field and culture N_2 fixation rates were obscured by a wide range of experimental conditions among the studies. Bottle sizes ranged from 14 ml to 10 L, the amount of $^{15}N_2$ injected varied from 0.2 to 40.8 ml $^{15}N_2$ per L seawater and incubation times ranged from 0.25 to 48 hours, with the majority of the field studies using 2–4 L bottles and 24 h incubations. In addition, information on agitation was, in general, not available. There were no obvious trends of reported N_2 fixation rates with either bottle size, incubation time or the amount of injected $^{15}N_2$ gas probably because of the large variability of geographic locations and environmental conditions prevailing in the individual studies, which would have a dominant effect on the local diazotrophic communities and their N_2 fixation rates. An evaluation of the degree of possible underestimation of $^{15}N_2$ fixation rates in environmental studies is further confounded by diel periodicity of N_2 fixation [25–27]. The lack of knowledge on the exact timing and magnitude of the individual N_2 fixation activity of the different diazotrophs relative to the timing of $^{15}N_2$ gas injection hinders back-calculation of published N_2 fixation data. This can be illustrated, for example, with a hypothetical diazotroph community that is dominated by unicellular cyanobacteria which fix nitrogen during the night period only (Fig. 5A). In this microbial community, measurements of N_2 fixation using the direct injection of a $^{15}N_2$ gas bubble during a 24 hour incubation will lead to a variable underestimation of the true N_2 fixation rate, depending on the timing of the incubation start relative to the peak in the nitrogenase activity (Fig. 5C, solid lines). The underestimation will be more pronounced if the start of the incubation is coincident with the onset of the active N_2 fixation period. In contrast, incubations with enriched $^{15}N_2$ seawater, will not lead to an underestimate, regardless of the incubation start relative to the diel cycle (Fig. 5C, dashed lines).

The discrepancies and mismatches/imbalances observed in field and laboratory studies could, in part, be explained by the variable underestimation of the true N_2 fixation rate due to the methodological uncertainty reported here. We propose the addition of $^{15}N_2$-enriched seawater to incubations to assess N_2 fixation rates in laboratory and field studies. We suggest that measurements using this approach are likely to increase measurements and estimates of N_2 fixation at species, regional and global level and lead to a reduction in the apparent oceanic nitrogen imbalance.

Table 1. Discrepancies observed between $^{15}N_2$ fixation, ARA and carbon fixation or biomass-specific rates[a].

Organism/area	C_2H_2:$^{15}N_2$	C:N fixation ratio	biomass-specific rate [d^{-1}]	Reference
Trichodesmium/Pacific, Atlantic, north of Australia		808[b]		[30]
cyanobacterial bloom/Baltic	3–20			[18]
Trichodesmium IMS 101	3–22	75–133		[17]
Trichodesmium IMS 101	1.5–6.9		0.002–0.011[c]	[16]
Trichodesmium/Gulf of Mexico		10–107[b]		[31]
Trichodesmium/Bermuda Atlantic Time Series station (BATS)		13–437	0.006–0.03[d]	[32]

[a]C:N fixation ratio is based on $^{15}N_2$-fixation measurements.
[b]Ratio calculated from DI^{13}C and $^{15}N_2$ fixation rates.
[c]Calculated from $^{15}N_2$ fixation rate divided by PON.
[d]Calculated from doubling time with biomass-specific rate = ln (2)/doubling time.
doi:10.1371/journal.pone.0012583.t001

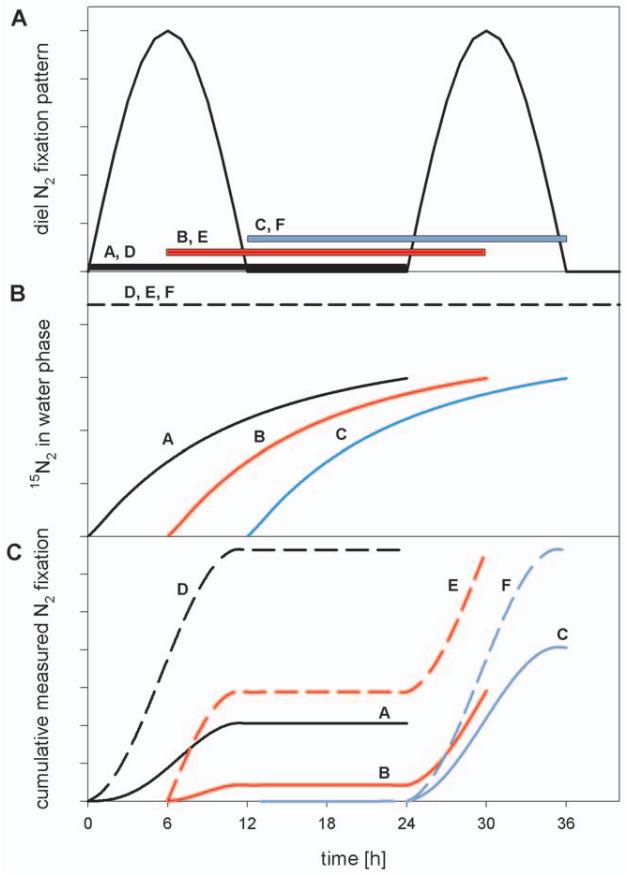

Figure 5. Influence of diel N_2 fixation patterns on the magnitude of N_2 fixation rates. Schematic diagram illustrating the influence of diel N_2 fixation patterns on N_2 fixation rates when determined with the direct injection of a $^{15}N_2$ gas bubble. A hypothetical diel N_2 fixation pattern is shown (panel A) with a duration of the N_2-fixing period of 12 h. Three possible time periods for 24 h incubations are indicated by the solid bars (A–F). The corresponding ^{15}N enrichment in the dissolved N_2 pool (panel B) is shown for the three incubation periods using the direct injection of a $^{15}N_2$ gas bubble (solid lines; A, B and C) and the addition of $^{15}N_2$-enriched seawater (dashed line; D, E and F). The resulting cumulative N_2 fixation in each of the incubations (panel C) demonstrates that the timing of the incubation relative to diel N_2 fixation patterns introduces a variable underestimation in the total N_2 fixation rate measured during the incubation after a $^{15}N_2$ gas bubble is injected (solid lines; A, B and C) as compared to the N_2 fixation measured with the addition of $^{15}N_2$-enriched seawater (dashed lines; D, E and F). The diagram is based on the observations made in the experiments described in this study.
doi:10.1371/journal.pone.0012583.g005

Materials and Methods

Culture and growth conditions

The diazotrophic cyanobacterium *Crocosphaera watsonii* WH8501 was grown in batch cultures in N-free YBCII media [28] at 28°C in a temperature-controlled growth chamber. *C. watsonii* was subjected to 12:12 h dark:light cycles.

Direct injection of a $^{15}N_2$ gas bubble in water

We first examined the rate of equilibration between an injected bubble of $^{15}N_2$ gas and seawater. Two series of incubations were started by injecting 140 µl of $^{15}N_2$ into 133 ml of an artificial seawater media (YBCII) contained in headspace-free, septum-capped glass bottles. In the first series (isotopic equilibration experiments), all bottles were inverted fifty times (~3 min) after injection of the $^{15}N_2$ gas bubble and left at room temperature in the laboratory. One bottle was sampled immediately after the agitation in order to determine how much $^{15}N_2$ gas had dissolved initially. The other bottles were opened and sampled after standing for periods from 1 to 24 h. Upon opening of the bottles, samples to measure the dissolved $^{15}N_2$ were taken and stored in gas-tight glass vials (Exetainer®) until analysis.

In the second series (culture experiments), the YBCII media was pre-heated to 28°C in a temperature-controlled chamber before being used to fill septum-capped glass bottles. As with the first series, samples were agitated and left standing for varying periods of time after the injection of a $^{15}N_2$ gas bubble. Instead of taking subsamples for $^{15}N_2$ analysis, 13 ml of media were replaced by *C. watsonii* WH8501 culture upon opening of the bottles. This series of experiments was timed so that the introduction of culture into the media took place at the start of a dark phase of the 12:12h dark:light-adapted *C. watsonii* culture. The samples with the culture were then incubated for 12 h at culture growth conditions (28°C, dark phase, *i.e.* N_2-fixing) and filtered onto pre-combusted GF/F (Whatman; 450°C for 4 h) filters at the end of the incubation. Filters were dried immediately after (50°C, 6 h) and stored at room temperature until analysis. To obtain a measure of underestimation using the direct injection of a $^{15}N_2$ gas bubble, one bottle containing 13 ml of *C. watsonii* culture was incubated for 12 h after the injection of 140 µl $^{15}N_2$ gas at the start of the dark phase and without release of the bubble, essentially resembling a laboratory or field incubation.

Direct addition of $^{15}N_2$ tracer-enriched seawater

An alternative, modified $^{15}N_2$ tracer addition method was developed, which involved addition of an aliquot of $^{15}N_2$-enriched water to incubations. This alternative method was based on earlier approaches used to study oxygen cycling using $^{18}O_2$ [29] and the release of DON using $^{15}N_2$ [24]. The preparation of the $^{15}N_2$-enriched water was started by degassing 0.2 µm-filtered artificial seawater (YBCII media). Degassing was carried out by applying vacuum (≤200 mbar absolute pressure) to continuously stirred (stir bar) media for about 30 min. The degassed water was transferred rapidly but gently into septum-capped glass bottles until overflow, and 1 ml of $^{15}N_2$ gas (98 at%; Campro Scientific) was injected per 100 ml of media. The bottles were shaken vigorously until the bubble disappeared. Aliquots of this $^{15}N_2$-enriched water were then added to the incubation bottles, with the enriched water constituting no more than 10% of the total sample volume. This alternative enrichment method was applied to the two series of experiments described above.

Assessment of additional factors contributing to variation in $^{15}N_2$ enrichment

We assessed possible effects of varying bottle size, amounts of injected gas and different amounts of agitation on their contribution to the equilibration between a bubble of $^{15}N_2$ gas and the surrounding seawater. For the bottle size comparison, incubations were performed in 0.13 L bottles and in 1.15 L bottles. The amount of injected gas varied between 1 ml $^{15}N_2$ per 1 L seawater up to 8 ml $^{15}N_2$ per 1 L seawater. The incubations were agitated either by inverting fifty times manually (~3 min) or by continuous agitation on a rotating bench-top shaker (Biometra WT 17) at 50 rpm (rotations per minute). We also added marine broth (Difco 2216; 0.2 µm filter-sterilized; 230 mg DOM L^{-1} media) to some bottles to examine the effect of dissolved organic matter (DOM).

$^{15}N_2$ analysis in the artificial seawater and ^{15}N analysis in the particulate organic nitrogen (PON)

Subsamples taken during the equilibration experiments were analysed for $^{15}N_2$ concentration with a membrane-inlet mass spectrometer (MIMS; GAM200, IPI) within one week of subsampling. Dried GF/F filters were pelletized in tin cups, and PON as well as isotope ratios were measured by means of flash combustion in an elemental analyser (Carlo Erba EA 1108) coupled to a mass spectrometer (Thermo Finnigan Delta S).

Calculations

The expected concentration of $^{15}N_2$ following bubble injections was calculated assuming rapid and complete isotopic equilibration between bubble and surrounding seawater and considering atmospheric equilibrium concentrations of dissolved N_2 [21]. When $^{15}N_2$-enriched aliquots were added, the amount of $^{15}N_2$ originally dissolved in the degassed seawater and the volume of the aliquot added were taken into account. The calculations of N_2 fixation rates in the culture incubations were made according to Equation 1 and are presented as a percentage of the highest rate measured. For the comparison between methods, the measured $^{15}N_2$ concentrations are presented as a percentage of the expected concentration calculated as follows

$$\frac{V_{15_{N_2}}}{MV \times V_{TOTAL}} = \left[mol\ ^{15}N_2\ L^{-1}\right]\ (i.e.\ 100\%) \qquad (2)$$

for the direct injection of a $^{15}N_2$ gas bubble where $V_{15_{N_2}}$ is the volume of the $^{15}N_2$ gas bubble, MV is the molar volume and V_{TOTAL} is the total (water) volume of the incubation. The expected concentration was corrected for the amount of $^{15}N_2$ gas which remains in the bubble at isotopic equilibrium with the surrounding water. For the addition of $^{15}N_2$-enriched water the expected concentration is

$$\frac{V_{15_{N_2}}}{MV \times V_{DG}} \times \frac{V_{EW}}{V_{TOTAL}} = \left[mol\ ^{15}N_2\ L^{-1}\right]\ (i.e.\ 100\%) \qquad (3)$$

where V_{DG} is the volume of degassed water, V_{EW} is the volume of $^{15}N_2$-enriched water added to the incubation and V_{TOTAL} is the total (water) volume of the incubation.

Acknowledgments

We thank Marcel Kuypers and Hannah Marchant (Max Planck Institute for Marine Microbiology Bremen) for providing access to and advice on the membrane-inlet mass spectrometry. The assistance and suggestions of Gert Petrick and Karen Stange (IFM-GEOMAR) concerning the early analyses of $^{15}N_2$ is also gratefully acknowledged.

Author Contributions

Conceived and designed the experiments: WM DWRW JL. Performed the experiments: WM. Analyzed the data: WM TG DWRW JL. Wrote the paper: WM. Contributed to figure preparation/schematic diagrams: TG.

References

1. Gruber N (2008) The marine nitrogen cycle: Overview and challenges. In: Capone DG, Bronk DA, Mulholland MR, Carpenter EJ, eds. Nitrogen in the marine environment. Amsterdam, The Netherlands: Elsevier. pp 1–50.
2. Karl D, Michaels A, Bergman B, Capone D, Carpenter E, et al. (2002) Dinitrogen fixation in the world's oceans. Biogeochemistry 57/58: 47–98.
3. Goebel NL, Edwards CA, Church MJ, Zehr JP (2007) Modeled contributions of three diazotrophs to nitrogen fixation at Station ALOHA. ISME J 1: 606–619.
4. Gruber N, Sarmiento JL (1997) Global patterns of marine nitrogen fixation and denitrification. Global Biogeochem Cy 11: 235–266.
5. Deutsch C, Sarmiento JL, Sigman DM, Gruber N, Dunne JP (2007) Spatial coupling of nitrogen inputs and losses in the ocean. Nature 445: 163–167.
6. Montoya JP, Carpenter EJ, Capone DG (2002) Nitrogen fixation and nitrogen isotope abundances in zooplankton of the oligotrophic North Atlantic. Limnol Oceanogr 47: 1617–1628.
7. Montoya JP, Voss M, Kähler P, Capone DG (1996) A simple, high-precision, high-sensitivity tracer assay for N_2 fixation. Appl Environ Microbiol 62: 986–993.
8. Capone DG, Montoya JP (2001) Nitrogen fixation and denitrification. In: Paul J, ed. Methods in Microbiology, Volume 30. London, UK: Academic Press. pp 501–515.
9. Capone DG (1993) Determination of nitrogenase activity in aquatic samples using the acetylene reduction procedure. In: Kemp PF, Sherr BF, Sherr EB, Cole JJ, eds. Handbook of Methods in Aquatic Microbial Ecology. Boca RatonFL, , USA: Lewis Publishers. pp 621–631.
10. Mahaffey C, Michaels AF, Capone DG (2005) The conundrum of marine N_2 fixation. Am J Sci 305(SI): 546–595.
11. Codispoti LA, Brandes JA, Christensen JP, Devol AH, Naqvi SWA, et al. (2001) The oceanic fixed nitrogen and nitrous oxide budgets: Moving targets as we enter the anthropocene? Sci Mar 65: 85–105.
12. Codispoti LA (2007) An oceanic fixed nitrogen sink exceeding 400 Tg N a^{-1} vs the concept of homeostasis in the fixed-nitrogen inventory. Biogeosciences 4: 233–253.
13. Brandes JA, Devol AH (2002) A global marine-fixed nitrogen isotopic budget: Implications for Holocene nitrogen cycling. Global Biogeochem Cy 16: 1120. doi:10.1029/2001GB001856.
14. Altabet MA (2007) Constraints on oceanic N balance/imbalance from sedimentary N-15 records. Biogeosciences 4: 75–86.
15. Mulholland MR (2007) The fate of nitrogen fixed by diazotrophs in the ocean. Biogeosciences 4: 37–51.
16. Mulholland MR, Bronk DA, Capone DG (2004) Dinitrogen fixation and release of ammonium and dissolved organic nitrogen by *Trichodesmium* IMS 101. Aquat Microb Ecol 37: 85–94.
17. Mulholland MR, Bernhardt PW (2005) The effect of growth rate, phosphorus concentration, and temperature on N_2 fixation, carbon fixation, and nitrogen release in continuous culture of *Trichodesmium* IMS 101. Limnol Oceanogr 50: 839–849.
18. Gallon JR, Evans AM, Jones DA, Albertano P, Congestri R, et al. (2002) Maximum rates of N_2 fixation and primary production are out of phase in a developing cyanobacterial bloom in the Baltic Sea. Limnol Oceanogr 47: 1514–1521.
19. Zehr JP, Montoya JP (2007) Measuring N_2 fixation in the field. In: Bothe H, Ferguson SJ, Newton WE, eds. Biology of the nitrogen cycle. Amsterdam, The Netherlands: Elsevier. pp 193–205.
20. Weiss RF (1970) The solubility of nitrogen, oxygen and argon in water and seawater. Deep-Sea Res 17: 721–735.
21. Hamme RC, Emerson SR (2004) The solubility of neon, nitrogen and argon in distilled water and seawater. Deep-Sea Research I 51: 1517–1528.
22. Frew NM (1997) The role of organic films in air-sea gas exchange. In: Liss PS, Duce RA, eds. The sea surface and global change. Cambridge, UK: Cambridge University Press. pp 121–172.
23. Asher WE, Pankow JF (1991) Prediction of gas/water mass transport coefficients by a surface renewal model. Environ Sci Technol 25: 1294–1300.
24. Glibert PM, Bronk DA (1994) Release of dissolved organic nitrogen by marine diazotrophic cyanobacteria, *Trichodesmium* spp. Appl Environ Microb 60: 3996–4000.
25. Colón-López M, Sherman DM, Sherman LA (1997) Transcriptional and translational regulation of nitrogenase in light-dark- and continuous-light grown cultures of the unicellular cyanobacterium *Cyanothece* sp. strain ATCC 51142. J Bacteriol 13: 4319–4327.
26. Chen YB, Dominic B, Mellon MT, Zehr JP (1998) Circadian rhythm of nitrogenase gene expression in the diazotrophic filamentous nonheterocystous cyanobacterium *Trichodesmium* sp. strain IMS 101. J Bacteriol 180: 3598–3605.
27. Mohr W, Intermaggio MP, LaRoche J (2010) Diel rhythm of nitrogen and carbon metabolism in the unicellular, diazotrophic cyanobacterium *Crocosphaera watsonii* WH8501. Environ Microbiol 12: 412–421.
28. Chen YB, Zehr JP, Mellon M (1996) Growth and nitrogen fixation of the diazotrophic filamentous nonheterocystous cyanobacterium *Trichodesmium* sp. IMS 101 in defined media: Evidence for a circadian rhythm. J Phycol 32: 916–923.
29. Kana T (1990) Light-dependent oxygen cycling measured by an oxygen-18 isotope dilution technique. Mar Ecol Prog Ser 64: 293–300.
30. Burns JA, Zehr JP, Montoya JP, Kustka AB, Capone DG (2006) Effect of EDTA additions on natural *Trichodesmium* spp. (Cyanophyta) populations. J Phycol 42: 900–904.

31. Mulholland MR, Bernhardt PW, Heil CA, Bronk DA, O'Neil JM (2006) Nitrogen fixation and release of fixed nitrogen by *Trichodesmium* spp. in the Gulf of Mexico. Limnol Oceanogr 51: 1762–1776.

32. Orcutt KM, Lipschultz F, Gundersen K, Arimoto R, Michaels AF, et al. (2001) A seasonal study of the significance of N_2 fixation by *Trichodesmium* spp. at the Bermuda Atlantic Time-Series study (BATS) site. Deep-Sea Res Pt 2 48: 1583–1608.

2.5 Closing the gap

1

2 **Closing the gap – Doubling in global N_2 fixation rates by direct measurements**

3

4 Tobias Großkopf[1,*], Wiebke Mohr[1,*,†], Tina Baustian[1], Harald Schunck[1], Diana Gill[1],
5 Marcel M.M. Kuypers[2], Gaute Lavik[2], Ruth A. Schmitz[3], Douglas W.R. Wallace[4], Julie
6 LaRoche[1,‡]

7

8 [1]Helmholtz-Centre for Ocean Research Kiel (GEOMAR), Düsternbrooker Weg 20,
9 24105 Kiel, Germany
10 [2]Max-Planck-Institute for Marine Microbiology, Celsiusstraße 1, 28359 Bremen,
11 Germany
12 [3]Institute for General Microbiology, Christian-Albrechts University Kiel, Am
13 Botanischen Garten 1-9, 24118 Kiel, Germany
14 [4]Oceanography Department, Dalhousie University, 1355 Oxford Street, PO Box 15000,
15 Halifax, Nova Scotia, B3H 4R2, Canada
16 [*]Equally contributed to this work
17 [†] Present address: Harvard University, Department of Earth and Planetary Sciences, 20
18 Oxford Street, Cambridge, MA 02138, USA
19 [‡] Corresponding author

20

Biological dinitrogen (N_2) fixation provides the largest input of nitrogen (N) to the ocean, therefore exerting critical control on the ocean's nitrogen inventory and primary productivity [1-3]. Despite the importance and demonstrated sensitivity of the N cycle to human influence [4, 5], there is controversy about the global magnitude of the gain and loss processes with the N loss exceeding the gain by approximately 200 Tg N yr^{-1} [6, 7]. Here we show that the most widely applied method used to measure N_2 fixation rates in natural open ocean settings leads to a large underestimation of the contribution of N_2-fixing microorganisms (diazotrophs) to fixed N in the Atlantic Ocean. Using molecular techniques to quantify the abundance of specific clades of diazotrophs and $^{15}N_2$ incorporation into particulate organic matter, we demonstrated that the magnitude of underestimation in N_2 fixation rates measured with the established method[8] relative to a new method[9] was related to the diazotrophic community composition. Our data show that in areas dominated by *Trichodesmium,* underestimation by the established method averaged 62%. However, where unicellular and symbiotic cyanobacteria and γ-proteobacteria dominated the diazotrophic community, the newly developed method yielded N_2 fixation rates over six fold higher than with the established method. Based on average areal rates measured over the whole Atlantic Ocean, we calculated basin wide N_2 fixation rates of 14 and 24 Tg N yr^{-1} for the established and new method, respectively. If our findings can be extrapolated to other ocean basins, this suggests that the global marine N_2 fixation should be raised from 103 Tg N yr^{-1} to 177 Tg N yr^{-1} and that the contribution of N_2-fixers other than *Trichodesmium* is much more significant than previously thought.

The oceans support approximately half of the earth's biological carbon fixation [10]. Carbon itself is rarely considered to be limiting in the ocean, rather nutrient elements such as nitrogen (N), phosphorus (P) or iron (Fe) control primary productivity [2]. Of these elements, nitrogen is special because it is always present in large amounts as dissolved dinitrogen (N_2) but this form is available only to the diazotrophs, a restricted group of prokaryotes[1]. Biological N_2 fixation is the largest input of fixed nitrogen into the ocean and has been proposed to control marine primary productivity on geological timescales [11]. While phytoplankton appear to be limited in growth over large areas by the availability of fixed N (e.g. nitrate, nitrite, ammonium), the productivity of

diazotrophs is controlled by other environmental factors, such as the availability of Fe and P [12]. Thus, increased desertification due to land use change may promote marine N_2 fixation through increased aeolian input of iron [13], whereas the increased usage of fertilizers and riverine runoff or increased atmospheric N deposition may have a contrary effect [5, 14]. An understanding of marine N_2 fixation and its response to anthropogenic forcing is crucial for assessing the future of oceanic primary productivity. Yet, recent attempts to produce a balanced N budget usually leave a major gap on the input side [6, 7] which creates a paradox, because stable isotopes recorded in ocean sediments suggest that the ocean's N inventory has been balanced for the last 3000 years [15]. The paradox can be reconciled in three ways [7]: One hypothesis is that current, transient N-loss rates are exceeding N_2 fixation, but that over timescales of several thousand years, variable losses and gains act to maintain a steady-state fixed-N inventory [16, 17]. Two alternate hypotheses invoke the possibilities that either the N-loss or the N-gain terms are in error. Several lines of evidence point out that even the most conservative estimates of oceanic N losses are higher than current estimates of N-input based on field-measurements of N_2 fixation and suggest that contemporary N_2 fixation rates may have been underestimated grossly [6, 7].

Over the last decade, molecular techniques have led to the discovery of a variety of previously unrecognized diazotrophs that express their nitrogenase genes and fix N_2, thereby illustrating gaps in our knowledge of marine N_2 fixation [18-22]. The discovery of N_2 fixation in mesopelagic waters in the Pacific [23, 24] and the possibility of significant involvement of heterotrophic bacteria in global N_2 fixation [25, 26] reinforces the idea that we are missing a large fraction of global N input by N_2 fixation. While biogeochemical modeling and geochemical tracer approaches have been used to estimate regional and global magnitudes of N_2 fixation, these indirect approaches rely on assumptions that require verification by direct biological rate measurements of N_2 fixation.

However, a recent laboratory study showed that the established method for measuring oceanic N_2 fixation leads to underestimation of rates due to slow and incomplete equilibration between the $^{15}N_2$ tracer added as a gas bubble and the water sample [9].

In fall 2009, we examined the consequences of these findings by measuring the magnitude of the underestimation of N_2 fixation rates in open ocean settings. During two research cruises in the Atlantic Ocean between 25°N and 45°S we compared the established $^{15}N_2$ tracer method (hereafter called the "bubble-addition method") for

measuring N_2 fixation[8] with a recently developed method[9] in which the $^{15}N_2$ tracer is added as a dissolved gas (the "dissolution method"). Our sampling covered a wide variety of oceanic conditions with sea surface temperatures ranging from 10°C to >28°C (Fig.1). At each sampling station we conducted parallel incubations with the dissolution and the bubble-addition methods, using dual labeling with $NaH^{13}CO_3$ and $^{15}N_2$ gas in the same incubation bottles to measure dissolved inorganic carbon (DIC) assimilation and N_2 fixation simultaneously with both methods (see supplementary online material for experimental details).

The ^{13}C labeled DIC was added to check for systematic differences in biological activity due to the differences in methods, and the results showed that carbon fixation rates were in good agreement between the two experimental methods (Fig. 2B). The N_2 fixation rates, on the other hand, showed a large difference between the two methods and a poor overall correlation (Fig. 2A). Average depth integrated rates of N_2 fixation over the whole Atlantic Ocean (25°N to 45°S) differed by a factor of 1.7 (91 +/- 37 and 54 +/- 16 μmol N m^{-2} d^{-1} for the dissolution and bubble-addition methods, respectively, n=17). Further, a geographical pattern emerged among the differences in the rates measured with the two methods. In the northern part of the 23°W section (15°N – 5°S), the depth-integrated N_2 fixation rates derived from 4 vertical profiles were, on average, 62% higher with the dissolution method relative to the bubble-addition method (194 ± 30 and 120 ± 13 μmol N m^{-2} d^{-1}, respectively). In the Equatorial Atlantic Ocean (4.5°N – 5°S), a region previously not considered important for N_2 fixation [27], the depth integrated N_2 fixation rates derived from 7 vertical profiles were on average 570 % higher with the dissolution method (55 ± 17.7 μmol N m^{-2} d^{-1}) relative to the bubble-addition method (8 ± 3.4 μmol N m^{-2} d^{-1}) (Fig. 3). Moreover, in the South Atlantic Gyre (38°S) and in the Falklands (Malvinas) Current (44°S), where water temperatures were as low as 16°C and 10°C, respectively, considerable N_2 fixation was detected with the dissolution method (0.44 +/- 0.1 and 0.54 +/- 0.1 μmol N m^{-3} d^{-1}). In contrast, the comparative rates with the bubble method were substantially lower (0.10 +/- 0.01 and 0.18 +/- 0.03 μmol N m^{-3} d^{-1} for 38°S and 44°S , respectively) [20, 22].

TaqMan assays based on *nifH* gene presence were used to quantify the relative abundance of the diazotrophic phylotypes known to occur in the Tropical Atlantic Ocean [21, 22]. Two geographically separated areas, dominated by distinct diazotrophic phylotypes could be identified (Fig. 4, Fig. S2). The most abundant diazotroph was *Trichodesmium* with *nifH* copy numbers peaking at 9°N with 5 x 10^5 *Trichodesmium*

nifH copies L^{-1}. The highest N_2 fixation rates were measured inside a *Trichodesmium* bloom at 13.75°N with 360 ± 8.5 μmol N m^{-2} d^{-1} and 219 ± 8.2 μmol N m^{-2} d^{-1} measured with the dissolution and bubble-addition methods, respectively. Although *Trichodesmium* was detectable throughout the whole area (Fig. 4, note the logarithmic scale), its abundance declined rapidly south of 5°N. Diatom associated heterocystous diazotrophs (DDA's), unicellular cyanobacteria and γ-proteobacteria (AO) showed a peak of abundance within the *Trichodesmium* bloom and a second peak in the Equatorial Atlantic region where they outnumbered *Trichodesmium*. We therefore characterize the Tropical North Atlantic region (5°N-15°N) as an area of *Trichodesmium* dominance where underestimation of N_2 fixation rates by the bubble-addition method was less severe (but significant). In contrast, the largest underestimation (570%) with the bubble-addition method was found in the Equatorial Atlantic (4.5°N-5°S), which was as an area dominated by diazotrophs other than *Trichodesmium* (Fig. S4 and S5). Hence the combined results indicate that the magnitude of underestimation in N_2 fixation rates measured with the bubble-addition method relative to the dissolution method was related to the diazotrophic community composition.

The species composition of the diazotrophic community can affect the level of underestimation by the bubble-addition method for a variety of reasons. The equilibration time for a $^{15}N_2$ gas bubble in a bubble-addition type of incubation is longer than the typical incubation time of 24 hours, despite manual shaking at the onset of incubation [9] (Fig. S6). Hence, the $^{15}N_2$ label will remain highly enriched within the bubble and its immediate surroundings, whereas water at the bottom of the incubation bottle will have lower $^{15}N_2$ enrichment (see supplementary online material). Consequently, *Trichodesmium,* which are buoyant, may be exposed to a higher fraction of the added $^{15}N_2$ label. In contrast, diatom-associated diazotrophs will tend to accumulate at the bottom of incubation bottles due to the size and silicate frustules of their hosts[28]. Hence, diatom-associated cyanobacteria may be amongst the organisms most affected by the underestimation bias of the established bubble-addition method. Underestimation bias will also be greater when the start of an incubation coincides with the peak of N_2 fixation activity of the dominant diazotrophs (e.g. *Crocosphaera* or UCYNA, for night-time and day-time incubations, respectively). These biases are avoided with the dissolution method because $^{15}N_2$ label is added via seawater which is mixed uniformly in the incubation vessel at the start of the incubation.

Using published measurements of N_2 fixation rates obtained with the bubble-addition method, we calculated basin-wide and global budgets of N_2 fixation. The basin wide averages are 14 Tg N yr^{-1} for the Atlantic, 63 Tg N yr^{-1} for the Pacific and 26 Tg N yr^{-1} for the Indian Ocean giving a global total of 103 Tg N yr^{-1} (see supplementary online material). Our own average N_2 fixation rates, as measured with the bubble-addition method and extrapolated over the Atlantic Ocean (25°N to 45°S) result in an input of 14 Tg N yr^{-1}, which is identical to the value for the Atlantic Ocean calculated from the published data. In contrast, using the average of our N_2 fixation measurements made with the dissolution method raises the Atlantic Ocean N_2 fixation rate to 24 Tg N yr^{-1}. Applying this relative difference in rates measured in the Atlantic Ocean (i.e. 14 versus 24 Tg N yr^{-1}) to all ocean basins (103 Tg N yr^{-1}), implies a global N_2 fixation rate, based on direct measurements, of 177 Tg N yr^{-1}.

Our study directly confirms that field measurements of N_2 fixation made with the most widely applied $^{15}N_2$ bubble-addition method have significantly and variably underestimated N_2 fixation rates, with major implications for global budgets. Our data reveal regional variations in the magnitude of underestimation which we hypothesize are related to diazotrophic community composition. Specifically, the contribution of diazotrophs other than *Trichodesmium* may have been severely underestimated in prior field studies leading to a biased view of the key players in this globally important process.

1. Karl, D. et al. Dinitrogen fixation in the world's oceans. Biogeochemistry 57, 47-+ (2002).
2. Falkowski, P. G., Barber, R. T. & Smetacek, V. Biogeochemical controls and feedbacks on ocean primary production. Science 281, 200-206 (1998).
3. Deutsch, C., Sarmiento, J. L., Sigman, D. M., Gruber, N. & Dunne, J. P. Spatial coupling of nitrogen inputs and losses in the ocean. Nature 445, 163-167 (2007).
4. Diaz, R. J. & Rosenberg, R. Spreading Dead Zones and Consequences for Marine Ecosystems. Science 321, 926-929 (2008).
5. Duce, R. A. et al. Impacts of atmospheric anthropogenic nitrogen on the open ocean. Science 320, 893-897 (2008).
6. Mahaffey, C., Michaels, A. F. & Capone, D. G. The conundrum of marine N-2 fixation. American Journal of Science 305, 546-595 (2005).

7. Codispoti, L. A. An oceanic fixed nitrogen sink exceeding 400 Tg Na-1 vs the concept of homeostasis in the fixed-nitrogen inventory. Biogeosciences 4, 233-253 (2007).
8. Montoya, J. P., Voss, M., Kahler, P. & Capone, D. G. A simple, high-precision, high-sensitivity tracer assay for N-2 fixation. Applied and Environmental Microbiology 62, 986-993 (1996).
9. Mohr, W., Grosskopf, T., Wallace, D. W. R. & LaRoche, J. Methodological Underestimation of Oceanic Nitrogen Fixation Rates. Plos One 5 (9), e12583. doi:10.1371/journal.pone.0012583 (2010).
10. Behrenfeld, M. J. & Falkowski, P. G. Photosynthetic rates derived from satellite-based chlorophyll concentration. Limnology and Oceanography 42, 1-20 (1997).
11. Falkowski, P. G. Evolution of the nitrogen cycle and its influence on the biological sequestration of CO2 in the ocean. Nature 387, 272-275 (1997).
12. Mills, M. M., Ridame, C., Davey, M., La Roche, J. & Geider, R. J. Iron and phosphorus co-limit nitrogen fixation in the eastern tropical North Atlantic. Nature 429, 292-294 (2004).
13. Moore, J. K., Doney, S. C., Lindsay, K., Mahowald, N. & Michaels, A. F. Nitrogen fixation amplifies the ocean biogeochemical response to decadal timescale variations in mineral dust deposition. Tellus Series B-Chemical and Physical Meteorology 58, 560-572 (2006).
14. Naqvi, S. W. A. et al. Increased marine production of N2O due to intensifying anoxia on the Indian continental shelf. Nature 408, 346-349 (2000).
15. Altabet, M. A. Constraints on oceanic N balance/imbalance from sedimentary N-15 records. Biogeosciences 4, 75-86 (2007).
16. Gruber, N. & Galloway, J. N. An Earth-system perspective of the global nitrogen cycle. Nature 451, 293-296 (2008).
17. Gruber, N. & Sarmiento, J. L. Global patterns of marine nitrogen fixation and denitrification. Global Biogeochemical Cycles 11, 235-266 (1997).
18. Zehr, J. P. et al. Unicellular cyanobacteria fix N-2 in the subtropical North Pacific Ocean. Nature 412, 635-638 (2001).
19. Zehr, J. P. et al. Globally Distributed Uncultivated Oceanic N-2-Fixing Cyanobacteria Lack Oxygenic Photosystem II. Science 322, 1110-1112 (2008).
20. Moisander, P. H. et al. Unicellular Cyanobacterial Distributions Broaden the Oceanic N-2 Fixation Domain. Science 327, 1512-1514 (2010).

21. Langlois, R. J., LaRoche, J. & Raab, P. A. Diazotrophic diversity and distribution in the tropical and subtropical Atlantic ocean. Applied and Environmental Microbiology 71, 7910-7919 (2005).
22. Langlois, R. J., Hummer, D. & LaRoche, J. Abundances and distributions of the dominant nifH phylotypes in the Northern Atlantic Ocean. Applied and Environmental Microbiology 74, 1922-1931 (2008).
23. Hamersley, M. R. et al. Nitrogen fixation within the water column associated with two hypoxic basins in the Southern California Bight. Aquatic Microbial Ecology 63, 193-+ (2011).
24. Fernandez, C., Farias, L. & Ulloa, O. Nitrogen Fixation in Denitrified Marine Waters. Plos One 6 (2011).
25. Farnelid, H. et al. Nitrogenase Gene Amplicons from Global Marine Surface Waters Are Dominated by Genes of Non-Cyanobacteria. Plos One 6 (2011).
26. Halm, H. et al. Heterotrophic organisms dominate nitrogen fixation in the South Pacific Gyre. ISME J (2011).
27. Moore, C. M. et al. Large-scale distribution of Atlantic nitrogen fixation controlled by iron availability. Nature Geoscience 2, 867-871 (2009).
28. Subramaniam, A. et al. Amazon River enhances diazotrophy and carbon sequestration in the tropical North Atlantic Ocean. Proceedings of the National Academy of Sciences of the United States of America 105, 10460-10465 (2008).

Supplementary Information is linked to the online version of the paper at www.nature.com/nature

Acknowledgements We thank Gabriele Klockgether and Thomas Max for mass spectrometry measurements. We further thank Sandra Fehsenfeld for helping with sampling and Hilda Nurlaeli for her experimental work on *Nodularia*. We also thank Captain and Crew of the research vessels Meteor and Polarstern, as well as the Chief Scientists Peter Brandt and Andreas Macke. We thank Dhwani Desai for conducting statistical analyses with the data. This work is a contribution of the Sonderforschungsbereich 754 "Climate - Biogeochemistry Interactions in the Tropical Ocean" (www.sfb754.de) which is supported by the Deutsche Forschungsgemeinschaft. We thank the Max Planck Gesellschaft for financial support. We thank the

Bundesministerium für Bildung und Forschung (BMBF) for financial support through the SOPRAN II (Surface Ocean Processes in the Anthropocene) project.

Author contributions W.M. designed the dissolution method. T.G., T.B., H.S. and D.G. collected samples and performed *nifH* gene quantification, M.M.M.K. and G.L. did the measurements on the mass spectrometer. T.G. wrote the manuscript with W.M. and J.LR. M.M.M.K., G.L., R.A.S., D.W.R.W., J.L.R, W.M. and T.G. designed the experiments and analyzed the data.

Author information Reprints and permissions information is available at www.nature.com/reprints. The authors declare no competing financial interests. Correspondence and requests for materials should be addressed to jlaroche@ geomar.de and tgrosskopf@geomar.de

Figure1: Sampling sites and sea surface temperature. Map of average night time sea surface temperature in °C (SST) in fall 2009 in the Atlantic Ocean (http://oceancolor.gsfc.nasa.gov/), overlaid with Stations sampled on the METEOR 80/1 (triangles) and the POLARSTERN ANT-XXVI/1 (circles) cruises. Triangles also correspond to 11 vertical profile stations used in Figure 3. The equatorial station was sampled twice during the course of the cruise, and therefore two triangles are superimposed at this location.

Figure 2: Comparison between bubble-addition and dissolution method. A: N_2 fixation rates for all stations and depths. Inlay shows zoom on 0-2 nmol L^{-1} d^{-1} range. B: Carbon fixation rates for all stations and depths. Error bars indicate standard errors of triplicate incubations.

Figure 3: Mixed layer inventory of N_2 fixation rates in the Tropical and Equatorial Atlantic Ocean. Stations correspond to triangles in Fig. 1A. Upper panel: N_2 fixation rates measured with the bubble-addition method. Lower panel: N_2 fixation rates measured with the dissolution method.

Figure 4: Relative abundance (logarithm of (gene copies +1)) of various phylotypes of diazotrophic bacteria from the same stations as the N_2 fixation rate measurements, estimated with TaqMan *nifH* gene assays. From top to bottom: Unicellular cy. = GroupA, GroupB and GroupC cyanobacteria, Het1+2 = diatom associated heterocystous cyanobacteria (DDA's), Gamma AO = diazotrophic γ-proteobacteria, *Trichodesmium*. There was no DNA sampling at the 3.5° N station. Note that the *nifH* gene copies L^{-1} of diatom-associated heterocystous cyanobacteria (e.g. *Richelia*) detects all cells of the symbionts not just the heterocysts where N_2 fixation is actively taking place.

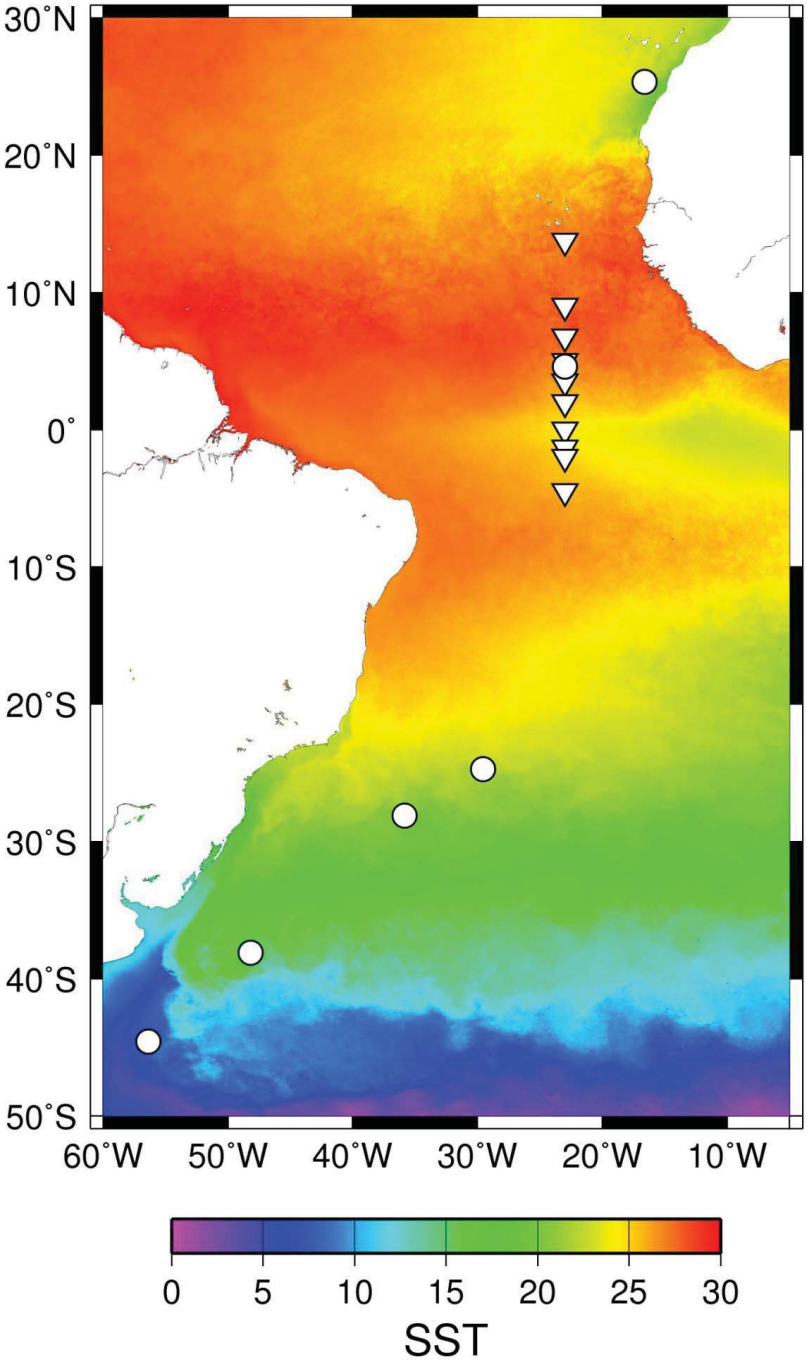
30˚N
20˚N
10˚N
0˚
10˚S
20˚S
30˚S
40˚S
50˚S
60˚W
50˚W
40˚W
30˚W
20˚W
10˚W
0
5
10
15
20
25
30
SST

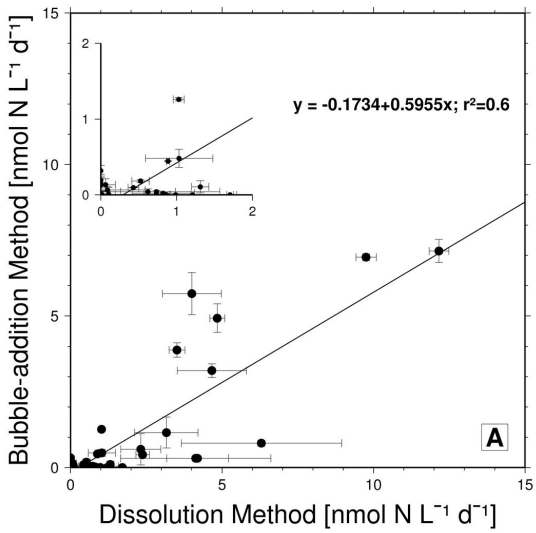
y = -0.1734+0.5955x; r²=0.6
A
Bubble-addition Method [nmol N L⁻¹ d⁻¹]
Dissolution Method [nmol N L⁻¹ d⁻¹]

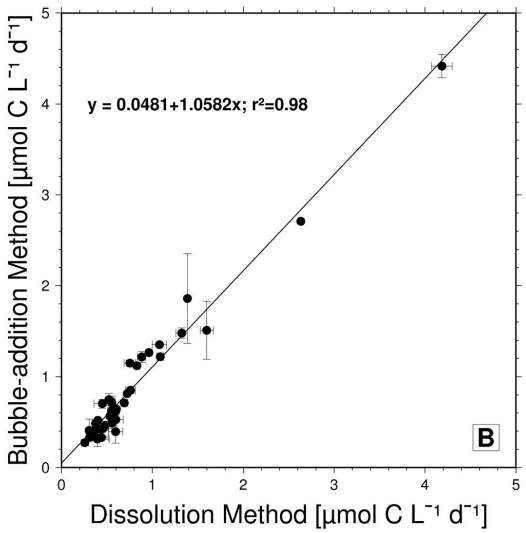
y = 0.0481+1.0582x; r²=0.98
B
Bubble-addition Method [µmol C L⁻¹ d⁻¹]
Dissolution Method [µmol C L⁻¹ d⁻¹]

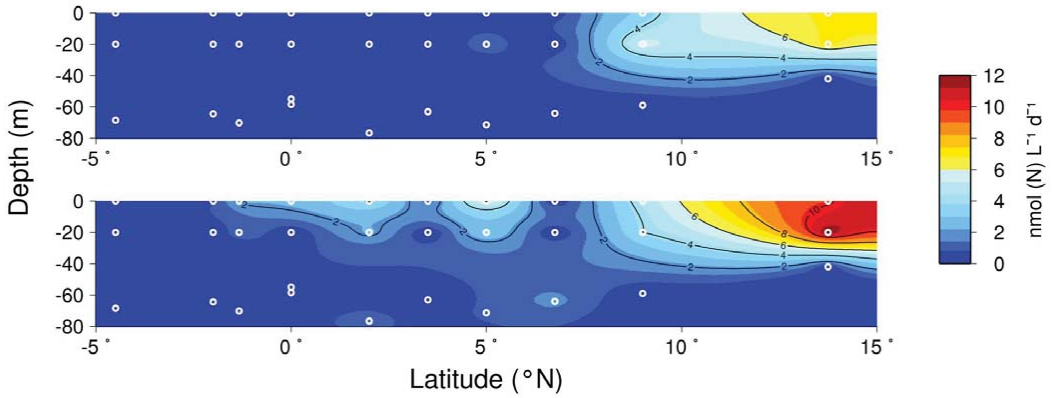
Depth (m)
0
-20
-40
-60
-80
-5 °
0 °
5 °
10 °
15 °
Latitude (°N)
12
10
8
6
4
2
0
nmol (N) L⁻¹ d⁻¹

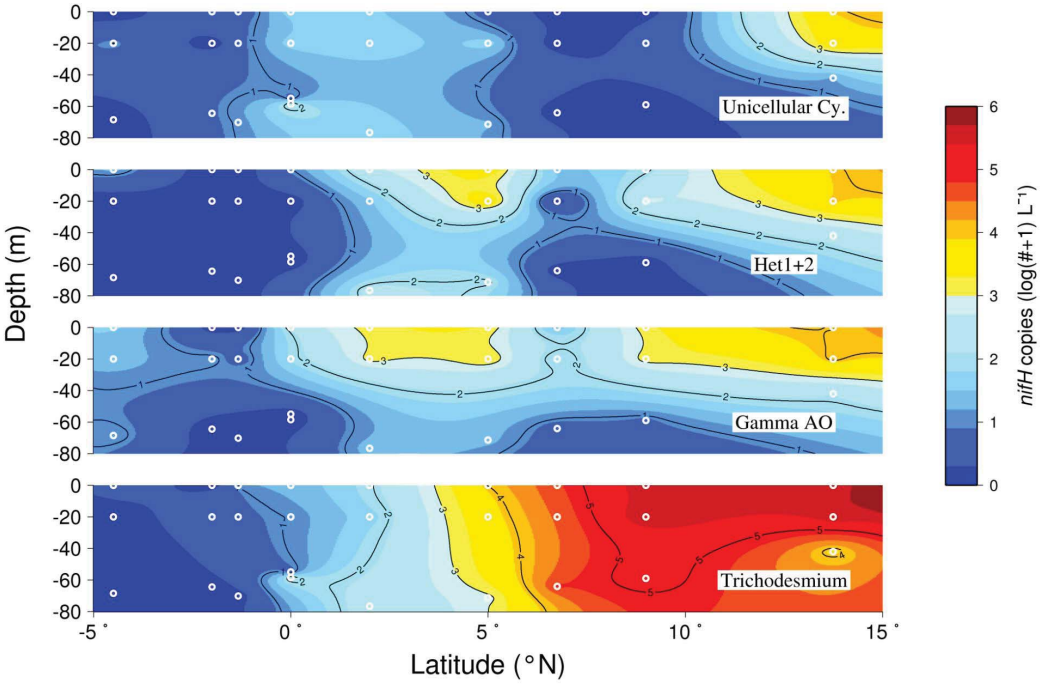
Unicellular Cy.
Het1+2
Gamma AO
Trichodesmium
Depth (m)
Latitude (°N)
nifH copies (log(#+1) L⁻¹)

Material and Methods

Sampling

In order to compare the commonly used $^{15}N_2$ tracer addition method to measure N_2 fixation [1] with the addition of $^{15}N_2$-enriched water as suggested by Mohr et al. (2010)[2], seawater was sampled on two cruises in the Atlantic Ocean, the first on board R/V Meteor (M80/1) on a longitudinal transect (23°W) between 15°N and 5°S, the second on board R/V Polarstern (ANT-XXVI/1) on a transect between 54°N and 54°S (Bremerhaven, Germany to Punta Arenas, Chile). In total 39 triplicate incubations were conducted with both methods in parallel. On the M80/1 cruise, seawater was sampled at 11 stations from the surface (bucket), 20 m depth and the chlorophyll maximum (CTD rosette sampler) at 7:00 in the morning, whereas on the ANT-XXVI/1 cruise, seawater was sampled at 6 stations at 16:00 from the ship's clean seawater supply which is installed at 11 m depth (keel of the ship).

Incubations

Seawater samples were filled headspace-free (bubble addition method) or with a 100-150 ml headspace (dissolved method) into 4.5 L polycarbonate bottles and closed with Teflon® -coated butyl rubber septum caps. To determine N_2 fixation rates with the bubble-addition method, a 4.5 mL $^{15}N_2$ gas bubble (Sigma-Aldrich, ≥98 atom%) was injected through the septa into each of triplicate bottles (yielding a theoretical enrichment of ~12 atom% assuming a rapid isotopic equilibration between the added $^{15}N_2$ gas and the ambient dissolved N_2 of the water sample). After injection, bottles were gently inverted one hundred times. For comparison of N_2 fixation rates, we added $^{15}N_2$-enriched seawater to a second set of triplicate bottles (dissolution method). In detail, the preparation of the $^{15}N_2$-enriched seawater was started by degassing filtered seawater (0.2 µm filtered, Durapore) using a membrane flow-through system (Mini-Module, Membrana) in which the seawater flowed on the inside of the membrane and a vacuum (-960 mbar, water jet pump) was applied to the outer side of the membrane. The seawater flow rate was about 400 – 500 mL min^{-1} and seawater was recirculated for the first 10-15 min of the degassing step. Degassed seawater was then filled directly from the flow-through system into evacuated gas-tight 3L Tedlar® bags without a headspace. Addition of $^{15}N_2$ gas was dependent on the amount of seawater in the Tedlar® bag and was added at a ratio of 10 ml $^{15}N_2$ per 1L seawater. The volume of degassed seawater in

1

the Tedlar® bag was estimated using a balance. During the Meteor cruise, dissolution of the $^{15}N_2$ gas was achieved by 'slapping' the bubble with a ruler. The 'slapping' lead to a dispersion of the large bubble into numerous small bubbles and thus an increase in the surface area to volume ratio which facilitated gas diffusion. After complete dissolution of the added $^{15}N_2$ gas ($^{15}N_2$-enriched seawater), an aliquot of the $^{15}N_2$ enriched water was collected for each preparation of enriched seawater and stored in an Exetainer until return to the laboratory where the isotopic composition was measured by membrane-inlet mass spectrometry[3]. Overall, the average concentration of $^{30}N_2$ in the prepared batches of enriched water was 246 µM (standard deviation =24.7 µM). This yielded a ^{15}N-enrichment of about 2% when 100 mL enriched seawater are added to 4.5 L of incubation volume (depending on temperature and salinity). Next, 100-150 ml of $^{15}N_2$-enriched seawater were added to each of triplicate bottles before capping the bottles headspace-free with Teflon®-coated butyl rubber septum caps. Bottles were inverted 100 times. Primary production rates were determined in all incubation bottles by the addition of $NaH^{13}CO_3$ (~3.5 atom% final) after the addition of $^{15}N_2$ gas or $^{15}N_2$-enriched water. All bottles were placed into on-deck incubators with a surface seawater flow-through and a 25% in situ light level established with a light foil layer (Blue Lagoon, Lee Filters). Incubations were stopped after 24 hours by filtering 2-3 liters of each incubation onto pre-combusted (450°C, 5 hours) GF/F filters (Whatman) under gentle vacuum (-200 mbar). Filters were oven-dried (50°C, 24 hours) (Meteor) and stored over desiccant until analysis or frozen at -20°C directly after filtration (Polarstern). On the Meteor, the remainder of the samples was pooled for nucleic acid sampling within each set of triplicate bottles and a total of 2 L were filtered onto Durapore filters (47 mm, 0.2 µm pore size; Millipore). Samples were shock-frozen in liquid nitrogen and stored at -80°C until analysis.

To determine the natural abundance (*NA-control*) of ^{15}N and ^{13}C isotopes in the incubations, two different controls were incubated alongside with the six experimental bottles. The control for the bubble-addition method was untreated seawater, while the control for the dissolved method received an aliquot of seawater which had previously been degassed but instead of the addition and dissolution of $^{15}N_2$ for the preparation, ambient air was used. Both controls were processed as described above for the experimental bottles.

Elemental stoichiometry and isotopic composition of particulate organic material

GF/F filters were acidified over fuming HCl overnight in a dessicator. Filters were then oven-dried for 2 hours at 50°C and pelletized in tin cups. Samples were analyzed for particulate

organic carbon and nitrogen (POC and PON) and isotopic composition using a CHN analyzer coupled to an isotope ratio monitoring mass spectrometer.

Calculation of nitrogen and carbon fixation rates

N_2 fixation rates were calculated based on the final isotopic composition of the particulate organic nitrogen after the incubation using the following equation (1):

$$N_2\,fixation\ rate = \frac{\left(A^{PN}_{sample} - A^{PN}_{NA-control}\right)}{\left(A_{N_2} - A^{PN}_{NA-control}\right)} x \frac{[PN]}{\Delta t} \qquad (1)$$

With A = atom% ^{15}N in the particulate organic nitrogen (PN) in incubations to which $^{15}N_2$ was added (A^{PN}_{sample}), in control incubations ($A^{PN}_{NA-control}$) which were simultaneously incubated with the other bottles or in the dissolved N_2 pool (A_{N_2}). For the bubble-addition method, the atom% in the N_2 pool was calculated from the predicted$^{15}N_2$ concentrations according to Mohr *et al*. (2010) [2]. For the dissolution method the $^{15}N_2$ concentration was calculated from the MIMS measurement value in the batch of enriched water for individual experiments and the measured volume of enriched water added to the incubation bottle. Carbon fixation rates were calculated as described for N_2 fixation rates. All rates are displayed as means of triplicate incubations with a standard error.

DNA extraction and determination of nifH phylotype gene copy number

DNA was extracted according to Langlois et al. 2008 using the AllPrep DNA/RNA extraction kit (QIAGEN) following the manufacturer's instructions[4]. Amplification of *nifH* genes was performed on an ABI-PRISM 7000 thermocycler, using phylotype specific probes and primers described in Langlois et al. 2008 [4] and Foster et. al. 2007 [5] (Table S1). *nifH* gene copy numbers were calculated based on the attained Ct values and a linear regression from plasmid standards ranging from 10^7 to 10^1 copies and simultaneously amplified on the same plate.

Table S1. Primers and Probes used in Taqman assays during this study. All sequences reported in 5'-3' direction.

	Reverse (5'-3')	Pos	Forward (5'-3')	Pos	Probe (5'-3')	Pos
UCYN-A	TCAGGACCACCGGACTCAAC	127-146	TAGCTGCAGAAAGAGGAACTGTAGAAG	50-76	TAATTCCTGGCTATAACAAC	98-117
Filamentous (Fil)	GCAAATCCACCGCAAACAAC	256-275	TGGCCGTGGTATTATTACTGCTATC	165-189	AAGGAGCTTATACAGATCTA	206-225
Croco (UCYN-B)	TCAGGACCACCAGATTCTACACACT	122-146	TGCTGAAATGGGTTCTGTTGAA	54-75	CGAAGACGTAATGCTC	87-102
UCYN-C	GGTATCCTTCAAGTAGTACTTCGTCTAGCT	83-112	TCTACCCGTTTGATGCTACACACTAA	1-26	AAACTACCATTCTTCACTTAGCAG	32-55
GamAO	AACAATGTAGATTTCCTGAGCCTTATTC	294-321	TTATGATGTTCTAGGTGATGTG	240-266	TTGCAATGCCTATTCG	275-290
Het-1 (Rich-Rizo)	AATACCACGACCCGCACAAC	158-177	CGGTTTCCGTGGTGTACGTT	105-124	TCCGGTGGTCCTGAGCCTGGTGT	133-155
Het-2 (Rich-Hemi)	AATGCCGCGACCAGCACAAC	158-177	TGGTTACCGTGATGTACGTT	106-124	TCTGGTGGTCCTGAGCCTGGTGT	133-155

Statistical analysis

To test if the grouping of the Meteor dataset into Equatorial and Tropical North Atlantic stations was statistically significant, we used the PRIMER (v. 6[6]) to perform a principal component analysis (PCA) and an analysis of similarity (ANOSIM) with the input parameters sample depth, phosphate concentration, *Trichodesmium* dominance (filamentous *nifH* abundance relative to other *nifH* genes), temperature, oxygen, ammonium concentration, salinity and the measured N_2 fixation rates for the bubble addition and dissolution methods (Fig. S2). The PCA showed that temperature, oxygen and phosphate were driving a spread of the data according to water depth, while the dominance of *Trichodesmium*, the measured N_2 fixation rates, salinity and ammonium were responsible for the separation in latitude (Fig.

S2A). The ANOSIM indicated that the division into the equatorial and tropical areas was highly significant ($p<0.01$).

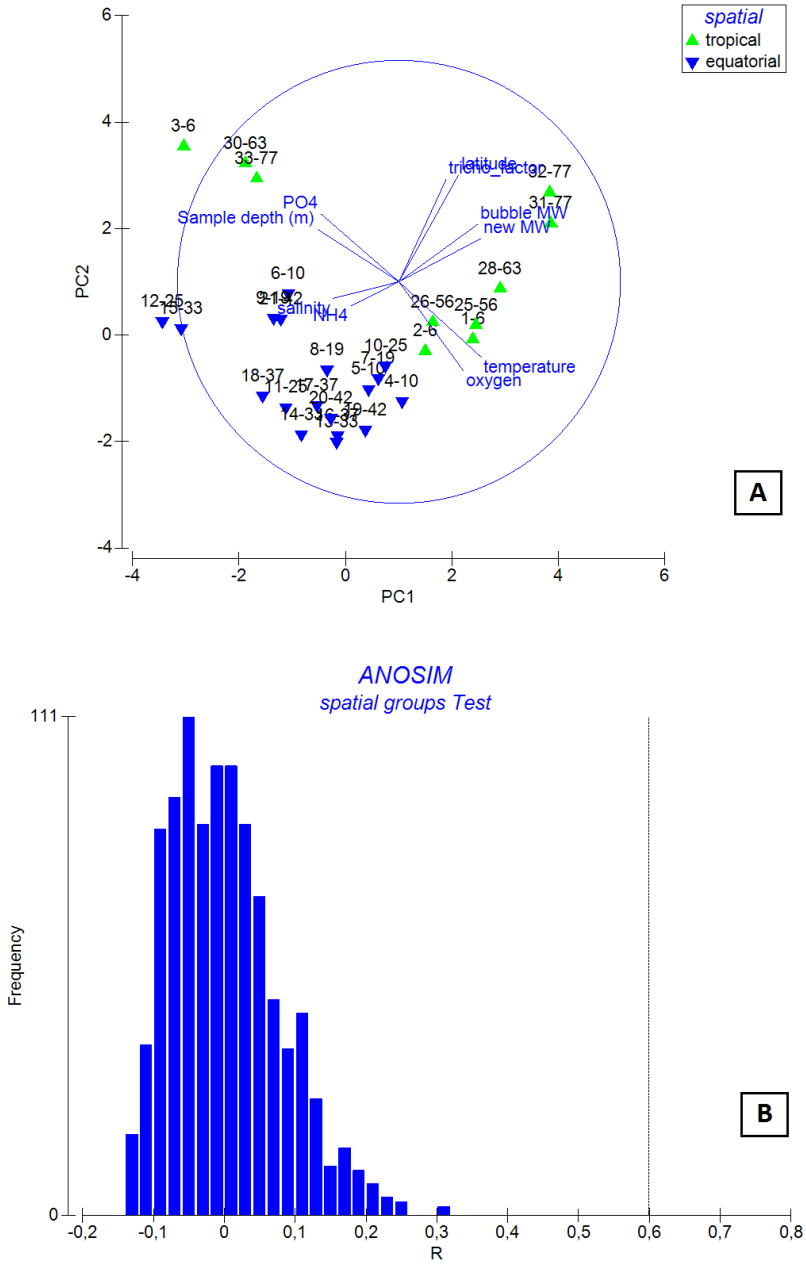

Figure S2. A: PCA analysis showing the samples of the METEOR 23°W transect and the clustering into the tropical (green triangles) and equatorial (blue triangles) groups. The blue lines show the strength and the direction of the influence of the variable over the direction of the data distribution. B: The observed R value of 0.6 (black line) is to the right beyond the

distribution function of random sampling of the variables (blue frequency bars), hence showing the statistical significance ($p<0.01$) of the grouping in the PCA of Fig. S2A.

Areal rates

Areal rates were calculated for the Meteor cruise (15°N – 5°S) according to equation (2):

$$N_{fix}\ (\mu mol\ N\ m^{-2}\ d^{-1}) = \frac{(r_0 + r_{20})}{2} x20m + \frac{(r_{20} + r_{DCM})}{2} x(z_{DCM} - 20m) \qquad (2)$$

With the areal N_2 fixation rate N_{fix}, r_0, r_{20} and r_{DCM} the N_2 fixation rates at surface, 20 meters and the chlorophyll maximum respectively and z_{DCM} the depth of the chlorophyll maximum. Standard errors were calculated according to error propagation techniques.

The areal N_2 fixation rates (µmol N m^{-2} d^{-1}) calculated according to equation 2 showed a strong linear correlation (Fig. S3, r^2 = 0.92) with the N_2 fixation rates (nmol N l^{-1} d^{-1}) measured for the surface waters during the Meteor cruise. This linear correlation (equation 3) was subsequently used to convert the N_2 fixation rates at 11m water depth from the Polarstern cruise to areal N_2 fixation rates.

$$N_{fix}\ (\mu mol\ N\ m^{-2}\ d^{-1}) = 35.872\ x\ N_{fix(surface)} (nmol\ N\ L^{-1}\ d^{-1}) \qquad (3)$$

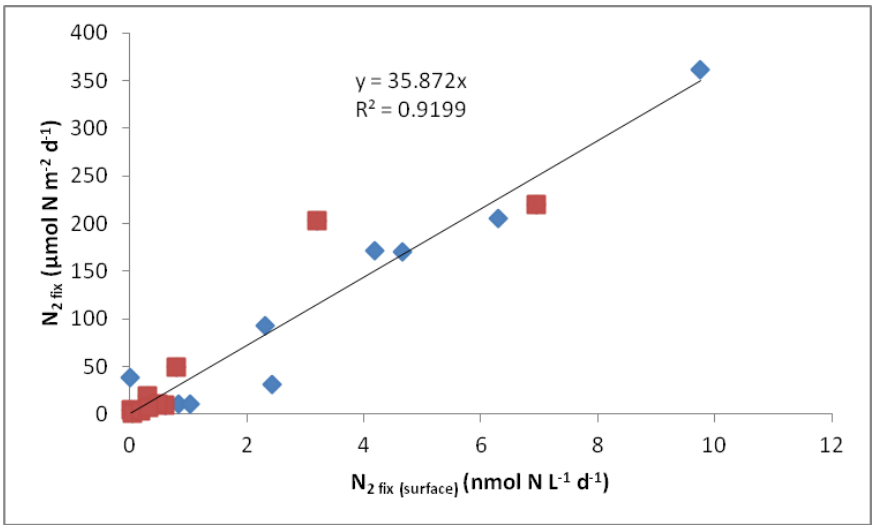

Figure S3. Correlation between N_2 fixation rates measured for the surface waters and calculated (equation 2) areal rates for the Meteor transect for both the bubble addition (red

squares) and the dissolution method (blue diamonds). The black line represents the linear relationship for the entire data set with both methods, forced through zero ($r^2 = 0.92$). The slopes of the regressions for the individual regressions of the two methods separately are 36.826 ($r^2 = 0.946$) for the dissolution and 35.851 ($r^2 = 0.8624$) for the bubble-addition method.

Global N_2 fixation estimates from literature values

For the global estimates of N gain via N_2 fixation, published values of bulk water N_2 fixation rates measured with the bubble-addition method (Table S2) were weighted according to the number of stations and averaged over six ocean basins: North and South Pacific, North and South Atlantic and North and South Indian Ocean (Table S3). The basin wide average was multiplied by the dimension of the basin, whose extent was defined by the most northerly and most southerly observation of N_2 fixation mentioned. Since the Indian Ocean is poorly constrained in terms of measurements by the bubble-addition method, we used average rates from the North and South Pacific for the North and South Indian Ocean, respectively.

Table S2: Collection of publications using the bubble-addition method in the Atlantic and Pacific Oceans. S.e., standard error. [+] Treated as outlier, * as quoted in Mahaffey2005, ** Considering stations 11, 12, 21, 22, 31, 32, 41, 51, 52 and 71 as upwelling stations, [‡] values from supporting online material, *** used for North and South Atlantic with half the stations weighted

Publication	Ocean domain	North limit (°N)	South limit (°N)	West limit (°E)	East limit (°E)	Stations	Areal rate (µmol N m^{-2} d^{-1})	S.e.
Rees *et al.* 2009	Atlantic, English channel[7]	50.2	49	-5	-4	2	350	
Fernandez *et al.* 2010	Atlantic, North[8]	40	15	-29	-28	8	18	3
Voss *et al.* 2004	Atlantic, Western Tropical North[9]	10	10	-55	-40	4	24	9
Voss *et al.* 2004	Atlantic, Eastern Tropical North[9]	10	5	-25	-15	6	140	32
Voss *et al.* 2004	Atlantic, Equatorial[9]	0	0	-26	-24	2	4	
Fernandez *et al.* 2010	Atlantic, Equatorial[8]	15	-5	-29	-28	14	60	5
Mourino-Carballido *et al.* 2011	Atlantic, North[10]	30	16	-29	-15	6	11	4
Mourino-Carballido *et al.* 2011 ***	Atlantic, Equatorial[10]	16	-12	-29	-28	7	56	19
Sohm *et al.* 2011	Atlantic, South East[11]	-14	-11	-5	0	2	24	
Sohm *et al.* 2011	Atlantic, South East[11]	-14.75	-14.75	12	12.2	1	85	
Fernandez *et al.* 2010	Atlantic, South[8]	-5	-30	-29	-28	12	7	1

Mourino-Carballido *et al.* 2011	Atlantic, South[10]	-12	-31	-36	-28	7	10	4
Shiozaki *et al.* 2009	Pacific, North[12]	44	30	-155	-155	3	0	
Montoya *et al.* 2004	Pacific, Eastern North Gyre[13]	35	25	-160	-125	10	520	160
Needoba *et al.* 2007	Pacific, North East[14]	34	34	-129	-129	24	15	
Hamersley *et al.* 2011	Pacific, North East[15]	34	34	-119	-119	15	150	
White *et al.* 2007	Pacific, North East[16]	30	22	-122	-122	4	106	55
Shiozaki *et al.* 2009	Pacific, North[12]	30	0	-155	-155	8	55	16
Sohm *et al.* 2011 ‡	Pacific, North[17]	24	19	-160	-154	23	143	21
Sohm *et al.* 2011 ‡	Pacific, North[17]	23	19	-162	-156	11	216	21
Sohm *et al.* 2011 ‡	Pacific, North[17]	28	23	-180	-161	8	137	16
Church *et al.* 2009	Pacific, ALOHA[18]	22.75	22.75	-158	-158	34	111	11
Zehr *et al.* 2001	Pacific, ALOHA[19]	22.75	22.75	-158	-158	1	95	
Montoya *et al.* 2004	Pacific, ALOHA[13]	22.75	22.75	-158	-158	7	66	19
Grabowski *et al.* 2008	Pacific, ALOHA[20]	22.75	22.75	-158	-158	9	72	4
Dore *et al.* 2002 *	Pacific, ALOHA[21]	22.75	22.75	-158	-158	4	69	13
Voss *et al.* 2006 **	Pacific, North West[22]	13.5	10	108	110.5	10	26	17
Voss *et al.* 2006	Pacific, North West[22]	13.5	10	108	110.5	18	71	16
Bombar *et al.* 2010	Pacific, North West[23]	13	10	108	111	4	23	3
Bombar *et al.* 2010	Pacific, North West[23]	13	10	108	111	7	138	45
Bombar *et al.* 2010	Pacific, North West[23]	13	10	108	111	4	88	49

Bombar *et al.* 2010	Pacific, North West[23]	13	10	108	111	4	59	23
Fernandez *et al.* 2011	Pacific, South East[24]	2	-18	-86	-74	8	8	2
Raimbault *et al.* 2008	Pacific, South West[25]	-7	-15	-141	-134	4	110	15
Fernandez *et al.* 2011	Pacific, South East[24]	-13	-20	-78	-70	8	190	29
Raimbault *et al.* 2008	Pacific, South West[25]	-15	-20	-133	-123	4	70	35
Garcia *et al.* 2007	Pacific, South West[26]	-20	-22	166	167	6	290	86
Raimbault *et al.* 2008	Pacific, South West[25]	-20	-30	-123	-101	4	60	15
Raimbault *et al.* 2008	Pacific, South West[25]	-30	-33	-100	-81	6	30	2
Raimbault *et al.* 2008	Pacific, South West[25]	-33	-35	-80	-72	2	90	47
Montoya *et al.* 2004+	Pacific, Arafura Sea[13]	-10	-20	120	150	2	3955	
Montoya *et al.* 2004	Pacific, Kaneohen Bay[13]	-9.5	-9.5	135	135	6	24	12
Montoya *et al.* 2004	Pacific, Arafura Sea[13]	-10	-20	120	150	7	126	47

Table S3: Global rates of annual N_2 fixation. The rates are basin wide averages, obtained by station weighted averaging over the four domains (North Atlantic, South Atlantic, North Pacific and South Pacific Ocean) from table S2. * For the Indian Ocean areal rates of the Pacific Ocean were used.

Ocean Basin	North limit (°N)	South limit (°N)	Stations	Areal rate (μmol N m^{-2} d^{-1})	Area (10^6 km^2)	Areal rate (mol N m^{-2} yr^{-1})	Basin (mol N y^{-1})	Basin rate (tg N y^{-1})
Atlantic North and Equatorial (weighted average)	50	-5	46	64	39.2	0.023	9.08E+11	12.7
Atlantic South (weighted average)	-5	-30	26	19	15.9	0.007	1.08E+11	1.5
Pacific North (weighted average)	30	0	208	115	56.3	0.042	2.36E+12	33.0
Pacific South (weighted average)	0	-35	55	103	56.1	0.038	2.11E+12	29.5
Indian North	25	0	0	115*	15.8	0.042*	6.62E+11	9.3
Indian South	0	-35	0	103*	31.8	0.038*	1.20E+12	16.7
Global Sum					215.1			**102.7**

Supplementary Online Material and Figures

Comparison of mean N_2 fixation rates measured by the bubble-addition and the dissolution methods in the tropical and equatorial regions

A pairwise comparison (t-test for dependent samples) of the mean N_2 fixation rates determined with the bubble-addition and the dissolution methods within the tropical and equatorial areas (Fig. S4) indicated that the underestimation by the bubble-addition method was statistically significant in both regions. Moreover, this underestimation was substantially higher in the equatorial region, which was dominated by diazotrophs other than *Trichodesmium.*

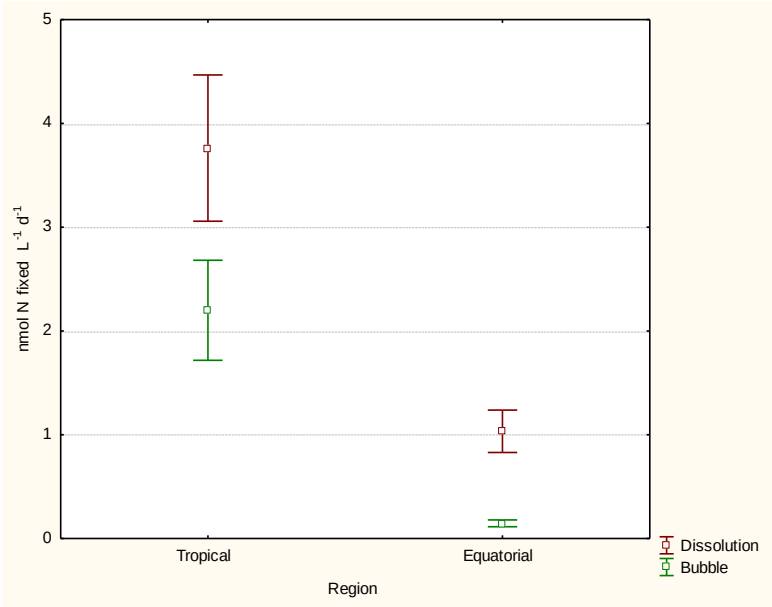

Figure S4: Plot of means with standard error for the dissolution method (red boxes) and bubble-addition method (green boxes). Rates were pooled over all depths for the Equatorial (4.5°N - 5°S) and the Tropical North Atlantic (15°N - 5°N) region. The mean N_2 fixation rates measured by the dissolution and the bubble-addition methods were significantly different for both the equatorial region (t-test for dependent samples, p = 0.000025, df = 61), and the tropical region (t-test for dependent samples, p = 0.001, df= 38).

Magnitude of the underestimation by the bubble-addition method relative to the dissolution method

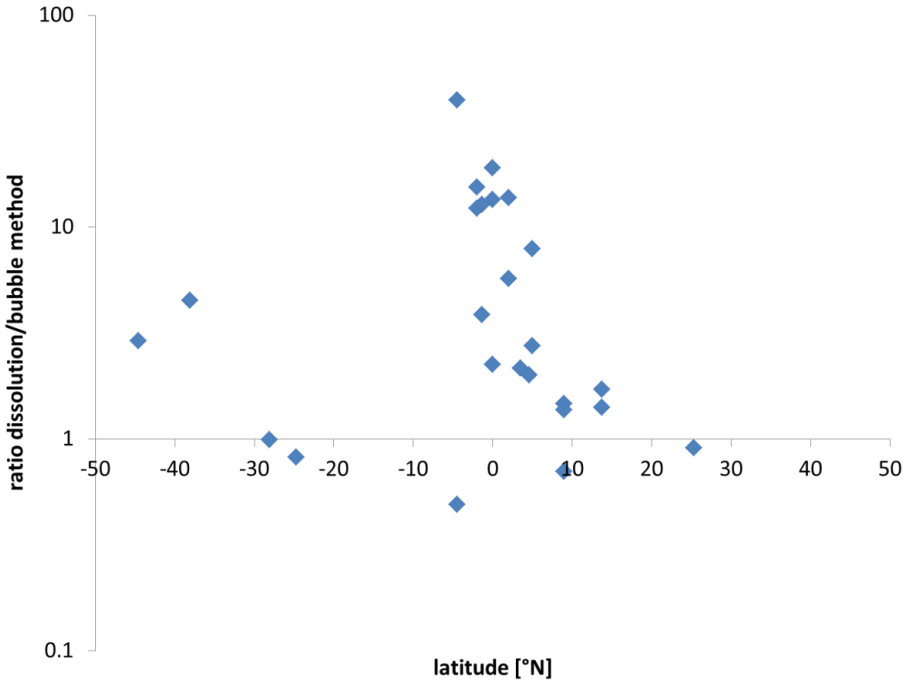

Figure S5: Ratio of N_2 fixation rates measured by dissolution method relative to the bubble-addition method (note the log-scale) as a function of latitude. Ratios were calculated for the paired measurements where N_2 fixation rates were detectable with both methods (n=25). Note that the ratio is particularly large (i.e. the underestimation of N_2-fixation rates by the bubble method is large) in the tropical regions where diazotrophs other than *Trichodesmium* dominate.

Summary and implications of the results presented in Mohr et al. (2010)

Mohr et al. (2010) showed that the equilibration of a $^{15}N_2$ gas bubble in seawater is slow, taking up to 12 hours to reach ~ 80% of the calculated value based on complete equilibration of the $^{15}N_2$ label with seawater (Fig. S6, upper panel). In contrast, the $^{15}N_2$ label added as dissolved $^{15}N_2$ remained constant with time (Fig. S6, lower panel). Mohr et al. (2010) shows that the strength of agitation (their Figure 2 and 4), bottle size and bubble size (their Figure 3 and 4), affect the kinetics of the $^{15}N_2$ gas equilibration with the surrounding seawater. The consequence of the slow and variable equilibration time of the $^{15}N_2$ gas in field incubations

carried out by the bubble addition method[1] is that the rates will be underestimated in most cases. The underestimation will be variable and depend on physical factors (e.g. amount of agitation), specific species composition of the diazotrophic community (e.g. floaters vs. sinkers, night fixers vs. day fixers), the time of onset for the incubations (e.g. morning vs. evening, Mohr et al 2010, their Figure 5) and length of incubation. The strong linear correlation between the ^{15}N-labeling % of dissolved N_2 in the medium and ^{15}N-labeling of *Crocosphaera* biomass (Fig. S7) shows that variations in $^{15}N_2$, and total dissolved N_2 concentrations have no significant effect on the N_2-fixation rate itself.

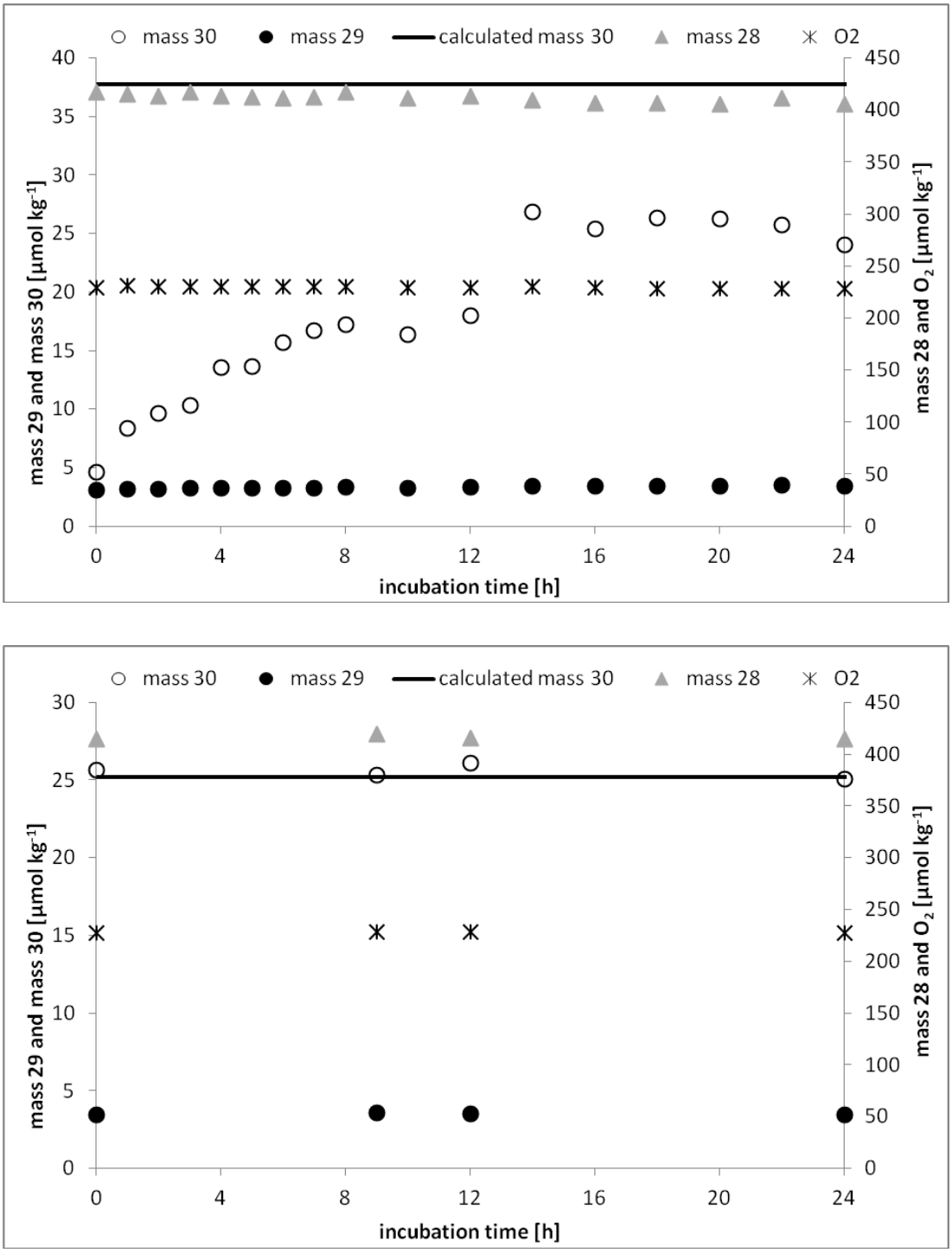

Figure S6: Membrane inlet mass spectrometry measurements of $^{28}N_2$, $^{29}N_2$, $^{30}N_2$, and dissolved oxygen ($^{32}O_2$) concentrations versus equilibration time for the bubble-addition method (top panel) and the dissolution method (lower panel). The calculated (expected)

values for $^{15}N_2$ (mass 30) are 37.7 and 25.2 µmol kg^{-1} for the bubble-addition and the dissolution method, respectively (black solid lines) (data redrawn from Mohr et al. (2010).

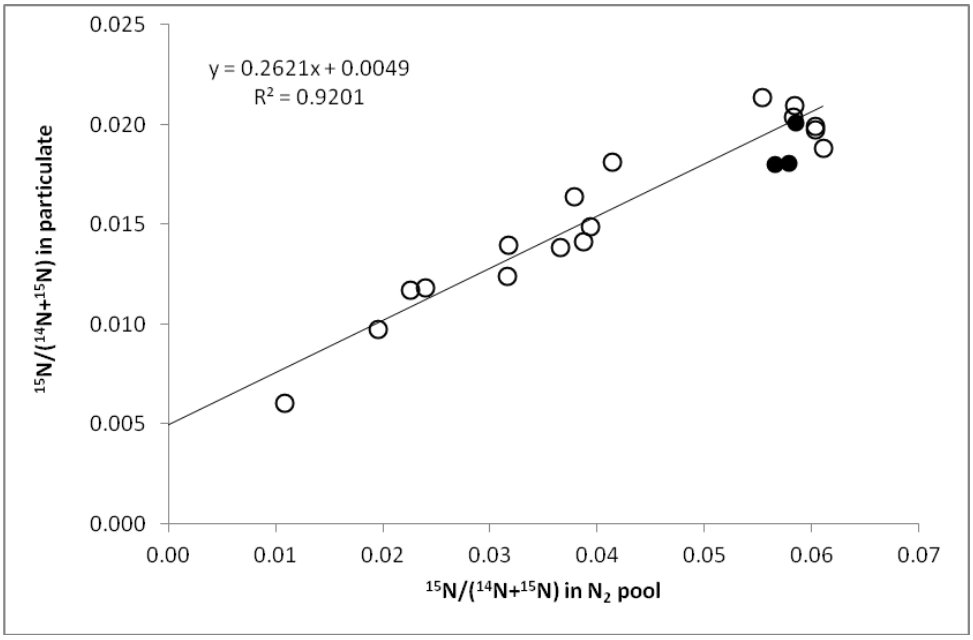

Figure S7: Linear correlation between the $^{15}N/(^{14}N+^{15}N)$ ratio for dissolved N_2 and the corresponding $^{15}N/(^{14}N+^{15}N)$ ratio for particulate nitrogen from the *Crocosphaera watsonii* culture after 12 h incubation. The linear relationship shows that ^{15}N-assimilation by these diazotrophs is directly proportional to the ^{15}N-labeling % for dissolved N_2 in the medium. The slope of the regression line is 0.26 indicating that the N-based doubling times for *Crocosphaera* were ~2 days in our incubations, which is comparable to published growth rates[27]. The different levels of ^{15}N enrichment in seawater were achieved by pre-equilibrating a gas bubble for times varying from 1 to 24 hours prior to the inoculation with the *Crocosphaera* cultures. For comparison, the values of incubations to which dissolved $^{15}N_2$ was added are displayed (filled circles). Data redrawn from Mohr et al. (2010).

Considerations about the change in gas composition in an incubation

An incubation of seawater in a bottle always presents a situation that is ideally close to, but not identical to *in situ* conditions. Since a bottle offers a very limited space, it is possible that in a 24 hour incubation some organisms or particulate matter sinks to the bottom of the bottle, where oxygen will get more depleted than in the upper part of the bottle.

However, such bottle effects are inherent to any kind of incubation and would not differentially affect the methods used here. In both the bubble-addition and the dissolution method a minor part of the gas composition is replaced by the added $^{15}N_2$ label. This volume needs to be kept as low as possible, but on the other hand the desire is to maximize the addition of $^{15}N_2$ label, to increase the detection limit. By adding 100 mL of degassed water to a 4.5 L incubation (= 2.2%), the oxygen concentration for example drops theoretically from 225 µM to 220 µM. Such a change in oxygen concentration is within the natural variability of surface oxygen concentration due to photosynthesis and respiration. In a bubble-addition type of incubation with 1 mL $^{15}N_2$ gas per L of seawater the drop in oxygen concentration would be from 225 µM to ~216 µM, since the bubble would hold ~20% oxygen after complete equilibration. The manipulation in the gas composition is therefore similar in both methods and within the range of natural variability. In Mohr et al, (2010), the concentrations of the nitrogen isotopes as well as dissolved oxygen were measured in water samples that were incubated with a $^{15}N_2$ gas bubble as well as with dissolved $^{15}N_2$ additions (see Fig. S6 above). The measured data confirm the theoretical changes mentioned here.

Examples of potential bias introduced by the species composition for the bubble-addition method

There are several ways in which the diazotrophic community composition can affect the magnitude of underestimation in a bubble-addition method incubation. One example is via the time of N_2 fixation activity relative to the beginning of the incubation. Diazotrophic communities dominated by diazotroph species fixing at night (e.g. *Crocosphaera*) will suffer less underestimation than one that is dominated by diazotrophs fixing during the day (e.g. UCYN-A) when the incubation is set up at sunrise, since the $^{15}N_2$ label had more time to equilibrate with the water phase [2] and vice versa. The second way is via the relative position in the water, i.e. the "closeness" of the diazotroph to the source of label, the $^{15}N_2$ bubble. The following experiment with *Nodularia*, a buoyant diazotrophic cyanobacterium, suggests that this may also happen in natural communities. A culture of the heterocystous cyanobacterium *Nodularia spumigena* IOW-2000/1 was grown in modified artificial seawater [28] supplemented with phosphate and trace metals (ASW). The culture was transferred twice into fresh medium before the experiment. For the experiment, three 450 ml sub-cultures (1 week after last transfer) were transferred from culture flasks into 1.15 L sterile glass bottles. The cultures were supplemented with fresh media up to ~ 1.13 L. Cultures were left over-night to allow

filaments to float to the top of the bottle. The next day, cultures were filled with fresh media from the bottom with a syringe in order to keep the floating filaments in place. The bottles were closed headspace-free with Teflon®-coated butyl rubber septum caps and 5 mL of $^{15}N_2$ gas were injected just underneath the septum. At the end of the ~ 6 h incubation period during the day time, the floating filaments were separated from the non-floating ones and both were separately filtered onto pre-combusted GF/F filters (Whatman). A natural abundance sample was also filtered at the end of the incubation. Filters were treated as previously described.

The nitrogen fixation rate measured in the floating fraction was significantly higher (t-test, $p < 0.05$, $n = 3$) than the measured rate of the bulk phase (Fig. S8). However, N_2 fixation rates measured with the $^{15}N_2$ isotope added as a dissolved gas (dissolution method) measured during the same experiment were approximately 2 and 6 times higher than those measured with the bubble-addition method for the floating and the non-floating fractions, respectively. Although our experimental design does not rule out that the floating and sinking fraction may have been in a different physiological state and fixing N_2 at different rates, the right panel of Figure S8 shows that a small layer of filaments close to the bubble of pure $^{15}N_2$ gas would have been exposed to very high concentration of $^{15}N_2$ gas during the incubation period. The calculated rates for the floating and non-floating fraction are in agreement with this hypothesis and suggest that such situation may also develop during calm field conditions. The culture results presented here are also congruent with the observation of less discrepancy between the bubble-addition and dissolution method in areas which were dominated by *Trichodesmium* vs. areas not dominated by *Trichodesmium* which suffered from larger discrepancies.

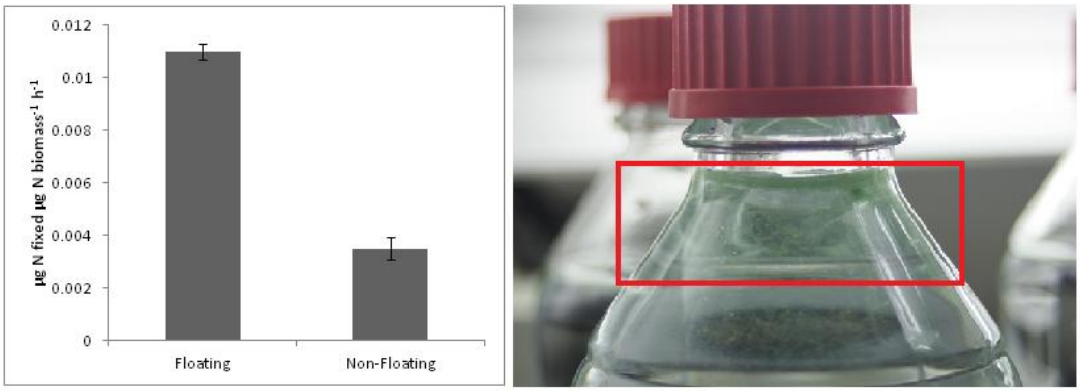

Figure S8. Left: Biomass-specific N_2 fixation rates of *N.spumigena* measured with the bubble-addition method. Filaments at the very surface of the incubation bottle (floating) were

analyzed separately from the bulk liquid phase (non-floating). Error bars indicate standard errors of triplicate incubations. Right: Filaments of *Nodularia* in the incubation bottles. Red box marks the floating fraction analyzed in this experiment.

Literature survey of incubation conditions used for $^{15}N_2$ fixation measurements

Since many factors besides the diazotrophic species composition (see upper section) have the potential to influence the magnitude of difference between the two methods, like bottle size, incubation time and bubble size, it is of interest to know how our experimental conditions compared to those in other studies. Table S4 gives an overview of the published literature and the experimental setup used. The global mean of $^{15}N_2$ gas added per liter of sample is 2.6 mL L^{-1}, the median is 1.0 mL L^{-1}. In this study we used 1 mL L^{-1} of $^{15}N_2$ gas, which is a representative value of the previously published work. The incubation time and bottle size in this study were 24 h and 4.5 liters, respectively, both representative of conditions used for whole water incubations in oligotrophic regions. In addition, a 24 h incubation also ensures that the N_2 fixation measurement covers a full daily cycle. However, the table below shows the range of incubation times used and that the underestimation or rates may be highly variable especially considering the timing effect of incubation vs. the timing of N_2 fixation activity.

Table S4: Published literature about studies using the $^{15}N_2$ tracer addition (bubble-addition) method and the parameters used in their incubation setup.

Reference	Year published	Ocean	Study area or organism	Incubation time [h]	$^{15}N_2$ [ml L^{-1}]	bottle size [L]
Benavides *et al.*	2011[29]	Atlantic	NE Atlantic	24	1.6	1.24
Bombar *et al.*	2011[30]	South China Sea	Mekong River Plume	6-12	0.9	2.3
Bombar *et al.*	2010[31]	South China Sea	upwelling	6	1.1	2.3
Bonnet *et al.*	2009[32]	Pacific	Equatorial W Pacific	24	0.7	4.5

Bonnet *et al.*	2011[33]	Mediterranean		24	0.9	4.5
Burns *et al.*	2006[34]	Atlantic / Pacific	*Trichodesmium*	4	0.4	0.25
Capone *et al.*	2005[35]	Atlantic	*Trichodesmium*	2	0.3	0.31
Chen *et al.*	2008[36]	South China Sea	Kuroshio and South China Sea Basin, *Trichodesmium*	3	1.7	0.12
Chen *et al.*	2011[37]	Pacific	NW Pacific / Kuroshio / *Trichodesmium*	3-5	1.7	0.12
Chen *et al.*	2011[37]	culture	*Trichodesmium*	24	5	1.2
Church *et al.*	2009[18]	Pacific	N Pacific subtropical gyre, station ALOHA	24	0.7	4.5
Degerholm *et al.*	2008[38]	Baltic Sea		4	18.4	0.25
Dore *et al.*	2002[21]	Pacific	subtropical N Pacific	24	0.2	4.7
Falcón *et al.*	2004[39]	Atlantic / Pacific	Unicellular	24	0.64	0.014
Fernandez *et al.*	2010[40]	Atlantic	Atlantic	24	1	2
Fernandez *et al.*	2011[24]	Pacific	tropical SE Pacific	24	2	2
Fong *et al.*	2008[41]	Pacific	N Pacific subtropical gyre	24	0.7	4.5
Gandhi *et al.*	2011[42]	Indian Ocean	Arabian Sea	4	1.6	1.25
Garcia *et al.*	2011[43]	culture	*Trichodesmium*	12	1	0.16
Garcia *et al.*	2007[26]	Pacific	SW Pacific	12	1.7	1.2
Goebel *et al.*	2010[44]	Atlantic	tropical Atlantic	24	0.1	3.8
Grabowski *et al.*	2008[20]	Pacific	ALOHA	24	0.25	4.5*

Grosse *et al.*	2010[45]	South China Sea	Mekong River Plume	6-12	0.9	2.3
Holl *et al.*	2007[46]	Atlantic	W Gulf of Mexico / *Trichodesmium*	6	0.96	0.25
Ibello *et al.*	2010[47]	Mediterranean		24	1	4.6
Konno *et al.*	2010[48]	Pacific	NW Pacific	24-72	2-4	0.25-0.5
Law *et al.*	2011[49]	Pacific	SW Pacific	12-36	1	2.4
Maranon *et al.*	2010[50]	Atlantic	central Atlantic	24	1	2
Mills *et al.*	2004[51]	Atlantic	eastern tropical N Atlantic	24	0.85	1.18
Moisander *et al.*	1996[52]	Baltic Sea	Field and culture	2	40	0.0245
Moore *et al.*	2009[53]	Pacific	Fiji to Hawaii	24	0.7	4.5
Mourino-Carballido	2011[54]	Atlantic	tropical and subtropical Atlantic	24	1	2
Moutin *et al.*	2008[55]	Pacific	tropical S Pacific	24	1.7	0.6
Mulholland and Bernhardt	2005[56]	culture	*Trichodesmium*	1	1	0.16
Mulholland *et al.*	2004[57]	culture	*Trichodesmium*	2	1	0.16
Needoba *et al.*	2007[14]	Pacific	oligotrophic N Pacific Ocean	48	2	4
Orcutt *et al.*	2001[58]	Atlantic	BATS/*Trichodesmium*	6	14.3	0.014
Ploug *et al.*	2010[59]	Baltic Sea	*Aphanizomenon*	3-6	8	0.25
Raimbault and Garcia	2008[25]	Pacific	S Pacific Ocean	24	3.5	0.58
Rees *et al.*	2009[7]	Atlantic	western English Channel	24	2	0.64
Rees *et al.*	2006[60]	Mediterranean	E Mediterranean Sea	24	2	10

Ridame *et al.*	2011[61]	Mediterranean		24	1.1	4.5
Rijkenberg *et al.*	2011[62]	Atlantic	subtropical NE Atlantic	≥24	1	4
Sandroni *et al.*	2007[63]	Mediterranean	NW Mediterranean Sea	12	1.7	0.6
Shiozaki *et al.*	2009[12]	Pacific	NW Pacific (along 155°E)	24	0.5	4.5
Sohm *et al.*, A	2011[11]	Atlantic	South Atlantic Gyre	24	0.7	4.5
Sohm *et al.*, B	2011[17]	Pacific	whole water and *Trichodesmium*	24	0.7	4.5
Ternon *et al.*	2011[64]	Mediterranean		24	1.1	4.5
Turk *et al.*	2011[65]	Atlantic	tropical NE Atlantic	6	2	1
Twomey *et al.*	2007[66]	Indian	SW coast of Australia	6	0.8	4
Voss *et al.*	2004[9]	Atlantic	tropical N Atlantic, transect at 10°N	6	1	1
Voss *et al.*	2006[22]	South China Sea	Off Vietnam	6	1.1	2.3
Wannicke *et al.*	2010[67]	Atlantic	NE Atlantic	1-20	1	2.5
Wasmund *et al.*	2005[68]	Baltic Sea		2	2	0.25
Wasmund *et al.*	2001[69]	Baltic Sea		8	4	0.25
Watkins-Brandt *et al.*	2011[70]	Pacific	North Pacific	24	0.5	4.4
White *et al.*	2007[16]	Pacific	Gulf of California	24	0.3	2
Yogev *et al.*	2011[71]	Mediterranean	E Mediterranean Sea	24-30	2	4.5
Mean				**15**	**2.6**	**2.2**
Median				**18**	**1.0**	**2.0**

This study	**2012**	**Atlantic**		**24**	**1**	**4.5**

References

1. Montoya, J. P., Voss, M., Kahler, P. & Capone, D. G. A simple, high-precision, high-sensitivity tracer assay for N-2 fixation. Applied and Environmental Microbiology 62, 986-993 (1996).
2. Mohr, W., Grosskopf, T., Wallace, D. W. R. & LaRoche, J. Methodological Underestimation of Oceanic Nitrogen Fixation Rates. Plos One 5 (9), e12583. doi:10.1371/journal.pone.0012583 (2010).
3. Gao, H. et al. Aerobic denitrification in permeable Wadden Sea sediments. Isme Journal 4, 417-426 (2010).
4. Langlois, R. J., Hummer, D. & LaRoche, J. Abundances and distributions of the dominant nifH phylotypes in the Northern Atlantic Ocean. Applied and Environmental Microbiology 74, 1922-1931 (2008).
5. Foster, R. A. et al. Influence of the Amazon River plume on distributions of free-living and symbiotic cyanobacteria in the western tropical north Atlantic Ocean. Limnology and Oceanography 52, 517-532 (2007).
6. Clarke, K. R. Nonparametric Multivariate Analyses of Changes in Community Structure. Australian Journal of Ecology 18, 117-143 (1993).
7. Rees, A. P., Gilbert, J. A. & Kelly-Gerreyn, B. A. Nitrogen fixation in the western English Channel (NE Atlantic Ocean). Marine Ecology-Progress Series 374, 7-12 (2009).
8. Fernandez, A., Mourino-Carballido, B., Bode, A., Varela, M. & Maranon, E. Latitudinal distribution of Trichodesmium spp. and N-2 fixation in the Atlantic Ocean. Biogeosciences 7, 3167-3176 (2010).
9. Voss, M., Croot, P., Lochte, K., Mills, M. & Peeken, I. Patterns of nitrogen fixation along 10N in the tropical Atlantic. Geophysical Research Letters 31 (2004).
10. Mourino-Carballido, B. et al. Importance of N(2) fixation vs. nitrate eddy diffusion along a latitudinal transect in the Atlantic Ocean. Limnology and Oceanography 56, 999-1007 (2011).
11. Sohm, J. A. et al. Nitrogen fixation in the South Atlantic Gyre and the Benguela Upwelling System. Geophysical Research Letters 38 (2011).

12. Shiozaki, T., Furuya, K., Kodama, T. & Takeda, S. Contribution of N(2) fixation to new production in the western North Pacific Ocean along 155 degrees E. Marine Ecology-Progress Series 377, 19-32 (2009).
13. Montoya, J. P. et al. High rates of N-2 fixation by unicellular diazotrophs in the oligotrophic Pacific Ocean. Nature 430, 1027-1031 (2004).
14. Needoba, J. A., Foster, R. A., Sakamoto, C., Zehr, J. P. & Johnson, K. S. Nitrogen fixation by unicellular diazotrophic cyanobacteria in the temperate oligotrophic North Pacific Ocean. Limnology and Oceanography 52, 1317-1327 (2007).
15. Hamersley, M. R. et al. Nitrogen fixation within the water column associated with two hypoxic basins in the Southern California Bight. Aquatic Microbial Ecology 63, 193-+ (2011).
16. White, A. E., Prahl, F. G., Letelier, R. M. & Popp, B. N. Summer surface waters in the Gulf of California: Prime habitat for biological N-2 fixation. Global Biogeochemical Cycles 21 (2007).
17. Sohm, J. A., Subramaniam, A., Gunderson, T. E., Carpenter, E. J. & Capone, D. G. Nitrogen fixation by Trichodesmium spp. and unicellular diazotrophs in the North Pacific Subtropical Gyre. Journal of Geophysical Research-Biogeosciences 116 (2011).
18. Church, M. J. et al. Physical forcing of nitrogen fixation and diazotroph community structure in the North Pacific subtropical gyre. Global Biogeochemical Cycles 23 (2009).
19. Zehr, J. P. et al. Unicellular cyanobacteria fix N-2 in the subtropical North Pacific Ocean. Nature 412, 635-638 (2001).
20. Grabowski, M. N. W., Church, M. J. & Karl, D. M. Nitrogen fixation rates and controls at Stn ALOHA. Aquatic Microbial Ecology 52, 175-183 (2008).
21. Dore, J. E., Brum, J. R., Tupas, L. M. & Karl, D. M. Seasonal and interannual variability in sources of nitrogen supporting export in the oligotrophic subtropical North Pacific Ocean. Limnology and Oceanography 47, 1595-1607 (2002).
22. Voss, M., Bombar, D., Loick, N. & Dippner, J. W. Riverine influence on nitrogen fixation in the upwelling region off Vietnam, South China Sea. Geophysical Research Letters 33 (2006).
23. Bombar, D. et al. Sources of new nitrogen in the Vietnamese upwelling region of the South China Sea. Journal of Geophysical Research-Oceans 115 (2010).

24. Fernandez, C., Farias, L. & Ulloa, O. Nitrogen Fixation in Denitrified Marine Waters. Plos One 6, e20539 (2011).
25. Raimbault, P. & Garcia, N. Evidence for efficient regenerated production and dinitrogen fixation in nitrogen-deficient waters of the South Pacific Ocean: impact on new and export production estimates. Biogeosciences 5, 323-338 (2008).
26. Garcia, N., Raimbault, P. & Sandroni, V. Seasonal nitrogen fixation and primary production in the Southwest Pacific: nanoplankton diazotrophy and transfer of nitrogen to picoplankton organisms. Marine Ecology-Progress Series 343, 25-33 (2007).
27. Goebel, N. L., Edwards, C. A., Carter, B. J., Achilles, K. M. & Zehr, J. P. Growth and carbon content of three different-sized diazotrophic cyanobacteria observed in the subtropical North Pacific. Journal of Phycology 44, 1212-1220 (2008).
28. Kester, D. R., Duedall, I. W., Connors, D. N. & Pytkowicz, R. M. Preparation of artificial seawater. Limnology and Oceanography 12, 176-179 (1967).
29. Benavides, M., Agawin, N. S. R., Aristegui, J., Ferriol, P. & Stal, L. J. Nitrogen fixation by Trichodesmium and small diazotrophs in the subtropical northeast Atlantic. Aquatic Microbial Ecology 65, 43-53 (2011).
30. Bombar, D. et al. Distribution of diazotrophic microorganisms and nifH gene expression in the Mekong River plume during intermonsoon. Marine Ecology-Progress Series 424, 39-U55 (2011).
31. Bombar, D. et al. Sources of new nitrogen in the Vietnamese upwelling region of the South China Sea. Journal of Geophysical Research-Oceans 115 (2010).
32. Bonnet, S., Biegala, I. C., Dutrieux, P., Slemons, L. O. & Capone, D. G. Nitrogen fixation in the western equatorial Pacific: Rates, diazotrophic cyanobacterial size class distribution, and biogeochemical significance. Global Biogeochemical Cycles 23 (2009).
33. Bonnet, S., Grosso, O. & Moutin, T. Planktonic dinitrogen fixation along a longitudinal gradient across the Mediterranean Sea during the stratified period (BOUM cruise). Biogeosciences 8, 2257-2267 (2011).
34. Burns, J. A., Zehr, J. P., Montoya, J. P., Kustka, A. B. & Capone, D. G. Effect of EDTA additions on natural Trichodesmium spp. (Cyanophyta) populations. Journal of Phycology 42, 900-904 (2006).

35. Capone, D. G. et al. Nitrogen fixation by Trichodesmium spp.: An important source of new nitrogen to the tropical and subtropical North Atlantic Ocean. Global Biogeochemical Cycles 19 (2005).
36. Chen, Y.-l. L., Chen, H.-Y., Tuo, S.-h. & Ohki, K. Seasonal dynamics of new production from Trichodesmium N-2 fixation and nitrate uptake in the upstream Kuroshio and South China Sea basin. Limnology and Oceanography 53, 1705-1721 (2008).
37. Chen, Y.-l. L., Tuo, S.-h. & Chen, H.-Y. Co-occurrence and transfer of fixed nitrogen from Trichodesmium spp. to diatoms in the low-latitude Kuroshio Current in the NW Pacific. Marine Ecology-Progress Series 421, 25-38 (2011).
38. Degerholm, J., Gundersen, K., Bergman, B. & Soderback, E. Seasonal significance of N-2 fixation in coastal and offshore waters of the northwestern Baltic Sea. Marine Ecology-Progress Series 360, 73-84 (2008).
39. Falcon, L. I., Carpenter, E. J., Cipriano, F., Bergman, B. & Capone, D. G. N-2 fixation by unicellular bacterioplankton from the Atlantic and Pacific oceans: Phylogeny and in situ rates. Applied and Environmental Microbiology 70, 765-770 (2004).
40. Fernandez, A., Mourino-Carballido, B., Bode, A., Varela, M. & Maranon, E. Latitudinal distribution of Trichodesmium spp. and N(2) fixation in the Atlantic Ocean. Biogeosciences 7, 3167-3176 (2010).
41. Fong, A. A. et al. Nitrogen fixation in an anticyclonic eddy in the oligotrophic North Pacific Ocean. Isme Journal 2, 663-676 (2008).
42. Gandhi, N. et al. First direct measurements of N(2) fixation during a Trichodesmium bloom in the eastern Arabian Sea. Global Biogeochemical Cycles 25 (2011).
43. Garcia, N. S. et al. Interactive Effects of Irradiance and Co(2) on Co(2) Fixation and N(2) Fixation in the Diazotroph Trichodesmium Erythraeum (Cyanobacteria). Journal of Phycology 47, 1292-1303 (2011).
44. Goebel, N. L. et al. Abundance and distribution of major groups of diazotrophic cyanobacteria and their potential contribution to N(2) fixation in the tropical Atlantic Ocean. Environmental Microbiology 12, 3272-3289 (2010).
45. Grosse, J., Bombar, D., Hai Nhu, D., Lam Ngoc, N. & Voss, M. The Mekong River plume fuels nitrogen fixation and determines phytoplankton species distribution in the South China Sea during low- and high-discharge season. Limnology and Oceanography 55, 1668-1680 (2010).

46. Holl, C. M. et al. Trichodesmium in the western Gulf of Mexico: N-15(2)-fixation and natural abundance stable isotope evidence. Limnology and Oceanography 52, 2249-2259 (2007).
47. Ibello, V., Cantoni, C., Cozzi, S. & Civitarese, G. First basin-wide experimental results on N(2) fixation in the open Mediterranean Sea. Geophysical Research Letters 37 (2010).
48. Konno, U. et al. Determination of total N (2) fixation rates in the ocean taking into account both the particulate and filtrate fractions. Biogeosciences 7, 2369-2377 (2010).
49. Law, C. S. et al. Response of surface nutrient inventories and nitrogen fixation to a tropical cyclone in the southwest Pacific. Limnology and Oceanography 56, 1372-1385 (2011).
50. Maranon, E. et al. Degree of oligotrophy controls the response of microbial plankton to Saharan dust. Limnology and Oceanography 55, 2339-2352 (2010).
51. Mills, M. M., Ridame, C., Davey, M., La Roche, J. & Geider, R. J. Iron and phosphorus co-limit nitrogen fixation in the eastern tropical North Atlantic. Nature 429, 292-294 (2004).
52. Moisander, P., Lehtimaki, J., Sivonen, K. & Kononen, K. Comparison of 15N2 and acetylene reduction methods for the measurement of nitrogen fixation by Baltic Sea cyanobacteria. Phycologia 35, 140-146 (1996).
53. Moore, R. M., Punshon, S., Mahaffey, C. & Karl, D. The relationship between dissolved hydrogen and nitrogen fixation in ocean waters. Deep-Sea Research Part I-Oceanographic Research Papers 56, 1449-1458 (2009).
54. Mourino-Carballido, B. et al. Importance of N(2) fixation vs. nitrate eddy diffusion along a latitudinal transect in the Atlantic Ocean. Limnology and Oceanography 56, 999-1007 (2011).
55. Moutin, T. et al. Phosphate availability and the ultimate control of new nitrogen input by nitrogen fixation in the tropical Pacific Ocean. Biogeosciences 5, 95-109 (2008).
56. Mulholland, M. R. & Bernhardt, P. W. The effect of growth rate, phosphorus concentration, and temperature on N(2) fixation, carbon fixation, and nitrogen release in continuous cultures of Trichodesmium IMS101. Limnology and Oceanography 50, 839-849 (2005).

57. Mulholland, M. R., Bronk, D. A. & Capone, D. G. Dinitrogen fixation and release of ammonium and dissolved organic nitrogen by Trichodesmium IMS101. Aquatic Microbial Ecology 37, 85-94 (2004).
58. Orcutt, K. M. et al. A seasonal study of the significance of N-2 fixation by Trichodesmium spp. at the Bermuda Atlantic Time-series Study (BATS) site. Deep-Sea Research Part Ii-Topical Studies in Oceanography 48, 1583-1608 (2001).
59. Ploug, H. et al. Carbon and nitrogen fluxes associated with the cyanobacterium Aphanizomenon sp. in the Baltic Sea. Isme Journal 4, 1215-1223 (2010).
60. Rees, A. P., Law, C. S. & Woodward, E. M. S. High rates of nitrogen fixation during an in-situ phosphate release experiment in the Eastern Mediterranean Sea. Geophysical Research Letters 33 (2006).
61. Ridame, C. et al. Nutrient control of N(2) fixation in the oligotrophic Mediterranean Sea and the impact of Saharan dust events. Biogeosciences 8, 2773-2783 (2011).
62. Rijkenberg, M. J. A. et al. Environmental Forcing of Nitrogen Fixation in the Eastern Tropical and Sub-Tropical North Atlantic Ocean. Plos One 6, e28989 (2011).
63. Sandroni, V., Raimbault, P., Migon, C., Garcia, N. & Gouze, E. Dry atmospheric deposition and diazotrophy as sources of new nitrogen to northwestern Mediterranean oligotrophic surface waters. Deep-Sea Research Part I-Oceanographic Research Papers 54, 1859-1870 (2007).
64. Ternon, E., Guieu, C., Ridame, C., L'Helguen, S. & Catala, P. Longitudinal variability of the biogeochemical role of Mediterranean aerosols in the Mediterranean Sea. Biogeosciences 8, 1067-1080 (2011).
65. Turk, K. A. et al. Nitrogen fixation and nitrogenase (nifH) expression in tropical waters of the eastern North Atlantic. Isme Journal 5, 1201-1212 (2011).
66. Twomey, L. J., Waite, A. M., Pez, V. & Pattiaratchi, C. B. Variability in nitrogen uptake and fixation in the oligotrophic waters off the south west coast of Australia. Deep-Sea Research Part Ii-Topical Studies in Oceanography 54, 925-942 (2007).
67. Wannicke, N., Liskow, I. & Voss, M. Impact of diazotrophy on N stable isotope signatures of nitrate and particulate organic nitrogen: case studies in the north-eastern tropical Atlantic Ocean. Isotopes in Environmental and Health Studies 46, 337-354 (2010).

68. Wasmund, N., Nausch, G., Schneider, B., Nagel, K. & Voss, M. Comparison of nitrogen fixation rates determined with different methods: a study in the Baltic Proper. Marine Ecology-Progress Series 297, 23-31 (2005).
69. Wasmund, N., Voss, M. & Lochte, K. Evidence of nitrogen fixation by non-heterocystous cyanobacteria in the Baltic Sea and re-calculation of a budget of nitrogen fixation. Marine Ecology-Progress Series 214, 1-14 (2001).
70. Watkins-Brandt, K. S. et al. Addition of inorganic or organic phosphorus enhances nitrogen and carbon fixation in the oligotrophic North Pacific. Marine Ecology-Progress Series 432, 17-29 (2011).
71. Yogev, T. et al. Is dinitrogen fixation significant in the Levantine Basin, East Mediterranean Sea? Environmental Microbiology 13, 854-871 (2011).

3 Discussion

3 Discussion

Deutsch *et al.* 2007 proposed a mechanism explaining how the high N-loss rates in oxygen minimum zones could be balanced by N_2 fixation. Due to upwelling of water with high P compared to N concentrations, the surface phytoplankton would rapidly draw down N concentrations to a level that limits their growth, with residual P opening the stage for diazotrophs. After degradation, the diazotrophic biomass would be converted to ammonium and then to nitrate, thereby resupplying the lost N to the ocean, shifting the nutrient stoichiometry (N:P) back towards the Redfield ratio. As predicted by Deutsch *et al.* 2007, we found high rates of N_2 fixation on the Peruvian shelf, at a station where nitrate was nearly completely depleted and P remained at very high concentrations in the water column. Yet, most of the diazotrophic organisms detected in the Peruvian upwelling system were previously unknown (Cluster P1-P7), showing distinct patterns of distribution throughout the water column, with sometimes high abundances inside the OMZ. Cyanobacteria, the best studied contributors to marine N_2 fixation were absent, except for *Crocosphaera*. The N_2 fixation rate as measured along the 10°S transect showed a broad peak throughout the OMZ, where oxygen concentrations were sometimes below the detection limit (2 μmol kg^{-1}). Furthermore, the addition of glucose to incubations always triggered an increase in N_2 fixation rates measured. The Peruvian upwelling system therefore represented a unique habitat of diazotrops, where cyanobacteria only play a minor role and heterotrophs seem to be the dominant diazotrophs.

The whole South Pacific receives very low quantities of Aeolian iron input; therefore phytoplankton productivity is limited by iron availability over large areas (Behrenfeld & Kolber 1999). Diazotrophic cyanobacteria have high iron requirements, because both N_2 fixation and photosynthesis involve enzymes with high iron content. This could explain the absence of diazotrophic cyanobacteria, at least in the areas that are iron limited. All along the 10°S and 12°S transects of the M77/3 cruise we detected a cyclic signal in the Fv/Fm value 2.2 that is indicative of iron limitation (Behrenfeld *et al.* 2006), yet nutrient addition experiments at the ends of the 10°S and 12°S transects did not show any limitation on phytoplankton growth, apart from a weak Si limitation at 12°S. In N-limited regions, as those identified via a nutrient addition experiment at 17.45°S 073°W, the high loading of organic material in the water possibly favours the growth of heterotrophic diazotrophs rather than diazotrophic cyanobacteria. A route of supply of reduced organic compounds could be via the upwelling itself. Dissolved organic carbon (DOC) accumulates as a byproduct of remineralisation in the ocean interior. The relatively old water masses upwelled off Peru therefore hold high concentrations of DOC. Although DOC encompasses thousands of different compounds, the majority of the deep ocean DOC is relatively stable and refractory and is not believed to play a major role in microbial energy

cycling (Hansell *et al.* 2009). However, once the sunlight penetrates into water that has not received solar irradiance for several hundred years, it is possible that at least a fraction of the DOC is broken down by UV radiation and is made bio-available. The major source of DOC comes from phytoplankton itself, that can leak DOC either actively, due to overproduction and exudation of organic carbon (Wohlers *et al.* 2009), or due to cell breakage. Under N limited conditions, phytoplankton tends to exude DOC and accumulate more carbon relative to nitrogen in their cellular material. The same effect has been described for non limited production under high CO_2 concentrations (Riebesell *et al.* 2007). This accumulation of reduced carbohydrates in the ocean surface certainly has the potential to fuel heterotrophic productivity and surface dwelling heterotrophic diazotrophs in the southern Peruvian upwelling, both N-limited and with high CO_2 concentrations.

The detection of high abundances of diazotrophs actively fixing N_2 in the mesopelagic ocean, inside the oxygen minimum zone, where nitrate is available at high concentrations, cannot be explained by the classical niche concept of diazotrophs. In chapter 2.1 the bioenergetic requirements of N_2 fixation under different concentrations of oxygen were analyzed. Thus, under low oxygen concentrations the fixation of N_2 could be considered energetically more advantageous than the uptake of nitrate. Although the specific model organism used was *Crocosphaera watsonii*, a phototrophic diazotroph, the results may also apply to heterotrophic organisms. The concentration of oxygen that would favor the switch from nitrate assimilation to N_2 fixation would be determined by the size and respiration rate of the organism in question. This concept of an alternative niche for diazotrophs presents a theoretical basis for the observed abundance of diazotrophs in OMZs (chapter 2.3).

Thus, the proposed niches of diazotrophy in the Peruvian upwelling system are threefold: First, heterotrophs living in the surface on the carbon overproduction of N-limited phytoplankton and secondly, heterotrophs living inside the OMZ on sinking organic matter that is enriched in carbon due to the above named effects. In regions of complete N-loss the N_2 fixation rates were the highest measured in the system. This blooming of diazotrophs in regions with high P* values (high N-loss) represents the third niche of diazotrophy in the Peruvian upwelling system. The result of this diazotrophy should be a drawdown in P concentrations without concomitant reduction of the N concentrations (lowering P*), therefore this last type of diazotrophy generates the effect predicted by Deutsch *et al.* 2007. Upwelling areas certainly represent a very interesting niche for diazotrophs that requires further in depth research. Previously undiscovered diazotrophs and niches of diazotrophy such as those described in chapter 2.1 and 2.3 may help to fill the proposed gap between the N-input via N_2 fixation and the N-loss via denitrification and anammox (Codispoti 2007) and the gap between global N_2 fixation estimates derived from distribution of geochemical tracers and those derived from actual measurements

(Mahaffey *et al.* 2005).

The last chapter of this thesis dealt with an additional reason for the gap in the N-cycle which has a more subtle origin: The variable underestimation of N_2 fixation rates by the $^{15}N_2$ tracer addition method as described in chapters 2.4 and 2.5. Since over the last 15 years the method was used to assess N_2 fixation rates all over the oceans, our budget calculations relying on direct measurements must have underestimated the contribution of diazotrophs to the oceanic N input. Also the models and simulations, designed to make predictions about the behavior of various parameters in the oceans of the future are calibrated and tuned with input parameters obtained by direct measurements. To understand how the $^{15}N_2$ tracer assay could become an accepted method in oceanography I would like to pose a rather philosophical question: What is the true N_2 fixation activity of a liter of ocean water? We can measure the $^{15}N_2$ uptake into the biomass contained in this liter or the activity of acetylene reduction to ethylene in this liter. However, to ensure that the measured value is accurate, i.e. close to the real N_2 fixation activity present in this liter, we have to determine the accuracy of the method in question. In the absence of any reference material, the measured rates of N_2 fixation in the past have been verified by comparing the measured value against the expected activity, either by quantifying the diazotrophs present (microscopy counts or *nifH* qPCR) or by doing $^{15}N_2$ incubations in parallel to acetylene reduction measurements.

The initial verification of the $^{15}N_2$ tracer method was done by incubating field samples from the Baltic Sea against acetylene reduction measurements of the same samples (Montoya *et al.* 1996). However, as briefly explained in the introduction of this thesis, the acetylene reduction assay suffers from the same problem of the slow equilibration of acetylene gas as does the $^{15}N_2$ tracer assay. The authors of that initial study obtained a value of mol acetylene reduced per mol N_2 fixed that was reasonably close to 4 (4.68), the theoretically predicted value from electron stochiometry (8 electrons to produce NH_3 and H_2 from ammonium, 2 electrons to reduce acetylene to ethylene), which was close enough to make the method an oceanographic standard method. Since then there have been reports on ratios measured between acetylene reduction assay and $^{15}N_2$ tracer assay that range from 1.5 to over 20 (Mohr *et al.* 2010a), which could in large parts rseult from the slow equilibration effect.

Trichodesmium stands a long tradition as a known diazotroph and for a long time was believed to be the only diazotroph in the marine environment that has a significant impact on the global N-input (Capone *et al.* 1997). This most certainly relates to the macroscopic aspect of *Trichodesmium* colonies, which can reach several millimeters in length and accumulate in great numbers during bloom events. With the introduction of molecular methods into biological oceanography, thousands of new organisms were detected in the oceans capable of fixing N_2 (Zehr & McReynolds 1989, Gaby & Buck-

ley 2011), some of which have since repeatedly been detected during different research cruises, often in numbers comparable to *Trichodesmium* (Langlois *et al.* 2008, Moisander *et al.* 2010). In chapter 2.4 and 2.5 it was shown that the underestimation of N_2 fixation rates by the $^{15}N_2$ tracer assay is related to species composition and that *Trichodesmium* dominated areas suffer less underestimation than areas dominated by other diazotrophs, like the recently discovered unicellular cycanobacteria or γ-proteobacteria. Thus, as long as *Trichodesmium* dominated in the perception of the scientific community as the key diazotroph in the marine realm, the $^{15}N_2$ tracer method produced N_2 fixation rates matching the expectations, i.e. high rates in areas with high *Trichodesmium* numbers and low rates in their absence.

As for other biological rate measurements, what is lacking in N_2 fixation research is a true standard of N_2 fixation rate measurements. A standard should be any reference material that ideally yields the same value whenever measured under the same set of conditions. In contrast to other areas of oceanography (chemical and physical) this is difficult to achieve for rate mesurements with live microorganisms. However, working with the unicellular cyanobacterium *Crocosphaera watsonii* WH8501, I was always impressed about its steady growth and N_2 fixation rates compared to other cultured marine diazotrophs, like *Trichodesmium*. Once the dissolution method, explained in chapter 2.4 and 2.5 of this thesis, was developed, it allowed for the first time an entirely closed N budget of *C. watsonii*, where the measured N_2 fixation rates matched the observed N increase in biomass over the day (chapter 2.5, supplementary material). Therefore, a defined number of *C. watsonii* cells growing under defined light and temperature conditions in N-free medium could serve as a standard, for new methods testing and intercalibration excercises.

A standard like described above would help to make the results obtained by different research groups in different ocean areas comparable to each other and hopefully lead to the full resolution of the N_2 fixation activity in the marine environment. Since we are only beginning to understand the importance of the newly discovered diazotrophs in the marine ecosystem it should be of major interest to have a method available capable of resolving the full extent of N_2 fixation, even by groups not yet discovered or that only get minor importance ascribed.

References

References

Altabet, M. A. (2007) Constraints on oceanic N balance/imbalance from sedimentary N-15 records. *Biogeosciences* 4(1):75–86.

Behrenfeld, M. J. and Kolber, Z. S. (1999) Widespread iron limitation of phytoplankton in the South Pacific Ocean. *Science* 283(5403):840–843.

Behrenfeld, M. J., Worthington, K., Sherrell, R. M., Chavez, F. P., Strutton, P., McPhaden, M. and Shea, D. M. (2006) Controls on tropical Pacific Ocean productivity revealed through nutrient stress diagnostics. *Nature* 442(7106):1025–1028.

Bergman, B., Siddiqui, P. J. A., Carpenter, E. J. and Peschek, G. A. (1993) Cytochrome-Oxidase - Subcellular-Distribution and Relationship to Nitrogenase Expression in the Nonheterocystous Marine Cyanobacterium *Trichodesmium thiebautii*. *Applied and Environmental Microbiology* 59(10):3239–3244.

Berman-Frank, I., Lundgren, P., Chen, Y. B., Kupper, H., Kolber, Z., Bergman, B. and Falkowski, P. (2001) Segregation of nitrogen fixation and oxygenic photosynthesis in the marine cyanobacterium *Trichodesmium*. *Science* 294(5546):1534–1537.

Bertsova, Y. V., Bogachev, A. V. and Skulachev, V. P. (2001) Noncoupled NADH : ubiquinone oxidoreductase of *Azotobacter vinelandii* is required for diazotrophic growth at high oxygen concentrations. *Journal of Bacteriology* 183(23):6869–6874.

Boyd, E. S., Anbar, A. D., Miller, S., Hamilton, T. L., Lavin, M. and Peters, J. W. (2011) A late methanogen origin for molybdenum-dependent nitrogenase. *Geobiology* 9(3):221–232.

Breitbarth, E., Oschlies, A. and LaRoche, J. (2007) Physiological constraints on the global distribution of *Trichodesmium* - effect of temperature on diazotrophy. *Biogeosciences* 4(1):53–61.

Brigle, K. E., Newton, W. E. and Dean, D. R. (1985) Complete Nucleotide-Sequence of the *Azotobacter vinelandii* Nitrogenase Structural Gene-Cluster. *Gene* 37(1-3):37–44.

Burgess, B. K. and Lowe, D. J. (1996) Mechanism of molybdenum nitrogenase. *Chemical Reviews* 96(7):2983–3011.

Capone, D. (1993) Determination of nitrogenase activity in aquatic samples using the acetylene reduction procedure. *E.B. Sherr [ed.] Handbook of methods in aquatic microbial ecology, Lewis* 621–631.

Capone, D. G., Zehr, J. P., Paerl, H. W., Bergman, B. and Carpenter, E. J. (1997) *Trichodesmium*, a globally significant marine cyanobacterium. *Science* 276(5316):1221–1229.

Carpenter, E. J., Montoya, J. P., Burns, J., Mulholland, M. R., Subramaniam, A. and Capone, D. G. (1999) Extensive bloom of a N-2-fixing diatom/cyanobacterial association in the tropical Atlantic Ocean. *Marine Ecology-Progress Series* 185:273–283.

Carr, M. E. and Kearns, E. J. (2003) Production regimes in four Eastern Boundary Current systems. *Deep-Sea Research Part Ii-Topical Studies in Oceanography* 50(22-26):3199–3221.

Cheng, Q. (2008) Perspectives in biological nitrogen fixation research. *Journal of Integrative Plant Biology* 50(7):786–798.

Chisnell, J. R., Premakumar, R. and Bishop, P. E. (1988) Purification of a 2nd Alternative Nitrogenase from a *nifhdk* Deletion Strain of *Azotobacter vinelandii*. *Journal of Bacteriology* 170(1):27–33.

Church, M. J., Short, C. M., Jenkins, B. D., Karl, D. M. and Zehr, J. P. (2005) Temporal patterns of nitrogenase gene (*nifH*) expression in the oligotrophic North Pacific Ocean. *Applied and Environmental Microbiology* 71(9):5362–5370.

Codispoti, L. A. (2007) An oceanic fixed nitrogen sink exceeding 400 Tg Na-1 vs the concept of homeostasis in the fixed-nitrogen inventory. *Biogeosciences* 4(2):233–253.

Colon-Lopez, M. S. and Sherman, L. A. (1998) Transcriptional and translational regulation of photosystem I and II genes in light-dark- and continuous-light-grown cultures of the unicellular cyanobacterium *Cyanothece sp.* strain ATCC 51142. *Journal of Bacteriology* 180(3):519–526.

ColonLopez, M., Sherman, D. M. and Sherman, L. A. (1997) Transcriptional and translational regulation of nitrogenase in light-dark- and continuous-light grown cultures of the unicellular cyanobacterium *Cyanothece sp*. strain ATCC 51142. *Journal of Bacteriology* 179(13):4319–4327.

Danyal, K., Dean, D. R., Hoffman, B. M. and Seefeldt, L. C. (2011) Electron Transfer within Nitrogenase: Evidence for a Deficit-Spending Mechanism. *Biochemistry* 50(43):9255–9263.

Deutsch, C., Sarmiento, J. L., Sigman, D. M., Gruber, N. and Dunne, J. P. (2007) Spatial coupling of nitrogen inputs and losses in the ocean. *Nature* 445(7124):163–167.

Diaz, R. J. and Rosenberg, R. (2008) Spreading Dead Zones and Consequences for Marine Ecosystems. *Science* 321(5891):926–929.

Duce, R. A., LaRoche, J., Altieri, K., Arrigo, K. R., Baker, A. R., Capone, D. G., Cornell, S., Dentener, F., Galloway, J., Ganeshram, R. S., Geider, R. J., Jickells, T., Kuypers, M. M., Langlois, R., Liss, P. S., Liu, S. M., Middelburg, J. J., Moore, C. M., Nickovic, S., Oschlies, A., Pedersen, T., Prospero, J., Schlitzer, R., Seitzinger, S., Sorensen, L. L., Uematsu, M., Ulloa, O., Voss, M., Ward, B. and Zamora, L. (2008) Impacts of atmospheric anthropogenic nitrogen on the open ocean. *Science* 320(5878):893–897.

Dugdale, R. (1972) Chemical oceanography and primary productivity in upwelling regions. *Geoforum* 3(3):47–61.

Dyhrman, S. T. and Haley, S. T. (2006) Phosphorus scavenging in the unicellular marine diazotroph *Crocosphaera watsonii*. *Applied and Environmental Microbiology* 72(2):1452–1458.

Falkowski, P. G. (1997) Evolution of the nitrogen cycle and its influence on the biological sequestration of CO2 in the ocean. *Nature* 387(6630):272–275.

Farnelid, H., Andersson, A. F., Bertilsson, S., Abu Al-Soud, W., Hansen, L. H., Sorensen, S., Steward, G. F., Hagstrom, A. and Riemann, L. (2011) Nitrogenase Gene Amplicons from Global Marine Surface Waters Are Dominated by Genes of Non-Cyanobacteria. *Plos One* 6(4).

Fay, P. (1992) Oxygen Relations of Nitrogen-Fixation in Cyanobacteria. *Microbiological Reviews* 56(2):340–373.

Fernandez, C., Farias, L. and Ulloa, O. (2011) Nitrogen Fixation in Denitrified Marine Waters. *Plos One* 6(6): e20539.

Foster, R. A., Subramaniam, A., Mahaffey, C., Carpenter, E. J., Capone, D. G. and Zehr, J. P. (2007) Influence of the Amazon River plume on distributions of free-living and symbiotic cyanobacteria in the western tropical north Atlantic Ocean. *Limnology and Oceanography* 52(2):517–532.

Foster, R. A., Subramaniam, A. and Zehr, J. P. (2009) Distribution and activity of diazotrophs in the Eastern Equatorial Atlantic. *Environmental Microbiology* 11(4):741–750.

Fu, F. X., Zhang, Y. H., Bell, P. R. F. and Hutchins, D. A. (2005) Phosphate uptake and growth kinetics of *Trichodesmium* (Cyanobacteria) isolates from the North Atlantic Ocean and the Great Barrier Reef, Australia. *Journal of Phycology* 41(1):62–73.

Gaby, J. C. and Buckley, D. H. (2011) A global census of nitrogenase diversity. *Environmental Microbiology* 13(7):1790–1799.

Galloway, J. N., Dentener, F. J., Capone, D. G., Boyer, E. W., Howarth, R. W., Seitzinger, S. P., Asner, G. P., Cleveland, C. C., Green, P. A., Holland, E. A., Karl, D. M., Michaels, A. F., Porter, J. H., Townsend, A. R. and Vorosmarty, C. J. (2004) Nitrogen cycles: past, present, and future. *Biogeochemistry* 70(2):153–226.

Garcia, R. A. L. T. P. B. J. I. A. O. K. B. M. M. Z., H. E. and Johnson, D. R. (2010) World Ocean Atlas 2009, Volume 3: Dissolved Oxygen, Apparent Oxygen Utilization, and Oxygen Saturation. *S. Levitus, Ed. NOAA Atlas NESDIS 70, U.S. Government Printing Office, Washington, D.C., 344 pp.* .

Gruber, N. and Galloway, J. N. (2008) An Earth-system perspective of the global nitrogen cycle. *Nature* 451(7176):293–296.

Gruber, N. and Sarmiento, J. L. (1997) Global patterns of marine nitrogen fixation and denitrification. *Global Biogeochemical Cycles* 11(2):235–266.

Hales, B. J., Case, E. E., Morningstar, J. E., Dzeda, M. F. and Mauterer, L. A. (1986) Isolation of a New Vanadium-Containing Nitrogenase from *Azotobacter Vinelandii*. *Biochemistry* 25(23):7253–7255.

Hallenbeck, P. C. (1983) Nitrogenase Reduction by Electron Carriers - Influence of Redox Potential on Activity and the Atp/2e-Ratio. *Archives of Biochemistry and Biophysics* 220(2):657–660.

Halm, H., Lam, P., Ferdelman, T. G., Lavik, G., Dittmar, T., LaRoche, J., D'Hondt, S. and Kuypers, M. M. M. (2011) Heterotrophic organisms dominate nitrogen fixation in the South Pacific Gyre. *ISME J* .

Hamersley, M. R., Turk, K. A., Leinweber, A., Gruber, N., Zehr, J. P., Gunderson, T. and Capone, D. G. (2011) Nitrogen fixation within the water column associated with two hypoxic basins in the Southern California Bight. *Aquatic Microbial Ecology* 63(2):193–+.

Hansell, D. A., Carlson, C. A., Repeta, D. J. and Schlitzer, R. (2009) Dissolved Organic Matter in the Ocean a Controversy Stimulates New Insights. *Oceanography* 22(4):202–211.

Karl, D., Michaels, A., Bergman, B., Capone, D., Carpenter, E., Letelier, R., Lipschultz, F., Paerl, H., Sigman, D. and Stal, L. (2002) Dinitrogen fixation in the world's oceans. *Biogeochemistry* 57(1):47–+.

Kasting, J. F. and Siefert, J. L. (2002) Life and the evolution of Earth's atmosphere. *Science* 296(5570):1066–1068.

Knowles, R. (1982) Denitrification. *Microbiological Reviews* 46(1):43–70.

Kupper, H., Ferimazova, N., Setlik, I. and Berman-Frank, I. (2004) Traffic lights in *Trichodesmium*. Regulation of photosynthesis for nitrogen fixation studied by chlorophyll fluorescence kinetic microscopy. *Plant Physiology* 135(4):2120–2133.

Kuypers, M. M. M., Lavik, G., Woebken, D., Schmid, M., Fuchs, B. M., Amann, R., Jorgensen, B. B. and Jetten, M. S. M. (2005) Massive nitrogen loss from the Benguela upwelling system through anaerobic ammonium oxidation. *Proceedings of the National Academy of Sciences of the United States of America* 102(18):6478–6483.

Lam, P. and Kuypers, M. M. M. (2011) Microbial Nitrogen Cycling Processes in Oxygen Minimum Zones. In Annual Review of Marine Science, Vol 3, volume 3 of *Annual Review of Marine Science*, 317–345.

Lam, P., Lavik, G., Jensen, M. M., van de Vossenberg, J., Schmid, M., Woebken, D., Dimitri, G., Amann, R., Jetten, M. S. M. and Kuypers, M. M. M. (2009) Revising the nitrogen cycle in the Peruvian oxygen minimum zone. *Proceedings of the National Academy of Sciences of the United States of America* 106(12):4752–4757.

Langlois, R. J., Hummer, D. and LaRoche, J. (2008) Abundances and distributions of the dominant nifH phylotypes in the Northern Atlantic Ocean. *Applied and Environmental Microbiology* 74(6):1922–1931.

LaRoche, J. and Breitbarth, E. (2005) Importance of the diazotrophs as a source of new nitrogen in the ocean. *Journal of Sea Research* 53(1-2):67–91.

Long, S. R. (1989) Rhizobium-Legume Nodulation - Life Together in the Underground. *Cell* 56(2):203–214.

Mahaffey, C., Michaels, A. F. and Capone, D. G. (2005) The conundrum of marine N-2 fixation. *American Journal of Science* 305(6-8):546–595.

Martinez-Argudo, I., Little, R., Shearer, N., Johnson, P. and Dixon, R. (2004) The NifL-NifA system: a multidomain transcriptional regulatory complex that integrates environmental signals. *Journal of Bacteriology* 186(3):601–610.

Milligan, A. J., Berman-Frank, I., Gerchman, Y., Dismukes, G. C. and Falkowski, P. G. (2007) Light-dependent oxygen consumption in nitrogen-fixing cyanobacteria plays a key role in nitrogenase protection. *Journal of Phycology* 43(5):845–852.

Mohr, W., Grosskopf, T., Wallace, D. W. R. and LaRoche, J. (2010a) Methodological Underestimation of Oceanic Nitrogen Fixation Rates. *Plos One* 5 (9)(9):e12583. doi:10.1371/journal.pone.0012583.

Mohr, W., Intermaggio, M. P. and LaRoche, J. (2010b) Diel rhythm of nitrogen and carbon metabolism in the unicellular, diazotrophic cyanobacterium *Crocosphaera watsonii* WH8501. *Environmental Microbiology* 12(2):412–421.

Moisander, P. H., Beinart, R. A., Hewson, I., White, A. E., Johnson, K. S., Carlson, C. A., Montoya, J. P. and Zehr, J. P. (2010) Unicellular Cyanobacterial Distributions Broaden the Oceanic N-2 Fixation Domain. *Science* 327(5972):1512–1514.

Montoya, J. P., Voss, M., Kahler, P. and Capone, D. G. (1996) A simple, high-precision, high-sensitivity tracer assay for N-2 fixation. *Applied and Environmental Microbiology* 62(3):986–993.

Morrison, J. M., Codispoti, L. A., Smith, S. L., Wishner, K., Flagg, C., Gardner, W. D., Gaurin, S., Naqvi, S. W. A., Manghnani, V., Prosperie, L. and Gundersen, J. S. (1999) The oxygen minimum zone in the Arabian Sea during 1995. *Deep-Sea Research Part Ii-Topical Studies in Oceanography* 46(8-9):1903–1931.

Moutin, T., Karl, D. M., Duhamel, S., Rimmelin, P., Raimbault, P., Van Mooy, B. A. S. and Claustre, H. (2008) Phosphate availability and the ultimate control of new nitrogen input by nitrogen fixation in the tropical Pacific Ocean. *Biogeosciences* 5(1):95–109.

Ohlendieck, U., Stuhr, A. and Siegmund, H. (2000) Nitrogen fixation by diazotrophic cyanobacteria in the Baltic Sea and transfer of the newly fixed nitrogen to picoplankton organisms. *Journal of Marine Systems* 25(3-4):213–219.

Paerl, H. W., Pinckney, J. L. and Kucera, S. A. (1995) Clarification of the Structural and Functional Roles of Heterocysts and Anoxic Microzones in the Control of Pelagic Nitrogen-Fixation. *Limnology and Oceanography* 40(3):634–638.

Paulmier, A. and Ruiz-Pino, D. (2009) Oxygen minimum zones (OMZs) in the modern ocean. *Progress in Oceanography* 80(3-4):113–128.

Peschek, G. A., Villgrater, K. and Wastyn, M. (1991) Respiratory Protection of the Nitrogenase in Dinitrogen-Fixing Cyanobacteria. *Plant and Soil* 137(1):17–24.

Pickett, C. J. (1996) The Chatt cycle and the mechanism of enzymic reduction of molecular nitrogen. *Journal of Biological Inorganic Chemistry* 1(6):601–606.

Ramos, J. L. and Guerrero, M. G. (1983) Involvement of Ammonium Metabolism in the Nitrate Inhibition of Nitrogen-Fixation in *Anabaena Sp* Strain Atcc-33047. *Archives of Microbiology* 136(2):81–83.

Redfield, A. C. (1958) The biological control of chemical factors in the environment. *American Scientist* 46:205–221.

Riebesell, U., Schulz, K. G., Bellerby, R. G. J., Botros, M., Fritsche, P., Meyerhofer, M., Neill, C., Nondal, G., Oschlies, A., Wohlers, J. and Zollner, E. (2007) Enhanced biological carbon consumption in a high CO2 ocean. *Nature* 450(7169):545–U10.

Riemann, L., Farnelid, H. and Steward, G. F. (2010) Nitrogenase genes in non-cyanobacterial plankton: prevalence, diversity and regulation in marine waters. *Aquatic Microbial Ecology* 61(3):225–237.

Robson, R. L. and Postgate, J. R. (1980) Oxygen and Hydrogen in Biological Nitrogen-Fixation. *Annual Review of Microbiology* 34:183–207.

Rubin, M., Berman-Frank, I. and Shaked, Y. (2011) Dust- and mineral-iron utilization by the marine dinitrogen-fixer *Trichodesmium*. *Nature Geoscience* 4(8):529–534.

Saito, M. A., Bertrand, E. M., Dutkiewicz, S., Bulygin, V. V., Moran, D. M., Monteiro, F. M., Follows, M. J., Valois, F. W. and Waterbury, J. B. (2011) Iron conservation by reduction of metalloenzyme inventories in the marine diazotroph *Crocosphaera watsonii*. *Proceedings of the National Academy of Sciences of the United States of America* 108(6):2184–2189.

Schindelin, N., Kisker, C., Sehlessman, J. L., Howard, J. B. and Rees, D. C. (1997) Structure of ADP center dot AIF(4)(-)-stabilized nitrogenase complex and its implications for signal transduction. *Nature* 387(6631):370–376.

Schmitz, R. A., Klopprogge, K. and Grabbe, R. (2002) Regulation of nitrogen fixation in *Klebsiella pneumoniae* and *Azotobacter vinelandii*: NifL, transducing two environmental signals to the *nif* transcriptional activator NifA. *Journal of Molecular Microbiology and Biotechnology* 4(3):235–242.

Schneegurt, M. A., Sherman, D. M., Nayar, S. and Sherman, L. A. (1994) Oscillating Behavior of Carbohydrate Granule Formation and Dinitrogen Fixation in the Cyanobacterium *Cyanothece Sp* Strain Atcc-51142. *Journal of Bacteriology* 176(6):1586–1597.

Seppala, J., Ylostalo, P., Kaitala, S., Hallfors, S., Raateoja, M. and Maunula, P. (2007) Ship-of-opportunity based phycocyanin fluorescence monitoring of the filamentous

cyanobacteria bloom dynamics in the Baltic Sea. *Estuarine Coastal and Shelf Science* 73(3-4):489–500.

Shah, V. K., Stacey, G. and Brill, W. J. (1983) Electron-Transport to Nitrogenase - Purification and Characterization of Pyruvate, Flavodoxin Oxidoreductase, the Nifj-Gene Product. *Journal of Biological Chemistry* 258(19):2064–2068.

Sherman, L. A., Meunier, P. and Colon-Lopez, M. S. (1998) Diurnal rhythms in metabolism: A day in the life of a unicellular, diazotrophic cyanobacterium. *Photosynthesis Research* 58(1):25–42.

Shi, T., Ilikchyan, I., Rabouille, S. and Zehr, J. P. (2010) Genome-wide analysis of diel gene expression in the unicellular N(2)-fixing cyanobacterium *Crocosphaera watsonii* WH 8501. *Isme Journal* 4(5):621–632.

Smil, V. (1999) Detonator of the population explosion. *Nature* 400(6743):415–415.

Staal, M., Meysman, F. J. R. and Stal, L. J. (2003) Temperature excludes N-2-fixing heterocystous cyanobacteria in the tropical oceans. *Nature* 425(6957):504–507.

Staal, M., Rabouille, S. and Stal, L. J. (2007) On the role of oxygen for nitrogen fixation in the marine cyanobacterium *Trichodesmium sp*. *Environmental Microbiology* 9(3):727–736.

Stoeckel, J., Welsh, E. A., Liberton, M., Kunnvakkam, R., Aurora, R. and Pakrasi, H. B. (2008) Global transcriptomic analysis of *Cyanothece* 51142 reveals robust diurnal oscillation of central metabolic processes. *Proceedings of the National Academy of Sciences of the United States of America* 105(16):6156–6161.

Stramma, L., Johnson, G. C., Sprintall, J. and Mohrholz, V. (2008) Expanding oxygen-minimum zones in the tropical oceans. *Science* 320(5876):655–658.

Stramma, L., Visbeck, M., Brandt, P., Tanhua, T. and Wallace, D. (2009) Deoxygenation in the oxygen minimum zone of the eastern tropical North Atlantic. *Geophysical Research Letters* 36.

Subramaniam, A., Brown, C. W., Hood, R. R., Carpenter, E. J. and Capone, D. G. (2002) Detecting *Trichodesmium* blooms in SeaWiFS imagery. *Deep-Sea Research Part Ii-Topical Studies in Oceanography* 49(1-3):107–121.

Thorneley, R. N. F. and Ashby, G. A. (1989) Oxidation of Nitrogenase Iron Protein by Dioxygen without Inactivation Could Contribute to High Respiration Rates of *Azotobacter* Species and Facilitate Nitrogen-Fixation in Other Aerobic Environments. *Biochemical Journal* 261(1):181–187.

Ting, C. S., Rocap, G., King, J. and Chisholm, S. W. (2002) Cyanobacterial photosynthesis in the oceans: the origins and significance of divergent light-harvesting strategies. *Trends in Microbiology* 10(3):134–142.

Tripp, H. J., Bench, S. R., Turk, K. A., Foster, R. A., Desany, B. A., Niazi, F., Affourtit, J. P. and Zehr, J. P. (2010) Metabolic streamlining in an open-ocean nitrogen-fixing cyanobacterium. *Nature* 464(7285):90–94.

Tuit, C., Waterbury, J. and Ravizzaz, G. (2004) Diel variation of molybdenum and iron in marine diazotrophic cyanobacteria. *Limnology and Oceanography* 49(4):978–990.

Tyrrell, T., Maranon, E., Poulton, A. J., Bowie, A. R., Harbour, D. S. and Woodward, E. M. S. (2003) Large-scale latitudinal distribution of *Trichodesmium spp.* in the Atlantic Ocean. *Journal of Plankton Research* 25(4):405–416.

Valladares, A., Maldener, I., Muro-Pastor, A. M., Flores, E. and Herrero, A. (2007) Heterocyst development and diazotrophic metabolism in terminal respiratory oxidase mutants of the cyanobacterium *Anabaena sp* strain PCC 7120. *Journal of Bacteriology* 189(12):4425–4430.

Walsby, A. E. (2007) Cyanobacterial heterocysts: terminal pores proposed as sites of gas exchange. *Trends in Microbiology* 15(8):340–349.

Ward, B. B., Devol, A. H., Rich, J. J., Chang, B. X., Bulow, S. E., Naik, H., Pratihary, A. and Jayakumar, A. (2009) Denitrification as the dominant nitrogen loss process in the Arabian Sea. *Nature* 461(7260):78–U77.

Webb, E. A., Ehrenreich, I. M., Brown, S. L., Valois, F. W. and Waterbury, J. B. (2009) Phenotypic and genotypic characterization of multiple strains of the diazotrophic cyanobacterium, *Crocosphaera watsonii*, isolated from the open ocean. *Environmental Microbiology* 11(2):338–348.

Weiss, R. (1970) The solubility of nitrogen, oxygen and argon in water and seawater. *Deep Sea Research* 17:721–735.

Wohlers, J., Engel, A., Zollner, E., Breithaupt, P., Jurgens, K., Hoppe, H. G., Sommer, U. and Riebesell, U. (2009) Changes in biogenic carbon flow in response to sea surface warming. *Proceedings of the National Academy of Sciences of the United States of America* 106(17):7067–7072.

Wyrtki, K. (1962) The Oxygen Minima in Relation to Ocean Circulation. *Deep-Sea Research* 9(1):11–23.

Zehr, J. P. (2009) New twist on nitrogen cycling in oceanic oxygen minimum zones. *Proceedings of the National Academy of Sciences of the United States of America* 106(12):4575–4576.

Zehr, J. P., Bench, S. R., Carter, B. J., Hewson, I., Niazi, F., Shi, T., Tripp, H. J. and Affourtit, J. P. (2008) Globally Distributed Uncultivated Oceanic N-2-Fixing Cyanobacteria Lack Oxygenic Photosystem II. *Science* 322(5904):1110–1112.

Zehr, J. P. and McReynolds, L. A. (1989) Use of Degenerate Oligonucleotides for Amplification of the *nifH* Gene from the Marine Cyanobacterium *Trichodesmium thiebautii*. *Applied and Environmental Microbiology* 55(10):2522–2526.

Zehr, J. P., Waterbury, J. B., Turner, P. J., Montoya, J. P., Omoregie, E., Steward, G. F., Hansen, A. and Karl, D. M. (2001) Unicellular cyanobacteria fix N-2 in the subtropical North Pacific Ocean. *Nature* 412(6847):635–638.

Acknowledgements

Eidesstattliche Erklärung

Acknowledgements

Many people contributed to the success of this work. I would like to thank a few of them here:

Thank you, Julie LaRoche, for offering me the opportunity to work in your group in this interesting field. You guided me through my years as a PhD student and always encouraged me in my ideas, also those more or less of the track. I have learned a lot and am gratefull for the experience I gathered on various cruises and in Kiel.

I would further like to thank Julie LaRoche and Ruth Schmitz-Streit for opening up the projekt on OMZs that I have been part of.

Thank you Diana Gill and Tania Klüver for being the best lab-technicians and office buddies. You were always very helpful in showing me new methods and assisting in endless repetitions of already known ones. It would not have worked without you!

I would like to say thank you to Marcel Kuypers and Gaute Lavik from the Max Planck Institute in Bremen. I have learned a lot from you two and I have always enjoyed working with you!

My thanks to all people of the LaRoche group, Markus, Rebecca, Dwhani, Falguni, Diana, Steffi, Tania, Harry, Sophie, Wiebke and everyone I forgot to mention but who feels like she or he should be on the list! Also thanks to Caro Löscher, for a fun cooperation on the B3 project!

I would like to thank the crew and captain of the FS METEOR and RRS DISCOVERY from the M77/3, M80/1 & 2 and D361 cruises, as well as all the chief scientists and all the colleagues that shared good moments and hard work.

Alexandra-Sophie Roy, I enjoyed having you as an office mate. Thousands of liters of your coffee and milk kept me running while writing this thesis and (all) my plant(s) would have died without you. Merci beaucoup!

My fellow colleagues and friends Harald (Harry) Schunck, Kai Lohbeck, Lars Nichelmann and Patricia Grasse were always open for discussions about old problems and new ideas. Thank you all! Thank you Kai for critically reading parts of this thesis and giving your suggestions and comments.

Mein Dank gilt auch Natalia Wagner, für ihre moralische Unterstützung besonders in schwierigen Zeiten!

Besonderer Danke gilt meiner Mutter, Gudrun Großkopf. Du hast mich immer unterstützt und nie den Glauben an mich verloren. Dafür möchte ich Dir von Herzen Danken!

Eidesstattliche Erklärung

Hiermit versichere ich an Eides statt, dass die von mir vorgelegte Dissertation, abgesehen von der Beratung durch meine Betreuerin, nach Inhalt und Form meine eigene Arbeit ist und unter Einhaltung der Regeln guter wissenschaftlicher Praxis der Deutschen Forschungsgemeinschaft (DFG) angefertigt wurde. Genutzte Quellen, Hilfsmittel und Zusammenarbeit mit anderen Wissenschaftlern wurden kenntlich gemacht. Desweiteren versichere ich, dass die von mir vorgelegte Dissertation weder im Ganzen noch im Teil einer anderen Fakultät oder anderen Hochschule im Rahmen eines Prüfungsverfahrens vorgelegt wurde. Veröffentlichte oder zur Veröffentlichung eingereichte Manuskripte wurden kenntlich gemacht.

Tobias Großkopf

Kiel, den 27. März 2012